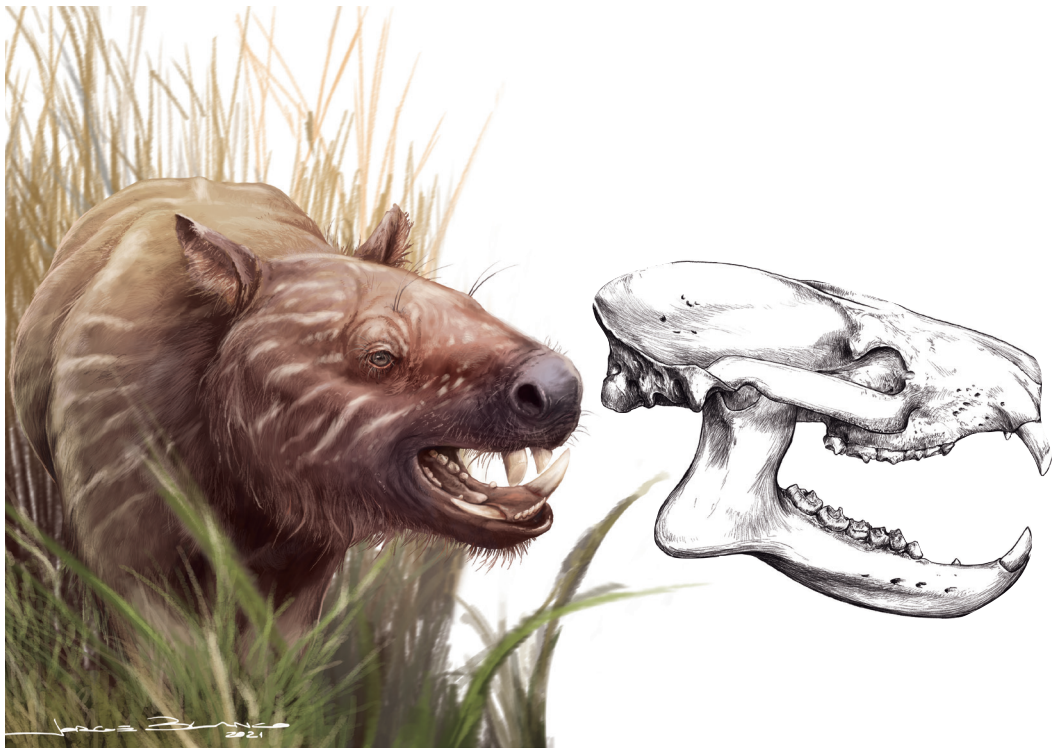# CRANIAL MORPHOLOGY AND PHYLOGENETIC RELATIONSHIPS OF *TRIGONOSTYLOPS WORTMANI*, AN EOCENE SOUTH AMERICAN NATIVE UNGULATE

R.D.E. MACPHEE, SANTIAGO HERNÁNDEZ DEL PINO,
ALEJANDRO KRAMARZ, ANALÍA M. FORASIEPI,
MARIANO BOND, AND R. BENJAMIN SULSER

CRANIAL MORPHOLOGY AND PHYLOGENETIC RELATIONSHIPS OF *TRIGONOSTYLOPS WORTMANI*, AN EOCENE SOUTH AMERICAN NATIVE UNGULATE

R.D.E. MacPHEE
Department of Mammalogy/Vertebrate Zoology and Richard Gilder Graduate School,
American Museum of Natural History

SANTIAGO HERNÁNDEZ DEL PINO
IANIGLA, CCT-CONICET Mendoza, Argentina

ALEJANDRO KRAMARZ
Sección Paleontología de Vertebrados, Museo Argentino de Ciencias Naturales
Bernardino Rivadavia, CONICET, Buenos Aires, Argentina

ANALÍA M. FORASIEPI
IANIGLA, CCT-CONICET Mendoza, Argentina

MARIANO BOND
Departamento Científico de Paleontología Vertebrados, Museo de La Plata,
Paseo del Bosque s/n, 1900 La Plata, Argentina

R. BENJAMIN SULSER
Department of Mammalogy/Vertebrate Zoology and Richard Gilder Graduate School,
American Museum of Natural History

CONTENTS

Reconstruction of *Trigonostylops wortmani* by Jorge Blanco.

ABSTRACT

In 1933 George G. Simpson described a remarkably complete skull of *Trigonostylops*, an Eocene South American native ungulate (SANU) whose relationships were, in his mind, quite uncertain. Although some authorities, such as Florentino Ameghino and William B. Scott, thought that a case could be made for regarding *Trigonostylops* as an astrapothere, Simpson took a different position, emphasizing what would now be regarded as autapomorphies. He pointed out a number of features of the skull of *Trigonostylops* that he thought were not represented in other major clades of SANUs, and regarded these as evidence of its phyletic uniqueness. Arguing that the lineage that *Trigonostylops* represented must have departed at an early point from lineages that gave rise to other SANU orders, Simpson reserved the possibility that Astrapotheriidae might still qualify (in modern terms) as its sister group. Even so, he argued that the next logical step was to place *Trigonostylops* and its few known allies in a separate order, Trigonostylopoidea, coordinate with Astrapotheria, Notoungulata, Litopterna, and Pyrotheria. Simpson's classification was not favored by most later authors, and in recent decades trigonostylopids have been almost universally assigned to Astrapotheria. However, his evaluation of the allegedly unique characters of *Trigonostylops* and its allies has never been systematically treated, which is the objective of this paper. Using computed tomography, the skull of *Trigonostylops* is compared, structure by structure, to a variety of representative SANUs as well as extant perissodactylans (which together comprise the clade Panperissodactyla) and the "condylarthran" *Meniscotherium*. In addition to placing Simpson's character evaluations in a comparative context, we also provide detailed assessments of many vascular and pneumatization-related features of panperissodactylans never previously explored. Overall, we found that this new assessment strengthened the placement of *Trigonostylops* within a monophyletic group that includes *Astrapotherium* and *Astraponotus*, to the exclusion of other SANU clades. Although *Trigonostylops* cannot be considered as morphologically distinct or unusual as Simpson thought, our comparative and phylogenetic analyses have helped to generate a number of hypotheses about character evolution and function in SANUs that may now be fruitfully tested using other taxon combinations.

INTRODUCTION

Trigonostylops wortmani AMNH VP-28700 (figs. 1, 2), the only substantially complete skull of a representative of Trigonostylopidae, is the source of most of what we know about cranial morphology in this clade of early South American placentals. George G. Simpson, on whose 1930–1931 Scarritt Patagonian Expedition this specimen was collected at a terminal Middle Eocene locality south of Lago Colhuéhuapí,[1] thought it was "one of the most extraordinary mammalian skulls ever discovered, being unusual in almost every detail and having some

striking characters otherwise quite unknown in the Class Mammalia" (Simpson, 1933a: 1).

To modern eyes Simpson's exuberance may seem misplaced, for he was essentially referring to features that would now be judged as relatively uninformative autapomorphies, however striking they might be on other grounds. However, given his "evolutionist" approach to systematics (e.g., Simpson, 1975), such characters were worth emphasizing because they represented "specializations not absolutely excluding the possibility of [discovering a] very remote relationship" (Simpson, 1933a: 18), in this case between *Trigonostylops* and its presumed closest relatives among South American native ungulates (hereafter, SANUs). In light of the geological age of AMNH VP-28700 and its alleged distinctiveness, Simpson reasoned that trigonostylopids must have diverged from the other main lineages of

---

[1] Simpson did not mention a specific locality or stratigraphic context in his 1933a paper. According to his field notes (Simpson MS, p. 6), the skull (field number 60 = AMNH VP-28700) was recovered at Colhuéhuapí in section A3, lower part of the lower tuff (= marker bed Y), equivalent to level 2 in Cifelli's (1985) figure 3, section I. The specimen was collected by Justino Hernández, October 31, 1930.

SANUs no later than the earliest part of the Cenozoic. While they might have shared a general "condylarthran" ancestry with other SANU groups, he considered that such relationships woiuld have otherwise been remote. In this Simpson differed from Ameghino (1901), Scott (1928, 1937a), and other authorities of the time who favored the view (on the basis of then quite limited dental evidence) that *Trigonostylops* was best regarded as an early astrapothere. In his view the taxon was sui generis, "as unlike litopterns as astrapotheres" (Simpson, 1933a: 27). He changed his mind somewhat in a subsequent paper (Simpson, 1934; see also Simpson, 1957), allowing that trigonostylopids might conceivably be astrapotheres in a general classificatory sense, but should be placed in a separate suborder. Later, Simpson (1967) withdrew even this concession, making *Trigonostylops* and several other taxa previously incertae sedis the sole representatives of order Trigonostylopoidea. His justification for this maneuver was basically the same as before, i.e., their marked differences from other early SANUs in certain aspects of the dentition and ear region (see Rose, 2006). In his view the existence of such distinctions meant that only a general "patristic" or grade position for *Trigonostylops* could be established: "their resemblances [to astrapotheres] could equally well be explained by remote common ancestry, such as within the Condylarthra, perhaps with a limited degree of convergence" (Simpson, 1967: 210).

In phylogenetic terms, little was actually clarified by Simpson's (1933a, 1957, 1967) analyses, and his later publications referencing trigonostylopid relationships did not differ from the first in either content or conclusions. In these papers he did not attempt to provide a broad comparative framework for his assessments, limiting his nondental comparisons to a few of the better-known (and mostly late-diverging) taxa representing other orders. As a separate order Trigonostylopoidea was never widely endorsed by other workers, and more recent systematic and morphological analyses have generally recommended reincorporation of the family into Astrapotheria (e.g., Carbajal et al., 1977; Soria and Bond, 1984; Soria, 1988; Cifelli, 1985; Kramarz and Bond, 2009; Kramarz et al., 2017; Billet, 2010, 2011; Billet et al., 2015). At the same time, none of these later studies has provided a thorough reinvestigation of the skull and dentition of *T. wortmani*, nor of the osteological features that Simpson regarded as "quite unknown" elsewhere among mammals.

In this contribution we not only reevaluate many of Simpson's morphological inferences in a wider context, but also describe cranial features of AMNH VP-28700 that would have been impossible for him to explore without modern imaging technology. We also provide evaluations of less complete cranial specimens of *Trigonostylops* in Argentinian and other collections that help to clarify morphological aspects that cannot be adequately studied on the AMNH skull. These new categories of information provide a basis for reassessing the phylogenetic position of *Trigonostylops* (fig. 34), using a modified version of the character set developed by Billet et al. (2015). See p. 131, Phylogenetic Analyses, and appendix 3.

That such a study can be usefully undertaken at this time is a credit not only to a wide range of relevant systematic and comparative studies published in the last several decades, but also to the increased availability of micro-CT scanning for examining vascular, otic, and cerebral endocast morphology at unprecedented levels of visualization. Given new molecular evidence that at least some SANU groups are more closely related to Perissodactyla than they are to any other mammalian order with extant representation (Owen, 1854; Welker et al., 2015; Buckley, 2015; Westbury et al., 2017), we include extensive comparative remarks on horses, tapirs, and rhinos to aid in the interpretation of trigonostylopid morphology. This allows us to conveniently convey new morphology, much of which does not (yet) lend itself to character construction and analysis because of the lack of comparable studies.

MATERIALS AND METHODS

Comparative Set

The comparative set (table 1) lists specimens that were extensively used to investigate morphological features or to ascertain character states, together with their technical names, institutional acronyms, and other data. For abbreviations used in figures 1–42, see table 2. Tables 3–6 provide data on specimens and other information relevant to analyses in the text. Taxon names for extant perissodactylans follow Grubb (2005). For fossil taxa, the names utilized are ones judged to be valid and current. We are aware that "condylarthrans" do not constitute a natural group, but as this paper is not centrally concerned with the ultimate ancestry of SANUs, it is adequate for our purposes to employ this term, but in quotes. Panperissodactyla minimally includes extinct and extant members of Perissodactyla as usually defined plus the SANU orders Notoungulata and Litopterna, as established by proteomic and genomic evidence presented by Welker et al. (2015) and Westbury et al. (2017). Other traditional SANU orders, sometimes grouped with the foregoing in superorder Meridiungulata, may also be members of Panperissodactyla (e.g., Pyrotheria); so might other taxa (e.g., Cooper et al., 2014; but see Rose et al., 2019), although delimiting this larger potential clade is not the focus of this paper. "No data" (ND) specimens of extant species (table 1) are ones, usually from zoos, that lack a native geographical origin; they were used for scanning and dissection in several instances because of their excellent preservation and availability for these purposes.

Trigonostylops and Astrapotheriidae: Physical Status of Selected Specimens

Although it is not feasible to comment on the physical condition of each of the numerous fossils utilized in this study, we have done so below for most of the high-quality trigonostylopid and astrapotheriid specimens available to us:

Trigonostylops wortmani AMNH VP-28700. Simpson (1933a: 1) described AMNH VP-28700 as being "nearly complete with preservation unusually favorable for study" (figs. 1A–E; 2A, B). This assessment is substantially correct, but it should be noted that, as was common practice at the time, a fair amount of reconstruction was undertaken to improve the fossil's appearance. On the specimen's left side (fig. 1D), much of the face, floor of the orbit, and rostral part of the zygomatic arch are reconstructed in plaster, their shapes based on the somewhat more intact right side. Plaster likewise holds together the nasal cavity's surviving right wall, which is minutely fractured and crushed inward (fig. 24). The meso- and neurocranium are internally much fragmented, although the caudal cranium is in surprisingly good condition. Some sutures and plaster/bone contacts were traced in India ink, perhaps by Simpson (e.g., fig. 25). During the original preparation of the specimen, matrix was removed from all external surfaces; foramina were subjected to especially deep cleaning, with inevitable (if mostly minute) loss of bone as a result. Matrix lodged in the endocranium was removed by tunneling through the foramen magnum, which resulted in additional damage to some structures (e.g., to internal walls of extratympanic sinuses, so that they now artificially open into the cranial cavity; figs. 11, 12).

The basicranium as it appears at present (fig. 26) differs slightly from the illustration in Simpson's (1933a: fig. 5) paper. This indicates that AMNH VP-28700 has undergone additional preparation by unknown hands since Simpson's time, especially on the specimen's right side where additional work on the auditory region has obviously occurred. Internally, the portion of the skull that housed the olfactory bulbs and adjacent parts of the forebrain are extensively damaged and could not be usefully reconstructed (fig. 8). The ubiquitous presence of mineral sinter on internal surfaces complicated endocast rendering (e.g., figs. 11, 12).

The skull may have been discovered in two or more parts, or perhaps it broke after collection or
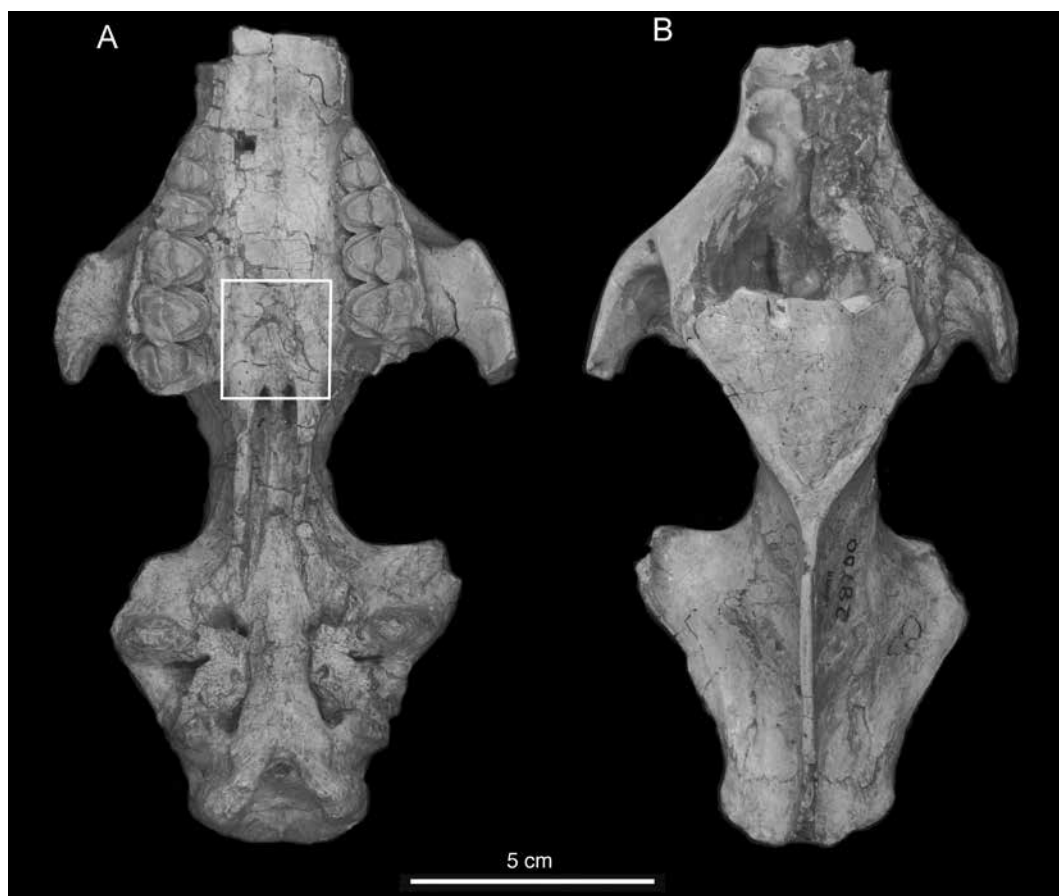
FIG. 1. *Trigonostylops wortmani* AMNH VP-28700, skull: **A,** ventral; **B,** dorsal; **C,** right lateral; **D,** left lateral; and **E,** caudal views (on this and facing page). In A**,** rectangle encloses palatal alate process (see fig. 20). For details of orbital and basicranial regions, see figures 25 and 26.

during preparation. In any case, the pieces were expertly glued together, albeit with a slight loss of bone as the pieces were fitted along fractures. The most obvious break can be seen ventrally, where the fracture line passes from side to side just caudal to the opening of the choanae. Large fractures were treated with a filler (?polyethylene glycol) at some stage of preparation.

OTHER *TRIGONOSTYLOPS* SPECIMENS. Three additional cranial fragments ascribed to *T. wortmani* were available for study: a partial face (MLP 52-X-5-98; fig. 21), a partial rostrum (MACN Pv 47 [cast of MNHN-CAS 187]), and another incomplete rostrum in poorer condition but preserving parts of the nasals and maxillae (MACN

A 11078). A nearly complete jaw, MPEF PV 5483 (fig. 3), is also briefly described and illustrated in connection with the summary of dental features (see p. 69, Dentition and Upper Jaw).

MLP 52-X-5-98 is the only specimen of *Trigonostylops* discovered to date that substantially preserves the nasal aperture and rostral portion of the face. The rostrum has been distorted by lateral crushing, with the result that the left palatal process of the maxilla has been partly jammed under the right. There is also a significant fracture passing through the palate that principally affects the teeth, but has no other consequences for present purposes. There is some loss of bone on projecting margins, but the nasal aperture

5 cm
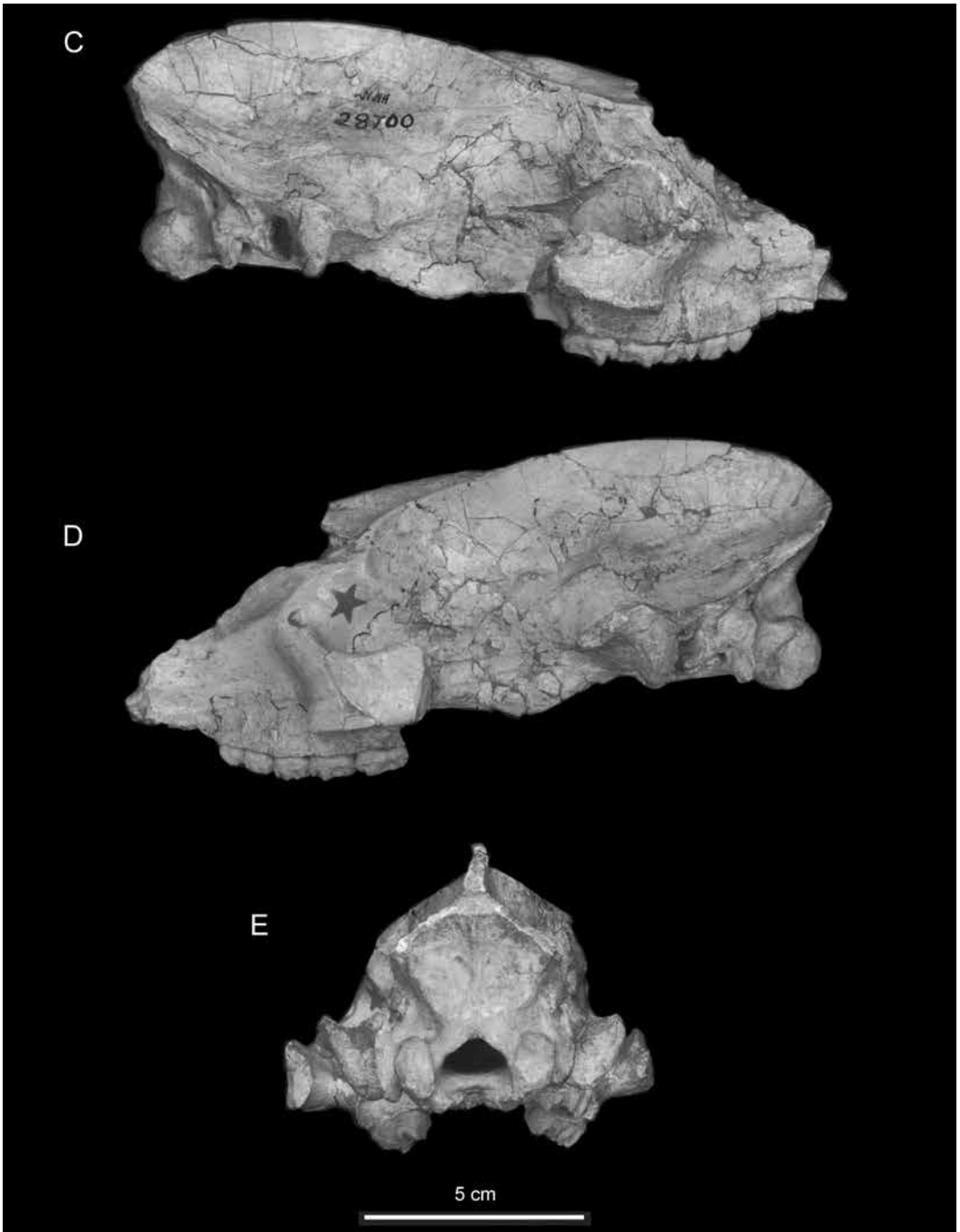
TABLE 1

Comparative Set[1]

Taxon	Institution	Accession No.	Specimen(s)[2]	Age/Gender	Geographical Origin[3]	Geological Age/Fm
EXTANT TAXA						
Tapiridae						
Tapirus indicus	AMNH	M-77875	skull	young juvenile	ND	Holocene
Tapirus indicus	AMNH	M-130108	skull	adult (M)	ND	Holocene
Tapirus indicus[4]	**AMNH**	**M-200300**	skull	subadult	ND	Holocene
Tapirus terrestris	AMNH	M-77576	skull	adult (M)	Venezuela	Holocene
Tapirus terrestris	MACN	Ma 24.30	skull	adult	Alto Amazonas, Brazil	Holocene
Tapirus terrestris	MACN	Ma 27200	skull	adult	ND	Holocene
Tapirus terrestris	MACN	Ma 52.77	skull	juvenile	Misiones, Argentina	Holocene
Rhinocerotidae						
Ceratotherium simum	**AMNH**	**M-51882**	skull	juvenile (F)	Democratic Republic of Congo	Holocene
Dicerorhinus sumatrensis	AMNH	M-81892	skull	adult (M)	Malaysia	Holocene
Rhinoceros unicornis	**AMNH**	**M-274636**	skull	perinatal	ND	Holocene
Equidae						
Equus asinus	AMNH	M-204141	skull	adult	ND	Holocene
Equus caballus	**AMNH**	**M-204155**	skull	young juvenile (F)	ND	Holocene
Bovidae						
Saiga tatarica	AMNH	M-85305	skull	adult	Kazakhstan	Holocene
FOSSIL TAXA						
Astrapotheria						
Trigonostylops wortmani	**AMNH**	**VP-28700**	skull	young adult	Colhué-Huapí, Argentina	M. Eocene; Sarmiento Fm.
Trigonostylops wortmani	MLP	52-X-5-98	partial rostrum	adult	Pampa de María Santísima, Argentina	M. Eocene; Sarmiento Fm.

TABLE 1 *continued*

Taxon	Institution	Accession No.	Specimen(s)[2]	Age/ Gender	Geographical Origin[3]	Geological Age/Fm
Trigonostylops wortmani	MACN	Pv 47	partial rostrum	adult	Punta Casamayor, Argentina	M. Eocene; Sarmiento Fm.
Trigonostylops wortmani	MACN	A 11078	partial rostrum	?	Colhué-Huapí, Argentina	M. Eocene; Sarmiento Fm.
Trigonostylops wortmani	MPEF	PV 5483	jaw	adult	Valle Hermoso, Argentina	M. Eocene; Sarmiento Fm.
Tetragonostylops apthomasi	DGM	355-M	partial skull	adult	Itaboraí, Brazil	E. Eocene; Itaboraí Fm.
Tetragonostylops apthomasi	DGM	216-M	left maxilla	adult	Itaboraí, Brazil	E. Eocene; Itaboraí Fm.
Granastrapotherium snorki	IGM SCG	MGJRG-2018 V4	skull	adult	La Venta, Colombia	M. Miocene; Villavieja Fm.
Astraponotus sp.	MPEF	PV 1279	skull	adult	Gran Hondonada, Argentina	L. Eocene; Sarmiento Fm.
Astraponotus sp.	MPEF	PV 1084	skull	adult	Gran Hondonada, Argentina	L. Eocene; Sarmiento Fm.
Astraponotus sp.	MPEF	PV 1296	right maxilla	juvenile	Gran Hondonada, Argentina	L. Eocene; Sarmiento Fm.
Astrapotherium magnum	YPM	PU 15117	skull, jaw	adult	Güer Aike, Argentina	E. Miocene; Santa Cruz Fm.
Astrapotherium magnum	YPM	PU 15261	skull	adult	Güer Aike, Argentina	E. Miocene; Santa Cruz Fm.
Astrapotherium magnum	**MACN**	**A 8580**	skull	adult	Corrigue Kaik, Argentina	E. Miocene; Santa Cruz Fm.
Astrapotherium magnum	**MACN**	**A 3208**	**skull**[5]	adult	Corrigue Kaik, Argentina	E. Miocene; Santa Cruz Fm.
Astrapotherium magnum	YPM	PU 15332	skull	adult	Coy Inlet, Argentina	E. Miocene; Santa Cruz Fm.
Astrapotherium magnum	AMNH	VP-9278	skull, jaw	juvenile	Río Gallegos, Argentina	E. Miocene; Santa Cruz Fm.
Astrapotherium sp.	MLP	38-X-30-1	partial skull	juvenile	Río Coyle, Argentina	E. Miocene; Santa Cruz Fm.
Astrapotherium magnum	FMNH	P14259	skull, jaw, LE	adult	Río Coyle, Argentina	E. Miocene; Santa Cruz Fm.
Astrapotherium guillei	MAPBAR	5322	skull, jaw	adult	Comallo, Argentina	M. Miocene; Collon Cura Fm.
Parastrapotherium sp.	AMNH	VP-29596	skull	juvenile	Las Cascadas, Argentina	L. Oligocene; Sarmiento Fm.
Parastrapotherium sp.	AMNH	VP-29575[6]	skull	adult	Las Cascadas, Argentina	L. Oligocene; Sarmiento Fm.
Parastrapotherium martiale	MACN	A 52-604	partial skull, jaw	adult	Argentina	?L. Oligocene
Scaglia kraglievichorum	MMP	M 207	skull	juvenile	Cañadón Vaca, Argentina	M. Eocene; Sarmiento Fm.
Scaglia cf. *kraglievichorum*	MPEF	PV 5478	skull	adult	Cañadón Vaca, Argentina	M. Eocene; Sarmiento Fm.
Eoastrapostylops riolorense	PVL	4216	skull, jaw	young adult	Río Loro, Argentina	?L. Paleocene; Río Loro Fm.
Eoastrapostylops riolorense	PVL	4217	skull, jaw	young adult	Río Loro, Argentina	?L. Paleocene; Río Loro Fm.

TABLE 1 *continued*

Taxon	Institution	Accession No.	Specimen(s)[2]	Age/Gender	Geographical Origin[3]	Geological Age/Fm
Notoungulata						
Nesodon imbricatus	YPM	PU 16012	skull	adult	Corpen Aike, Argentina	E. Miocene; Santa Cruz Fm.
Nesodon imbricatus	YPM	PU 15000	skull	adult	Güer Aike, Argentina	E. Miocene; Santa Cruz Fm.
Nesodon imbricatus	YPM	PU 15336	skull	adult	Güer Aike, Argentina	E. Miocene; Santa Cruz Fm.
Nesodon imbricatus	YPM	PU 15492	skull	adult	Güer Aike, Argentina	E. Miocene; Santa Cruz Fm.
Nesodon sp.	YPM	3384[7]	partial skull	?		
Adinotherium ovinum	YPM	PU 15986	skull	adult	Güer Aike, Argentina	E. Miocene; Santa Cruz Fm.
Adinotherium ovinum	YPM	PU 15114	skull	adult	Güer Aike, Argentina	E. Miocene; Santa Cruz Fm.
Piauhytherium sp.	MCL	5191	partial skull	adult	Procedência, Toca dos Ossos, Brazil	Pleistocene
Toxodon sp.	MCL	5192	partial skull	adult	Procedência, Toca dos Ossos, Brazil	Pleistocene
Toxodon sp.	MCL	5194	partial skull	juvenile	Procedência, Toca dos Ossos, Brazil	Pleistocene
Toxodon sp.	MACN	Pv 16615	skull	juvenile	Río Carcarañá, Argentina	L. Pleistocene
Puelia coarctatus	MLP	67-II-27-27	skull	adult	Gran Hondonada, Argentina	L. Eocene; Sarmiento Fm.
Homalodotherium sp.	**MPM**	**PV 17490**	skull	adult	Cañadon de la Vacas, Argentina	E. Miocene, Santa Cruz Fm.
Homalodotherium segoviae	FMNH	P13092	LE	adult	Cape Fairweather, Argentina	E. Miocene; Santa Cruz Fm.
Homalodotherium sp.	MACN	A 3206[8]	skull	adult	Monte Observacion, Argentina	E. Miocene; Santa Cruz Fm.
Rhynchippus equinus	FMNH	P13410	skull, LE	adult	Cabeza Blanca, Argentina	L. Oligocene; Sarmiento Fm.
Oldfieldthomasia debilitata	**AMNH**	**VP-28600**	skull	adult	Cerro Blanco, Argentina	M. Eocene; Sarmiento Fm.
Notopithecus adapinus	AMNH	VP-28949	skull	adult	Colhué-Huapí, Argentina	M. Eocene; Sarmiento Fm.
Cochilius volvens	**AMNH**	**VP-29651**	skull	adult	Colhué-Huapí, Argentina	E. Miocene; Sarmiento Fm.
Cochilius volvens	FMNH	P13424	skull	adult	Colhué-Huapí, Argentina	E. Miocene; Sarmiento Fm.
Interatherium robustum	FMNH	P13057	skull, jaw	adult	Estancia Felton, Argentina	E. Miocene; Santa Cruz Fm.
Campanorco inauguralis	MLP	79-IV-16-1	skull	adult	Cerro Campanorco, Argentina	M. Eocene; Lumbrera Fm.
Protypotherium sp.	FMNH	P13234	skull, jaw	adult	Güer Aike, Argentina	E. Miocene; Santa Cruz Fm.
Typotheriopsis internum	FMNH	P14420	skull	adult	Puerta de Corral Quemado, Argentina	L. Miocene; Chiquimil Fm.
Typotheriopsis internum	FMNH	P14477	skull	adult	Puerta de Corral Quemado, Argentina	L. Miocene; Chiquimil Fm.

TABLE 1 *continued*

Taxon	Institution	Accession No.	Specimen(s)[2]	Age/ Gender	Geographical Origin[3]	Geological Age/Fm
Mesotherium angustirostrum	MACN	Pv 6040	skull	adult	General Alvarado, Argentina	E. Pleistocene; "Pampean Fm."
Paedotherium chapadmalense	AMNH	VP-45914	skull	adult	Chapadmalal, Argentina	L.Pliocene; Chapadmalal Fm.
Argyrohyrax proavus	FMNH	P13415	skull	adult	Cabeza Blanca, Argentina	L. Oligocene; Sarmiento Fm.
Pyrotheria						
Pyrotherium romeroi	ACM	3207	partial skull	adult	Cabeza Blanca, Argentina	L. Oligocene; Sarmiento Fm.
Pyrotherium romeroi	FMNH	P13515	incomp. rostrum	adult	Pico Truncado, Argentina	L. Oligocene; Sarmiento Fm.
Litopterna						
Diadiaphorus majusculus	AMNH	VP-9270	skull	adult	Santa Cruz, Argentina	E. Miocene; Santa Cruz Fm.
Tetramerorhinus mixtum	MACN	A 8970	skull	adult	Corrigue Kaik, Argentina	E. Miocene; Santa Cruz Fm.
Tetramerorhinus cingulatum	MACN	A 5971	skull	adult	La Cueva, Argentina	E. Miocene; Santa Cruz Fm.
Tetramerorhinus cingulatum	MACN	A 8666	skull	adult	Corrigue Kaik, Argentina	E. Miocene; Santa Cruz Fm.
Tetramerorhinus lucarius	**AMNH**	**VP-9245**[9]	skull	adult	Río Gallegos, Argentina	E. Miocene; Santa Cruz Fm.
Tetramerorhinus sp.	YPM	PU 15368[9]	skull	adult	Killik Aike, Argentina	E. Miocene; Santa Cruz Fm.
Tetramerorhinus mixtum	YPM	PU 15107[9]	skull, jaw	adult	Lago Pueyrredón, Argentina	E. Miocene; Santa Cruz Fm.
Neobrachytherium morenoi	MACN	Pv 8428	skull	adult	Andalhualá, Argentina	L. Miocene; Corral Quemado Fm.
Thoatherium minusculum	**YPM**	**PU 15721**	skull	adult	Río Gallego, Argentina	E. Miocene; Santa Cruz Fm.
Scalabrinitherium bravardi	MACN	Pv 13082	caudal cranium	adult	Paraná, Argentina	L. Miocene; Ituzaingó Fm.
Promacrauchenia antiquua	MACN	Pv 7986	skull	adult	Monte Hermoso, Argentina	E. Pliocene; Monte Hermoso Fm.
Huayqueriana cf. cristata	**IANIGLA**	**Pv 29**	skull	adult	Huayquerías del Este, Argentina	L. Miocene; Huayquerías Fm.
Macrauchenia patachonica	MACN	Pv 2	skull	adult	Salto, Argentina	L. Pleistocene; "Pampean Fm."
Perissodactyla (Palaeotheriidae)						
Palaeotherium siderolithicum	MNHN	GY-523[10]	skull	adult	Montmartre, France	Eocene
Palaeotherium crassum	MACN	A 11538	maxilla	adult	France	Eocene

TABLE 1 *continued*

Taxon	Institution	Accession No.	Specimen(s)[2]	Age/ Gender	Geographical Origin[3]	Geological Age/Fm
Palaeotherium crassum	MACN	A 11539	jaw	adult	France	Eocene
Palaeotherium magnum	MACN	Pv 12998	maxilla	adult	France	Eocene
Palaeotherium muelhbergi	FMO	SEO-01	skull	adult	St Etienne de l'Olm, France	Eocene
Palaeotherium muelhbergi	FMO	SEO-02	skull, jaw	adult	St Etienne de l'Olm, France	Eocene
Palaeotherium robustum	FMO	FAV-16	skull	adult	Faveirol, France	Eocene
Palaeotherium lautricense	FMO	LTN-02	skull	adult	Lautrec, France	Eocene
Palaeotherium muelhbergi	FMO	UM-1756	skull	adult	Gypse de Pantin, France	Eocene
Palaeotherium curtum	MNHN	GY-424	skull	adult	Montmartre, France	Eocene
Palaeotherium sp.	MNHN	GY-410, 412, 470, 482	astragali	adult	Montmartre, France	Eocene
"Condylarthra"						
Phenacodus primaevus	AMNH	VP-15268	skull	adult	Elk Creek, Bighorn Basin	E. Eocene
Phenacodus primaevus	MACN	Pv 18808[11]	skull, jaw	adult	Wind River, Wyoming	E. Eocene
Meniscotherium chamense	**AMNH**	**VP-4412**	skull	adult	San Juan, San Juan Basin	E. Eocene

[1] Scanned specimens in bold.

[2] LE, latex endocast (FMNH Patterson collection); F, female; M, male.

[3] ND, no locality data (zoo specimens in the case of extant species). For fossils lacking locality data, only country of origin is listed.

[4] Accessioned as "*Tapirus* sp." in AMNH Mammalogy catalog, but cranial characters are those of *T. indicus* (cf. Moyano and Giannini, 2017).

[5] Left petrosal scanned.

[6] Specimen extensively reconstructed.

[7] Temporary accession number.

[8] Type of *Diorotherium aegregium*.

[9] Specimens usually included in *Protertotherium* (e.g., Billet et al., 2015, App. S1), but here placed in *Tetramerorhinus* following Soria (2001). YPM PU 15107 is type of *Proter- otherium dodgei*.

[10] Examined for pneumatization-related features; other *Palaeotherium* specimens used for scoring discrete traits.

[11] Cast of YPM PU 14864.

and the pillarlike projections in which the tusks were socketed are relatively well preserved.

Astrapotheriid Specimens. *Astrapotherium magnum* AMNH VP-9278. Although the morphological gap between Middle Eocene *Trigonostylops* and Early-Middle Miocene *Astrapotherium* is wide indeed, it is important to be able to compare similarities and differences visually. To enhance our descriptions we include illustrations of the complete, but partially reconstructed, skull of *Astrapotherium magnum* AMNH VP-9278 (figs. 4, 27A) that Simpson (1933a) used in making his comparisons (see also Scott, 1928). Many of the areas of greatest morphological interest on this specimen are either not intact or have been heavily reconstructed (e.g., most large processes, palatal area, auditory region). Fortunately, some of these regions are adequately preserved on specimens in the MACN collection (see below).

Astrapotherium magnum MACN A 8580. This is the only specimen of *Astrapotherium* for which cranial CT scans are currently available (figs. 13–15). It consists of a partial adult skull lacking the entire rostrum, the right zygomatic arch, and most of the occipital condyles (last named reconstructed in plaster). The auditory region is fairly well preserved on both sides.

Astrapotherium magnum MACN A 3208. This specimen is a markedly distorted skull of a subadult. The basicranium, nearly complete on discovery, was later dissected to enable better exploration of areas of interest. The left petrosal (fig. 27B) contains the stapes (fig. 33A–D), dislodged into the labyrinth (figs. 31, 33E) and reconstructed via CT segmental data.

Astrapotherium guillei MAPBAR 5322, recently described by Kramarz et al. (2019a), is an almost complete but laterally compressed skull preserving most of the bones and delicate structures of the basicranium, including the cranial portion of the hyoid apparatus and paracondylar processes. Unlike other *Astrapotherium* specimens used for comparisons, which derive from Early Miocene (Santacrucian) beds of southern Patagonia, *A. guillei* is Middle Miocene (Colloncuran) in age

and the youngest representative of the genus known to date.

Parastrapotherium sp. AMNH VP-29575 is not extensively referenced in our descriptions because the cranium is considerably damaged and much of it is reconstructed. Almost the entire facial region is plaster, including the nasal aperture and the rostral end of the palate, as are the zygomatic arches and much of the basicranium. Known errors in reconstruction include absence of apertures (adituses) in the reconstructed retromandibular processes. These apertures are consistently present in better-preserved skulls of both *Astrapotherium* and *Parastrapotherium*; absence does, however, occur in *Astraponotus* (p. 51, Interpreting Pneumatization).

Astraponotus sp. MPEF PV 1279 and MPEF PV 1084, described by Kramarz et al. (2010), were found in late Middle Eocene (Mustersan) contexts in central Patagonia. MPEF PV 1279 preserves an almost complete rostrum, the left half of the palate with partial dentition, and the braincase and zygomatic arch, but lacks the entire caudal basicranium. MPEF PV 1084 is a partial skull with nearly complete palate, basicranium and occiput, along with the right side of the braincase and zygoma. Together, the two specimens provide significant information on much of the cranial anatomy of *Astraponotus.*

Scaglia kraglievichorum MMP M-207 is a juvenile skull described by Simpson (1957, 1967), which he considered the basalmost astrapotheriid then known. The skull is somewhat distorted, but except for the petrosals and most of the occipital, which are lost, it is otherwise mostly intact. MMP M-207 comes from Middle Eocene (Casamayoran) rocks in central Patagonia. From the same locality and level, Kramarz et al. (2019b) described the partial skull *Scaglia* cf. *kraglievichorum* MPEF PV 5478, an adult of the ?same species. Preserved are the left side of the rostrum, palate, orbital region, zygomatic arch, and both sides of the braincase and the basicranium. The skull as a whole is somewhat distorted and almost all bones are seriously fractured, but a significant part of the basicranium is preserved well enough for cautious interpretation.

Agenda

Method of Description

In his initial publication on *Trigonostylops* Simpson (1933a) provided line drawings designed to bring out similarities and differences between AMNH VP-28700 and other SANUs, but by modern standards his report is underillustrated. Most of the new morphology presented here concerns "hidden" internal architecture brought to light by CT scanning and thus unavailable heretofore. To underscore this, the first section of the description is devoted to vascular and pneumatization-related structures, some of which have been rarely or never explored in fossil panperissodactylans. The second section is concerned with specific features of the skull of *Trigonostylops*, again within a broadly comparative framework. Simpson (1933a) should be consulted for a regionally oriented anatomy of AMNH VP-28700; our method concentrates on presenting detailed evaluations of individual features in a way suitable for making comparisons and scoring characters (see also appendices 1–4). When referenced in the main text, characters listed in appendix 3 are denoted by the letter C plus the list number in bold font (e.g., **C85**).

Recently, intensive descriptive morphology has gained a renewed importance in phenomic systematics (e.g., O'Leary, 2010; Muizon et al., 2018; Harper and Rougier, 2019). This approach requires thorough examination of relevant extant taxa, for which exhaustive detail can be collected on both hard and soft tissues. Information thus acquired is then applied to the interpretation of fossils. In this paper we especially emphasize comparative anatomy and ontogeny as key to the detection of primary or operational homologies (see Presley, 1993). For *Trigonostylops*, this approach turned out to be particularly important. With its combination of small and little-pneumatized neurocranium, relatively long face, and absence of marked basicranial flexion, among many other features, AMNH VP-28700 differs significantly from most post-Paleogene SANUs. This applies a fortiori to the astrapo-

theriids, especially the two best-known members of this clade, *Astraponotus* and *Astrapotherium*, with their extraordinarily modified facial regions (Kramarz and Bond, 2009). Despite Simpson's (1933a, 1967) understandable reservations about their relationship to *Trigonostylops*, more recent scholarship has shown that astrapotheres are the single most important SANU group to which trigonostylopids should be carefully compared, which explains our emphasis on them here.

Use of indicia. It is important to get new observations right, which is why we emphasize the importance of indicia (Latin, *indicium*, pl., indicia, "sign, mark"), defined for the purposes of this paper as bony or other features whose presence is known to strongly correlate with specific soft tissue entities in known extant taxa. In searching for strong indicia on a given fossil, the objective is to justify making an initial assumption of operational homology by making comparisons to similar features in extant forms, thereby enabling recovery of morphological information that would be difficult or impossible to acquire from the fossil alone. At the same time, it is just as important to take note of evidence that may serve to exclude other potential interpretations. This is normally the way that good inferences are made and tested in paleobiology; here we attempt to be as explicit as possible. In the text we concentrate on describing indicia for blood vessels and pneumatic spaces, especially ones whose description we are introducing into the literature for the first time. Terms such as "foramen," "incisure," "sulcus," and "canal" are used somewhat interchangeably depending on a given structure's appearance in segments (especially because each of these terms may apply to one or another part of a given trackway). Likewise, in figs. 7 and 8 certain vessels are named according to the osteological features transmitting them to reflect various uncertainties discussed in the text. We trust that alternative usages will be obvious and not cause confusion.

Cerebral and vascular reconstruction. Virtual cerebral and vascular reconstruc-
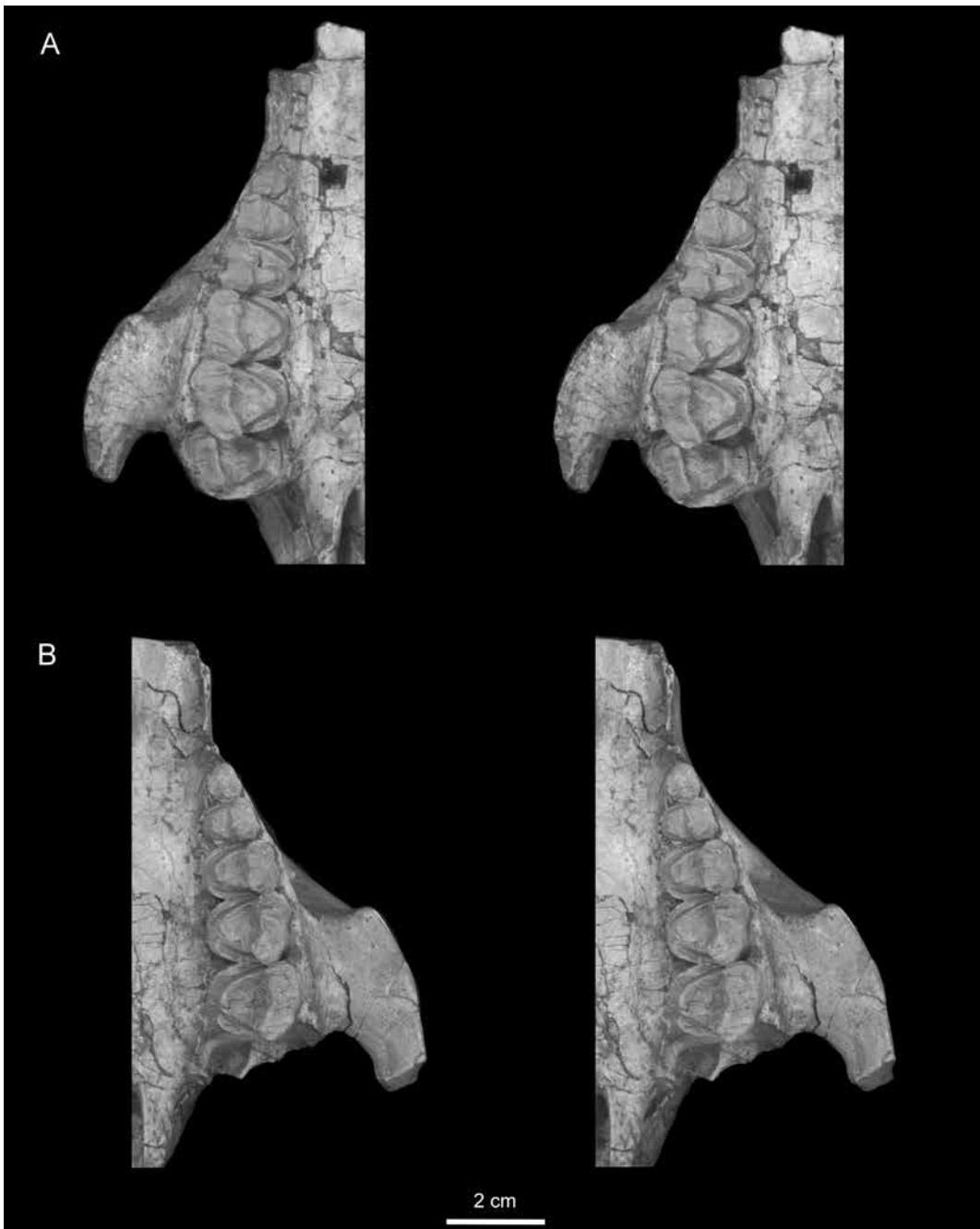
FIG. 2. *Trigonostylops wortmani* AMNH VP-28700, maxillary dentition (stereopairs): **A,** right side; **B,** left side. Defect on right side of palate is an artificial opening into palatal diverticulum (see text and fig. 12A).

TABLE 2

Abbreviations

ANATOMICAL		canine pr	canine-bearing process of maxilla
a	artery (used with other abbreviations)	car spin pr	carotid spinous process (of alisphenoid)
a diplo magn	arteria diploetica magna	car sulc	carotid sulcus
a diplo magn sulc	sulcus for arteria diploetica magna	caud	caudal (used with other abbreviations)
aam	anterior ampulla	caud car for	caudal (= posterior) carotid foramen
acc lac trans sin	accessory lacunae of transverse sinus(es)	caud car incis	caudal (= posterior) carotid incisure
adit	aditus (= pneumatic foramen)	caud cereb a	caudal cerebral artery
adit epitym sin	aditus to epitympanic sinus	caud commun a	caudal communicating artery
adit extrtym sin	aditus to extratympanic sinus	caud crus	caudal crus of ectotympanic
ala	ala of atlas vertebra	cav sin	cavernous sinus
alar can	alar canal	cav suprcoch	cavum supracochleare
aper aud tube	aperture of the auditory tube	ccr	caudal crus of stapes
aqu vest	aqueductus vestibuli	cerbel	cerebellum
artic pr teg	articular process of tegmen tympani	cerbel fos	cerebellar fossa
ASC	anterior semicircular canal	cereb car a	cerebral carotid artery
ASP	alisphenoid bone	choan	choana(e)
atlas	atlas vertebra	chor plx	choroid plexus
auric ram vagus n	auricular ramus of vagus nerve	chord tym	chorda tympani (of CN 7)
axis	axis vertebra	CN 2	optic nerve
basicap fen	basicapsular fenestra	CN 5	trigeminal nerve
basil a	basilar artery	CN 5.1	ophthalmic nerve
basil plx	basilar plexus	CN 5.2	maxillary nerve
BOC	basioccipital bone	CN 5.3	mandibular nerve
br	broken (in reference to damage)	CN 7	facial nerve
BSP	basisphenoid bone	CN 8	vestibulocochlear nerve
bucc n	buccal nerve	CN 9	glossopharyngeal nerve
bulla	auditory bulla	CN 10	vagus nerve
C/c	upper/lower canine	CN 11	accessory nerve
can	canal (used with other abbreviations)	CN 12	hypoglossal nerve
		coch	cochlea
can chord tym	canal chordae tympani	coch can	cochlear canaliculus
can Y	canal Y (for arteria diploetica magna/cranioorbital artery anastomosis)	cond v	condylar (emissary) vein
		cran cav	cranial cavity
can Y aperts	lateral and medial apertures of canal Y	cranorb a	cranioorbital artery
		cranorb can	cranioorbital canal

TABLE 2 *continued*

cranorb for	cranioorbital foramen	gtr palat n for	foramen for greater palatine nerve
cranorb sin	cranioorbital sinus	hiat fac can	hiatus of facial canal
cris tym	crista tympanica	hs	head of stapes
crph can	craniopharyngeal canal	HSB	Hunter-Schreger bands
crus com	crus commune	hyd rec	hyoid recess
crus com sec	secondary crus commune	hyp fos	hypophyseal fossa
dors pet sin	dorsal petrosal sinus	hypgl can	hypoglossal canal
dors sagit sin	dorsal sagittal sinus	hypgl for	hypoglossal foramen
ECT	ectotympanic bone	I/i	upper/lower incisor
ect-ent bulla	ectotympanoentotympanic bulla	INC	incus bone
ENT	(rostral) entotympanic bone	incis	incisure (used with other abbreviations)
EOC	exoccipital bone		
eoc-soc sut	exoccipitosupraoccipital suture	incis car	incisura carotidis
epitym rec	epitympanic recess	incis oval	incisura ovalis
epitym sin	epitympanic sinus	incis spin	incisura spinosa
epitym wing squ	epitympanic wing of squamosal	infrorb can	infraorbital canal
ethm a, n, v	(external) ethmoidal artery, nerve, vein	infrorb for	infraorbital foramen (-ina)
		infrorb n	infraorbital nerve
ethm for	ethmoidal foramen	int acous meat	internal acoustic meatus
ethm lab	ethmoidal labyrinth	int car a	internal carotid artery
ethm sin	ethmoidal sinus	int occ prot	internal occipital protuberance
ext acous can	external acoustic canal	int vert ven plx	internal vertebral venous plexus
ext acous meat	external acoustic meatus	intercar a	intercarotid artery
extrtym sin	extratympanic sinus	IPR	interparietal bone
fac sulc	facial sulcus	jug area	jugular area of basicapsular fenestra (= jugular foramen)
fen coch	fenestra cochleae		
fen vest	fenestra vestibuli	jug pr pet	jugular process of petrosal
for	foramen (used with other abbreviations)	L	length (measurement)
		LAC	lacrimal bone
for magn	foramen magnum	lac for	lacrimal foramen
for ovale	foramen ovale	lam	lateral ampulla
fp	facial process of premaxillae	lambd pr pet	lambdoidal process of petrosal
fps	footplate of stapes	ling n	lingual nerve
FRO	frontal bone	long vert sin	longitudinal vertebral sinus(es)
fron sin	frontal sinus	LSC	lateral semicircular canal
glas fis	glaserian fissure	M/m	upper/lower molar (with locus number)
gr	groove (used with other abbreviations)		
		MAL	malleus bone
grt cereb v	great cerebral vein	malar for	malar foramen
gtr pet n	greater petrosal n (of CN 7)		

TABLE 2 *continued*

mand alveol n	mandibular alveolar nerve	PAR	parietal bone
mand fos	mandibular fossa	paracond pr	paracondylar process
mast	mastoid region of petrosal	parietsqu can	parietosquamosal canal
MAX	maxillary bone	parietsqu for	parietosquamosal foramen
max for	maxillary foramen	PET	petrosal bone
med obl	medulla oblongata	pet-eoc sut	petrosoexoccipital suture
mid cereb a	middle cerebral artery	pet-soc sut	petrososupraoccipital suture
mpf	microperforation (in stapes)	pet-squ sut	petrososquamosal suture
mps	muscular process of stapes (for stapedial m.)	pirif lb	piriform lobe
musc brr	muscular branches	PMX	premaxilla bone
n	nerve (used with other abbreviations)	pons	pons (of brainstem)
		postemp can	posttemporal canal
n pte can	nerve of pterygoid canal	postemp for	posttemporal foramen
NAS	nasal bone	postemp sulc	posttemporal sulcus
nas apt	nasal aperture	postym pr	posttympanic process of squamosal
nas cav	nasal cavity		
nas sill	sill (border) of external nasal aperture	pp	palatal process of premaxillae
		prom	promontorium
naspal can	nasopalatine canal	prom sulc	promontorial sulcus for internal carotid artery
neopal	neopallium		
nuch cr	nuchal crest	PSC	posterior semicircular canal
occip a	occipital artery	PSP	presphenoid bone
occip a sulc	sulcus for occipital artery	PTE	pterygoid bone
occip cond	occipital condyle	pte can	pterygoid canal
occip for	occipital (emissary) foramen	pte plx	pterygoid plexus
occip v	occipital vein	pte pr	pterygoid process
occip-vert plx	occipital-vertebral venous plexus	ram anast occip v	ramus anastomoticus of occipital vein
olf blb	olfactory bulb or peduncle		
ophth v	ophthalmic vein	rcr	rostral crus of stapes
opt can	optic canal	reconst	reconstructed (used with other abbreviations)
opt chias	optic chiasma		
opt for	optic foramen	retroart can	retroarticular (= postglenoid) canal
OSP	orbitosphenoid bone		
P/p	upper/lower premolar (with locus number)	retroart for	retroarticular (= postglenoid) foramen
		retroart incis	retroarticular (= postglenoid) incisure
PAL	palatine bone		
palat alate pr	palatal alate process	retroart pr	retroarticular (= postglenoid) process
palat divert	palatal diverticulum	retroart v	retroarticular (= postglenoid) vein
pam	posterior ampulla	rhin sulc	rhinal sulcus

TABLE 2 *continued*

rost	rostral (used with other abbreviations)	to	to, toward (used with other abbreviations)
rost cereb a	rostral cerebral artery	trans sin	transverse sinus(es)
rost crus	rostral crus of ectotympanic	trans sin can	transverse sinus canal
rost tym pr pet	rostral tympanic process of petrosal	trans sin sulc	transverse sinus sulcus
		transcliv for	transclival foramen
rostvent cerbel a	rostroventral cerebellar artery	trib/tribs	tributary (-ies)
sagit cr	sagittal crest	tym aper prot can	tympanic aperture of prootic canal
sec fac for	secondary facial foramen	tym cav	tympanic cavity
sigm sin	sigmoid sinus	tym n	tympanic nerve (of CN 9)
sigm sin sulc	sulcus for sigmoid sinus	tym n sulc	tympanic nerve sulcus
sin commun	sinus communicans	tymhyl	tympanohyal
SOC	supraoccipital bone	v/vv	vein, veins (used with other abbreviations)
sphen	sphenoidal (used with other abbreviations)	vasc sulc	vascular sulcus
sphen sin	sphenoidal sinus	vent pet sin	ventral petrosal sinus
sphenorb can	sphenoorbital canal	vert a	vertebral artery
sphenorb fis	sphenoorbital fissure	vert v	vertebral vein
sphenpal a, n, v	sphenopalatine artery, nerve, vein	VOM	vomer bone
sphenpal for	sphenopalatine foramen	W	width (measurement)
spinal cd	spinal cord	zyg pr	zygomatic process
SQU	squamosal bone		

str sin	straight sinus	ACM	Amherst College Museum, Amherst, Massachusetts
styhyl	stylohyal	AMNH	American Museum of Natural History (M, Mammalogy collection; VP, Vertebrate Paleontology collection), New York
stylf pr	styliform process (of ectotympanic)		
stylmast for	stylomastoid foramen		
stylmast for prim	foramen stylomastoideum primitivum	DGM	Divisão de Geologia e Mineralogia do Departamento Nacional da Produção Mineral, Rio de Janeiro, Brazil
sulc	sulcus (used with other abbreviations)		
supf temp v	superficial temporal vein	FMNH	Field Museum of Natural History (P, Paleontology collection), Chicago
symp tr	sympathetic trunk		
temp can	temporal (sinus) canal	IGM SCG	Museo Geológico "José Royo y Gómez," Servicio Geológico Colombiano, Bogotá, Colombia
temp meat	temporal meatus		
temp meat v	vein of temporal meatus		
temp sin	temporal sinus	MACN	Museo Argentino de Ciencias Naturales "Bernardino Rivadavia" (A, Ameghino collection; Pv, Vertebrate Paleontology collection), Buenos Aires, Argentina
temp sin can	canal for temporal sinus		
temp sin sulc	sulcus for temporal sinus		
tens tym fos	tensor tympani fossa		

TABLE 2 *continued*

MAPBAR	Museo de la Asociación Paleontológica Bariloche, San Carlos de Bariloche, Argentina
MCL	Museo de Cîencias Naturais da Pontifícia Universidade Católica de Minas Gerais, Belo Horizonte, Brazil
MCNAM	Museo de Ciencias Naturales y Antropológicas "J. C. Moyano" (PV, Vertebrate Paleontology collection), Mendoza, Argentina
MLP	Departamento Científico de Paleontología Vertebrados, Museo de La Plata, Argentina
MMP	Museo Municipal de Ciencias Naturales de Mar del Plata "Lorenzo Scaglia," Mar del Plata, Argentina
MNHN	Muséum national d'Histoire naturelle (various separately designated Vertebrate Paleontology collections), Paris, France
MPEF	Museo Paleontológico "Egidio Feruglio" (PV, Vertebrate Paleontology collection), Trelew, Argentina
MPM	Museo Regional Provincial "Padre M. J. Molina" (PV, Vertebrate Paleontology collection), Río Gallegos, Argentina
PVL	Facultad de Ciencias Naturales e Instituto Miguel Lillo, Universidad Nacional de Tucumán (PVL, Colección Paleontología de Vertebrados Lillo), San Miguel de Tucumán, Argentina
YPM	Yale Peabody Museum (PU, ex Vertebrate Paleontological collection of Princeton University), New Haven, CT

OTHER

NAV	*Nomina Anatomica Veterinaria*, 6th ed. (2017)
SALMA	South American Land Mammal Age
SANU	South American native ungulate

tions are presented in figures 7–10. Indicia can often be traced with greater confidence on scan-derived reconstructions than on natural (matrix) or plaster/resin endocasts, although one has to be conscious of limitations even with scans of well-preserved material. Vascular identifications are based on the usual kinds of indicia (sulci, canals, foramina) that can be plausibly interpreted in light of known correlations in extant taxa. Because the vascular system of the horse is well investigated, we were usually able to directly compare conditions in other panperissodactylans to descriptions and illustrations in equine anatomy texts. Older works were of particular value because of the amount of descriptive and illustrative detail they typically contain (e.g., figs. 5, 6). Having a sense of conditions in *Equus* often made it easier to sort out features encountered in SANUs, but at the same time made us aware of how extensive the morphological gulf is between these distant relatives.

Arterial routings have long figured in morphological treatments of fossil mammals and nowadays detailed virtual reconstructions are commonplace thanks to the availability of CT. However, for several reasons this new tool has been little used to date for studying venous networks (but see Martínez et al., 2016, 2020). To begin with, and to make the undertaking worthwhile, physical trackways or other indicia have to be present and sufficiently stereotypical in their form and location (i.e., not subject to great individual variation) to permit recognition of primary homologies across taxonomic boundaries. Comparative information from extant taxa may be helpful in sorting out vessel identities and connections, but reconstructions based on fossils will necessarily be limited by the nature of the available evidence. Thus true cerebral veins (e.g., great cerebral and other veins traveling in the subarachnoid space and draining directly to dural sinuses) as well as sinuses in thick dural folds (e.g., tentorial sinuses) may be difficult or impossible to reconstruct because they leave limited traces on bony surfaces (Kielan-Jaworowska et al., 1986: 558).

TABLE 3

CT Scanning Parameters

Taxon	Institutional accession no.	Family	Order	Scan type[1]	Slice thickness[2] (μm)	Image resolution (px)	Total images
Astrapotherium magnum [3]	MACN A 3208	Astrapotheriidae	Astrapotheria	μCT	n.a.[4]	990×990	1000
Astrapotherium magnum	MACN A 8580	Astrapotheriidae	Astrapotheria	CT	1500	500×500	346
Ceratotherium simun	AMNH M-51882	Rhinocerotidae	Perissodactyla	μCT	141.7	1960×1960	2097
Cochilius volvens	AMNH VP-29651	Interatheriidae	Notoungulata	μCT	65.77	990×990	1448
Equus caballus	AMNH M-204155	Equidae	Perissodactyla	μCT	128.0	1960×1960	3602
Homalodotherium sp.	MPM PV 17490	Homalodotheri-idae	Notoungulata	CT	600	500×500	593
Huayqueriana cf. *H. cristata*	IANIGLA-PV19	Macraucheniidae	Litopterna	μCT	124.06	1619×1166	3585
Meniscotherium chamense	AMNH VP-4412	Phenacodontidae?	"Condylarthra"	μCT	43.9	1989×1000	3172
Tapirus indicus	AMNH M-200300	Tapiridae	Perissodactyla	μCT	141.7	1960×1960	2033
Tetramerorhinus lucarius [5]	AMNH VP-9245	Protherotheriidae	Litopterna	μCT	56.8	3273×2644	3467
Trigonostylops wortmani	AMNH VP-28700	Trigonostylopidae	Astrapotheria	μCT	72.24	1978×1978	2845

[1] CT, medical scanner; μCT, microscanner.

[2] As provided by CT program.

[3] Left petrosal only; other scans are of complete skulls.

[4] Not available.

[5] Formerly placed in *Proterotherium*; see Soria (2001) and text.

Even when vascular impressions are available, trackway edges and widths can be hard to capture, especially if resolution and density contrasts between bone and matrix are low. Editing and smoothing may be necessary to reduce noise and emphasize pattern, but these represent additional interpretative interventions. To limit such effects where feasible, in our reconstructions apparent gaps between channels (as seen in segmental data) were filled in only when there was reasonable certainty that the trackways on either side of the gap were truly continuous. Nevertheless, some instances of actual continuity were proba-

bly missed. Estimating vessel caliber from segmental information is also quite challenging, and vascular shapes as represented in our figures should not be taken too literally. Additional details on principal vessels and related features are provided in figure legends and the glossary (appendix 1).

Another interpretative difficulty arises when only a single trackway is seemingly present, even when there is reason to believe that it was occupied by both an artery and a vein traveling coaxially. If justified by other evidence, specific inferences can be made about the content of par-

ticular trackways even though virtual reconstructions may be ambiguous. To avoid making assumptions, in our reconstructions all vascular trackways are colored a uniform gray tone, with the single exception of one vessel in *Equus*, the probable homolog of the arteria diploetica magna (= caudal meningeal artery of equine anatomy; Wible, 1987), which is known to travel alone into the skull (see p. 113, Discussion: Vascular Indicia).

NOMENCLATURE. The names of structures used in the text mostly correspond to English equivalents of terms preferred by the International Committee on Veterinary Gross Anatomical Nomenclature, as presented in *Nomina anatomica veterinaria* (6th ed., 2017; hereafter, *NAV*). Even so, the *NAV* list is neither flawless nor comprehensive, and instances where *NAV* choices were not accepted are noted where appropriate. We emphasize that the *NAV* should be treated as a list of names, not secure homologies; these have to be worked out individually to the degree that they can be, especially given the kinds of material normally studied in vertebrate paleontology. We have allowed ourselves some latitude in translating comparative adjectives (e.g., "major" and "minor" vs. "greater" and "lesser"), depending on context and prevailing community usages. In cases where the *NAV* provides specialized names for structures in individual species, we have usually chosen the alternatives proposed for *Equus caballus*. We have introduced a few new terms to cover structures that have not been previously recognized in extant taxa or are otherwise of uncertain homology (see appendix 1).

COMPARATIVE CRANIAL MORPHOLOGY OF *TRIGONOSTYLOPS*

INTERPRETING VASCULATURE

The cranial vasculature of extinct panperissodactylans and their close relatives has long been of morphological and systematic interest (e.g., van Kampen, 1905; van der Klaauw, 1931; Simp-

son, 1933a; Patterson, 1934a, 1934b, 1936, 1937; Gabbert, 2004; Kramarz et al., 2010, 2017; Billet and Muizon, 2013; MacPhee, 2014; Billet et al., 2015; Forasiepi et al., 2015, 2016; García-López et al., 2017; Martínez et al., 2016, 2020). However, there is still much to be learned. In this section we first provide a practical guide to the vessels and vascular networks that typically leave interpretable indications of their passage on cranial bones as well as endocasts. Throughout we emphasize conditions in extant panperissodactylans—especially *Equus*—as well as other well-investigated placentals (including *Homo*, *Canis*) in order to provide a basis for interpreting SANU morphology (see also appendices 1, 2). Frequently referenced equine anatomies (e.g., Sisson and Grossman, 1953; Getty, 1975; Schummer et al., 1981; Budras et al., 2008) often do not illustrate endocranial and basicranial vasculature in a way that is useful for comparisons with fossil material. For this reason we have reproduced older illustrations from Leisering's (1888) *Atlas* and Montané and Bourdelle's (1913) detailed regional anatomy of the horse (figs. 5, 6). Although somewhat schematic, they illustrate points of interest that are less likely to be covered in more recent sources.

Knowing how something develops may help in its identification and interpretation. Relevant aspects of cranial artery development are covered in classic works (e.g., Tandler, 1899; Padget, 1948) as well as in more recent contributions listed in References (e.g., Presley, 1979; numerous papers by Wible and colleagues). Cranial veins have not been addressed to the same degree. Foundational works by Padget (1956, 1957), Butler (1957, 1967) and others mainly concern early stages of development. Missing in the literature for the most part are efforts to correlate fetal conditions in particular groups with those seen in adults—the only ontogenetic stage available for study in most paleontological contexts. This paper attempts to make a contribution to this need in the case of panperissodactylans, but much more can be done, especially with ever-improving modern imaging techniques.

TABLE 4

Endocranial measurements of scanned taxa based on 3D reconstructions

Abbreviations: **CBL**, maximum length of cerebellum; **CBW**, maximum width of cerebellum; **CRH**, maximum height of cerebrum; **CRL**, maximum length of cerebrum, excluding olfactory bulbs; **CRW**, maximum width of cerebrum; **EL**, maximum length of endocast; **EH**, maximum height of endocast; **FRW**, maximum width of frontal region of endocast; **HBH**, maximum height of hindbrain; **HPL**, maximum length of hypophysis; **HPW**, maximum transverse width of hypophysis; **NPH**, maximum neopallial height; **OBH**, maximum height of olfactory bulbs; **OBL**, maximum length of olfactory bulbs; **OBW**, maximum combined width of olfactory bulbs; **PLD**, maximum distance between ventral edges of piriform lobes. Approximate measurements are indicated in italics; missing values indicated by dash (–). Asterisk (*), estimated value based on mean of measurements of both sides, to minimize effect of distortion.

Taxon	Museum accession number	EL	EH	CRL	CRW	FRW	CRH	OBL	OBW	OBH	NPH	PLD	CBL	CBW	HBH	HPL	HPW
Trigonostylops wortmani	AMNH VP-28700	–	39.66	–	37.17	–	27.96	–	–	–	16.49	22.64	14.92	26.66	26.49	5.80	3.95
Astrapotherium magnum	MACN A-3208	150.10	114.01	95.01	89.70	67.39	76.01	19.85	50.31	35.68	40.61	79.14	39.47	73.19	79.87	13.94	10.24
Tetramerorhinus lucarius	AMNH VP-9245	85.53	43.64	45.03	46.08	28.22	37.73	14.05	20.55	13.69	16.43	22.28	24.36	23.68	35.08	7.89	3.70
Homalodotherium sp.	MPM-PV 17490	134.21	76.70	86.42	68.19	49.53	51.09	32.03	26.31	21.28	34.01	46.50	30.58	52.34	58.01	16.73	12.33
Cochilius volvens	AMNH VP-29651	47.30	21.72	26.64	27.96	19.81	14.96	7.96	12.16	5.44	7.64*	17.38	13.33	17.57	16.39	6.45	4.03
Meniscotherium chamense	AMNH VP-4412	106.89	59.38	86.63	63.47	46.19	48.03	20.26	31.69	23.45	17.45	31.76	29.21	49.51	43.54	11.82	9.88
Equus caballus	AMNH M-204155	102.65	81.51	73.61	70.81	50.02	67.15	15.72	29.24	23.45	48.33	38.55	34.53	44.81	50.24	8.53	10.54
Tapirus indicus	AMNH M-200300	110.45	89.23	76.13	79.16	64.79	65.94	14.73	53.81	33.63	54.34	57.17	23.32	48.81	63.33	13.94	9.31
Ceratotherium simum	AMNH M-51882	135.03	89.70	109.51	90.59	75.30	80.27	21.06	48.06	31.86	41.21	80.92	28.61	60.34	68.79	10.55	6.25

Although the notoungulate *Homalodotherium* is not one of our focal taxa, its vascular anatomy raises many questions of morphological interest and for that reason warrants inclusion here. Using conditions in *Homalodotherium* sp. MPM PV 17490 as a pictorial guide in figure 7, we illustrate key morphological divisions of the endocranial vascular network as defined in this paper, color-coded for ease of reference. Figures 8–10 depict selected extinct and extant panperissodactylans and their relatives in the same orientations. First or early mentions of important vessels and other structures are noted in bold type in the next section; appendix 1 should be consulted throughout for additional information.

Arteries

Although it is sometimes tacitly assumed that in basal eutherians only the vertebral/basilar arteries and the internal carotid artery were involved in transmitting blood to the circulus arteriosus, this is uncertain and probably too restrictive. Comparative anatomical studies (e.g., Daniel et al., 1953; Du Boulay and Verity, 1973; Bugge, 1974; Cartmill, 1975; MacPhee, 1981; Wible, 1984; Geisler and Luo, 1998; Fukuta et al., 2007; Wible and Shelley, 2020) reveal that there are at least five potential arterial sources for cerebral irrigation in extant mammals, which may occur in several combinations: (1) **internal carotid artery**, typically supplying the contents of the braincase and orbit; (2) branches of the **external carotid artery**, supplying the superficial parts of the face and jaw, and through retial networks and anastomoses often the cranial meninges, brain and orbit; (3) **vertebral/basilar arteries**, ventrally feeding the brain as well as contributing to the caudal portion of circulus arteriosus; and (4) **occipital arteries**, servicing the dorsum of the neck and scalp, but also the brain and meninges via anastomoses with the vertebral artery and the **arteria diploetica magna** (including annexed branch of **stapedial ramus superior**); and (5) **ascending pharyngeal artery**, variably providing blood to the pharynx, tympanic cavity, and middle cranial fossa, but occasionally also to the brain via anastomosis

with the cerebral carotid artery. In this paper we concentrate on the internal carotid artery and the arteria diploetica magna, for which reliable osteological indicia are comparatively abundant. Except for the stapedial artery and its branches, the other main channels referenced above generally leave limited evidence of their passage.

INTERNAL CAROTID ARTERY. From the standpoint of indicial interpretation, the carotid vasculature consists of two portions: the **(preendocranial) internal carotid artery** (from common carotid to final entry into endocranium) and the **(endocranial) cerebral carotid artery** (endocranial entry to participation in circulus arteriosus). Even when the preendocranial portion of the carotid involutes, the endocranial section is necessarily conserved in order to complete the circulus arteriosus. In this case the cerebral carotid's blood supply must come from other sources (see below). In the horse the right and left cerebral carotids are joined by an anastomotic branch (**intercarotid artery**; fig. 5). This last vessel is also known to be present in *Tapirus indicus* (fig. 37B; Du Boulay and Verity, 1973), but its presence in other panperissodactylans (including SANUs) has not been established.

Diagnostic indicia for the internal carotid artery have been considered difficult to recognize in SANU crania (Gabbert, 2004; Billet and Muizon, 2013; Martínez et al., 2016, 2020). However, with attention to detail the artery's functional presence can often be plausibly inferred (see p. 113, Discussion: Arterial Structures). Although it is conventional to distinguish extra- and intratympanic routings of the internal carotid artery in placentals (e.g., Gregory, 1910; MacPhee, 1981; Wible, 1984; Presley, 1993), indicia supporting this distinction can be ambiguous. Intratympanic routings that traverse the length of the petrosal promontorium, as in extant strepsirrhine primates and eulipotyphlans (MacPhee, 1981), seem to be rare in native South American ungulates and supposed examples are mostly unconfirmed or unconvincing. Presence of a shallow carotid sulcus on or near the rostral pole of the promontorium is found in some
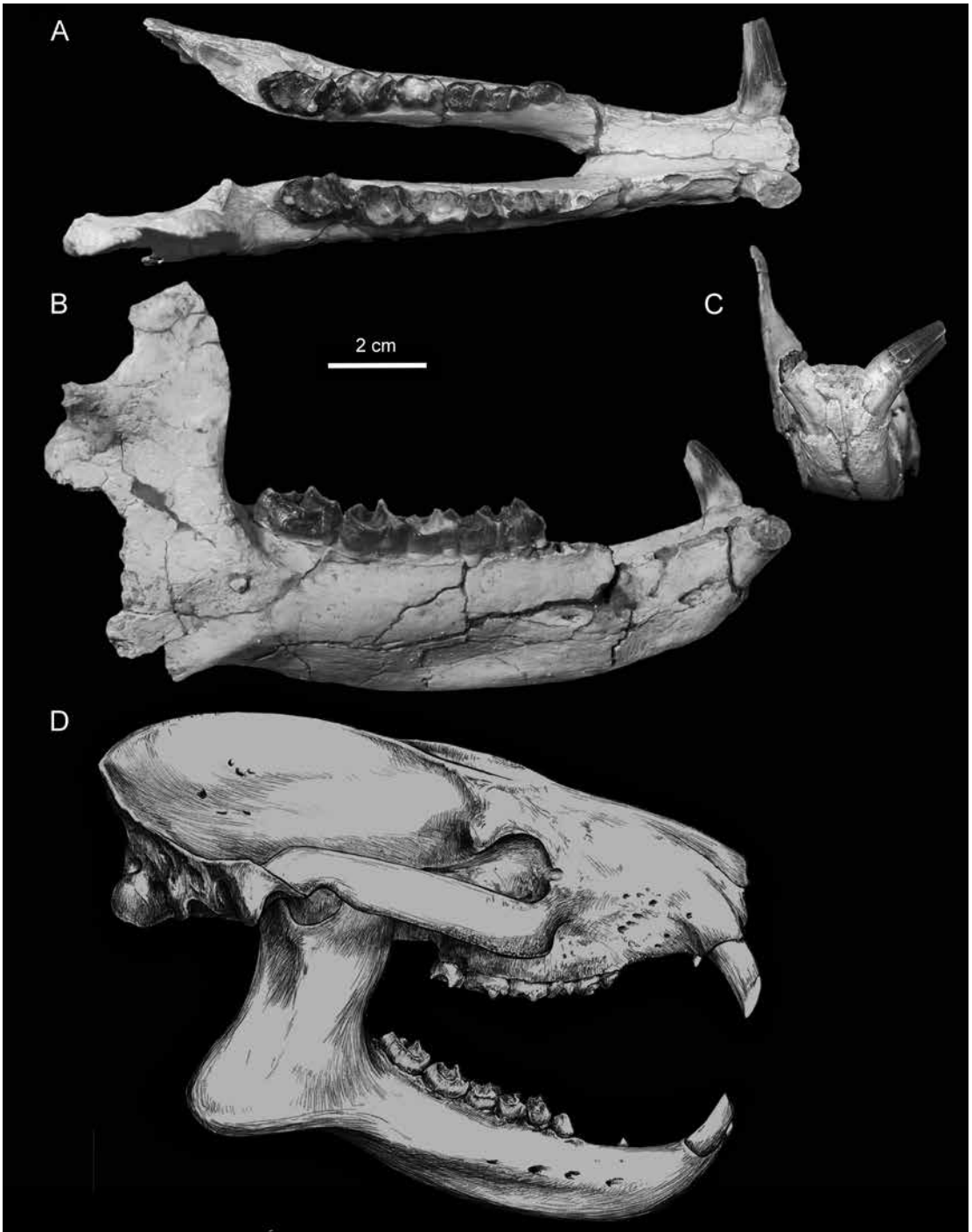
FIG. 3. *Trigonostylops wortmani*. **Top:** Mandible (MPEF PV 5483) with dentition: **A,** occlusal, **B,** rostral (mesial), and **C,** right lateral views. **D,** Reconstructed skull in right lateral aspect, chiefly based on AMNH 28700, MLP 52-X-5-98, and MPEF PV 5483.

extant perissodactylans, but whether it is meaningful to describe the routing in these cases as "intratympanic" needs reconsideration (see p. 113, Discussion: Arterial Structures). For criteria concerning the so-called transpromontorial vs. medial routings of the internal carotid artery, as well as earlier confusions regarding "medial" vs. "lateral" internal carotid arteries, not relevant here, see Presley (1979), Cartmill and MacPhee (1980), and Wible (1984, 1986).

It is reasonably certain that all extant perissodactylans possess an intact internal carotid artery in the adult stage, although dissection data are not available for all species (see Tandler, 1899; van Kampen, 1905; van der Klaauw, 1931; Cave, 1959; Wible, 1984, 1986). In *Equus*, the internal carotid artery at its origin is usually smaller than the occipital artery, with which it may share a common trunk (Tandler, 1899; Sisson and Grossman, 1953). As it passes rostrally beneath the basicranium toward the rostral or piriform portion of the basicapsular fenestra (= sphenotympanic fissure sensu Gabbert, 2004) it travels in company with the sympathetic trunk and the latter's chief cranial branch, the internal carotid nerve, bypassing the bulla and middle ear medially (fig. 5). As the artery crosses the basicapsular fenestra it characteristically bends into a half loop and crosses the carotid incisure on the trailing edge of the alisphenoid before piercing the fenestral membrane (Sisson and Grossman, 1953: 702). (Similar flexures of the internal carotid artery occur in *Equus quagga* and *Tapirus indicus* according to Du Boulay and Verity, 1973: 243.) Within the endocranium the cerebral carotid artery loops again through the cavernous sinus before anastomosing with the intercarotid artery and entering the circulus arteriosus (fig. 5).

The **pterygoid canal** is a constant feature of the mammalian skull because the autonomic nerves that it transmits conduct fibers to a number of intracranial targets (fig. 5), but its presence is not by itself an indication that the **vidian artery** (= artery of the pterygoid canal) is present (Wible, 1984, 1986). This artery appears to be absent in *Equus*; the so-called pterygoid arteries

(Sisson and Grossman, 1953: 659), which arise from the maxillary artery and feed pterygoid musculature, have a different origin and area of supply. In modern nomenclature Tandler's (1899) "canalis pterygoideus" is the **alar canal**, which transmits the maxillary artery.

EXTERNAL CAROTID ARTERY. Although the main trunks of the external carotid artery are extracranial, several of them release transcranial branches that may leave distinctive markings as they pass through or over cranial elements on their way to their targets. The most important of these is the **maxillary artery**, which in the horse travels through a fold of the guttural pouch to enter the alar canal of the alisphenoid bone. The canal opens rostrally immediately below or within the orifice of the sphenoorbital fissure; the artery then passes along a groove that conducts it along the dorsal aspect of the maxillary tuberosity, next to the medial wall of the orbit, where it travels in company with CN 5.1 and 5.2 toward the maxillary foramen. Important branches usually detectable by indicia in fossils include the **ethmoidal**, **sphenopalatine**, and **greater** and **lesser palatine arteries**. These are joined by similarly named veins and nerves to form discrete neurovascular bundles.

During the course of ontogenetic development in many extant mammals, the external carotid artery annexes vessels primordially associated with the internal carotid artery, especially the primary divisions of the **stapedial artery** (Bugge, 1974; MacPhee, 1981; Wible, 1984, 1987). Various forms of stapedial annexation can sometimes be inferred in fossil material (MacPhee and Cartmill, 1986; Diamond, 1991); however, verifiable examples of stapedial annexation in SANUs are few and covered only incidentally here. Also, although the main rostral and caudal branches of the stapedial artery are named as such in this paper, because of involution and reorganization in life these branches frequently appear as dependencies of other arteries in the adult. Thus in *Equus*, and probably all extant perissodactylans by virtue of their large body sizes, the proximal stapedial artery is absent in
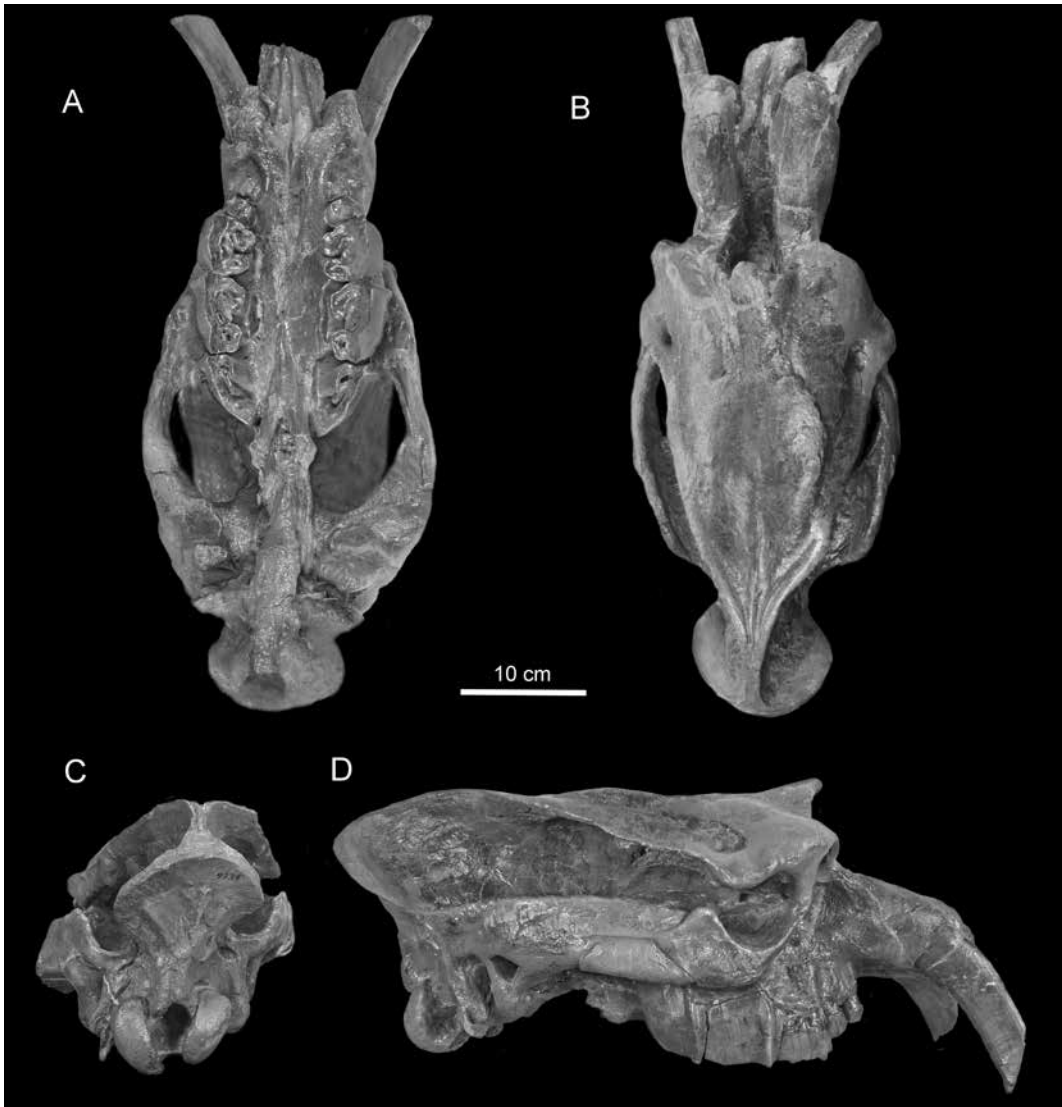
FIG. 4. *Astrapotherium magnum* AMNH VP-9278: **A,** ventral, **B,** dorsal, **C,** caudal, and **D,** right lateral views. Specimen is somewhat distorted and partly restored (see text). Apart from size, most noticeable external differences between *Astrapotherium* and *Trigonostylops* are concentrated in facial region (relative size of nasals and nasal cavity, rostral dentition, scale of pneumatization). Basicranial regions are also markedly different, but they share unusual derived features not found in non-astrapothere SANUs (see figs. 13–15, 27).

the adult, although a twig representing a segment of the stapedial ramus inferior is retained as the "arteria tympanica" (Tandler, 1899). The rostral branch of the ramus superior is represented in part by meningeal branches and a small twig attached to the ramus orbitalis, both annexed by the external carotid artery (Sisson and Gross-

man, 1953). The caudal branch is anastomotically linked to the occipital artery.

In certain euungulate taxa branches related to the external carotid artery are directly involved in cerebral irrigation. In all extant artiodactylans except tragulids (Fukuta et al., 2007; O'Brien and Bourke, 2015), the external carotid supplies the
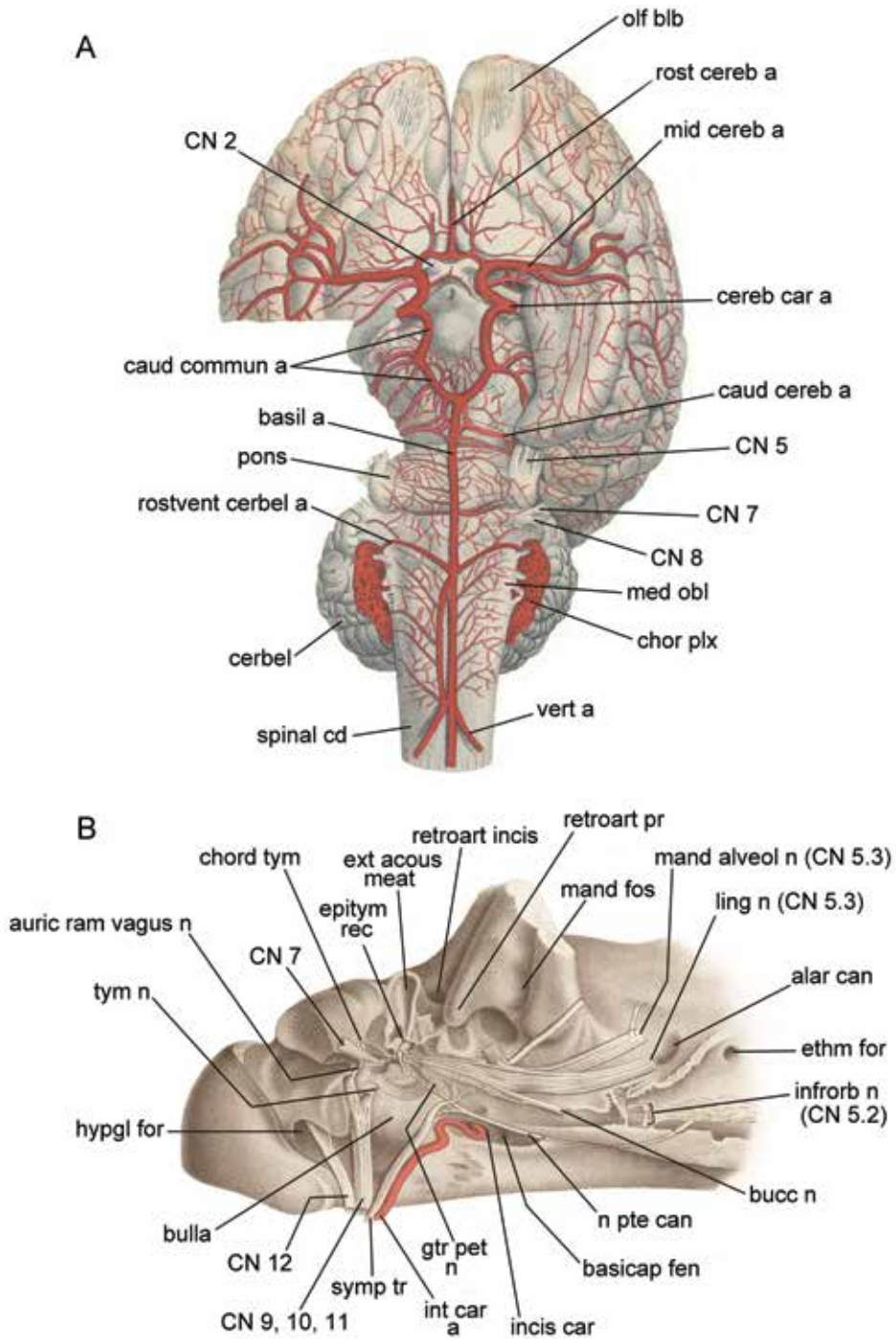
FIG. 5. *Equus caballus,* principal vasculature of brain and endocranium (on this and facing page). After Leisering (1888: pl. 30, figs. 1, 3; pl. 31, figs. 1, 2). **A,** Arterial network of brain, ventral aspect; **B,** deep dissection of right basicranium and infratemporal fossa in oblique lateral aspect, showing preendocranial course of internal carotid artery and principal nerves. **C,** deep dissection of ventral aspect of head and rostral cervicals,
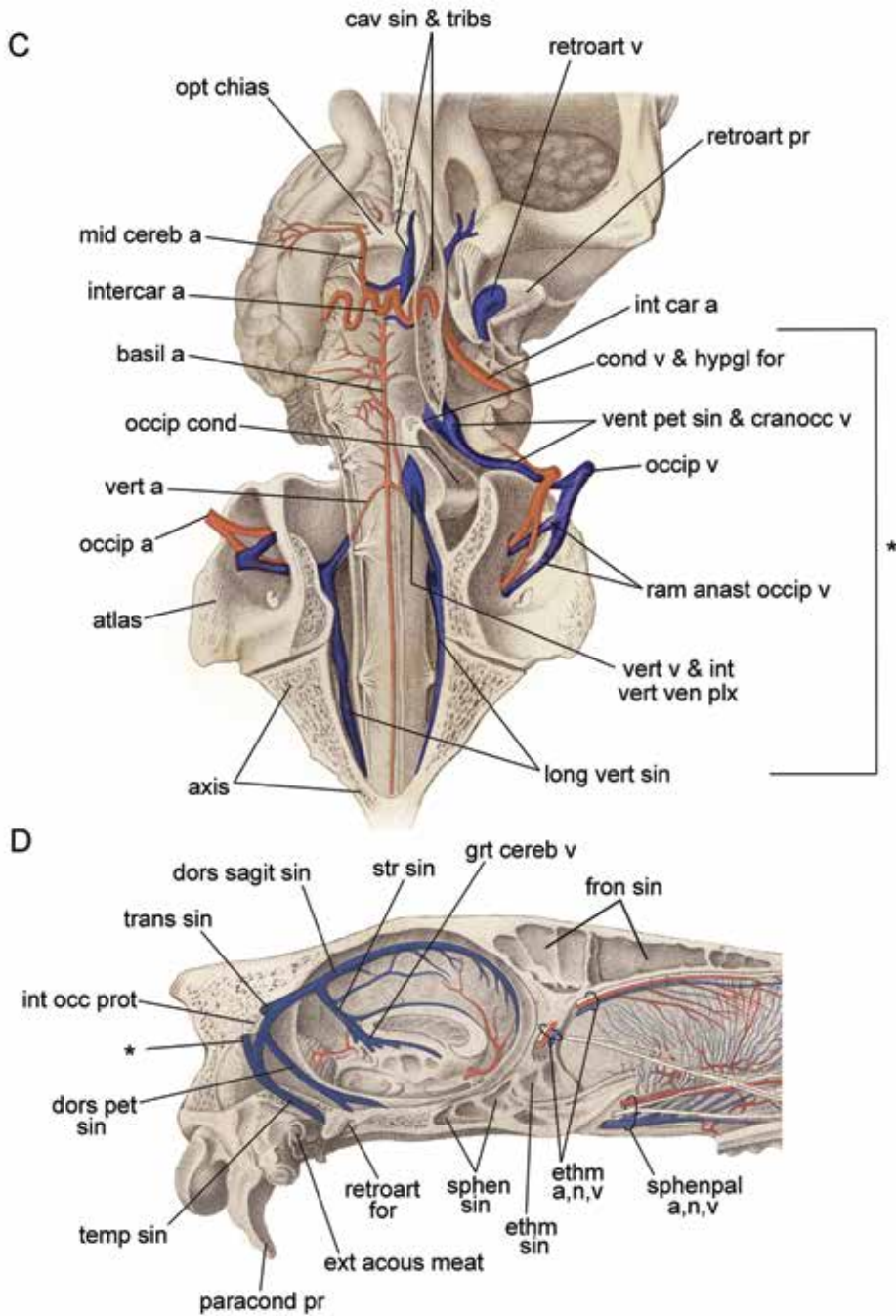
exposing brain stem, spinal cord, and vasculature of endocranium and rostral neck; and **D,** parasagittal section of skull with most of brain removed, exposing principal vessels of endocranium and caudal part of nasal cavity. In A and C basilar artery seems disproportionately small, but this conforms to dissection evidence (see Tandler, 1899: 698; Du Boulay and Verity, 1973: 238). In C, **bracket with asterisk** groups major vessels composing or contributing to cranial end of vertebral venous system (see also fig. 6A). In D, sinus communicans (**asterisk**), which links transverse sinuses, is seen emerging from its canal within supraoccipital bone.
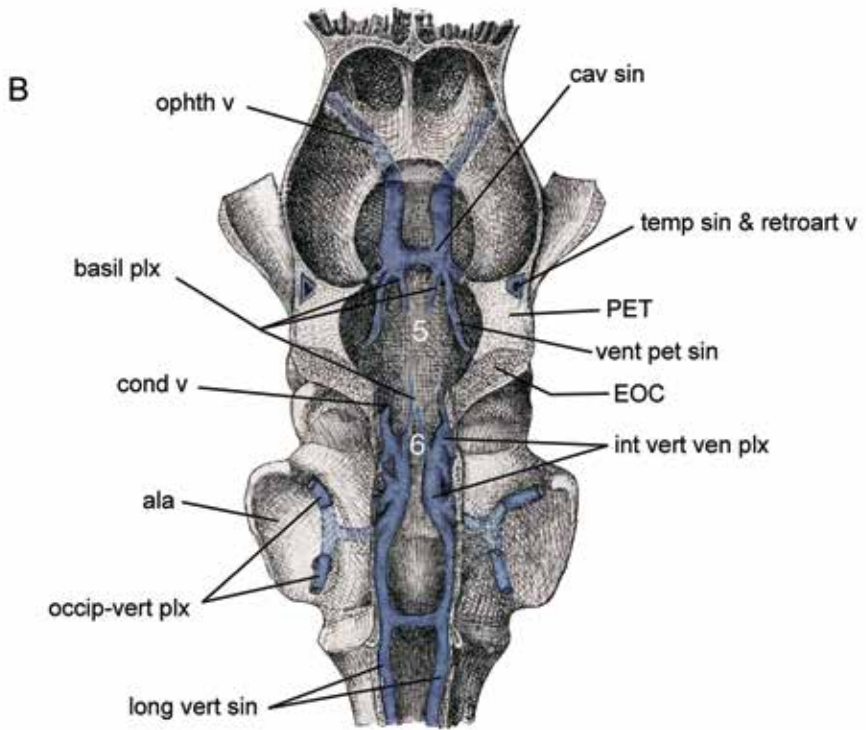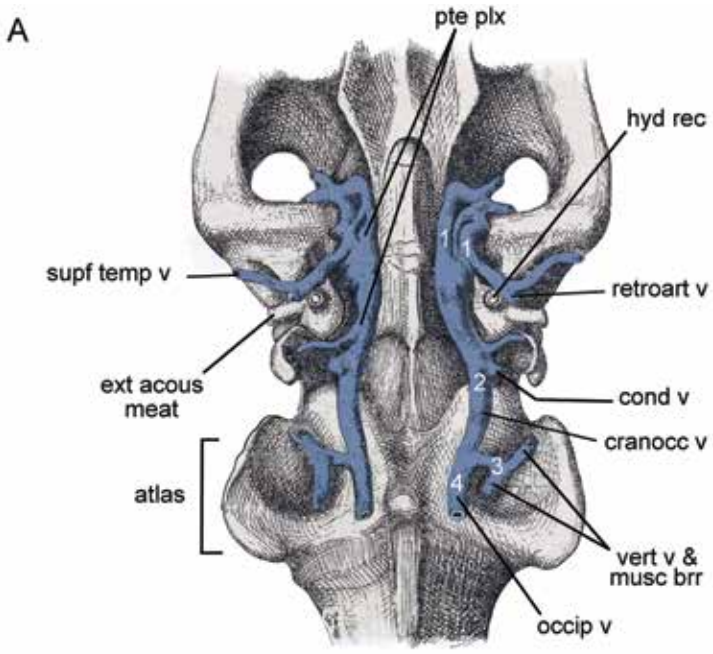
cerebral carotid and the endocranially situated **rete epidurale** by means of two transcranial links, the **arteria anastomotica** and the **ramus anastomoticus of the external carotid.** These branches enter the endocranium through, respectively, the rostral part of the basicapsular fenestra (or foramen ovale, if morphologically separate) and the sphenoorbital fissure, joining the cerebral carotid artery and the associated rete at the level of the hypophysis. In correlation with this, the internal carotid artery generally becomes a functionless thread in adult artiodactylans; more remarkably, the vertebral arteries also partly or wholly lose their functional connection with the circulus arteriosus (Tandler, 1899). Efforts to identify reliable osteological indicia in euungulates for vessels strongly associated with retial branches of the external carotid artery have to date been few (but see Geisler and Luo [1998] regarding cetaceans and O'Brien et al. [2016] regarding some other artiodactylans). While there is no express evidence for intracranial retia in basal placentals, including "condylarthrans" and early euungulates, it does not follow from this that they were necessarily absent when we do not know what to look for (see p. 113, Discussion: Arterial Structures).

The **ascending pharyngeal artery** as a dominant contributor to cerebral circulation is seen in only a few extant groups, such as various strepsirrhine primates and feliform carnivorans (Cartmill, 1975; MacPhee, 1981; Wible, 1984), but a connection with the circulus arteriosus may be more common than usually thought (e.g., Du Boulay and Verity, 1973; Du Boulay et al., 1998). However, as there is no indicial evidence for this artery's participation in cerebral irrigation in SANUs there is no reason to consider it further here.

Occipital and vertebral arteries. The occipital artery is a significant vessel in the horse, with a number of anastomotic links to other vessels in the proximal cervical region, including the vertebral arteries (Tandler, 1899; Sisson and Grossman, 1953; Du Boulay and Verity, 1973). Although the occipital artery is mainly associated with the blood supply of the muscles and other tissues of the upper back, neck and scalp, during ontogeny it plays an early and crucial role in the development of the brain and meninges (see Evans, 1912). In many mammals the meningeal role is maintained throughout life by the arteria diploetica magna, which is in effect the occipital artery's terminal endocranial branch.

The vertebral arteries originate from the subclavian and segmental arteries, pass through the lateral vertebral (= transverse) foramen of the atlas, and then enter the skull via the foramen magnum. On the ventral surface of the brain stem they coalesce to form the midline basilar artery (fig. 5A). This vessel then passes rostrally, branches from it supplying the cerebellum and pons, before it enters the caudal part of the circulus arteriosus.

Despite the foramen magnum's importance for reconstructing vascular patterns in fossil taxa, strong indicia for vasculature entering or leaving the endocranium through this aperture are rarely encountered in SANUs. *Homalodotherium* is notably different in this regard, as Patterson (1937: 292) briefly noted in his description of the endocast of FMNH P13092. In *Homalodotherium* sp. MPM PV 17490 (fig. 7C), as in Pat-

FIG. 6. *Equus caballus*, principal venous vasculature of basicranium and rostral cervical area (schematic). After Montané and Bourdelle (1913: figs. 125, 126), nomenclature updated and reinterpreted. **A,** external view, with basicranium and atlas in ventral aspect; **B,** internal view, horizontal section through endocranium and rostral cervical vertebrae in dorsal aspect. Anastomoses are complex in this region and portrayal here is simplified. On external surface of basicranium, pterygoid/pharyngeal plexuses (**1**) anastomose with rostral and caudal roots (**2, 3**) of definitive occipital vein (**4**), which continues distally and laterally to join (external) jugular vein. Rostral root is also known as craniooccipital vein, name preferred here. In B, on endocranial surface of central stem, basilar plexus (**5**) issues from cavernous sinus to join anastomotic channels connecting condylar emissary vein, ventral petrosal sinus, and sigmoid sinus. These may form one or several channels (to produce vertebral vein), which issues from foramen magnum, crosses atlantooccipital joint, and joins or becomes internal vertebral venous plexus (**6**). Inside vertebral canal of atlas, this plexus anastomoses with branches from occipital vein.

terson's specimen, a symmetrical series of shallow sulci are found on the ventral surface of the endocast, extending from the foramen magnum to a position on or near the basicapsular fenestra. There is another pair, situated more rostrally, which Patterson did not mention, that extend from the latter feature to the region of the optic chiasma. Patterson identified the caudal pair as impressions (sulci) for the vertebral arteries, an interpretation followed here. The caudal pair of impressions begin on the internal sidewalls of the foramen magnum, which is the same place that markings for vertebral veins are sometimes seen. What makes the trackways in *Homalodotherium* distinctive is that there is (1) midline convergence and ?fusion of trackways and (2) no evident connections with local dural sinuses such as the condylar and ventral petrosal sinuses.

In *Homo* and probably most placentals the vertebral arteries develop from paired longitudinal neural arteries that fuse rostrally in the embryo to form the basilar artery (Padget, 1948), but it is difficult to say from endocast evidence whether complete fusion occurred in *Homalodotherium* (fig. 7C). If it did, it was evidently for only a short distance. Note also that there is an asymmetry in MPM PV 17490, in that the impression on the specimen's left side is larger in caliber than the one on the right. Past the point of ostensible fusion, the apparent basilar impression bifurcates into features suggestive of right and left caudal cerebral arteries (i.e., caudal components of the circulus arteriosus). Rostrally, however, these indicia are interrupted and thus do not, as trackways, connect with the two more rostral sulci seen in figure 7C. These latter impressions run in a convergent course, medial to the trunks of CN 5.1 and 5.2, and terminate in the form of a small ?anastomotic bridge (fig. 7C).

Given the homological inferences made so far, it is tempting to think that these last branches represent the equivalent of rostral cerebral arteries, their morphological termini joining to form the rostral communicating artery, but this is far from certain. In *Equus* (fig. 5A), as in *Homo* and probably most placentals, the rostral communicating artery is formed in advance of the optic chiasma, whereas in the virtual endocast of MPM PV 17490 the communication between the putative rostral cerebral arteries is situated more caudally, perhaps where the tuber cinereum was located in life. Impressions for other expected vessels, such as the middle cerebral artery, are not found because they travel in the subarachnoid space. In sum, although it is reasonable to infer that these indicia represent arteries (as opposed to veins), their organization notably departs from the usual pattern expected for the arterial network at the base of the brain.

A final point of interest is that the inferred interruption between the major caudal and rostral trackways on each side occurs immediately medial to the impression for the piriform end of the basicapsular fenestra, which appears as a void in the reconstruction (fig. 7C). Although our endocast results are hard to interpret because of low resolution, it is conceivable that the internal carotid artery would have entered the endocranium through the void to merge with the circulus arteriosus. Unfortunately we found no interpretable indicia to support this inference; indeed, it is not even definite that the preendocranial part of the internal carotid existed in adult *Homalodotherium* (see below).

Although both Patterson (1937) and Simpson (1933b) reported finding evidence of endocranial arteries on natural endocasts of other taxa (e.g., *Phenacodus*), none matches *Homalodotherium* in regard to the number or extensiveness of the vessels represented. In the reconstruction of *Astrapotherium magnum* MACN A 8580 (fig. 8), ridges may be seen on the ventral aspect of the endocast in positions similar to the apparent vertebral arteries found in *Homalodotherium* sp. MPM PV 17490 (see fig. 14F). However, in this case the associated sulcus is associated with the hypoglossal canal. The prominent vascular impressions seen in *Tetramerorhinus* AMNH VP-9245 (fig. 40H: double asterisks) are quite lateral in position, do not converge in the midline, and communicate with the ventral petrosal sinuses. They are accordingly interpreted as venous channels (fig. 9: feature 6).

In specimens of both *Astrapotherium* and *Homalodotherium* the rostral or piriform portion of the basicapsular fenestra is widely open, without visible evidence of an incisura carotidis. However, in *Astrapotherium* there is a possible carotid groove on the promontorium (Kramarz et al., 2017) that is lacking in *Homalodotherium* (see p. 91, Promontorial vascular features). If the internal carotid artery was present at all in the latter taxon, it must have travelled outside the bulla-enclosed tympanic cavity (contra Patterson, 1934a, 1937; see fig. 28).

ARTERIA DIPLOETICA MAGNA. This vessel, which serves as a connector between the occipital artery with one of the end branches of the **ramus superior of the stapedial artery**, is arguably plesiomorphous at the level of Amniota (Wible, 1987). Although the presence of the arteria diploetica magna is frequently recorded for fossil material on the basis of osteological features, relatively few studies of the vessel's actual morphology or variation in extant mammals have been undertaken (but see Hyrtl, 1854; Wible, 1984, 2008, 2010, 2012; Archer 1976; Aplin, 1990; Wible and Hopson, 1995; Wible and Gaudin, 2004). This is of some importance because there are differences among extant mammals in the branching pattern and connections of this vessel (Wible and Hopson, 1995). Whereas Wible (1987: 120) defined the arteria diploetica magna as a branch of the stapedial system per se, Tandler (1899: 695), who is followed here, called this artery the "arteria occipitalis," or more specifically its "ramus mastoideus" (presumably because it serves as an anastomotic link between the occipital artery and derivatives of the stapedial ramus superior).

Typically, the artery enters the cranium by passing through the **posttemporal foramen** and **canal** (forming together the **posttemporal trackway complex**), in some cases at least with an accompanying vein termed the **vena diploetica magna**. In this paper, when reference is jointly made to the artery and vein, the expression **vasa diploetica magna** will be used (Latin, *vasum*, pl., *vasa*, "[blood] vessel"). As already mentioned, in equine anatomies the probable homolog of the arteria diploetica magna is called the **caudal meningeal artery**. When necessary for attribution or clarity we use the latter term in this paper, but its use should otherwise be avoided. To the unending confusion of students, the port by means of which the arteria diploetica magna enters the caudal cranium is called the "mastoid foramen" in equine anatomies ((Tandler, 1899; Sisson and Grossman, 1953: 651; appendix 2). This technical name should not be used at all, or placed in quotes, or (as here) reserved exclusively for the aperture of the mastoid emissary vein (see p. 119, Discussion: Venous Structures).

In the vascular reconstruction of extant *Equus* (fig. 10: features 1, i), the arteria diploetica magna is colored red because its nature is known for certain. Its assumed connection with meningeal supply via the channel here denoted as canal Y is indicated in figure 41B (see also appendix 2). In the absence of any relevant dissection evidence for extant ceratomorphs, the occupant(s) of the posttemporal foramen/sulcus are left undifferentiated, as vasa diploetica magna (fig. 10, *Ceratotherium*, *Tapirus*). This also applies to SANUs.

Sisson and Grossman (1953: 263) stated that the temporalis muscle in *Equus* is partly supplied by the caudal meningeal artery, but it is not obvious how this would be accomplished as extracranial branches have not been described for this vessel and its pathway lies ventral to the muscle's origin. However, even an incidental supply to the temporalis muscle by the arteria diploetica magna would be of interest: such an arrangement is in fact found in *Tachyglossus* and inferred for certain extinct nontherians (Wible, 1987).

Veins

Although markings for intracranial venous channels are sometimes identified in paleomammalogical descriptions, such treatments have traditionally favored arteries. This is unfortunate, because in many taxa veins may actually leave more indicia than arteries do. The problem is how to interpret them properly. Comparative and developmental information exists for some extant
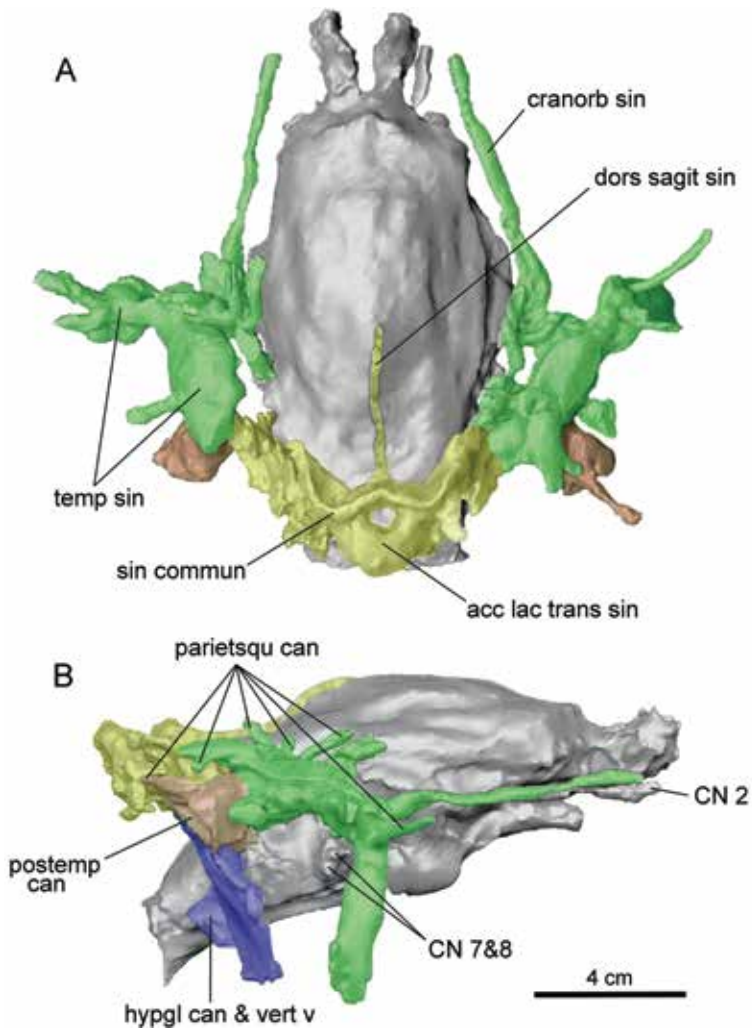
FIG. 7. *Homalodotherium* sp. MPM PV 17490, reconstructions of brain endocast and endocranial vasculature in **A,** dorsal; **B,** right lateral; **C,** ventral; and **D,** caudal views (on this and facing page). For neural features see text. Where possible, interpretations were checked against Patterson's (1937) latex endocast of *Homalodotherium segoviae* FMNH P13092. Morphological divisions of inferred dural sinuses and their connectors are color-coded to aid interpretation of similarly positioned (but uncolored) structures in figures 8-10. **Key: yellow,** dorsal sagittal sinus and transverse sinuses, including accessory lacunae of latter; **brown,** vasa diploetica magna (whether both arteria and vena diploetica magna were present is not determinable); **green,** temporal sinus and connectors (retroarticular vein, cranioorbital sinus, parietosquamosal veins); **blue,** sigmoid sinus and connectors (petrosal sinuses and condylar, vertebral, and internal jugular veins). In C, **red** indicates apparent trackways for putative rostral cerebral and vertebral arteries. **Inset,** segment at level of hypoglossal canals illustrating large sulci for inferred vertebral arteries (**white asterisks**). In this and following vascular reconstructions, CT resolution inadequate to detect separate trackways of arteries that typically accompany veins (e.g., arteria diploetica magna in posttemporal canal; meningeal arterial branches in parietosquamosal canals; cranioorbital artery accompanying cranioorbital sinus). Left side of specimen's basicranium is damaged, which accounts for incomplete reconstruction of some vessels (e.g., sigmoid sinus). Most vessels reconstructed from shallow sulci or other indicators and sizes cannot be considered dimensionally accurate. Supposed accessory vascular tissues (yellow) in extraneural space dorsal to cerebellum require further study (see text).
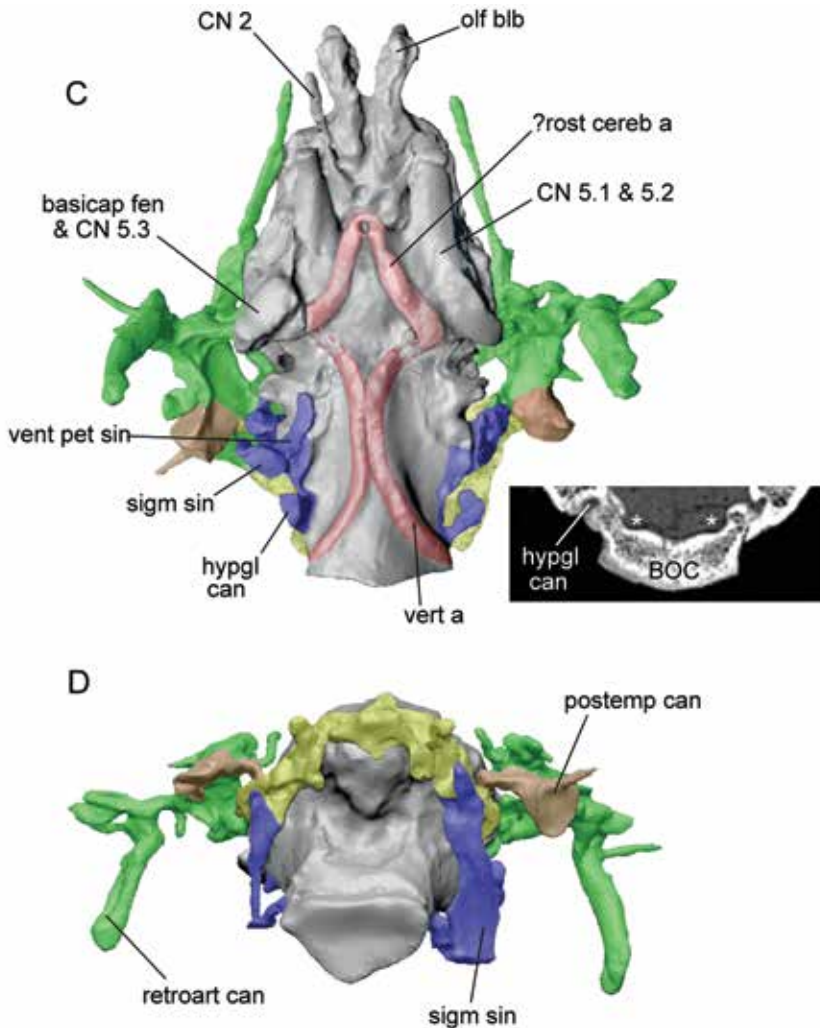
taxa, which may be helpful when making homology determinations in fossils, but most of the species for which such data exist are domesticants or other economically or experimentally significant species and thus represent only a small handful of clades. Another problem is variation: intracranial veins are valveless endothelial sacs lacking muscular tunics, which develop embryonically from extensively braided networks. In consequence their size, shape, course, and anatomical relationships can be expected to vary significantly, both within and among species. To make further headway with anatomical interpretation, high-quality digital information on venous networks in a wide variety of extant and extinct taxa is needed.

EMISSARY AND DIPLOIC VEINS. Emissary veins are valveless channels connecting intracranial dural venous sinuses with extracranial networks (Lang, 1983; Mortazavi et al., 2011; Tubbs et al., 2020). Although this description may seem to imply that emissaria are of secondary importance because they are merely connectors between large networks, in fact their distribution and development are critically important for understanding how venous systems have evolved in different clades (Butler, 1957, 1967). *NAV* lists 11 emissaria typically encountered in domesticants, but this is not a complete catalog for all of Mammalia.

Less directly relevant for present purposes are diploic veins, which resemble interconnected

endothelium-lined venous lakes within the diploe; they too are valveless and integrated with intracranial networks, and are highly variable. Hershkovitz et al. (1999) have shown that in anthropoid primates there is considerable individual variation, in which arrangements may vary from a few principal channels draining the calvarium to the much less organized so-called thousand lakes pattern. Other mammalian clades are doubtless similar.

Emissary and diploic veins are physiologically important. In *Homo*, diploic veins are thought to function in transdural drainage of cerebrospinal fluid (Tsutsumi et al., 2015), and, along with emissary veins, may also be implicated in brain cooling (Cabanac, 1996; Hershkovitz et al., 1999). Diploic veins are said to develop after birth, whereas emissary veins are laid down earlier in development (Butler, 1967), which may account for the latter's more extensive organizational role in network ontogeny. For example, mastoid and condylar emissary veins are already present by the third fetal month in *Homo*, which is probably why they are in a position to act as shunts if other parts of the dural network develop anomalously (Tubbs et al., 2020; see also p. 119, Discussion: Venous Structures). Apart from this, the great importance of emissary veins relates to the role they have been assumed to play in the evolutionary transformation or reorganization of cranial venous networks. Many of the normally small emissary veins recorded for adult *Homo* (Mortazavi et al., 2011), for example, are probable homologs of the sometimes much larger channels found in one or another mammalian clade, and knowledge of their development and relations may help in both identifying transformations and envisaging how one pattern might give rise to another. However, to support such inferences sufficient information must be collected and analyzed. As Butler (1967: 64) pointed out, although there seems to be a basic pattern of emissarial occurrence common to most mammalian embryos, it offers "no guide to the factors which determine the final pattern seen in any particular mammal. If the pattern of the mammalian head veins is to be used as a guide to phylogenetic relationships then the whole pattern must be considered and not one particular emissary vein."

It is helpful to divide dural venous sinuses of the endocranium into large **caudodorsal** and **rostroventral arrays**, comparable to the postero-superior and anteroinferior sets customarily described for *Homo* (Warwick and Williams, 1973; Tubbs et al., 2020). This introduction will be largely concerned with conditions in *Equus*, *Canis*, and *Homo* because the anatomical literature for them is abundant, and because most of the sinuses making up these arrays have obvious equivalents in other vertebrates. Known levels of dural sinus variation within humans (e.g., Lang, 1983; Moore, 1985; Curé et al., 1994) suggest that other mammals should also vary substantially, but probably they do so in generally similar ways. Although less attention will be paid to extracranial systemic veins because they leave few or no indicia on cranial elements, it is particularly important to mention how the arrays relate to the **cerebrospinal venous system** (see below). Legends for figures 5–10 provide further remarks on individual taxa.

CAUDODORSAL ARRAY. Tributaries in this array drain the brain by means of deep-lying intracerebral (ventricular) vessels and are not discussed here. The chief collector of their throughput is the **dorsal sagittal sinus** (= superior sagittal sinus) on the brain's dorsal midline. This channel connects with the **right and left transverse sinuses**, which develop from large plexuses on the caudal aspect of the developing brain (Padget, 1957; Lang, 1983; Tubbs et al., 2020) and which may persist as multiple, braided branches in the adult or resolve into single conduits. In humans and probably all mammals, one or more small midline **occipital sinuses** also link the transverse sinuses with the marginal system of veins around the foramen magnum and rostral portion of the vertebral canal. Although in *Homo* the transverse sinuses generally intersect in a crosslike arrangement (**confluence of the sinuses**, confluens sinuum), implying that blood from the dorsal sagittal sinus could be shunted either way across the midline, such an equipo-

tential configuration appears in only about two-thirds of cases (Lang, 1983). In most of the endocast reconstructions of members of the comparative set (figs. 7–10), connectivity between one or more of these sinuses appears to be lacking, but this is at least somewhat artifactual because in these cases part or all of the confluence failed to produce recoverable impressions on bone. For example, the dorsal sagittal sinus, enclosed in the dorsum of the falx cerebri, is surely always present but often fails to leave a separate trace on endocranial surfaces and is therefore not reconstructed, or is only reconstructed as far as its impression can be discerned. In adult *Equus* an endocranial impression for the confluence of the sinuses is frequently absent because the connector travels within a distinct canal, the **sinus communicans**, located in the **tentorial process** and **internal occipital protuberance** (Sisson and Grossman, 1953; Ghosal, 1975; figs. 5D, 10). Martínez et al. (2020: 17) identified this feature as a "transversal diploic communication between the temporal sinuses" in the notoungulate *Mendozahippus fierensis*, a point that requires additional discussion.

CT scanning reveals that, in at least some of the taxa described here, there is an elaborate set of enlarged intradiploic spaces associated with the transverse sinuses that extend deep into the diploe of the supraoccipital, parietal, and interparietal bones. These spaces, which we tentatively group together as **accessory lacunae of the transverse sinuses**, typically appear as a mazelike series of small channels and diverticula connected to larger networks that ultimately terminate in the transverse sinuses. They are demonstrably nonpneumatic in origin because they lack adituses and are not usually associated with areas of pneumatic activity. Accessory lacunae cannot be readily distinguished from the kinds of hematopoietic marrow spaces normally present in calvaria of mammals, which suggests that the production of red blood cells is the principal physiological function of all of them, any differences having to do only with scale. Large lacunae are negligible (at the available level of resolution) in examined

perissodactylans, but are abundantly developed in some SANUs in the comparative set, especially *Homalodotherium* (see fig. 7).

As in the case of the arteria diploetica magna, there is still much to be learned about the origin, incidence, and development of the **vena diploetica magna**. For extant species there are few direct observations relating to this vessel (but see Wible, 2010), which complicates its assessment in fossils. Based on what little relevant evidence there is, our conclusion is that it is probable, although not certain, that the SANU version of the vena diploetica magna is homologous with the mastoid emissary vein and not the occipital vein per se as in xenarthrans (see p. 119, Discussion: Venous Structures). Although the large size of the posttemporal trackway complex in SANUs may indicate that both members of the vasa diploetica magna were present, this cannot be demonstrated in our segmental data (figs. 7–9) and therefore should not be simply assumed.

In SANUs the intracranial **posttemporal sulcus** is typically short, terminating more or less immediately in grooves transmitting the transverse/temporal sinuses. In several of the reconstructions in figures 7–9, sinus junctions dorsal to the petrosal apex are marked by a conspicuous expansion or dilatation of the trackway. Both Simpson (1933b, 1936) and Patterson (1937) briefly remarked on this feature, Simpson (1933b: 12) even wondering whether the very large impression he saw on the endocast of a specimen of *Notostylops* was a preservational artifact of some sort. Patterson (1937) illustrated, but did not describe, dilatations of his "postero-lateral venous sinus" (= posttemporal + transverse trackways) in several taxa, including *Rhynchippus equinus* FMNH P13410 and *Leontinia gaudryi* FMNH P13285. More recently, Martínez et al. (2020: fig. 9B) have provided a dramatic example of dilatation in the related leontiniid *Gualta cuyana* MCNAM-PV 3951. Other impressive examples can be seen on the endocasts of *Astrapotherium magnum* MACN A 8580 (fig. 8) and FMNH P14259. "Bulbous expansions" have been detected in *Homo* at positions where certain dural sinuses
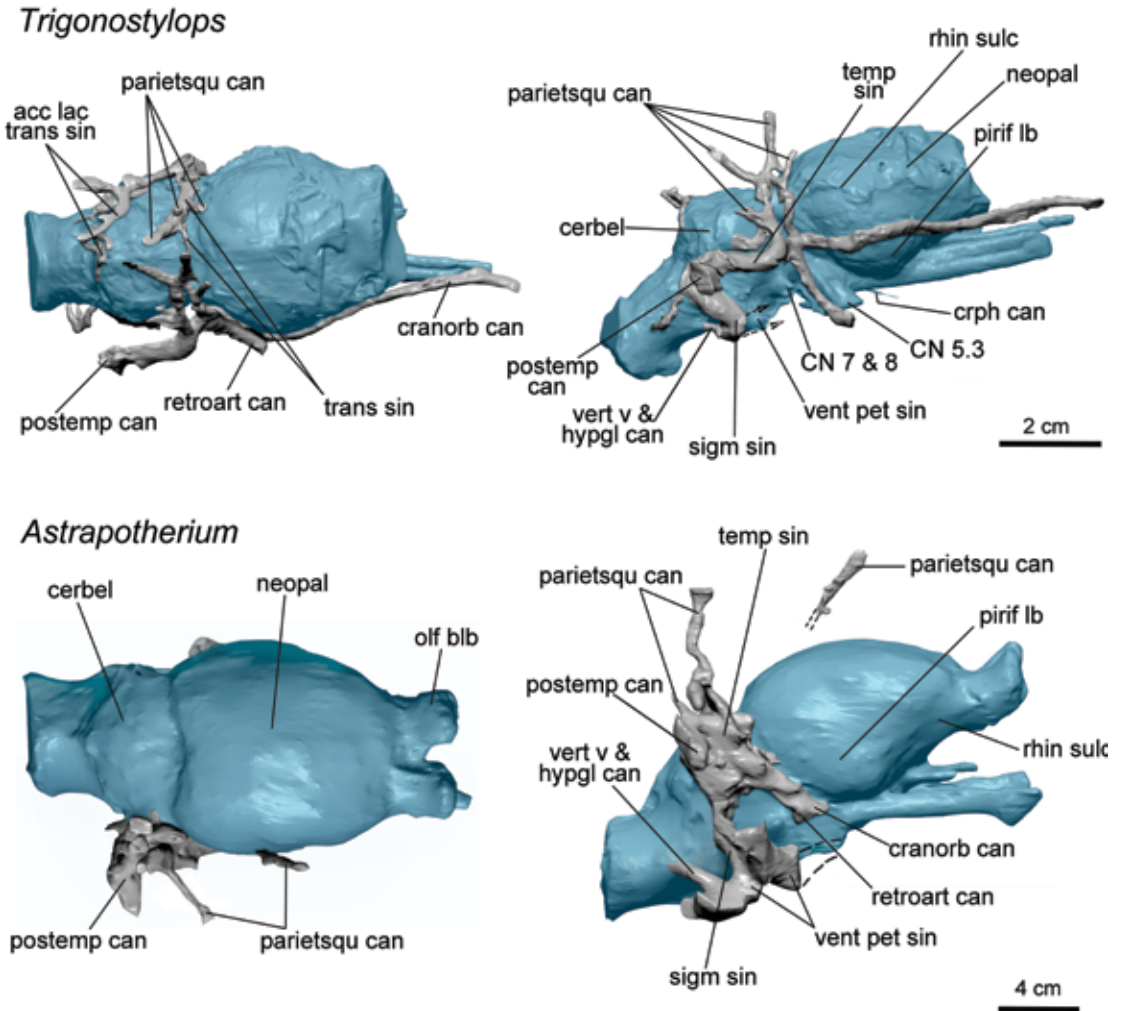
FIG. 8. *Trigonostylops wortmani* AMNH VP-28700 and *Astrapotherium magnum* MACN A 8580, reconstructions of brain endocast and endocranial vasculature in dorsal, right lateral, ventral, and caudal views (on this and facing page). Olfactory portion of brain mostly missing in *Trigonostylops* specimen; ventral petrosal sinus areas damaged in both. For neural features, see text. **Top row:** In vascular organization *Trigonostylops* resembles *Meniscotherium* and *Tetramerorhinus* (fig. 9) more than highly derived *Astrapotherium*. Despite unusual position in this taxon, hypoglossal canal communicates with sulcus for vertebral vein as in other SANUs. Small connector between transverse sinuses, possibly morphological equivalent of sinus communicans, was probably accompanied by other channels that left no impressions. Number and distribution of parietosquamosal canals is also noteworthy. Feature (**single black asterisk** in ventral view) seen on hindbrain/spinal cord is vascular, not neural, and composed of segmental vessels of uncertain homology. They drain from interior of occipital condyles toward endocast surface, and are therefore presumably tributary to vertebral venous system. **Bottom row:** Because of damage and scale of pneumatization, several expected channels, including
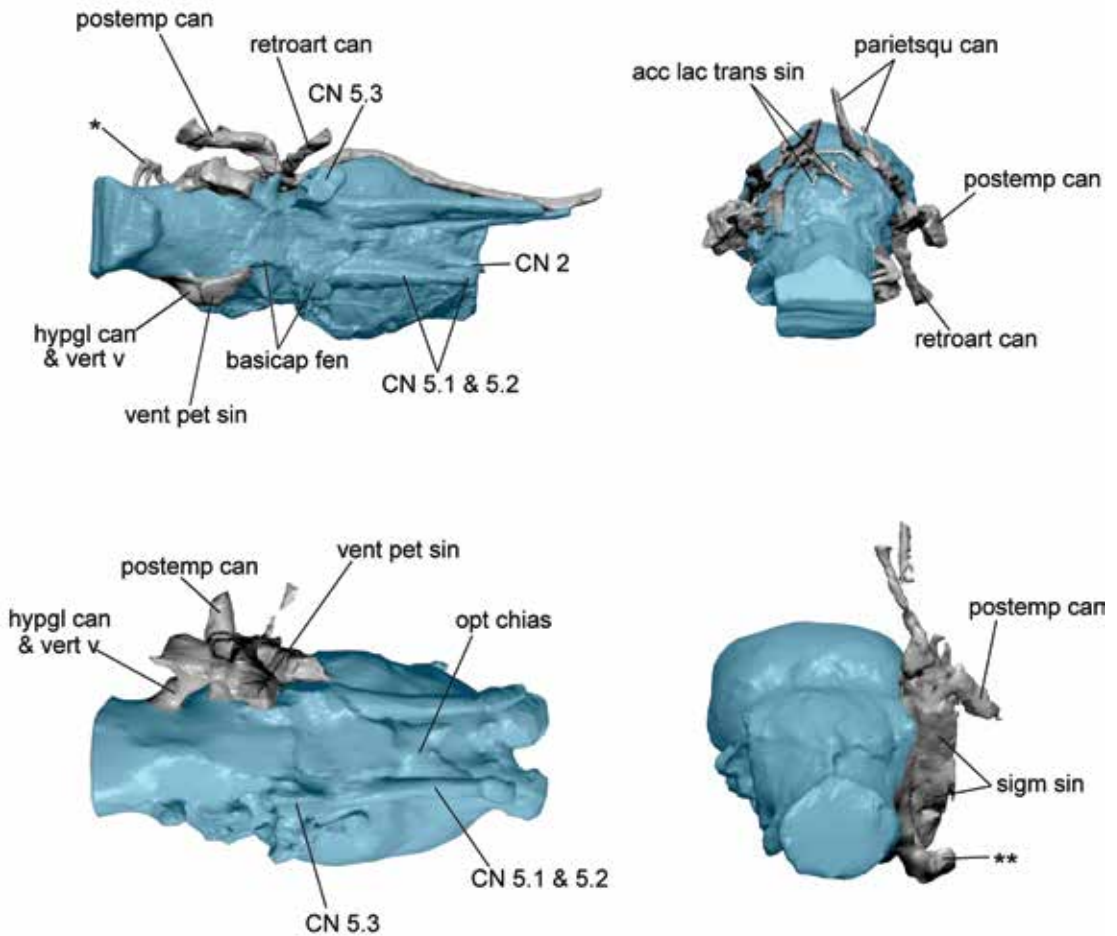
retroarticular vein and cranioorbital sinus, could not be continuously followed in specimen of *Astrapotherium*. Stumps representing these vessels are suggested on rostral end of temporal sinus. Great size of ventral petrosal and sigmoid sinuses implies commensurately large internal jugular vein (suggested by **double black asterisks** in caudal view), although as usual this vein's presence is difficult to independently verify from endocast evidence. Reconstruction of remaining part of ventral petrosal sinus follows contours of large fossa associated with jugular area. Similar fossa exists in *Parastrapotherium* sp. FMNH P13505, a fragmentary basicranium. Although faint ridges on ventral aspect of *Astrapotherium* endocast are in positions similar to possible vertebral artery impressions seen in *Homalodotherium* (fig. 7), a more intact specimen will be needed to clarify their nature. Although doubtless present in life, definite impressions for dorsal sagittal sinus and transverse sinuses were not found. Posttemporal, temporal, and sigmoid impressions form a single large dilatated mass dorsal to petrosal, with no distinct internal boundaries. Exceptional lengths of dorsalmost parietosquamosal canals reflect massive pneumatization of cranial roof (see figs. 13, 14).

meet (Lang, 1983: 106), suggesting that they may serve a cisternlike function for blood passing bidirectionally along valveless networks in correlation with the position of the head. This makes sense because intracranial venous development and function is characterized by frequent reversals in the direction of flow, not only in smaller vessels but even in major channels (Padget, 1956, 1957). The size of these dilatations in members of the comparative set is perhaps also correlated with the number of channels to which the transverse sinuses were connected (i.e., posttemporal, parietosquamosal, and temporal canals).

In most mammals each transverse sinus terminates by furcating into a rostral branch, the **temporal sinus**, which continues forward within a sulcus or bony canal, and a caudal branch, the **sigmoid sinus**, which passes around the caudal border of the petrosal to end morphologically in the jugular area. It is seemingly never enclosed in a canal. The temporal sinus is normally present in mammalian development and is often retained as a functional conduit in the adult (Diamond, 1992; figs. 7–9). In many taxa it terminates in (or as) the **retroarticular emissary vein** (= capsuloparietal emissary vein), which empties into the superficial temporal vein of the external jugular system (or equivalent) after passing out of the **retroarticular foramen** (= postglenoid foramen). Also, the temporal sinus may retain part or all of its original orbital connection, continuing across the endocranial aspect of the squamosal, parietal, and alisphenoid as the separately named **cranioorbital sinus** (= petrosquamous sinus).

Accompanying this sinus is the cranioorbital artery (retained portion of rostral branch of stapedial ramus superior), either as part of the proximal stapedial system if intact or as an annexed twig of another vessel (see Wible, 1987). Cranioorbital vessels normally release small meningeal branches within the middle cranial fossa, although these are rarely resolvable on low-resolution virtual endocasts unless very well preserved.

Relative to landmarks on the neopallium, the position of this sinus in SANUs varies from comparatively high, at or just below the level of the rhinal sulcus, to much lower, along the ventrolateral surface of the piriform lobe. Bearing in mind that these sinuses develop from plexiform networks, such differences as there are do not affect homology, although character states are a different matter. Cranioorbital channels to the orbit are not usually present as such in adult *Homo*, as the temporal sinus and unannexed parts of the rostral branch of the stapedial ramus superior normally involute more or less completely (Butler, 1957, 1967; Diamond, 1992; Marsot-Dupuch et al., 2001). Extant perissodactylans display some differences: the cranioorbital sulcus is absent or highly reduced in specimens of *Equus* (Vitums, 1979) and *Ceratotherium*, but present and large in *Tapirus* (fig. 10: feature 9).

Conroy (1982) linked the loss of the cranioorbital sinus in anthropoid evolution to the overgrowth of the cerebellum by the neopallium, correlating with the displacement of the transverse sinus from a more vertical orientation characteristic of the embryo to a more horizontal position. This led to regression of the cranioorbital sinus, with the sigmoid becoming the dominant discharge pathway for the transverse sinus. In mammals in which the neopallium does not cover the cerebellum, conditions typical of dural drainage in the embryo are retained, as is the cranioorbital sinus. This scenario does not, however, explain differences among extant perissodactylans, which display similar degrees of neopallial development but variability in the functional retention of the cranioorbital sinus.

The sigmoid sinus and internal jugular vein are also significantly variable, which has implications for endocast interpretation. In the specimen of *Equus* illustrated in figure 10 there is no osteological indication of the sigmoid sinus in the usual place, i.e., along the caudal border of the endocranial surface of the petrosal and associated petroexoccipital suture. In this instance absence is unsurprising, because in *Equus* a large vein homologous with the internal jugular vein of *Homo* (i.e., a large, direct continuation of the sigmoid sinus draining to the subclavian/innominate veins) is usually said either to be not present or

reduced to a thread (e.g., Ellenberger and Baum, 1894: 339ff.; Bradley, 1923: 2; Sisson and Grossman, 1953: 696; Vitums, 1979; Schummer et al., 1981: 217; but see *NAV* Angiologia, fn. 97). In equine anatomies the only named "jugular vein" is situated on the external body wall, where it drains most of the external aspect of the head and upper neck and thus does the job of the external jugular + facial vein of *Homo*. Martínez et al. (2016) were not able to discriminate with certainty the sigmoid sinus in *Rhynchippus*, although they did not consider whether it might have been functionally absent. By contrast, in *Tetramerorhinus* AMNH VP-9245 (figs. 9, 40H; appendix 2) the sulcus for the sigmoid sinus is very well marked, consistent with presence of a large internal jugular vein. *Cochilius volvens* AMNH VP-29651 (figs. 9, 16, 18) presents an intermediate condition in which the sulcus for the sigmoid sinus/internal jugular is identifiable but seems rather small in comparison with the size of the canal for the retroarticular vein, indicating perhaps that the caudal vessels had a reduced role in endocranial drainage. Obviously, these estimates are essentially impressionistic, but they make the point that one should not automatically assume that venous return through the internal jugular vein is always predominant in a given taxon.

In many mammals the caudodorsal array also plays a role in the vascular circulation of the dorsum of the head, via **parietosquamosal veins** (= rami temporales), which mostly drain to the temporal and related sinuses. Parietosquamosal canals probably carried arteries as well as veins in SANUs, as documented for various extant mammals (chiropterans, primates, eulipotyphlans, xenarthrans; Cartmill and MacPhee, 1980; Wible, 2008, 2010), although in our scanned material separate trackways could not be distinguished (but see Martínez et al., 2016: fig. 9). In the paleontological literature parietosquamosal channels are usually given scant attention and their function remains physiologically obscure. There are none in *Homo*, unless some veins usually counted as diploic veins (parietal diploic vein, occipital diploic vein) are counted as such, which is plausible (see Tubbs et al., 2020). All SANUs that we have investigated, as well as all living perissodactylans, possess at least some foramina in positions typical for parietosquamosal vessels (figs. 7–10). Horses and rhinos may exhibit only one or two such apertures, tapirs frequently more. SANUs display similar variability (e.g., *Cochilius*, fig. 9; see also numerous illustrations in Lydekker, 1893; Sinclair, 1909; Scott, 1910, 1912). Because these foramina open directly into the area of origin of the temporalis, it is reasonable to infer that the parietosquamosal vasculature supplied both the muscle and related tissues.

In the horse, one aperture on the sidewall of the neurocranium is much larger than the others, and is distinguished in equine anatomies as the **temporal meatus** (figs. 10, 39A, 40A). It is situated on the caudoventral margin of the parietal and opens directly from the temporal sulcus/canal, close to the latter's union with the short sulcus for the transverse sinus, and obviously gives passage to a large vessel. The meatus may go under other names in other taxa (e.g., ?subsquamosal foramen), but rather than viewing it as a novel opening on the skull's sidewall we regard it as an aperture for an enlarged parietosquamosal vein, here tentatively called the **vein of the temporal meatus**, as it bears the same relationship to the temporal sinus as do parietosquamosal veins in other panperissodactylans (see also appendix 1). The vein of the temporal meatus joins the superficial temporal vein according to Bradley (1923: 144), as does the more rostrally located retroarticular vein. There is no reported dissection evidence that these veins are closely accompanied by an artery.

In light of the foregoing, highly derived conditions of the temporal sinus in pachyrukhine hegetotheres may be briefly noted. The dorsal midcranial hiatus described for *Paedotherium* by MacPhee (2014) is situated in the same area as the temporal meatus of *Equus*, but it is relatively much larger. It is not clear how much of the hiatus would have been devoted to transmitting vasculature as opposed to facilitating klinocrany (cranial flexion) in this taxon.
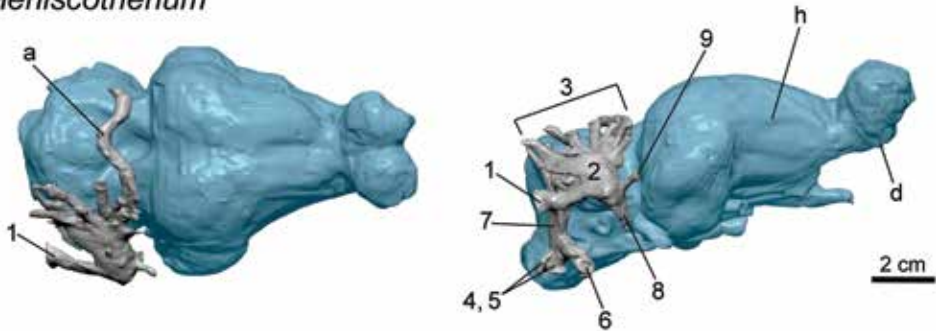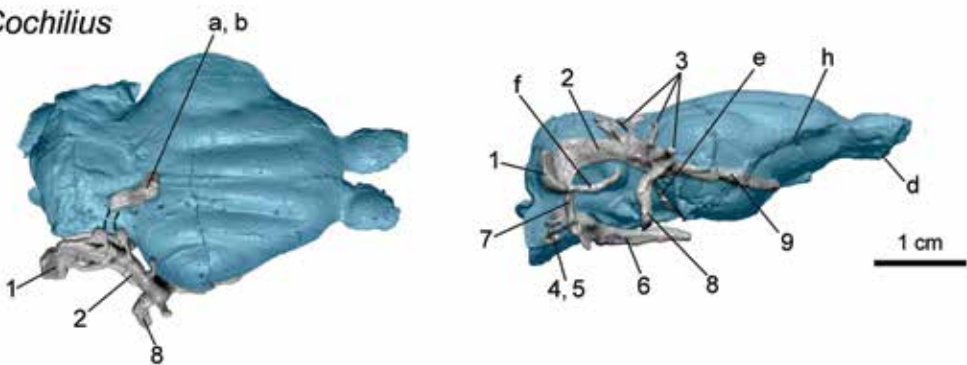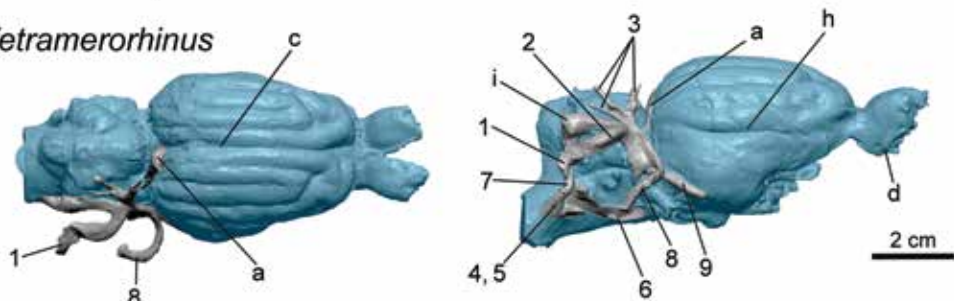
FIG. 9. *Meniscotherium chamense* AMNH VP-4412, *Cochilius volvens* AMNH VP-29651, and *Tetramerorhinus lucarius* AMNH VP-9245, reconstructions of brain endocast and endocranial vasculature in dorsal, right lateral, ventral, and caudal views (on this and facing page). For neural features, see text. **Key: 1,** posttemporal sulcus/canal (for vasa diploetica magna); **2,** temporal sulcus/canal (for temporal sinus); **3,** parietosquamosal canals (for parietosquamosal vessels); **4,** hypoglossal canal (for condylar emissary vein); **5,** sulcus for vertebral vein; **6,** sulcus for ventral petrosal sinus (may include part of cavernous sinus); **7,** sulcus for sigmoid sinus (may include proximal internal jugular vein); **8,** retroarticular sulcus/canal (for retroarticular emissary vein); **9,** cranioorbital sulcus/canal (for cranioorbital sinus); **a,** sulcus for transverse sinus or sinus communicans; **b,** accessory lacunae of transverse sinus (few in number, not reconstructed in detail); **c,** sulcus for dorsal sagittal sinus; **d,** ethmoidal canal (for ethmoidal neurovascular bundle); **e,** ?dorsal petrosal sinus; **f,** petromastoid canaliculus (for parafloccular vein); **g,** transclival
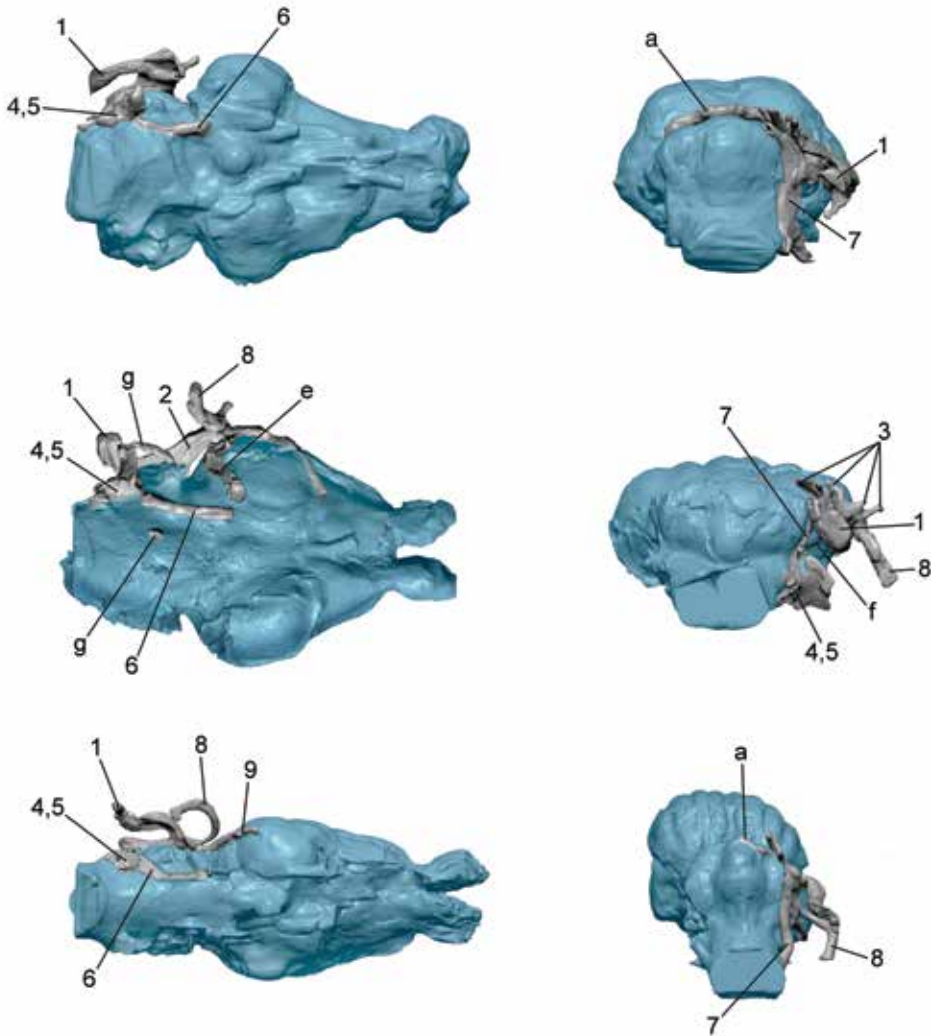
foramen (contents uncertain but probably related to vertebral venous system); **h,** rhinal sulcus; and **i,** sinus dilatation. In these specimens, impressions for transverse sinuses and dorsal sagittal sinus were few or absent. Accessory lacunae of transverse sinuses not reconstructed, although small channels are visible in transverse sections of illustrated *Cochilius* (fig. 17). Vascularization of dorsal surface of head via parietosquamosal canals (feature 3) seems to have been extensive in SANUs, in contrast to extant perissodactylans (fig. 10). Sulcus for cranioorbital sinus (feature 9), present in *Cochilius* and *Tetramerorhinus*, but could not be certainly identified in *Meniscotherium chamense* AMNH VP-4412; small channel emerging from temporal canal is interrupted by damage and could not be traced further (but see Orliac et al., 2012). In *Cochilius*, large endocranial channel (feature e) lies immediately rostral to auditory region between temporal canal and foramen ovale. In *Rhynchippus equinus*, Patterson (1937) identified an "anterior periotic sinus" with same relations, homology uncertain.

Small plexiform veins abound in the cerebellar region, but they rarely leave distinct impressions on endocasts and have not been uniformly reconstructed for the comparative set. The entirely endocranial **petromastoid canaliculus** for the parafloccular vein, which drains parts of the pars canalicularis to the transverse sinus, is evident in some of the vascular reconstructions (e.g., *Cochilius*, fig. 9). Its exit aperture, which in *Homo* may also carry a small artery (Lang, 1983: 386), is usually located within the confines of the subarcuate fossa.

ROSTROVENTRAL ARRAY. This portion of the mammalian cerebral venous system may be minimally defined as including the **cavernous, intercavernous**, **ventral petrosal**, **dorsal petrosal,** and **sphenoparietal sinuses**, plus the **middle meningeal, basilar**, and various **basicranial emissary veins**. The last-named pass through apertures located in the rostral and medial sides of the auditory region (i.e., hypoglossal canal and basicapsular fenestra or its subdivisions, including, where formed, the rostral carotid, ovale/spinosum, and jugular foramina). The dorsal petrosal sinus is normally a link between the two arrays, as it runs from the trasverse/temporal sinus to the cavernous sinus over the dorsal aspect of the petrosal. In *Homo* and probably most mammals the cavernous sinus is involved in the drainage of the eye and its adnexa, rostral part of the brain, meninges, and floor of the skull (Moore, 1985). In the horse this sinus communicates with the pterygoid/pharyngeal plexuses via emissaries passing through the basicapsular fenestra (Montané and Bourdelle, 1913; Sisson and Grossman, 1953), but indicative features are often wanting. Unfortunately, this applies to most of the named sinuses in the rostroventral array, which generally do not leave strong or well-bounded impressions on endocasts, and their portrayal in figures 7–10 should not be regarded as definitive (see also Martínez et al., 2020: 21–22).

A point of some morphological interest, because it concerns an extant panperissodactylan, is whether the caudodorsal and rostroventral dural venous arrays directly communicate in *Equus* via the dorsal petrosal sinus. According to

Vitums (1979) the developmental evidence suggests that they do not—a surprising finding. This is a difficult point to check in fossils. The dorsal petrosal sinus is enfolded within the tentorium cerebelli where the latter attaches to the dorsal rim of the petrosal, and it leaves few exclusive markings in this area (Oyanagi et al., 2020).

CEREBROSPINAL VENOUS SYSTEM. Although it is often tacitly assumed in the paleontological literature that the internal jugular is always a dominant channel for endocranial venous return in therians, this is incorrect as already noted (for further discussion see MacPhee, 1994; Wible and Rougier, 2000; Forasiepi et al., 2019). There is another caudal pathway for returning blood to the heart, the **cerebrospinal venous system**, which has been extensively studied in *Homo* and a few experimental mammals (see Arnautovic et al., 1997; Nathoo et al., 2011, and references cited therein). Like other parts of the body's total venous network, the components of the cerebrospinal system have many points of overlap (anastomosis) with other systems to ensure redundancy and uninterrupted blood flow. The cerebral component consists of the superficial and deep veins of the brain and endocranium (i.e., the dural sinuses and cerebral veins). The vertebral component consists of the **vertebral veins** and associated plexuses (see appendix 1), which are mainly extracranial but are anastomotically linked to various endocranial vessels (see below). The azygos vein ultimately receives most of the blood drained by the vertebral venous plexuses; it terminates in the rostral vena cava, as does (separately) the jugular system. The two systems meet anastomotically at multiple locations, the number and size of connections varying among species (e.g., Davis, 1964; Evans and de Lahunta, 2013).

In *Equus* the cavernous sinuses are linked, via emissaries, to a complicated series of plexuses lying beneath the skull base. Montané and Bourdelle (1913: 251) depict this network (termed by them the *confluent sous-sphénoïdal*) as significantly extensive, with tributaries arriving from the orbit, infratemporal region, retroarticular foramen, and basicranial apertures, the whole eventually terminating in the occipital and vertebral veins (fig. 6).

The portion of *NAV* Angiologia devoted to *Equus* does not specifically deal with these channels, evidently subsuming them under the general heading of the pterygoid plexus (plexus pterygoideus), which includes the pharyngeal veins/plexus. These vessels drain other head structures in addition to the brain, the network as a whole forming the **basicranial plexuses** of this paper. This is different from the situation in *Homo* (Warwick and Williams, 1973), in which the pterygoid plexus drains (via the plexiform maxillary vein) to the facial and (extracranial) retroarticular veins, with little or no direct communication with the occipital vein (see p. 119, Discussion: Venous Structures). Aplin (1990) provides useful dissection-based comparative notes on these understudied vascular features, mainly but not exclusively in Australian marsupials.

In conformity with a suggestion made by Sisson and Grossman (1953: 697, fn.) we use the term **craniooccipital vein** to refer to the end member of the pterygoid/pharyngeal plexuses, which anastomoses with the occipital vein as depicted in figure 6. This usage is preferred to "ventral cerebral vein," found in older equine anatomies (e.g., Ellenberger and Baum, 1908: 744) and often conflated with or poorly distinguished from the ventral petrosal (dural) sinus. (True vena cerebri ventrales recognized by *NAV* Angiologia, which are solely endocranial and drain the ventral parts of the brain to the cavernous and transverse sinuses, are not discussed here.)

The anatomy of the cerebrospinal venous system has been extensively studied in *Canis* (Evans and Christensen, 1979: figs. 12-8; Evans and de Lahunta, 2013). Much as in the horse, an extensive set of basicranial plexuses extend from the palatine and pharyngeal regions to the foramen magnum in the dog, draining caudally toward the craniocervical junction. The plexuses converge on a caudally directed channel, also as in the horse, but identified in *Canis* as the "internal jugular vein" because it receives a tributary (regarded as the v. emissaria jugularis) from the ventral petrosal sinus/sigmoid sinus via the jugular foramen. The course of this vessel does not conform to that of the internal jugular vein of *Homo* but resembles instead that of the craniooccipital vein, as characterized here, in crossing below the craniocervical junction to join the vertebral venous plexuses. Evans and Christensen (1979: 761) also recognize a "vertebral vein" that runs ventrally between the jugular area (where it anastomoses with the internal jugular vein) and the transverse foramen of the atlas; it does not enter the foramen magnum. Its route closely conforms to the rostral root of the occipital vein described for *Equus* (see fig. 6: feature 4).

A version of the craniooccipital vein, or at least one its tributaries, may even exist in *Homo* in the form of the inferior petrooccipital vein. This small vessel, which links the cavernous sinus with the internal jugular, is buried within the petrobasioccipital suture (i.e., the fully "closed" basicapsular fenestra seen in all crown primates), where it is separated from the overlying inferior petrosal sinus by a "thin plate of bone" according to Tubbs et al. (2014: 698). As these authors concluded, this primarily extracranial vessel cannot be the same as the ventral petrosal sinus, and should be considered an independent emissary vein. To cite another primate example, in the lorisiform primate *Galago* a relatively much larger version of the petrooccipital vein forms a complicated rete mirabile involving the ascending pharyngeal artery (MacPhee, 1981: 114), producing yet another variation on the basicranial plexus theme.

These facts suggest that the basicranial portion of the cerebrospinal venous system exists, and is similarly organized, in several distantly related placentals, which presumably has implications for its antiquity as well as its ontogeny. Similar networks are known in marsupials but are little investigated (but see Aplin, 1990). From the standpoint of function, multiple anastomotic links between the occipital, vertebral, and other systemic veins on the one hand, and the sigmoid sinus, ventral petrosal sinus, and basicranial emissary veins on the other, are surely important in the regulation of intracranial blood pressure in mammals generally (cf. Arnautovic et al., 1997).
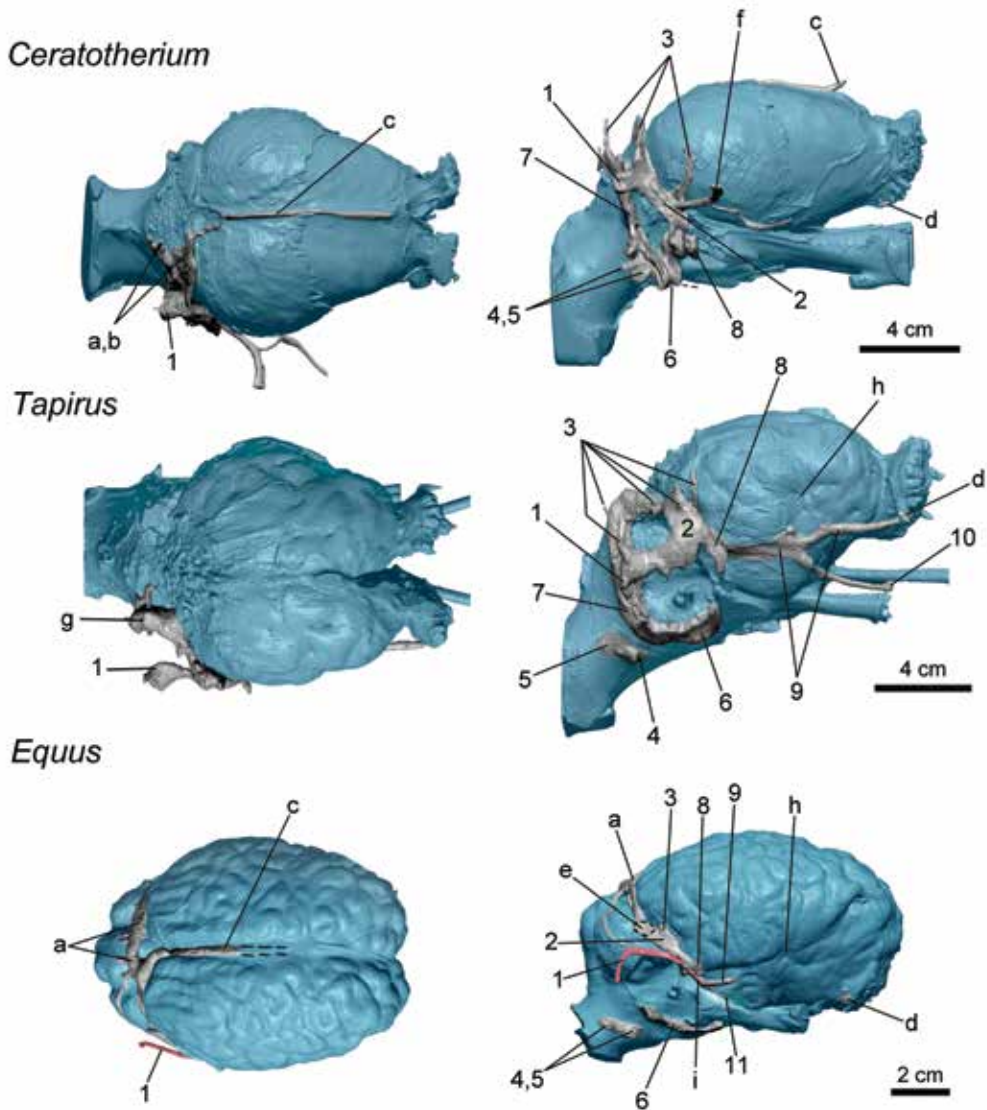
FIG. 10. *Ceratotherium simum* AMNH M-51882, *Tapirus indicus* AMNH M-200300, and *Equus caballus* AMNH M-204155, reconstructions of endocranial vasculature in dorsal, right lateral, ventral, and caudal views (on this and facing page). Specimens of *C. simum* and *E. caballus* are juveniles. For neural features, see text. As in previous figures in this series, vascular-related features are uniformly colored (**gray**), with exception of arteria diploetica magna (= caudal meningeal artery) (**red**) in *Equus* only. Posttemporal track-way contents in other taxa are grouped nonspecifically as vasa diploetica magna. See text. **Key: 1,** post-temporal sulcus/canal (for vasa diploetica magna); **2,** temporal sulcus/canal (for temporal sinus); **3,** parietosquamosal sulcus/canal (for parietosquamosal vessels); **4,** hypoglossal canal (for condylar emissary vein); **5,** sulcus for vertebral vein; **6,** sulcus for ventral petrosal sinus (may include part of cavernous sinus); **7,** sulcus for sigmoid sinus (may include proximal internal jugular vein); **8,** retroarticular sulcus/canal (for retroarticular emissary vein); **9,** cranioorbital sulcus/canal (for cranioorbital vessels); **10,** sulcus for ?oph-thalmic vein; **11,** sulcus for ?caudal rhinencephalic vein; **a,** sulcus for transverse sinus or sinus communi-

cans; **b,** sulci for accessory lacunae of transverse sinus; **c,** sulcus for dorsal sagittal sinus; **d,** ethmoidal canal (for ethmoidal neurovascular bundle); **e,** temporal meatus and vein (for *Equus* only; dashed outline of meatus suggests vessel size); **f,** foramen dorsal to external acoustic meatus (for ?suprameatal vein; *Ceratotherium* only); **g,** sinus dilatation; **h,** rhinal sulcus (not identifiable in *Ceratotherium simum* AMNH M-51882); and **i,** cranioorbital artery (dashed line, *Equus* only). In *Ceratotherium* and *Tapirus* there are several parietosquamosal canals, but *Equus* typically exhibits few or none (unless temporal meatus qualifies as such). After releasing retroarticular vein, temporal sinus ends in a short extension that cannot be traced further in *Equus* AMNH M-204155, but in hemisected skull of *E. asinus* AMNH M-20414 a groove for cranioorbital vasculature ends on floor of middle cranial fossa (see also related petrosal features in same specimen in fig. 41). Cerebellar (dorsal occipital) veins (**asterisk**) were reconstructed for *Equus* but not for other taxa. Possible caudal rhinencephalic vein in *Equus* (feature 11) is prominent during development but not in adult (Vitums, 1979).
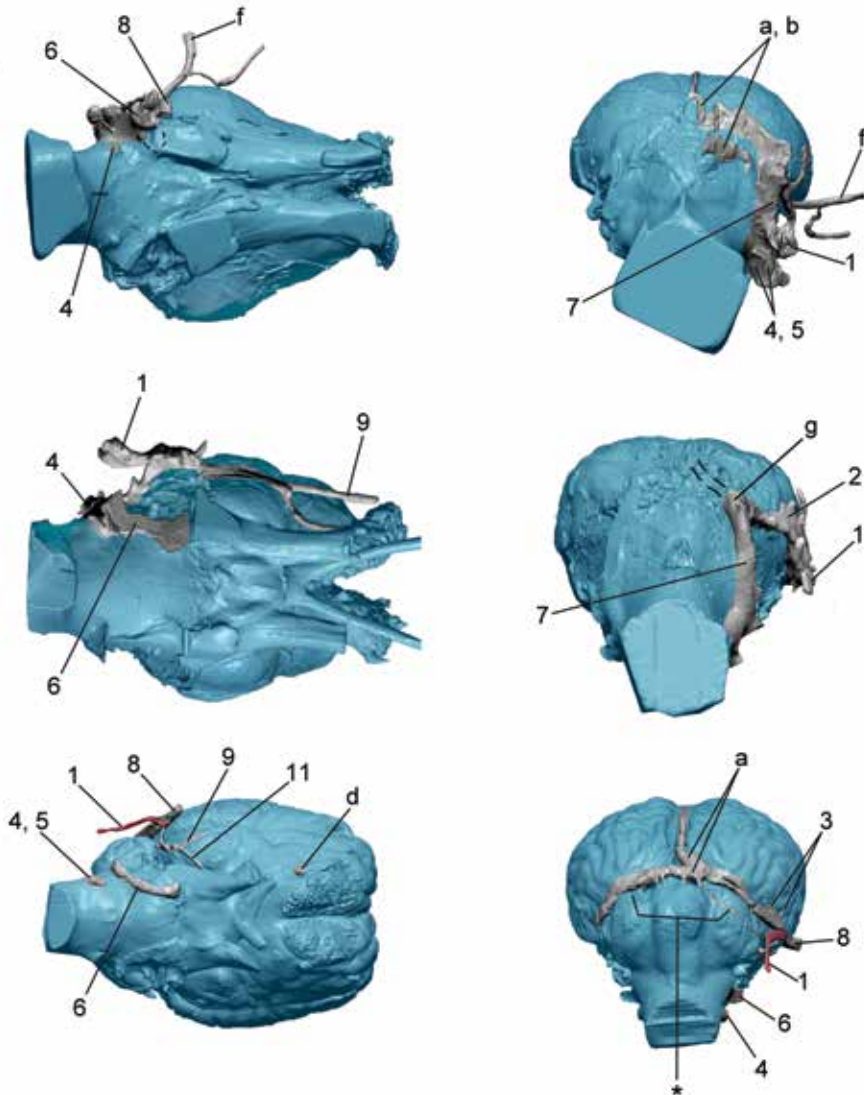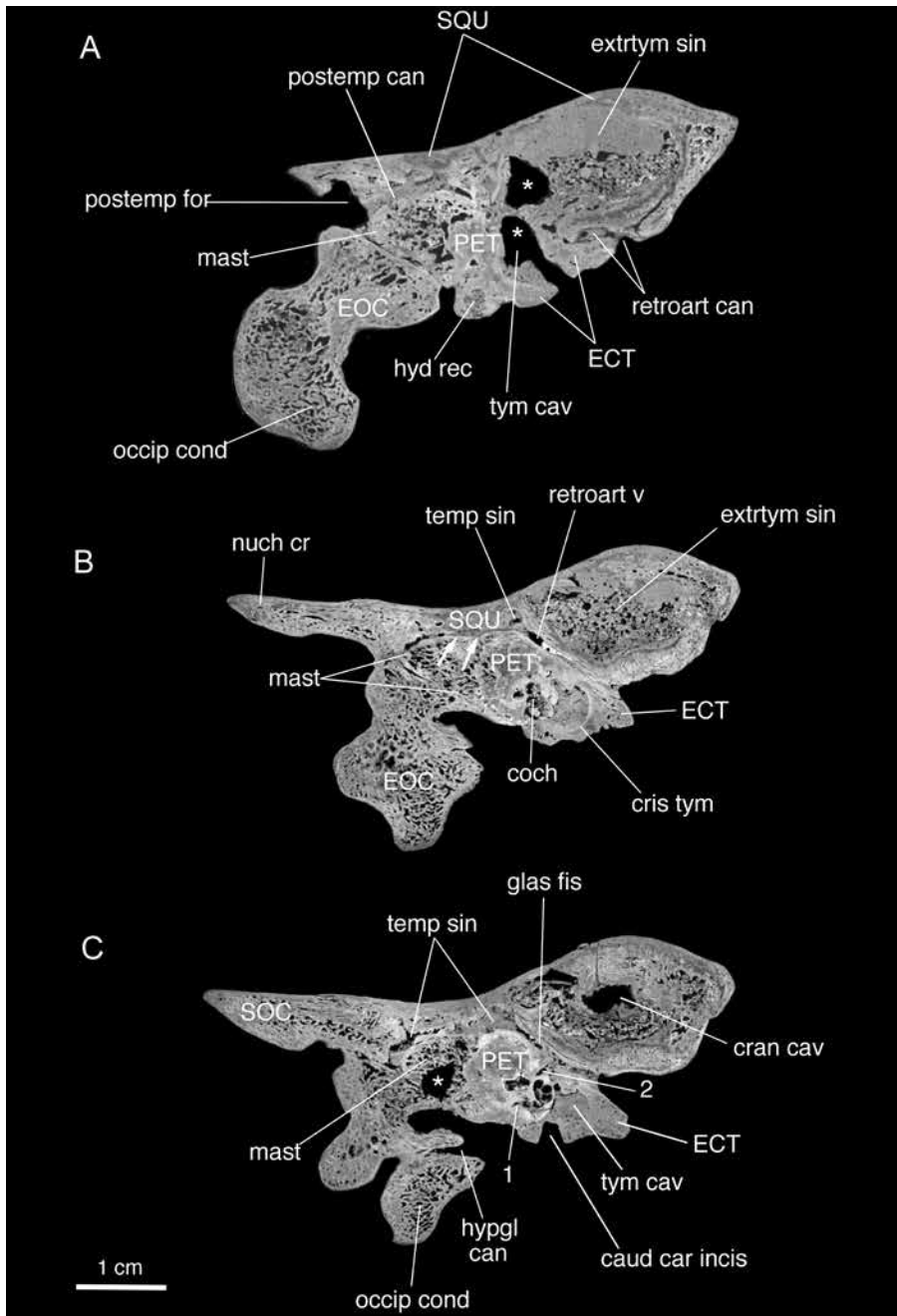
FIG. 11. *Trigonostylops wortmani* AMNH VP-28700, parasagittal segments through left side of caudal cranium, sequence lateral to medial. In **A,** note preparation artifacts (gaps in matrix) in tympanic cavity and aditus of extratympanic sinus (**asterisks**); in **B,** distinct crista tympanica, track of retroarticular vein departing temporal sinus, and area of petrosal-squamosal fusion (arrows); in **C,** hypoglossal canal in rear wall of basicapsular fenestra, notch in ectotympanic for carotid artery, and cranial cavity exposed by preparation in endocranial wall of extratympanic sinus. **Key: 1,** aqueductus cochleae; **2,** cavum supracochleare.

Interpreting Pneumatization

Ontogeny of Cranial Pneumatization

Caudal cranial pneumatization in placentals can vary from negligible (e.g., oryzorictine tenrecs; MacPhee, 1981) to massive (e.g., heteromyid rodents; Webster, 1975), for phylogenetic (heritage) as well as functional reasons. In some cases the ontogeny and position of such spaces may have systematic significance (e.g., MacPhee and Cartmill, 1986; Rossie, 2006), which makes their detailed exploration in SANUs of interest here. Significant cranial pneumatization is found in representatives of all major SANU clades for which adequate material exists, but there are important intertaxon differences and questions of homology that merit extended commentary.

As usually conceived, cranial pneumatization is the consequence of nasopharyngeal (including otic) mucous epithelium inducing the formation of continuous air spaces in cranial elements, largely through the tightly programmed production and destruction of bone on opposing surfaces during ontogeny (Rossie, 2006; Zollikofer and Weissmann, 2008; Anthwal and Thompson, 2016). In regard to what actually happens at the level of cellular processes, the phrase "spatial translation" (Aplin, 1990) of bone surfaces is perhaps preferable to the more metaphorical term "pneumatization." However, the latter name is readily understood as a covering term for a specific form of remodeling and its consequences. How pneumatization occurs at the level of cellular signal transduction is not well understood (Anthwal and Thompson, 2016).

Cranial bones typically affected by the remodeling activity induced by nasopharyngeal epithelium are the ethmoid, maxilla, frontal, presphenoid, alisphenoid, basisphenoid, and pterygoid, to greatly varying degrees in different species. Spaces originating along this pathway are classed as **paranasal sinuses**. Other bones affected by the same cellular processes, but in these cases involving the epithelial mucosal linings of the auditory tube and middle ear (thus producing **paratympanic sinuses**), include the
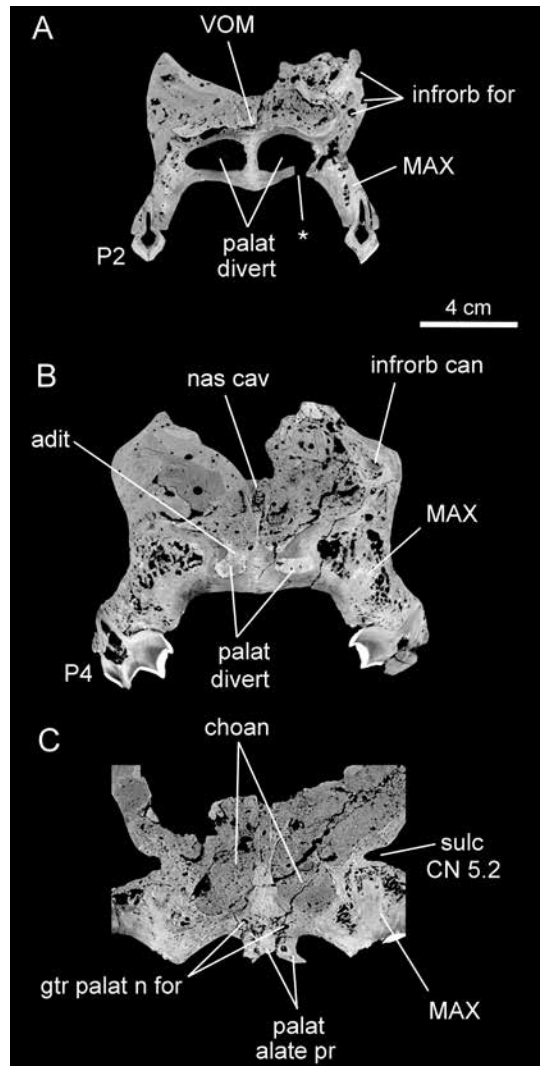
FIG. 12. *Trigonostylops wortmani* AMNH VP-28700, transverse segments through skull (on this and following two pages) in rostrocaudal sequence and at different scales. In **A–C,** note artificial entrance (**asterisk**) into right palatal diverticulum (filled with matrix in B), aditus of palatal diverticulum opening into nasal cavity, and palatal alate process (left side broken). In **D–G,** note frontal sinus in sagittal crest, matrix-filled extratympanic sinus occupying lateral sidewall of skull, and preparation artefacts (**asterisks**) occupying original positions of tympanic cavity and rostral carotid foramen. In **H–L,** note artificially widened aditus of extratympanic sinus, reconstructed position of tympanic membrane (**double-**
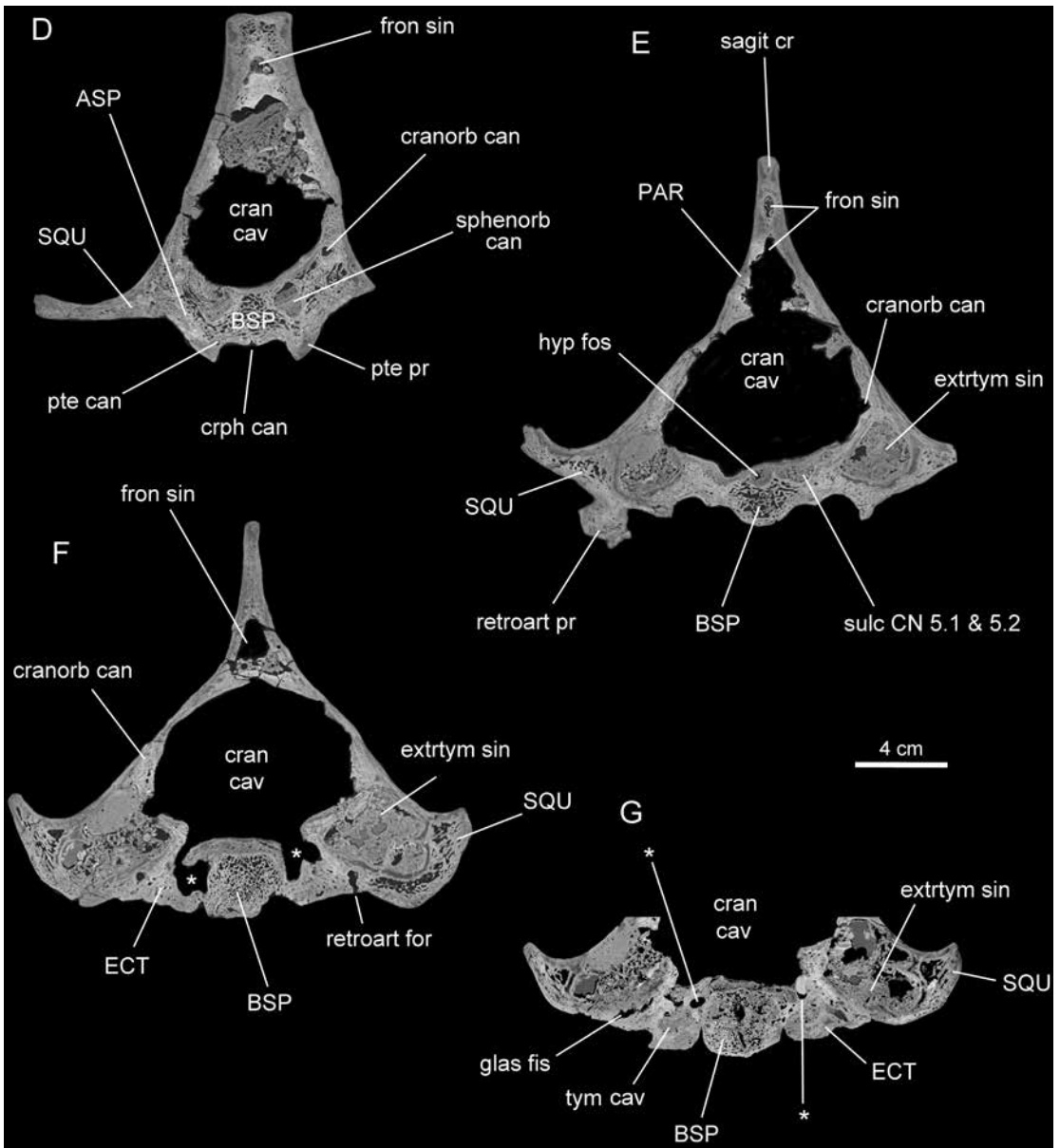
headed arrow, **asterisk**), and lambdoidal process of petrosal. In all segments, matrix or mineral sinter covers most internal surfaces as well as basicapsular fenestra (only partly cleaned). In A and B (right side), small canals leading to infraorbital foramina presumably emanate from main infraorbital canal. In J, in addition to obvious fine bone spicules, lighter-colored material within hyoid recess is matrix.
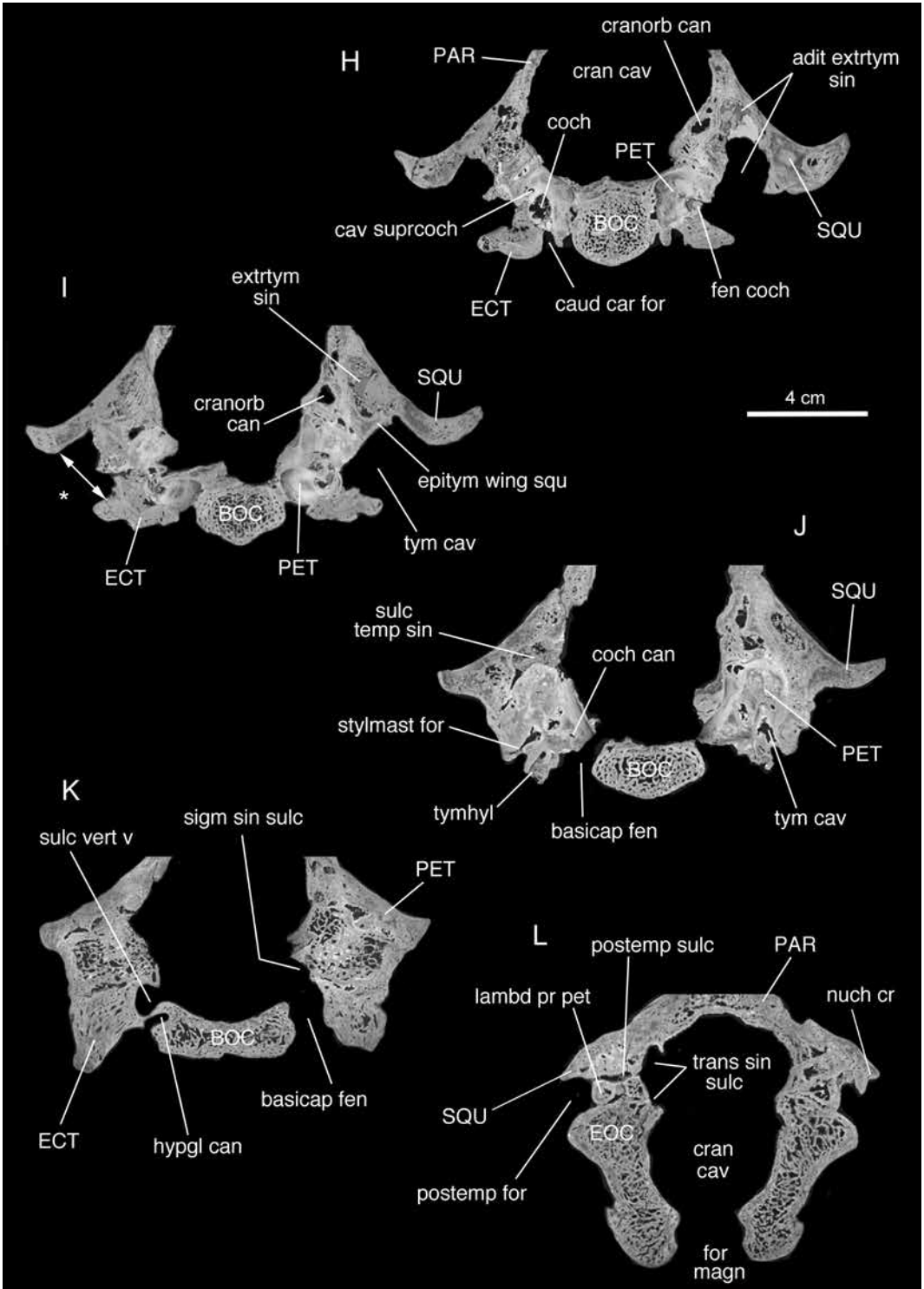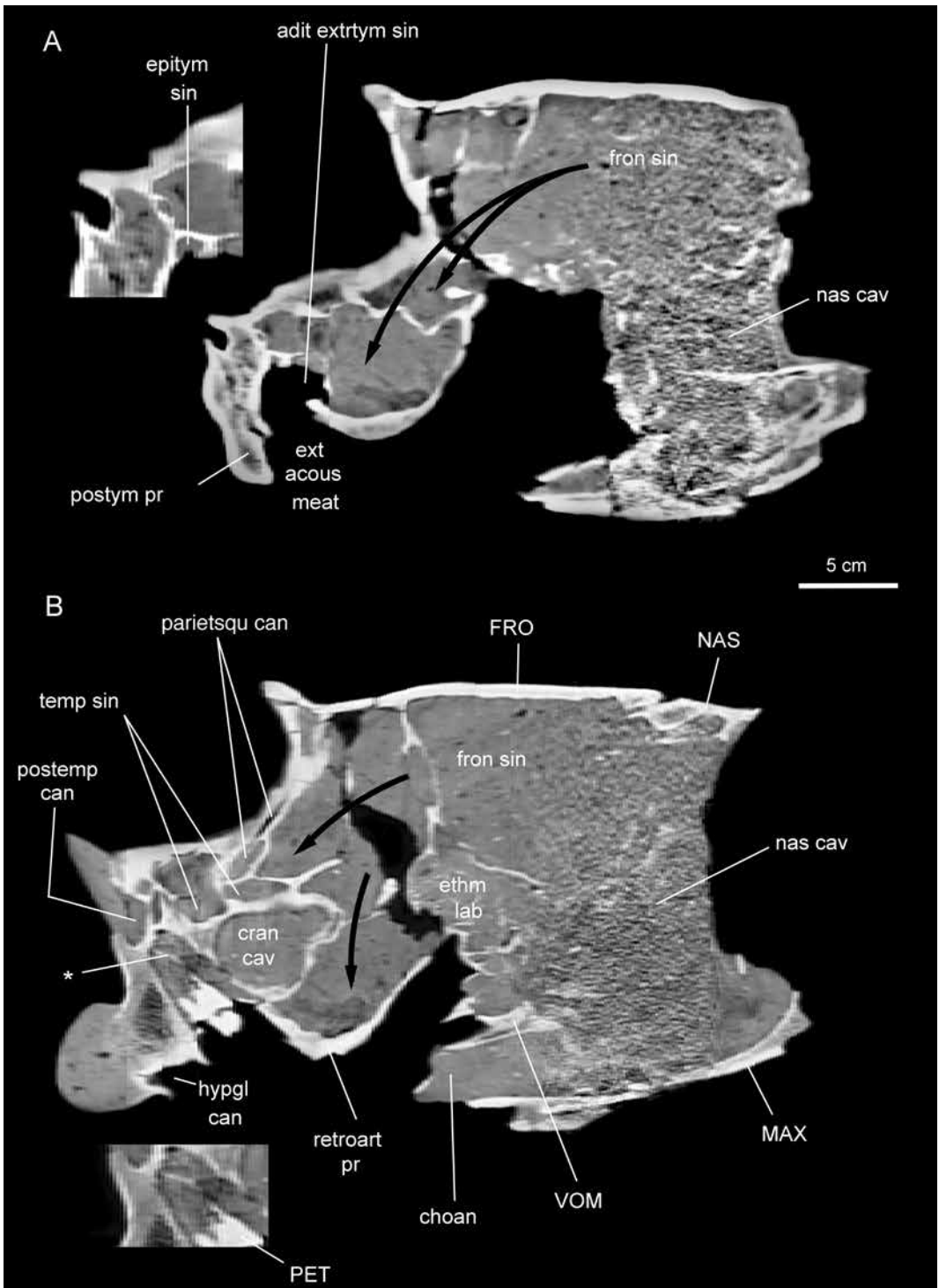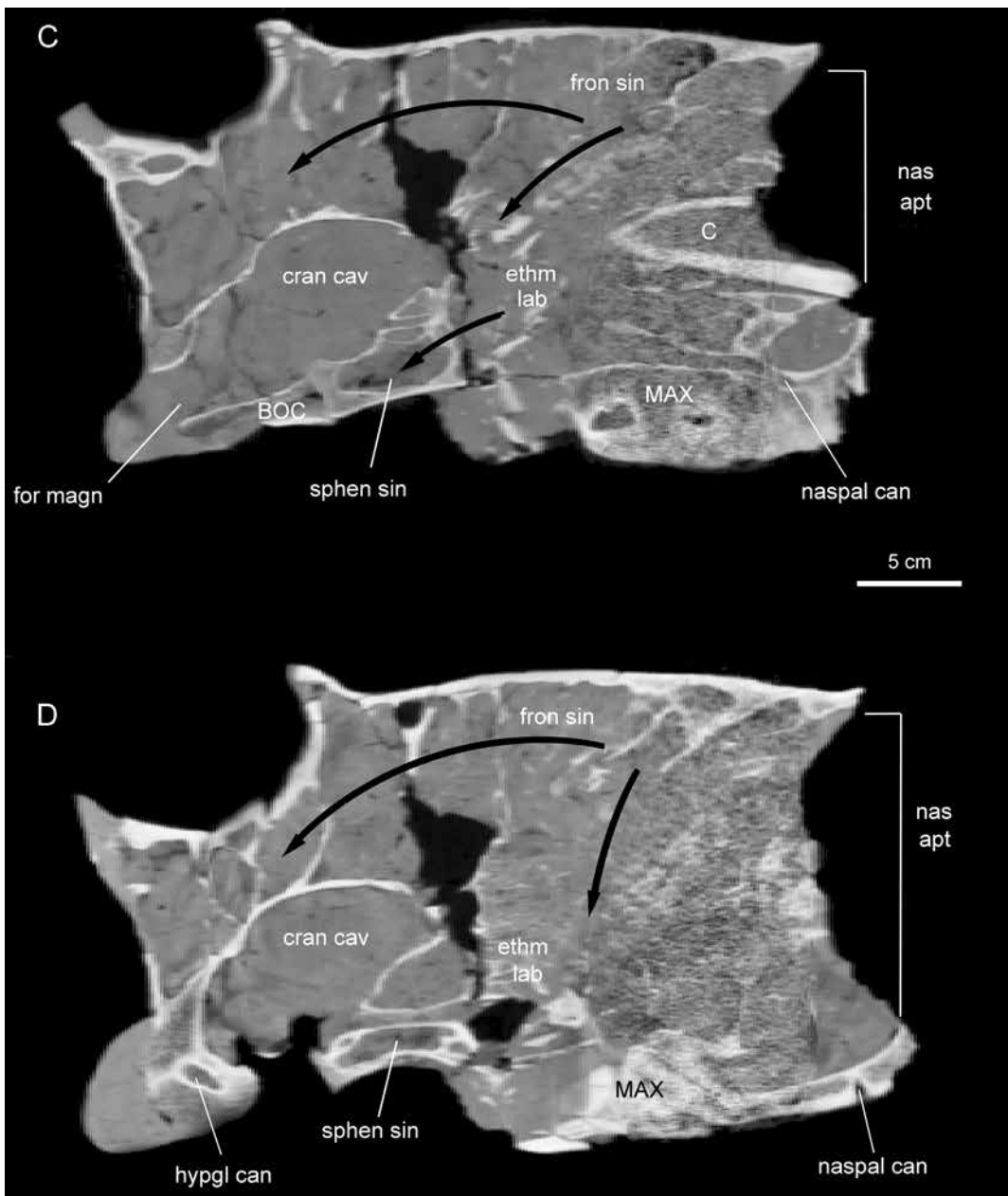
FIG. 13. *Astrapotherium magnum* MACN A 8580, parasagittal segments through left side of caudal cranium, sequence lateral to medial. In **A, inset** passes through skull just medial to the complete segment; note small epitympanic sinus and proximity of aditus of extratympanic sinus (see also fig. 27). In **B, asterisk** marks lambdoidal process of petrosal also seen in **inset** (see also fig. 14F). In **C, D, curved black arrows** indicate continuity between frontal sinus and air spaces throughout skull; note relatively small size of braincase. Cobbly appearance of bone and matrix in nasal region is due to artifacts in CT data. Premaxillae missing postmortem in this specimen (but see fig. 4).
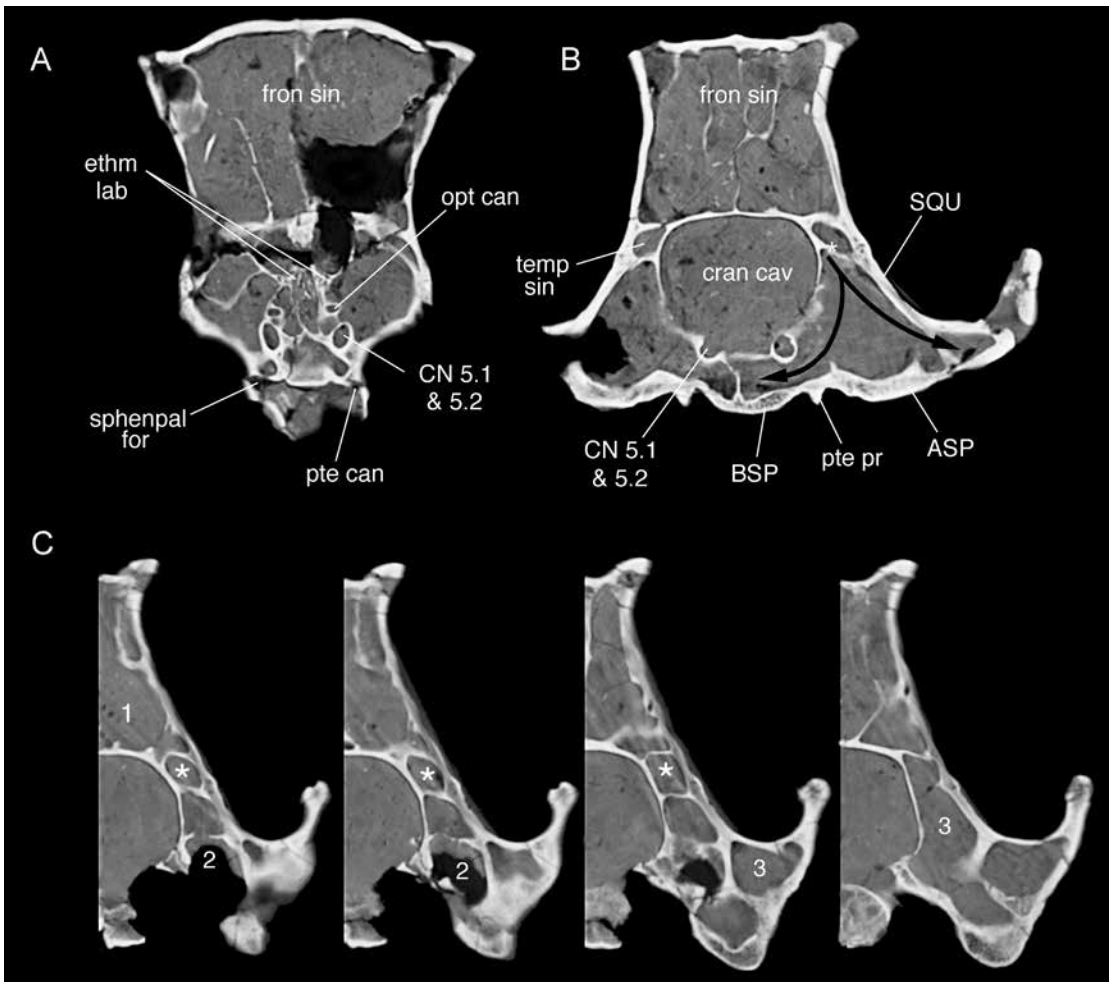
FIG. 14. *Astrapotherium magnum* MACN A 8580, transverse segments through skull in rostrocaudal order, all to same scale. In **A, B,** continuous chambers related to massive frontal sinus expansion serve to isolate cranial cavity from skull's sidewalls (suggested by **black arrows**); **C,** successive segments through apparent right side, illustrating relationship of frontal sinus (**1**) to extratympanic aditus (**2**) and other chambers in retroarticular process (**3**); **D,** segment through fenestra vestibuli (**4**) and aditus of epitympanic sinus, fully prepared on right side (**white arrow**) but still blocked by matrix on left; **E, F,** segments through rear of tympanic cavity and foramen magnum, illustrating positions of temporal sinus, posttemporal canal, sulcus for ?vertebral artery, lambdoidal process of petrosal, and paracondylar process (cf. *Tetramerorhinus*, fig. 40H). In **B, C, white asterisks** mark a large longitudinal conduit within cranial sidewall that corresponds, in other SANUs, to trackway of temporal sinus. But this feature also communicates with spaces that open into retroarticular process' aditus, indicating that both kinds of sinuses (pneumatic and venous) were housed in same bony chambers (see text).
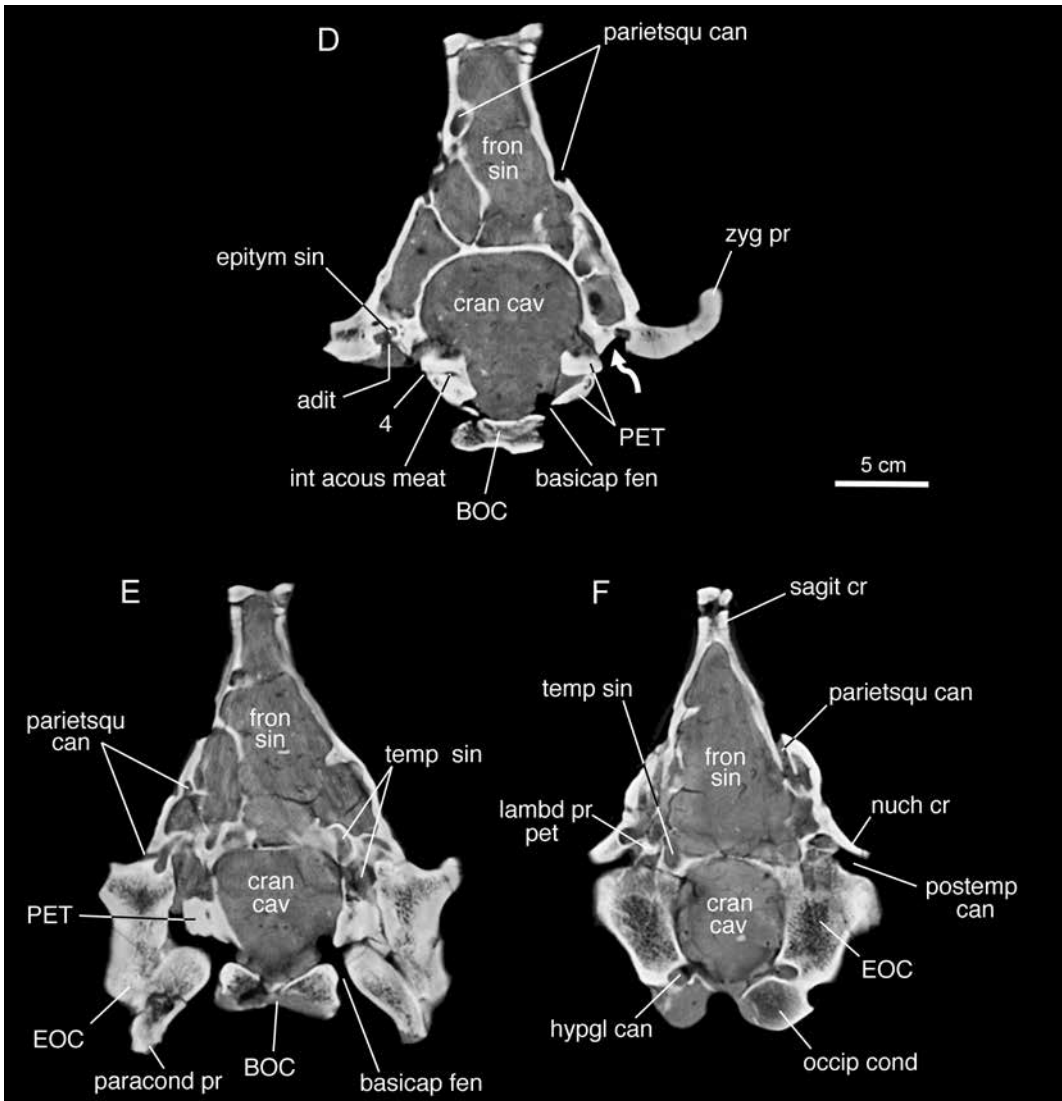
petrosal, squamosal, and sometimes the ecto-tympanic and entotympanic (if present). Other elements may be affected as well (e.g., exoccipital), but this is infrequent in placentals.

In some SANU taxa cranial pneumatization is so extensive that it penetrates bones that are rarely affected, such as the supraoccipital and the interparietal. In *Astrapotherium*, for example, almost all of the caudodorsal part of the skull is thoroughly pneumatized, with paranasal expansion seemingly responsible for virtually all of it (figs. 13, 14). From a structural standpoint, the main advantage of

pneumatization is that the volume of the skull or its components can be greatly increased during development without substantially affecting its weight, but there may be other benefits as well, such as increasing the area for muscular attachment (Zollikofer and Weissmann, 2008).

During normal development, the connections between the nasopharynx and intraosseous pneumatic cavities that develop from it become permanent passageways within local bones and are maintained as such into the adult stage (Anthwal and Thompson, 2016). Continuity is necessary, in
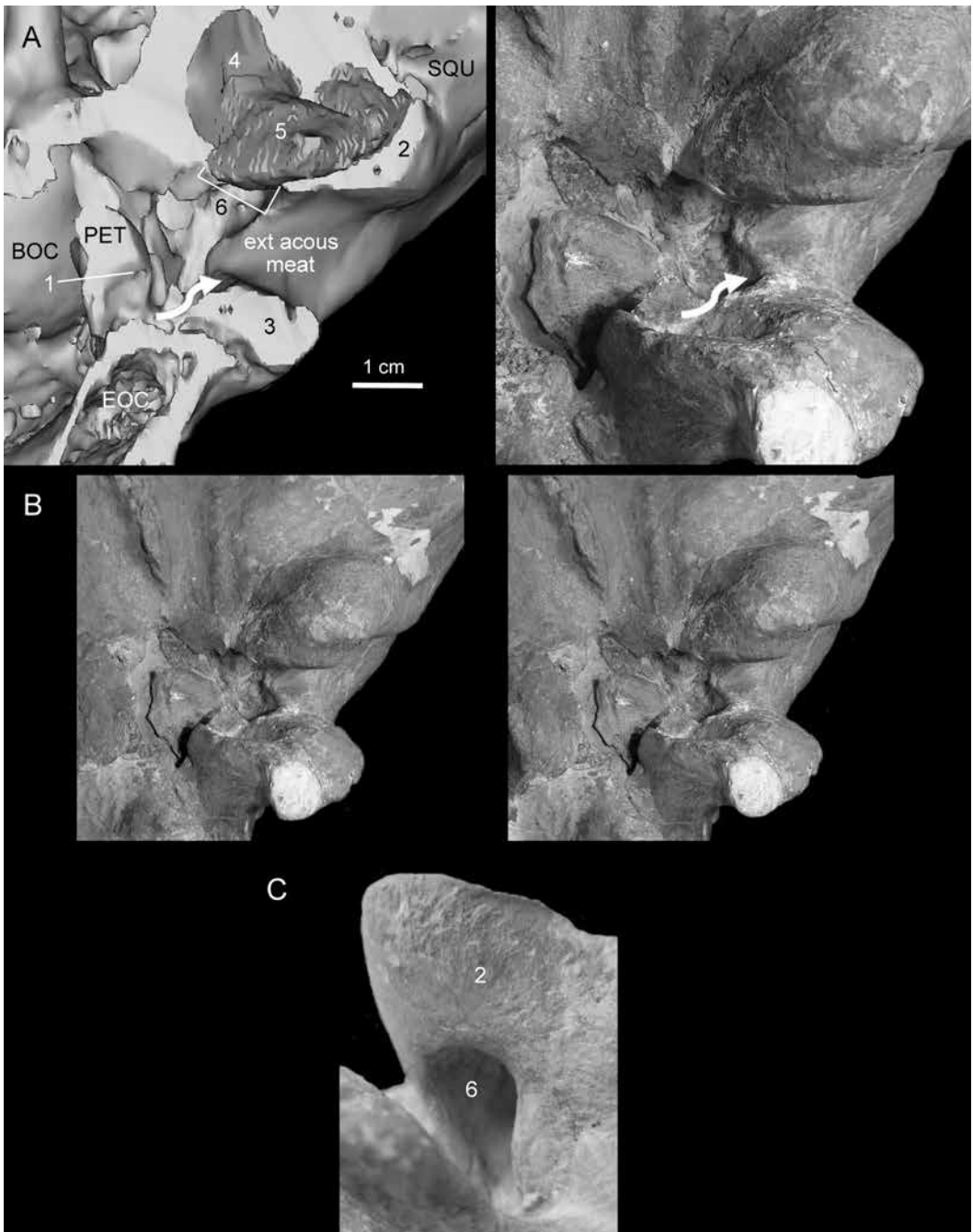
FIG. 15. *Astrapotherium magnum*, epitympanic and extratympanic sinuses and their adituses. **A,** MACN A 8580, virtual horizontal slice through left side of skull in ventral aspect, compared to photo of same skull in similar orientation; **B,** same skull and aspect, stereopair; **C,** MAPBAR 5322, extratympanic aditus in right retroarticular process, as seen from within external acoustic meatus. In A, **white arrow** points to small epitympanic sinus, situated lateral to position of (damaged) fenestra vestibuli (**1**); sinus slightly inflates tympanic roof near margin of

order to permit the physiological functioning of the mucous epithelia lining paranasal and paratympanic spaces. However, the intraosseous spaces are themselves normally sharply separated: the nose only communicates directly with its paranasal outpocketings, while the middle ear connects similarly with paratympanic spaces. This is important to emphasize, because separate development should provide a way to determine relationships between areas of pneumatization and their ultimate source in either the nasal cavity or the middle ear, no matter how complicated their disposition may appear in the adult (see Starck, 1967; Nickel et al., 1977: fig. 287; Boscaini et al., 2020). Whether this is always true is considered in relation to air sinus development in *Astrapotherium*.

The section of the tympanic roof situated directly over the incudomalleolar joint is recognized as a frequent site of pneumatic activity in extant therians (e.g., van der Klaauw, 1931; Aplin, 1990). If activity is relatively limited during ontogeny, only a small fossa will be produced, usually denoted as the epitympanic recess. If activity is greater, a very large chamber may eventually develop within the squamosal, usually termed the **epitympanic sinus** to distinguish it from the smaller, but ontogenetically primary, **epitympanic recess**. Depending on the constitution of the bony tympanic roof, in certain clades wings of the petrosal and alisphenoid may also be affected by epitympanic pneumatization (van der Klaauw, 1931; Fleischer, 1973). Significant development of epitympanic sinuses as defined here occurs sporadically in a diverse range of unrelated mammals, in marsupials as well as placentals (van der Klaauw, 1931; Aplin, 1990; Forasiepi et al., 2019), indicating that this topological space has evolved repeatedly. At the same time, not every inflation on the dorsal wall of the tympanic cavity can be considered a true epitympanic sinus.

Continuity between the tympanic cavity proper and the epitympanic sinus is characteristically provided by an **aditus** (= pneumatic foramen, ostium), usually fairly narrow, that connects the two spaces (van der Klaauw, 1931; Forasiepi et al., 2019). The aditus also marks the site where inflation began within the epitympanic recess during ontogeny. From the perspective of operational homology, an important indicium is the positional regularity of adituses in different groups, which is the chief ground for calling them by the same name. (Although the epitympanic recess is positionally defined by its relationship to the incudomalleolar joint, fossils rarely preserve ear ossicles in anatomical position and other indicia must be used, such as proximity to the fenestra vestibuli.) Although the mechanisms responsible for adital positioning have been little explored, that regularity exists at all implies that there must be ontogenetic "guidance cues" (Anthwal and Thompson, 2016) involved, whether these operate at the molecular or some other level of cellular interaction. Other adituses may occur wherever concentrated pneumatic activity occurs during development, such as the mastoid antrum situated in the rear of the tympanic cavity (in *Homo*) or the maxillary and frontal sinuses developed from the nasal cavity.

Finally, pneumatization of the promontorium itself has been described or inferred for a number of notoungulates (Billet and Muizon, 2013; Martínez et al., 2016) as well as for other mammals (van der Klaauw, 1931; O'Leary, 2010). One possibility is that it results ontogenetically from expansion of the epithelium of the auditory tube into the bone of pars cochlearis. If this is correct, it would represent a third area of pneumatic activity in SANUs in addition to those creating the epitympanic and extratympanic sinuses (see p. 51). Reconstructing the ontogeny and com-

---

external acoustic meatus, situated between retroarticular process (**2**) and posttympanic process (**3**). Inside the retroarticular process, complex volumes (**4, 5**) communicate with a large aditus (**6**) opening into meatus, as well as with other pneumatic spaces extending through much of skull. In C, retroarticular aditus apparently accommodated both retroarticular emissary vein and extratympanic paratympanic sinus, although subdivision into vascular and pneumatic spaces not possible in absence of soft tissues (see text and fig. 14).
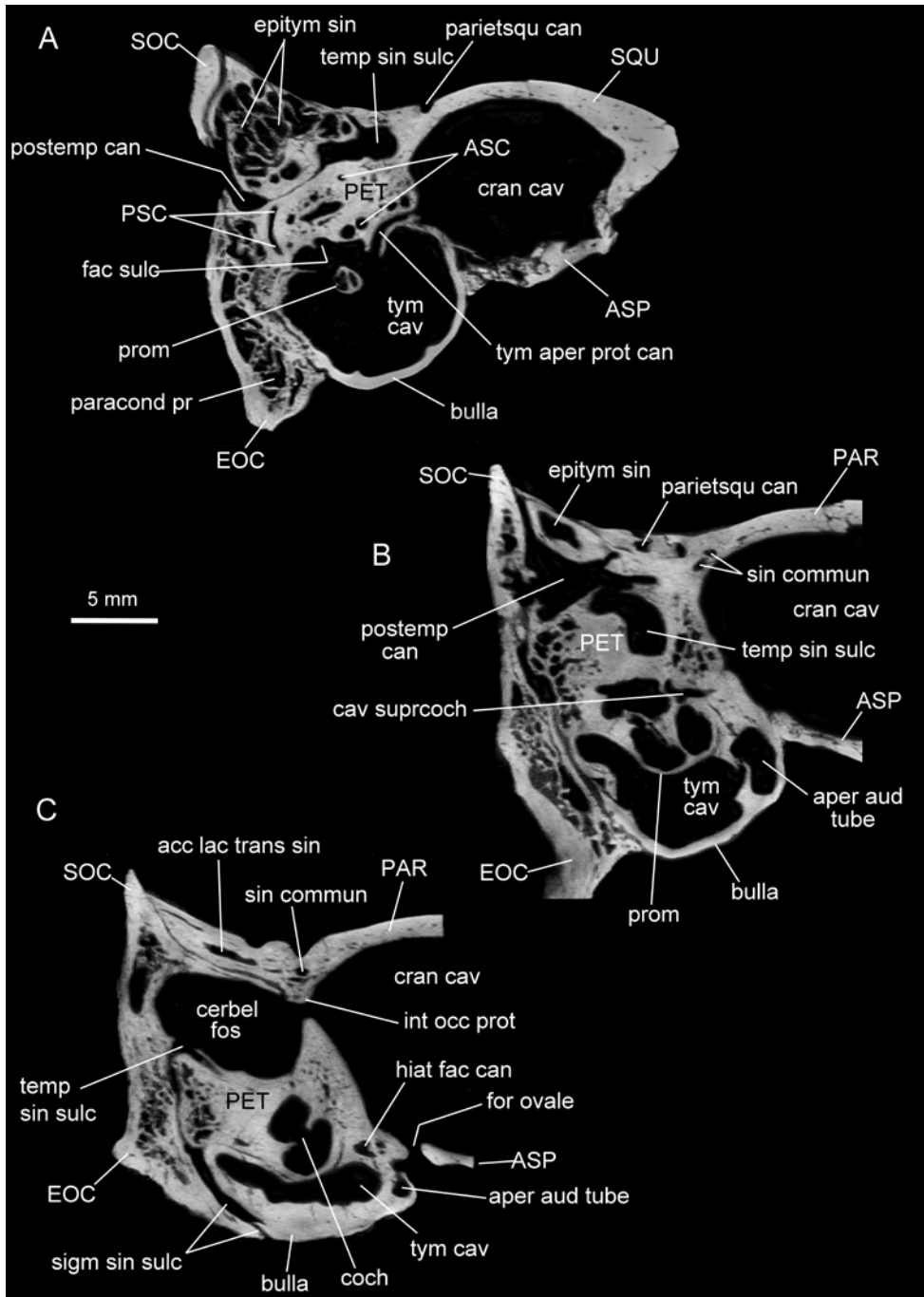
FIG. 16. *Cochilius volvens* AMNH VP-29651, parasagittal segments through caudal cranium, from lateral to medial. **A,** prootic canal traceable from temporal sinus within endocranium to track of facial nerve in tympanic cavity (see fig. 17). **B,** large vacuity dorsal to petrosal formed by confluence of posttemporal canal and sulcus for temporal sinus. **C,** channels for accessory lacunae of transverse sinus and sinus communicans housed in calvarial bones.

parative incidence of promontorial pneumatization in SANUs was not one of the targets of the present investigation, although such a study utilizing microtomography would be very useful.

Frontal Sinus Development. It is significant that the skull of *Trigonostylops* AMNH VP-28700 lacks evidence of extensive paranasal pneumatization, in strong contrast to astrapotheriids. Because little remains of the rostrum, the morphology of the nasal cavity itself cannot be assessed, although the slight doming of the frontal bone indicates that a modest amount of frontal sinus expansion occurred. In AMNH VP-28700 frontal sinus expansion extends for a short distance into the rostral part of the sagittal crest, as Simpson (1933a) surmised (fig. 12D–F), but the degree of inflation bears no comparison to the massive pneumatization of the cranial roof seen in *Astrapotherium* (figs. 13, 14) or large notoungulates such as *Toxodon*. Similarly, paranasal pneumatization in *Trigonostylops* is absent in the caudal calvarial bones and retroarticular process, whereas inflation from this source was extensive in Miocene astrapotheriids (figs. 13, 14). The single available skull of *Eoastrapostylops riolorense* (PVL 4216; Kramarz et al., 2017) is too damaged for interpretation.

Palatal Diverticulum of Maxillary Palatine Process. An unusual feature of AMNH VP-28700 not described by Simpson (1933a) is the diverticulum situated in each palatine process of the maxillary. As may be seen in figure 2A, the palatine process on the specimen's right side bears a large artificial opening, situated rostromedial to the position of the P2. If the hole had been made during preparation it seems likely that Simpson would have mentioned it, so we conclude that it was created subsequent to his study. In any case, scanning reveals that the hole intersects a natural space (hereinafter, **palatal diverticulum**) that is dorsally connected by means of an aditus to the nasal cavity (fig. 12A, B). An identical space, still intact, exists on the left side. Witmer et al. (1999: 261, fig. 7) described "a rostral extension of the ventral nasal meatus" in *Tapirus terrestris*, housed in a comparable part

of the maxilla and "formed into a complete tube by the contact of the septal part of the maxilloturbinate to the nasal septum." This is similar but obviously not identical to the condition in *Trigonostylops*, in which the maxilloturbinate was evidently not involved in diverticulum formation.

Whether small palatal spaces that communicate only with the nasal cavity occur in other SANU taxa is unknown. A small vacuity can be seen in CT segments of the proterothere *Tetramerorhinus* AMNH VP-9245, but in this case the diverticulum is more caudally situated, within the palatine bone itself and not the palatine process of the maxilla. In the toxodontian *Puelia coarctatus* MLP 67-II-27-27 there are very large (although somewhat nonsymmetrical) natural dehiscences that penetrate the palate, but such features can be seen in a variety of unrelated therians. In terms of their origin they are unlikely to be the result of pneumatic activity (as opposed to other kinds of remodeling). In *Bos* and *Ovis* very large paranasal spaces, termed palatine sinuses, substantially pneumatize the bones composing the rostral part of the hard palate, creating large intranasal spaces additional to the maxillary sinuses (Sisson and Grossman, 1953: 137; Hare, 1975: fig. 30-1). However, they are differently positioned and seem unlikely to be homologous with the vacuities present in *Trigonostylops*.

The proximity of the palatal diverticula in *Trigonostylops* to the nasal septum and rostral part of the nasal cavity raises the question whether each contained, or was otherwise related to, the ipsilateral vomeronasal organ. There seems to be no mammalian examples of the vomeronasal organ actually lying within, as opposed to on, the maxillary palatine process. In *Equus*, as in mammals generally, the vomeronasal organ is enclosed in a bony or cartilaginous capsule (cartilago paraseptalis) that lies entirely within the nasal cavity (Minett, 1925; Schliemann, 1987; Witmer et al., 1999; Zancanaro, 2014). Vomeronasal organ location in AMNH VP-28700 cannot be evaluated because of damage to the rostrum, and for the present no function can be ascribed to the palatal diverticulum.
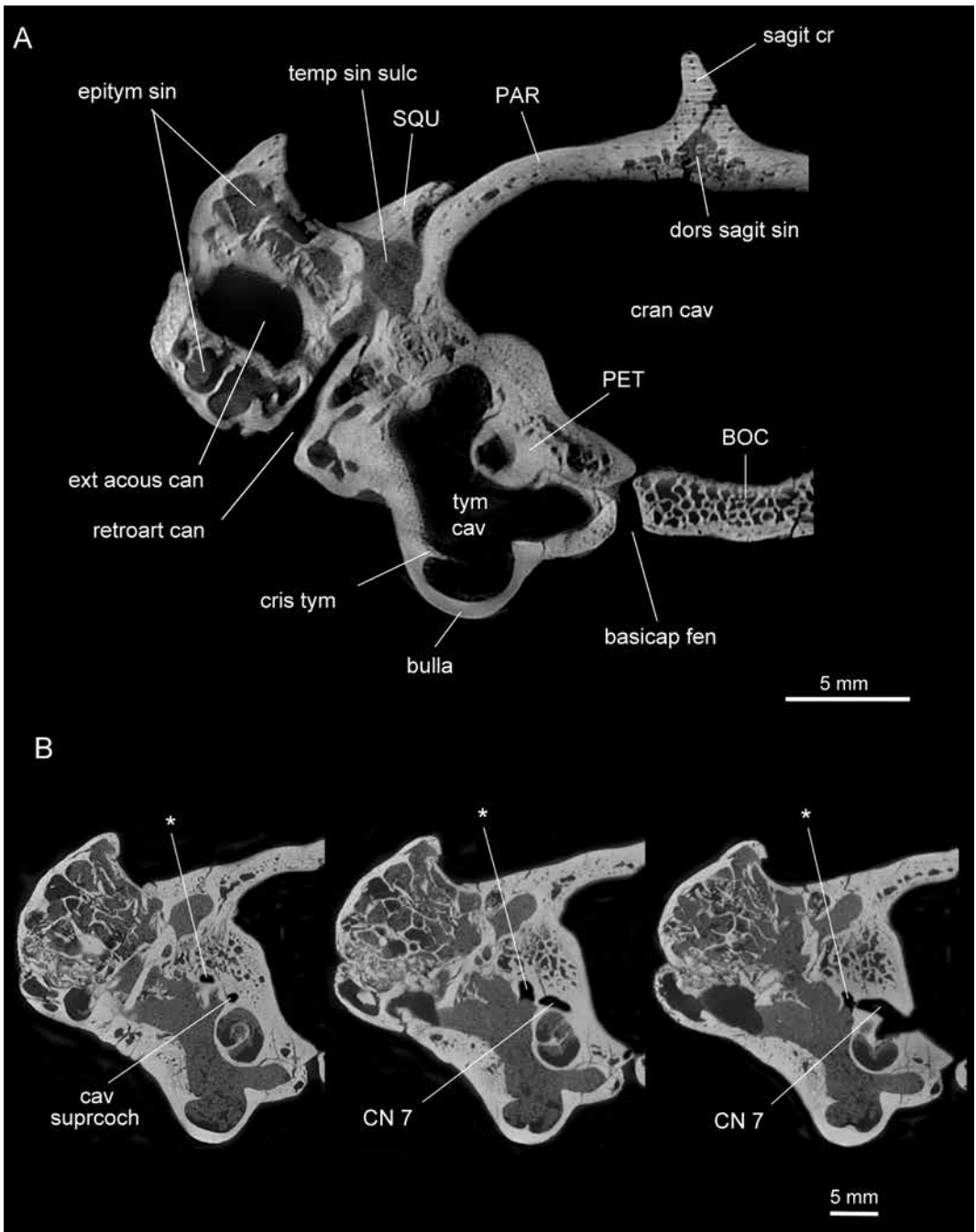
FIG. 17. *Cochilius volvens* AMNH VP-29651, transverse segments through caudal cranium in rostrocaudal sequence (on this and opposite page). Note different scales. In **A,** external acoustic canal bordered by epitympanic sinus, retroarticular canal. In **B,** closely spaced segments depict trajectory of channel (prootic canal) for lateral head vein/prootic sinus, which typically opens into tympanic cavity on margin of secondary facial foramen (**asterisks**). In **C, asterisk** marks distal part of intratympanic sulcus for
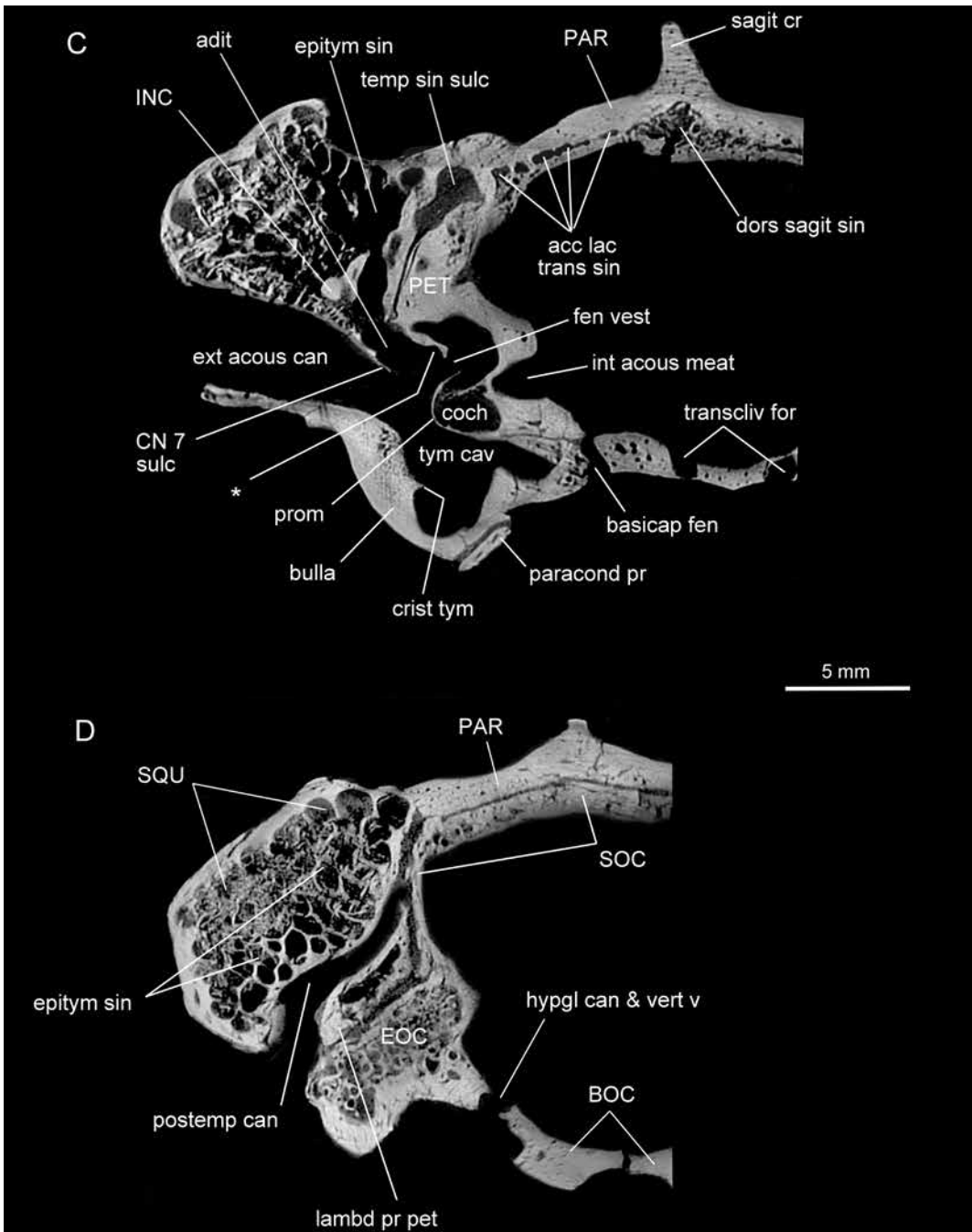
lateral head vein (and not proximal stapedial artery, which is absent) crossing dorsal wall of fenestra vestibuli on path to stylomastoid foramen. Note also numerous channels for accessory lacunae of transverse sinuses in skull roof, transclival foramina. In **D,** note lambdoidal process of petrosal in floor of posttemporal canal, parietal/supraoccipital overlap and latter's minor participation in bounding posttemporal canal.

FIG. 18. *Cochilius volvens* AMNH-VP 29651, left auditory region in slightly oblique ventral aspect. **A,** virtual horizontal slice through reconstructed left auditory region, with bulla digitally removed. **B,** same specimen, skull intact (stereopair). Bulla shifted slightly out of position post mortem, as it would normally cover caudal portion of basicapsular fenestra. Entotympanic-ectotympanic suture fully visible running parasagitally across bullar surface (see MacPhee, 2014). **Key: 1,** basisphenoid surface articulating with rostromedial portion of expanded bulla; **2,** caudal aperture of pterygoid canal; **3,** groove for greater petrosal and deep petrosal nerves; **4,** transclival foramina in basioccipital; **5,** groove connecting transclival foramen with small foramen in basioccipital-basisphenoid synchondrosis. In A, **asterisks** identify continuous basicapsular fenestra, covered by bulla in intact skull except for jugular area and foramen ovale. Dorsal wing of entotympanic (ENT) forms "medial flange," roofing over space between promontorium and medial bullar wall. For adital connection between epitympanic sinus and tympanic cavity, see figures 16 and 17.

A different feature, equally unusual, is the meatal diverticulum seen in tapirs. This is an epithelium-lined saclike extension of the nasal cavity that extends onto each side of the upper face of tapirs; its position is marked on the skull by bony gutters running along the external margin of the nasal aperture (Witmer et al., 1999; Moyano and Giannini, 2017). Somewhat similar features occur in an even more elaborate form in certain macraucheniids (Forasiepi et al., 2016), but have not been identified as such in any other SANUs, including trigonostylopids and astrapotheriids. Witmer et al. (1999) were unable to identify any distinctive features of the mucous epithelial lining of the meatal diverticulum in *T. terrestris* and *T. indicus*, and its function apart from contributing marginally to the volume of the nasal cavity is uncertain.

Epitympanic Sinus, Extratympanic Sinus, and Other Pneumatic Spaces

The epitympanic sinus has played an important role historically in adjudicating relationships among SANU major taxa (for recent treatments see Billet, 2010; Billet and Muizon, 2013; MacPhee, 2014; Martínez et al., 2020). Roth (1903) claimed that the epitympanic sinus was a defining feature of Notoungulata, with the implication that it was absent in other, nonnotoungulate SANUs (but see fig. 19). Although he briefly noted the existence of a large cavity in an unspecified part of the zygomatic process area of the squamosal in an unnamed proterotheriid, he also stated that he could not determine whether the air space communicated with the tympanic cavity and, in any case, held that it could not be the homolog of the epitympanic sinus of notoungulates in his view (Roth, 1903: 13). Simpson (1933a: 26) pointed out that the distribution of paratympanic spaces was wider than Roth had allowed: not only in proterotheriids, but also in astrapotheriids and *Trigonostylops*, there was "a small cavity in or near the base of the zygomatic process of the squamosal which communicates with the ear region by a canal running downward and slightly backward [which] may perhaps also be considered as liter-

ally an epitympanic sinus, although not strictly homologous with this structure in its more usual development [in notoungulates]."

How much Simpson (1933a) could have actually known about the fine details of paratympanic spaces in SANU taxa is impossible to say, but it is likely that he reached his conclusion after studying damaged specimens in which relevant features were exposed. Much greater detail can be captured with CT scanning, which in turn provides a stronger morphological basis for homology assessment than was available to Simpson or Roth. In the case of *Trigonostylops wortmani* AMNH VP-28700, segmental data show that the "small cavity" inflates much of the rostral part of the squamosal (fig. 12E–G), including the retroarticular process, base of the zygomatic process, and ventral part of the squama, whereas in notoungulates (fig. 19) the epitympanic sinus lies more dorsocaudally in the squamosal. This is especially obvious in pachyrhukines, mesotheriids, and other small taxa with proportionately large sinuses (Gabbert, 2004; MacPhee, 2014). Compared to *Cochilius* (fig. 19), which exhibits conditions typical of notoungulates, *Trigonostylops wortmani* AMNH VP-28700 differs in that the aditus lies significantly more laterally, on or slightly beyond the osteological border between the tympanic cavity proper and the external auditory meatus (fig. 26C, D). Despite this positioning, the inferred pneumatization pattern, as reconsidered here and discussed below, makes it highly likely that in *Trigonostylops* the aditus actually lay just inside the probable line of attachment of the pars flaccida of the tympanic membrane, and therefore functionally "inside" the tympanic cavity (contra MacPhee, 2014: 21, fn.). The chief reason for this conclusion is the nature of the space itself: it has no relationship with the nasal cavity or its dependent air spaces, so barring some unknown method of pneumatization in *Trigonostylops*, this **extratympanic sinus** must have had a single origin as a paratympanic extension of the middle ear.

How do these conditions compare with those in proterotheriids and astrapotheres? Scanning reveals that in the proterotheriid *Tetramerorhi-*
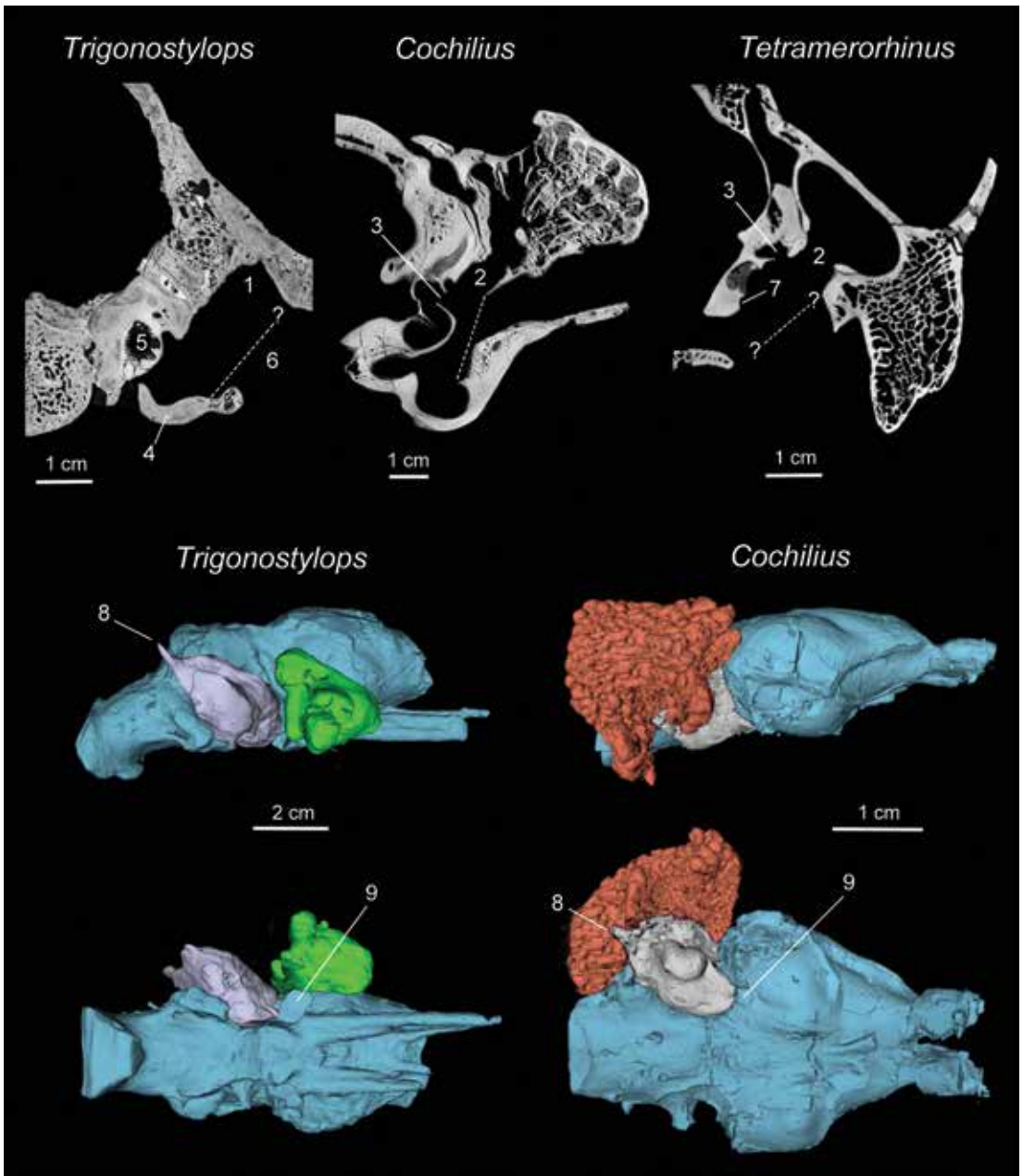
FIG. 19. Differences between epitympanic and extratympanic sinuses and other features in three members of comparative set: *Trigonostylops wortmani* AMNH VP-28700, *Cochilius volvens* AMNH VP-29651, and *Tetramerorhinus lucarius* AMNH VP-9245. **Top row:** Selected segments through external acoustic meatus; note differences in scale. In each segment, dashed line indicates inferred position of tympanic membrane in life. **Key** (structures not exhaustively identified on each segment): **1,** to aditus of extratympanic sinus (aperture not in plane of segment); **2,** aditus of epitympanic sinus; **3,** fenestra vestibuli; **4,** ectotympanic; **5,** cochlea; **6,** tympanic membrane (inferred); **7,** ?sulcus for internal carotid artery on caudal portion of promontorium. Note that adituses of epitympanic sinuses of notoungulate *Cochilius* and litoptern *Tetramerorhinus* are located

nus AMNH VP-9245 the tympanic roof is inflated by a modest squamosal air space (figs. 19, 40I) that communicates with the tympanic cavity via a relatively large aditus situated somewhat more rostrally than in notoungulates, but still directly lateral to the fenestra vestibuli and thus well inside the limits of the tympanic cavity. The air space continues into the portion of the squamosal medial to the base of the zygomatic process, but not further; a similar arrangement is seen in *Thoatherium minusculum* YPM PU 15721. In our opinion, small differences in the pneumatic penetration of the squamosal do not affect the equivalency of the epitympanic sinus in proterotheriids and notoungulates, whether or not they point to differences in function.

Conditions within astrapotheriids, however, are substantially different. Although Simpson inferred that *Astrapotherium* possessed a paratympanic sinus of some sort, his remarks are too terse to be useful. We surmise that he thought that the large opening within the retroarticular process, plainly evident in all adequately preserved *Astrapotherium* skulls (figs. 14, 15) and positioned very close to the lateral border of the tympanic cavity, was in fact an aditus (hereafter, **aditus of the extratympanic sinus**) resembling the one seen in *Trigonostylops*.

Difficult homological questions of this sort arise in comparative morphology all the time, but in this instance we argue that it can be provisionally answered. To begin with, it is important to underline the fact that in *Astrapotherium* an epitympanic sinus also exists, which we discovered in the course of examining the scan of MACN A 8580 (figs. 13, 14). The version of this space in *Astrapotherium* is best described as rudimentary, and is obvious only in well-preserved specimens in which the tympanic roof has been adequately cleaned. Although this space might be interpreted as simply a rather deep epitympanic recess, it exhibits a constriction that leads into a modest swelling, which is mushroom shaped in profile (fig. 15). The space is situated in proximity to the fenestra vestibuli and within the morphological limits of the tympanic cavity as defined by the meatal border of the squamosal. Furthermore, it is wholly contained in the ventral part of the squamosal and simply terminates there; it does not open up into the much larger chambers situated above it, which are inflated from the frontal sinus (and thus ultimately from the nasal cavity). Given the consistency of relevant indicia, which, apart from matters of size, appear to be much the same in notoungulates, proterotheriid litopterns, and astrapotheres examined to date, it seems reasonable to regard the epitympanic sinus in these major taxa as operational homologs. Unfortunately, due to overpreparation of the tympanic roof in *Trigonostylops wortmani* AMNH VP-28700 (fig. 12H) it cannot be determined whether this taxon possessed an equivalent to the small epitympanic sinus found in *Astrapotherium*. If a sinus existed at all in this taxon it could not have been very extensive.

We must now account for the additional and much larger extratympanic cavity in *Astrapotherium* and its possible correspondence to conditions in *Trigonostylops*, because Simpson's

in same topographical position relative to fenestra vestibuli. Ectotympanic is not known in *Tetramerorhinus*, but was probably relatively unexpanded (projecting piece of bone seen in figured segment is part of basioccipital, not ectotympanic). **Middle and bottom rows:** 3D reconstructions in right lateral (middle row) and ventral (bottom row) views of same specimens. **Key: blue,** brain endocast; **grey,** petrosal; **orange,** epitympanic sinus; **green,** extratympanic sinus; **8,** lambdoidal process of petrosal (extending into floor of posttemporal canal, latter not shown); **9,** basicapsular fenestra/foramen ovale. Epitympanic sinus of *Cochilius* is subdivided into numerous cellules, as in many typotheres; in *Tetramerorhinus* it is a single large vacuity, as is also generally the rule in notoungulates. Note that extratympanic sinus of *Trigonostylops* is located rostral to petrosal, whereas epitympanic sinus of *Cochilius* is dorsocaudal to latter element. Adituses for these spaces are also located in different relative positions, suggesting different ontogenies and nonhomology (see text, p. 65). Both kinds of pneumatic chambers are solely related to tympanic cavity, as paranasal inflation did not reach these areas in these taxa (contrast with *Astrapotherium*, figs. 13, 14).

(1933a) text does not reveal whether he considered the large opening in the retroarticular process to have also functioned as a port for the retroarticular vein. In *Astrapotherium guillei* MAPBAR 5322, which preserves both the retroarticular aperture and foramen magnum (see Kramarz et al., 2019a), the two openings have approximately the same measurements at their external margins (respectively, 3.5 × 2.0 cm vs. 3.0 × 3.0 cm), which means that the aperture's cross-sectional area would have been close to that of the brainstem. Even for an animal the size of *Astrapotherium*, it is questionable whether the retroarticular emissary vein would have attained such a size, especially in view of the number of other dural drainage channels in this taxon (fig. 8). Billet et al. (2015) logically viewed the adital opening in the retroarticular process as being at least partly devoted to the passage of the retroarticular vein, and our vascular reconstruction does not conflict with this interpretation. Unfortunately, in the scan of MACN A 8580 we were unable to track a continuous vascular pathway through the retroarticular air space all the way to the aditus (fig. 14C). Topologically, the retroarticular process houses a single complicated but continuous space (fig. 13A). In life there would have had to have been some form of histological separation between the air space and the vascular channel, even if this took the form of a few thicknesses of epithelia. In *Trigonostylops* there is good evidence for the retroarticular vein, but its relatively small foramen opens on the medial side of the retroarticular process, far from the proposed aditus (figs. 11A, 26D).

Apart from the retroarticular vein, an additional problem with having two air-filled sinuses of different ontogenetic origin within the retroarticular process is the fact that, in the skull, the aditus freely opens onto the external acoustic meatus. Considered without any further assessment, this arrangement seems to imply that there would have been a continuous, air-filled passageway from nose to ear entirely within the basicranium. The only interpretation that makes much sense would be to infer that, within the retroar-

ticular process, the paratympanic space was separated within its own membranous envelope from the much larger paranasal volume. There are no indicia to support such a speculation, although there may be analogies, such as the cranial fenestrations found in unusual places in certain groups (e.g., lateral maxillary fenestrations in some lagomorphs and heteromyids; occipital fenestrations in moles). However, these dehiscences occupy areas that are normally filled by bone in other taxa (see Russell and Thomason, 1993); their ontogeny is not related to pneumatization as defined here.

Conditions in other astrapotheriids have not been explored in detail, although fortuitous breakages in *Scaglia kraglievichorum* MMP M-207 and *Scaglia* cf. *kraglievichorum* MPEF PV 5478 (Kramarz et al., 2019b) indicate that this taxon lacked any form of retroarticular pneumatization. *Astraponotus* has not been investigated, but it is known for certain that no opening of any sort, vascular or pneumatic, existed on the caudal surface of the retroarticular process in this astrapothere (Kramarz et al., 2010).

The form and consequences of cranial pneumatization in other panperissodactylans cannot be covered in detail here, but a few observations are worth summarizing because they have a bearing on the morphological problems outlined in this section. Patterson (1977) determined that a notoungulatelike epitympanic sinus existed in *Pyrotherium romeroi* ACM 3207, the only relatively complete skull of this taxon so far discovered. Billet (2010) verified Patterson's conclusion and supplied additional observations that comport with our indicia for recognizing the epitympanic sinus and its aditus. Although Rusconi (1932) claimed that the epitympanic sinus existed in the macraucheniid *Scalabrinitherium bravardi* MACN Pv 13082, we were unable to confirm this on the specimen. There is a vacuity located on the dorsal border of the petrosal, but this is surely a vascular (temporal sinus?) rather than a pneumatic feature. In MACN Pv 13082 the retroarticular processes are mostly intact, but on the left side an area of damage reveals that the processes' interior is filled with cancellous tissue typical of dip-

loe. Beyond these facts, the preserved part of the skull is otherwise highly pneumatized, with the frontal sinus deeply penetrating the roof and side-walls of the skull. Conditions in other macraucheniids have not yet been adequately explored.

In the scan of *Meniscotherium chamense* AMNH VP-4412 an aperture of some sort can be detected in the roof of the tympanic cavity, in the area where an epitympanic recess would normally be expected. Because of damage to this specimen we cannot clarify its relations further. Gazin (1965, 1968) made no mention of this feature in his comparisons of various "condylarthrans," including *Meniscotherium*. In another specimen of this taxon, Cifelli (1982: fig. 2; see also Williamson and Lucas, 1992: fig. 6) identified what appears to be the same aperture as a "posterior petrosal epitympanic sinus," perhaps because of its position relative to the fenestra vestibuli. However, position alone is not dispositive because the prootic canal's tympanic aperture for the lateral head vein/prootic sinus, when present, is located in the same general area (see p. 119, Discussion: Venous Structures). If Cifelli's (1982) gap were truly a pneumatic aditus, it would be of great interest because it is situated well within the tympanic cavity, but O'Leary (2010) has shown on comparative grounds that this interpretation is probably incorrect.

Finally, on the skull of the palaeotheriid perissodactylan *Palaeotherium siderolithicum* MNHN GY-523 there is a depression (*recessus sus-méatique*) situated at the base of the retroarticular process, in close proximity to what would have been the limits of the tympanic cavity in life (Remy, 1992: 210). A large retroarticular foramen is also present, although its relationship, if any, to retroarticular air sinuses is unexplored. In panperissodactylans depressions or grooves of this kind adjacent to the retroarticular process are not unusual, but seem to have nothing to do with pneumatization. In *Equus* they appear to be sulci for large anastomotic vessels linking the basicranial plexuses with the retroarticular emissary vein (fig. 39A, B).

Tympanic roof pneumatization is almost completely absent in extant perissodactylans: there is an epitympanic recess, but no equivalent even to the small epitympanic sinus seen in *Astrapotherium*. Extratympanic adituses are also absent in *Equus*, *Ceratotherium*, and *Tapirus*, although damaged specimens reveal that there is a small degree of inflation within the retroarticular process (likely developed from the frontal sinus). Incidentally, the guttural pouch of *Equus*, although an evagination of the mucous lining of the auditory tube, does not penetrate bone and thus has no associated osseous indicia. The guttural pouch, relatively small in extant tapirs (Anthony, 1920), is apparently absent in rhinos (Fischer and Tassy, 1993).

Rostral Cranium and Mesocranium

Dentition and Upper Jaw

Major dental features of *Trigonostylops* compared to other SANUs. With regard to dentition, Simpson (1933a: 20) maintained that "the resemblances [between astrapotheriids and *Trigonostylops*], not very deep-seated, could equally well be explained as due only to a considerably more remote ancestry and a limited degree of convergence." In fact, in later astrapotheriids with highly derived dentitions such as *Astrapotherium*, molar morphology actually resembles that of notoungulates more than that of trigonostylopids in several respects (Scott, 1928). Simpson's (1933a) position concerning the lack of dental resemblance between *Trigonostylops* and late astrapotheres is thus well taken, and should be considered in any study that primarily relies on dental characters for detecting relationships (see p. 131, Phylogenetic Analysis).

At the time Simpson wrote there was uncertainty about the nature of the anterior dentition of *Trigonostylops* (especially as to whether the tusks were canines or incisors), and the important early astrapotheriid *Tetragonostylops apthomasi* (Paula Couto, 1952) had not been discovered. The following section is meant to briefly summarize what has been learned about the teeth of *Trigonostylops* since then, based on the authors' observations on a wide diversity of SANU dentitions. Upper and lower dentitions of

Trigonostylops and *Astrapotherium* are illustrated in figures 2–4 (see also fig. 42).

Dentally, *Trigonostylops* is characterized by the following features:

1. Enamel with vertical Hunter-Schreger bands (HSB), as in all known astrapotheres (**C159**). In *Trigonostylops*, as well as in *Albertogaudrya*, the vertical HSB are overlain by radial enamel, whereas in *Astrapotherium*, the portion exhibiting vertical HSB is overlain by a layer of enamel with transversal HSB, combined with slight vertical decussation (Lindenau, 2005; Koenigswald et al., 2014). *Pyrotherium* (Late Oligocene) presents vertical bands of decussating prisms that differ from HSB in having an internal, feathery structure (Koenigswald et al., 2014). Vertical HSB bands are unknown in *Eoastrapostylops*, Notoungulata, and Litopterna (with the exception of sparnotheriodontids, whose status as litopterns is controversial; Cifelli [1993]). Among perissodactylans, vertical HSB are found in rhinocerotids (Filippo et al., 2020).

2. Tusklike, divergent upper and lower canines (**C17, C18, C19, 158**), not as enlarged as in astrapotheriids, and rooted (rootless in later astrapotheriids). Enlarged canines are typical of but not exclusive to astrapotheres among SANUs (e.g., Early Eocene litoptern *Protolipterna ellipsodontoides*; Cifelli, 1983)

3. Cheekteeth are plesiomorphic, as in most SANUs and thus structurally far removed from those of derived astrapotheriids (e.g., *Astrapotherium*, Early-Middle Miocene), but closer to those of basal astrapotheriids such as Early Eocene *Tetragonostylops* and Middle Eocene *Albertogaudrya*.

4. P1 (known only from alveolus) small, situated immediately behind canine tusk, as in *Tetragonostylops* (P1 lost in later astrapotheriids).

5. Long diastema rostral to P2 (**C2**), as in Late Eocene *Astraponotus* (P2 lost in later astrapotheriids, but postcanine diastema present). Short diastema in *Tetragonostylops*.

6. P2 with a single, mesiodistally keeled cusp, and a small, noncuspidate, talonlike swelling on lingual side. Astrapotheriids have more complex P2s, with a parastylar lobe and lingual swelling well developed in *Tetragonostylops*, and a conspicuous lingual cusp in *Astraponotus* and *Maddenia* (Late Oligocene).

7. P3–M3 essentially trigonodont. Paraconule indistinct (**C35**), subsumed within large protoloph (**C23**), as in astrapotheriids (also pyrotheres and notoungulates), but unlike litopterns. P3–4 with distinct metacone, as in basal astrapotheriids (metacone secondarily reduced in later forms), unlike most (but not all) basal notoungulates and litopterns. Mesostyle absent (**C40**), as in all astrapotheres, unlike litopterns (i.e., Macraucheniidae and Proterotheriidae) and some basal notoungulates (e.g., *Oldfieldthomasia*). Postprotocrista connecting metaconule, and hypocone (**C46**) hardly indicated by lingually elevated postcingulum in M1–M2; trigon basin lingually isolated. Postmetaconular crista directed toward metastyle. Early Eocene *Tetragonostylops*, possessing a distinct cingular hypocone and transverse postmetaconular crista (directed toward metacone and metalophlike), is morphologically intermediate between *Trigonostylops* and the indisputable astrapothere *Albertogaudrya* (see Carbajal et al., 1977; Soria, 1982). Notoungulates are more likely to have had a pseudohypocone (derived from partition of protocone, at least on M1–M2), since an independent hypocone and postcingulum coexist in basal notoungulates (see Patterson, 1934c; Muizon et al., 2019).

8. Procumbent (**C56**), spatulate lower incisors (3 pairs), nonbilobate (**C55**).

9. In the lower jaw p1 variably present, isolated within postcanine diastema, single cusp with small distal heel, as in *Tetragonostylops* (p1 lost in all remaining astrapotheres). Also occurs in litoptern *Protolipterna ellipsodontoides*.

10. Mandibular p2 two-rooted, with a main cusp and a variably developed distal heel; variable, small mesial paraconidlike cusp and hypoconid-entoconid cusps on distal heel (incipient talonid). The most complex variant is closer to *Astraponotus* than to *Tetragonostylops* and *Albertogaudrya*.

11. Mandibular p3-p4 submolariform, exhibiting triangular trigonid with distinct protoco-
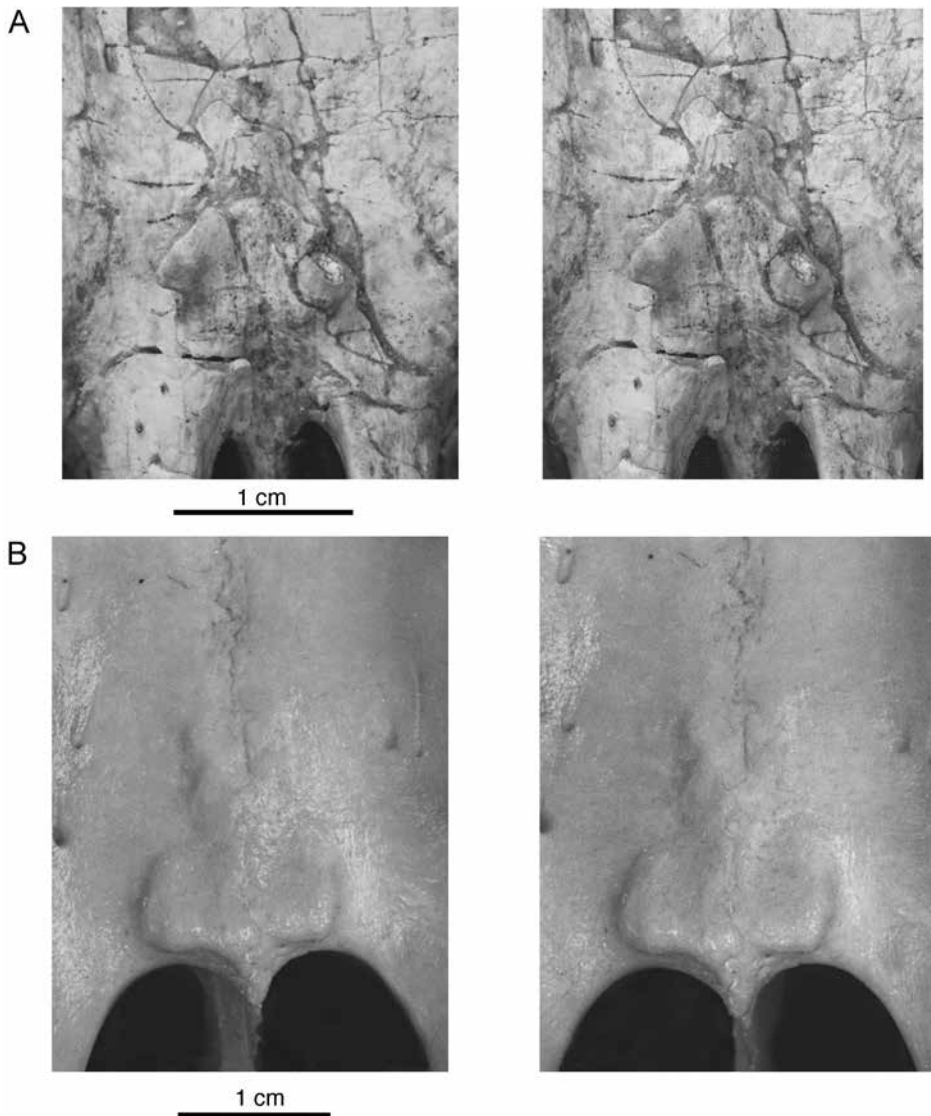
FIG. 20. Palatal alate process in **A,** *Trigonostylops wortmani* AMNH VP-28700 and **B,** *Tapirus indicus* AMNH M-77576, ventral aspect (stereopairs). For location on palate see fig. 1A. In A, left wing of process is broken, but right is intact. In B, although process of *Tapirus* is less developed, note similarity in position and conformation to that of *Trigonostylops*.

nid and metaconid (**C60**) and rudimentary "paraconid" enclosing trigonid basin. Short talonid with lophoid hypoconid. Lower p4 with three distinct talonid cusps, as in *Tetragonostylops* and *Astraponotus*. In basal litopterns and notoungulates, p3 is much simpler and p4 more molariform.

12. Lower molars (**C61, C62, C63**) with short and simple trigonid, paraconid/paralophid absent, unlike basal notoungulates and litopterns. Strong protoconid-metaconid postvallid. Long talonid, with lophoid hypoconid (hypolophid) connecting hypoconulid. Cristid obliqua abuts protocristid at a point nearer to
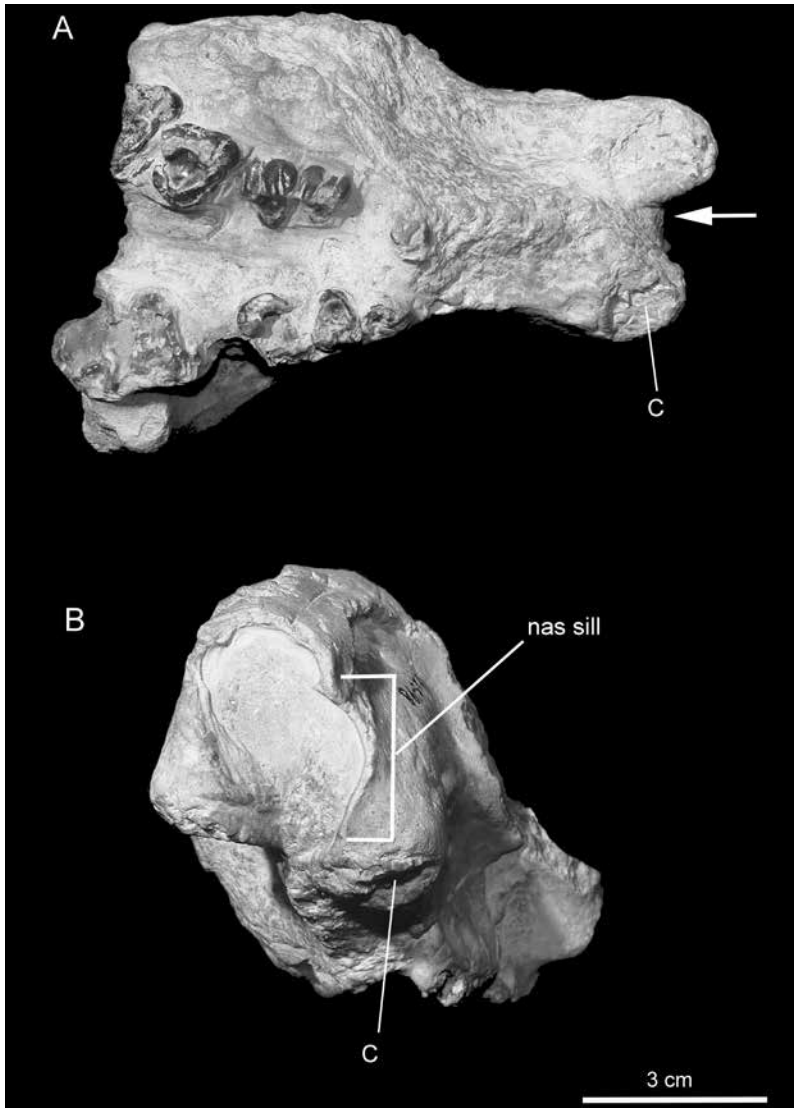
FIG. 21. *Trigonostylops wortmani* MLP 52-X-5-98, partial rostrum with C and P1 (roots only) and P2-4, M1, and M2 (crowns bilaterally present) in **A,** ventral; **B,** rostral; **C,** oblique dorsal; and **D,** left lateral views. In A, appearance of rostral end of palate implies but does not prove that it naturally furcated into relatively large canine-bearing processes, separated by an intervening cleft (**arrow**). A separate premaxillary element cannot be detected within this cleft, but specimen is distorted and actual appearance in life remains uncertain. In B, nasal aperture is dorsally damaged on both sides, but on specimen's left side its margin or sill seems to be essentially intact, especially ventrally. External wall of canine alveolus is smooth, with no evidence of a complex sutural surface for lateral maxillopremaxillary suture. *Trigonostylops* possessed nasals of normal proportionate length that extended to end of rostrum (B, C). In C, nasals and maxillae are not in contact along their shared borders (**arrow**), but this seems to be a consequence of postmortem separation of nasomaxillary sutures, not presence of intervening process of premaxilla. In D, note presence of 3–4 infraorbital foramina in a nearly linear arrangement.
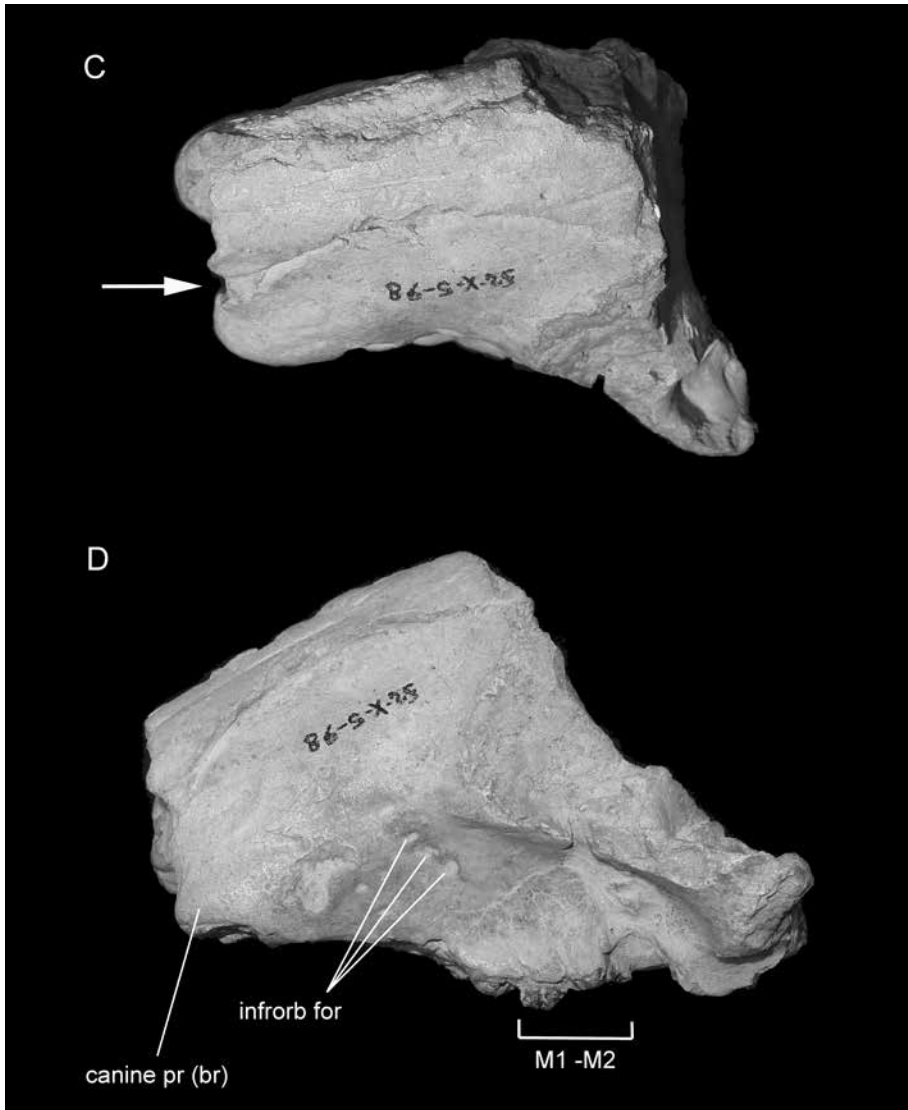
protoconid than to metaconid (unlike litopterns). Bunoid entoconid, not expanded transversally into entolophid (unlike notoungulates). Lower m3 without distinct posterior lobe, as in all astrapotheres (unlike litopterns and many basal notoungulates).

Absence of upper incisors and identification of canines. Scott (1937b: 349) pointed out that the highly distinctive mandibular incisors of *Astrapotherium* **(C3, C4)** (Gaudry, 1904; Lydekker, 1893: pl. 22) are sometimes encountered in a heavily worn condition, indicating that they must have occluded against something fairly resistant. Yet upper incisors are unknown in either trigonostylopids or astrapotheriids. This interesting problem is reserved for later discussion (see p. 77, Premaxillae).

Originally, possession of large, laterally projecting mandibular canines **(C17-C19)** was one of the few positive reasons for supporting an astrapothere affiliation for *Trigonostylops*, but Simpson (1933a) was dubious about evidence for
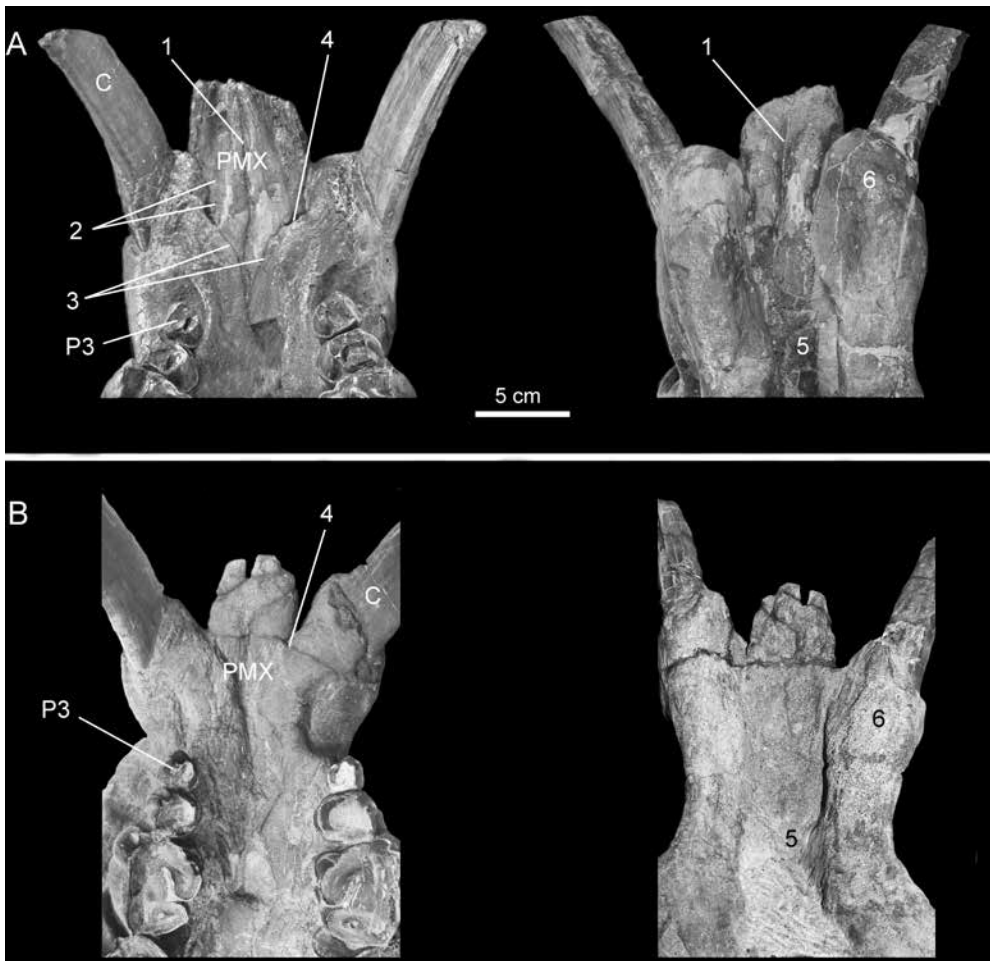
FIG. 22. *Astrapotherium magnum* **A,** AMNH VP-9278 and **B,** YPM PU 15261, rostral end of palate in ventral and dorsal aspects. Long tongue of bone in center of each view is composed of fused palatal processes of right and left premaxillae. In all examined astrapotheriid specimens preserving premaxillae, these elements are completely edentulous (in B, projections on rostral margin represent broken edge of premaxillae). In B, ventral and dorsal surfaces of premaxilla are flat without grooves; sutures are fused or hidden by matrix, and left premaxilla has been medially crushed onto right premaxilla. **Key: 1,** interpremaxillary suture (partly obliterated in YPM PU 15261); **2,** ?grooves, exposed by breakage (in AMNH VP-9278 only); **3,** medial (internal) maxillopremaxillary sutures; **4,** ?foramen exposed in latter suture; **5,** floor of nasal cavity; **6,** terminal part of maxilla bearing canine tusk. Incisive foramen not securely identified (see text). In figure 42, compare lengthy lateral maxillopremaxillary suture in *Mesotherium* with its absence in *Astrapotherium* (**C157,** facial process of maxilla).

canine conformation in this taxon. Gaudry (1904) had previously identified, as canines, a pair of tusklike teeth in a jaw assigned to *Trigonostylops*, but his inference regarding dental loci was not conclusive because the specimen he examined had only two pairs of lower incisors. Later work demonstrated that individuals of

Trigonostylops typically possessed three pairs of mandibular incisors in addition to the lower tusks (fig. 3C), confirming that the latter were indeed true canines.

In regard to the upper tusks, conditions in *Trigonostylops* MACN Pv 47 and MLP 52-X-5-98 (fig. 21) as well as *Tetragonostylops apthomasi*

DGM 355-M favored the idea that the large teeth implanted at the rostral end of the snout were canines rather than incisors (see Gaudry, 1904; Paula Couto, 1952: pl. 41, fig. 1), although without a lateral maxillopremaxillary suture as a guide this inference had to remain tentative (see p. 77, Premaxillae). Yet by 1967 Simpson had come to the conclusion that canine enlargement had indeed occurred in the course of trigonostylopoid evolution, in a direction similar to that seen in astrapotheriids. This presumably informed his decision to transfer *Albertogaudrya*, which exhibits large, projecting canines in both jaws, from Astrapotheria to Trigonostylopoidea (Simpson, 1967).

Palatal, Facial, and Nasal Regions

Palatal architecture. The palate of AMNH VP-28700 is essentially flat, lacking rugosities but with a slight midsagittal bulge that is more prominent rostrally than caudally (figs. 1A, 2). MACN Pv 47 and MACN A 11078 are similar but with a more noticeable bulge. In *Tapirus* by contrast the rostral part of the hard palate is markedly arched. To a lesser degree this is also the case in rhinos and horses. The palatal diverticulum of *Trigonostylops* is described above (see p. 51, Interpreting Pneumatization).

The palate is bordered by well preserved, slightly diverging rows of cheekteeth (P2–M3, last molar present on right side only). As already noted, the P2 is preceded by a long diastema that would have extended well beyond the end of the remaining part of the palate according to Simpson's (1933a: fig. 1) interpretation, which is in good agreement with palatal structure in MACN A 11078, a more complete specimen. The P1 is not present in AMNH VP-28700, although in CT segments a small, incomplete alveolus for it can be seen near the specimen's rostral end.

The rostralmost part of the palate is completely missing in AMNH VP-28700. Simpson's (1933a: fig. 1) drawing of the skull in lateral view implies that a considerable portion had been lost, a conclusion confirmed by MLP 52-X-5-98 (fig.

21). Interestingly, the incisive foramen, usually easy to identify in mammals as a wide embrasure at the front of the palate (fig. 23), is not represented in any obvious way in either of these specimens. Scott (1937b: 317) noticed apparent absence of this foramen in the astrapotheriid material available to him, a point that warrants further attention (see fig. 22).

Palatal alate process. In most mammals, the caudal margin of the hard palate is simply a flat, sometimes thickened rim supporting the tissues of the soft palate. Some SANUs display elaborate bony structures in this area (see Billet, 2011), which is also the case in *Trigonostylops wortmani*. AMNH VP-28700 bears an unusual eminence (fig. 20A) on the palate's caudal margin which Simpson (1933a: 7) termed the "alate posteromedian process" (hereafter, palatal alate process):

> The posterior border of the palate and the choanae likewise present very striking features which appear to be quite unique. Near the posterior end of the surface of the palate, the palatines form a prominent median process, with an anterior median crest, and a broad, shallow, irregular posterior groove running obliquely up into the choanae. On each side this process is produced into a pointed, wing-like process, between which and the general surface there is a large open groove.

The features that Simpson listed are indeed uncommon, as stated, although he did not go on to discuss their possible morphological or physiological significance. In transverse section, each winglike projection of the palatal alate process shields a deep groove (figs. 12C, 20A). The groove's radius of curvature is much larger than would be required to transmit a neurovascular bundle, but perhaps not for a muscle involved in controlling the oropharyngeal opening (see below). None of the other specimens of *Trigonostylops* available for this study preserves this part of the palate.

In *Homo*, the soft palate extends caudally from the hard palate as a flexible curtain, enclos-
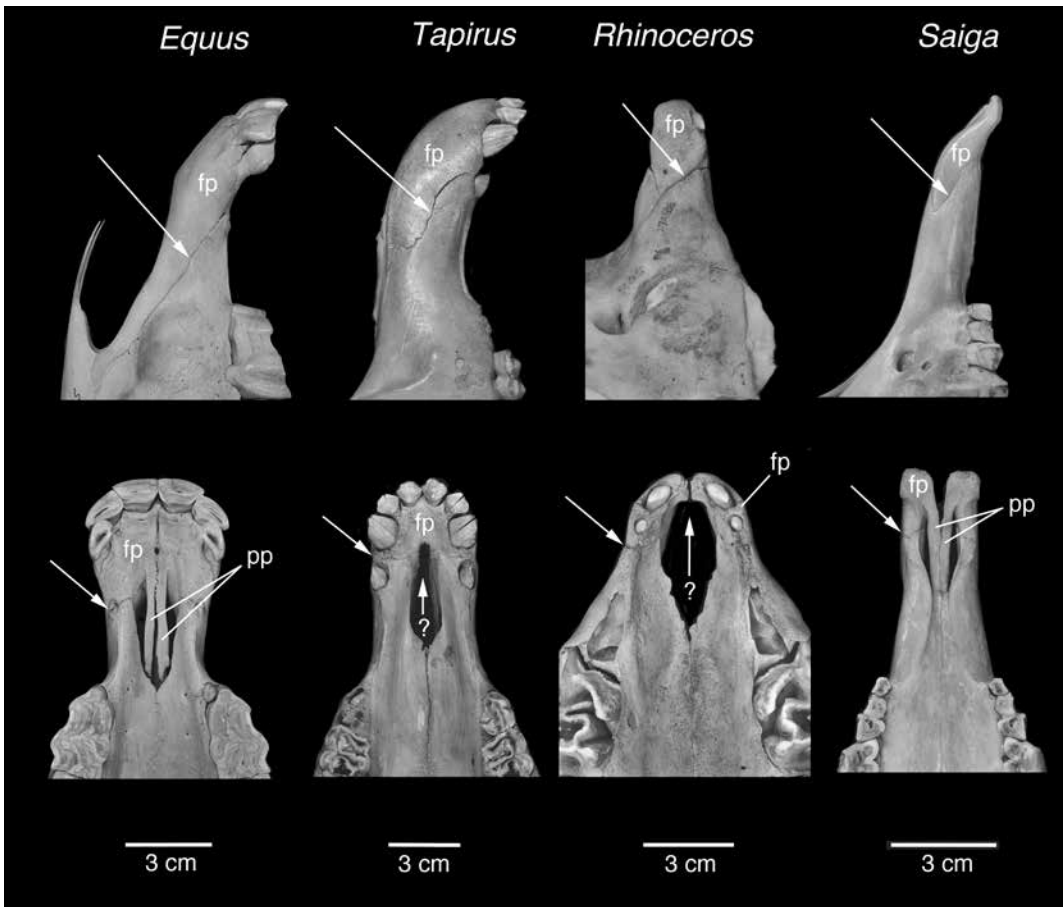
FIG. 23. Premaxilla morphology in extant euungulates in right lateral (**top**) and ventral (**bottom**) views (*Equus caballus* AMNH M-204155; *Tapirus indicus* AMNH M-200300; *Rhinoceros unicornis* AMNH M-274636; *Saiga tatarica* AMNH M-85305). Note differences in scale. **Key: fp,** facial process of premaxilla, tooth bearing in perissodactylans as well as most other mammals; **pp,** palatal processes of premaxilla, subdividing or flooring incisive foramen when present. On external surface of rostrum, **angled white arrow** points to lateral part of maxillopremaxillary suture, present in all specimens illustrated. In skulls of young *Tapirus* and *Rhinoceros*, palatal processes are either tiny or unrecognizable as such (**midline white arrows**), indicating possible non-development (hence question mark) even though premaxillae are otherwise robust. In *Saiga* and other pecorans, premaxillae develop complete facial and palatal processes, even in absence of upper incisors, along with lengthy maxillopremaxillary suture on rostrum's outer surface. In *Astrapotherium* (fig. 22), facial process and lateral portion of maxillopremaxillary suture are absent.

ing muscle fibers, vessels, nerves, and other structures, such as the uvula, which jointly define the boundary between the oral and pharyngeal portions of the upper throat (Warwick and Williams, 1973). Laterally bounding the soft palate and continuous with it are two symmetrical muscular arches formed by the palatoglossus and palatopharyngeus muscles. These in turn insert into other structures lining the throat to help frame the oropharyngeal aperture. In the case of the palatoglossus muscles, insertions include the side and dorsum of the tongue; when these muscles contract they not only narrow the distance between them but also raise the tongue's root

(Warwick and Williams, 1973). This has the effect of closing off the oral cavity from the pharynx, which, together with the synchronized actions of other muscles involved, provides part of the essential anatomical basis for swallowing.

The basic architecture of the muscular pharyngeal arches is probably similar in all terrestrial placentals, but there are many differences in detail. For example, in *Equus* the soft palate is relatively elongated, and its flaplike caudal margin contacts the epiglottis of the larynx (Sisson and Grossman, 1953). This arrangement creates a moveable barrier that may be used to close off the oral cavity from the nasal cavity and pharynx, an arrangement that is said to account for the fact that mouth breathing does not occur in horses under normal conditions (Hare, 1975). In *Trigonostylops* the wide lateral grooves on the palatal alate process may have borne robust versions of the palatoglossus muscles, possibly indicating that the soft palate was thick and muscular, thereby enhancing its sphinctering action for isolating the nasopharyngeal and oroesophageal pathways.

Simpson considered the palatal alate process of *Trigonostylops* to be unique. However, in our comparative set a close approach to conditions in *Trigonostylops* occurs in *Tapirus terrestris* AMNH M-77576, in which there is a wedge-shaped platform reminiscent of, but less projecting than, the alate process of AMNH VP-28700 (fig. 20B). Within *T. terrestris* this feature seems to be variable, other specimens showing only a slightly raised midline swelling with ill-defined margins. Nevertheless, the fact that such a specialization occurs at all in this region may imply a capacity for enhanced constriction at the pharyngeal entrance in *T. terrestris*. No similar feature was encountered in specimens of other tapir species (or in rhinos and horses).

In a later paper concerned with description of a skull of the Casamayoran astrapotheriid *Scaglia kraglievichorum* (MMP M-207), Simpson (1957: 14) noted that "there is a slight tubercle on the ventral aspect of the palatine at each side of the rim of the choanae, but it is much more lateral in position and is in any case not a strong process as in *Trigo-*

nostylops." (Only the right-hand tubercle is still present on this specimen.) Although differences certainly exist, the fact that both taxa exhibit a specialization of this part of the bony palate may reflect presence of a shared function. The caudal part of the palate is not preserved in the available material of *Tetragonostylops* (Paula Couto, 1952; Kramarz et al., 2019b) or *Astraponotus* (Kramarz et al., 2010).

Specializations of the caudal part of the palate also occur in notoungulates, although their configurations are rather different. In toxodontians especially (e.g., *Adinotherium*, *Toxodon, Nesodon*), but also in a variety of typotherians (e.g., *Protypotherium*, *Hegetotherium*, *Cochilius)*, the plane of the hard palate is continued by large, flat processes of the palatine bones (postpalatine platform) that project backward to ventrally border the choanae (see Lydekker, 1893; Scott, 1912; Simpson, 1932; Billet, 2011). Presumably, the platform functioned at least in part for muscular attachment and, given its position, may have likewise influenced oropharyngeal movements.

Premaxillae (C88, C89, C156). The fused premaxillae (for simplicity, "the premaxilla") may be described as consisting of two parts: a facial process, which in most mammals contains the incisor loci and is externally bounded by a lengthy suture (the lateral part of the maxillopremaxillary suture, or in some cases the nasopremaxillary suture); and a palatal process, which comprises the rest of the bone and is bounded by or includes the medial part of the maxillopremaxillary suture and (usually) the incisive foramen (figs. 23, 42). Developmental studies of the premaxilla in a variety of mammals (e.g., Fawcett, 1921; De Beer, 1937; Parrington and Westoll, 1940; Teng et al., 2019) are consistent with the view that in many taxa its facial and palatal components are ossified from discrete centers. This does not mean that they represent phylogenetically separate bones that fuse together primordially, but it does lay a basis for discussing whether one or the other constituent of the premaxilla may be lost or reduced during evolution without affecting the differentiation of the other (cf. loss of prenasal process of premaxilla in mammals due to fusion of external nasal openings; Maier, 2020).

At present there is no direct evidence bearing on the condition of the premaxilla in *Trigonostylops*. The only reasonably well-preserved rostrum available for this taxon, MLP 52-X-5-98, ends at the maxillary prominences containing the canine alveoli (fig. 21). On the fossil's more complete left side, a thin, slightly raised sill borders the nasal aperture and extends onto the ipsilateral prominence (fig. 21B), the rostral face of which lacks corrugations suggestive of a sutural surface. In this specimen a small cleft (best seen in ventral aspect, fig. 22A) divides the prominences in the midline, although whether this condition is natural or the result of postmortem deformation cannot be determined because the equivalent area is not preserved on other fossils. Nonetheless, this feature is of interest because Simpson (1933a: 6) remarked that the unknown premaxilla of *Trigonostylops* might have been reduced by "analogy with the functionally similar astrapotheres," in which a cleft between the maxillary palatal processes is not only present but also clearly natural. In well preserved specimens of *Astrapotherium* and *Parastrapotherium* (figs. 4, 22A, B), this gap is occupied by bony elements sutured in the midline to each other and caudolaterally to the maxillae. In less well preserved specimens the midline elements are often broken away, producing a divided rostrum somewhat similar to that of *Trigonostylops* MLP 52-X-5-98.

Scott (1928, 1937b) regarded these elements in astrapotheres as comprising the premaxilla, an identification supported here but with the proviso that they represent the palatal or paraseptal (Fawcett, 1921) component of the primitive mammalian premaxilla—the element's facial part supporting the incisor dentition having been lost or greatly reduced during evolution (cf. fig. 23). In *Astrapotherium magnum* AMNH VP-9278 the partially restored premaxilla juts well beyond a transverse line passed through the alveolar margins of the tusks (fig. 4), but not so far as to provide any likelihood that the lower incisors could have contacted it during occlusion (see below).

As Scott (1928: 318) also noted, the premaxilla in AMNH VP-9278 is ventrally incised by

deep parallel troughs (fig. 22A), whereas in most *Astrapotherium* specimens the ventral surface of the premaxilla is smooth and flat (e.g., fig. 22B). This is probably also the case in *Parastrapotherium*, and possibly in the uruguaytheriine astrapothere *Hilarcotherium castanedaii* (Vallejo-Pareja et al., 2015). It has not been possible to establish whether the grooves in AMNH VP-9278 are natural, the result of damage, or due to the method of restoration.

The scan of MACN A 8580 reveals a large canal passing through the palatal process of the maxilla on each side (fig. 13C, D). This feature appears to be the nasopalatine canal, which typically transmits to the incisive foramen a neurovascular bundle consisting of the nasopalatine nerve of CN 5.2 and the sphenopalatine artery and vein. In MACN A 8580 the nasopalatine canals are truncated because the premaxilla is missing. It is therefore not clear where the contained vessels and nerve might have emerged on the palatal surface, because there is no conventional incisive foramen in the expected midline position. This is also the case in *Hilarcotherium castanedaii* (Vallejo-Pareja et al., 2015). Scott (1928) noticed the foramen's absence, and thought that the nasopalatine canal's contents must have passed through the notch between the maxilla and premaxilla. In AMNH VP-9278 possible foramina appear to lie within the medial part of the maxillopremaxillary suture on each side, but in MACN A 8580 a similar feature is only seen on the specimen's left side (the right side is distorted) (fig. 22: feature 4). As already mentioned, whether the grooves on the ventral surface of the premaxilla in AMNH VP-9278 transmitted anything is uncertain, but it is relevant to note that exit foramina are never seen on the premaxilla's rostralmost edge in other specimens preserving this element.

However the nasopalatine neurovascular bundle might have emerged from its canal in astrapotheriids, comparative anatomy indicates that the nerve's only target area would have been the palatal mucosa and gums, as in mammals generally (Sisson and Grossman, 1953; Warwick and Wil-

liams, 1973). Speculatively, the sphenopalatine artery and vein might have been in a position to communicate with vasculature in the upper lip and base of the nose, and thus help to supply the proboscis—if *Astrapotherium* in fact possessed such a structure (Scott, 1937b). *Tapirus* possesses a small proboscis, but Witmer et al. (1999) found that the infraorbital artery is its main supplier of blood, with some assistance from anastomoses with branches of the facial artery. Anastomoses with the sphenopalatine or greater palatine arteries were not mentioned, which suggests that their involvement was negligible or nonexistent. Apart from this, it is reasonable to infer that any trunk-like muscular structure associated with the external face of *Astrapotherium* would have received motor innervation exclusively from CN 7, exactly as in elephants (cf. Sprinz, 1952), while sensory innervation would have been supplied by the infraorbital nerve, not the nasopalatine nerve. The routing of the nasopalatine ducts of the vomeronasal organ is uncertain. Because the ducts are always situated close to the midline on either side of the nasal septum, perhaps they passed through another part of the maxillopremaxillary suture.

Lack of a facial process of the premaxilla in astrapotheriids may have had other morphological consequences, some of which might have affected soft tissues. Commenting on the almost-certain absence of upper incisors in *Astrapotherium* (see p. 69, Dentition and Upper Jaw), Scott (1937a: 534) suggested that the high level of attrition on lower incisor crowns, noted earlier, might have been a result of these teeth wearing against a "horny band" on the underside of the inferred proboscis. Although there is no extant model for such a pattern of incisor/proboscis occlusion in mammals, it is hard to suggest an alternative. In an earlier paper Scott (1928: 318) briefly developed a different explanation for incisor wear in this taxon: the lower incisors may have occluded against a resistant dental pad reminiscent of the pulvinus dentalis of ruminant artiodactylans. This structure consists of heavily keratinized stratified squamous epithelium overlying a thick layer of dense, irregular connective tissue, firmly

seated on the palatal portion of the premaxilla (Sisson and Grossman, 1953; Habel, 1975: fig. 29-4; Frappier, 2006). Extant ruminants also lack upper incisors (except for the laterals, present in Camelidae only: Janis and Theodor, 2014), but they are able to efficiently crop plant stems or leaves by working the lower incisors against the premaxillary dental pad. The trouble with this argument, as Scott (1937a: 534) later realized, is that the rostral end of the jaw in *Astrapotherium* AMNH VP-9278 extends well beyond the bony limits of the upper jaw, obviating any possibility that lower incisors wore against structures supported on the edentulous premaxillae. This seems definitive as—uniquely for this genus—the AMNH skull and jaw are said to represent a single animal. As there are no associated skulls and jaws of *Trigonostylops*, our reconstructions omit both underbite and proboscis (see fig. 3D and p. 4).

Finally, in the few known cases of a cartilago proboscidis or os proboscidis in extant mammals (e.g., *Solenodon*; Wible, 2008), the lower jaw does not extend far enough rostrally to contact this feature, and the role of this rarely encountered skeletal element seems to be unrelated to mastication. In any case, such speculations are interesting but do not solve the puzzle of incisor function in astrapotheriids.

Although very incomplete, the partial rostrum of *Eoastrapostylops riolorense* PVL 4217 (paratype) lacks any positive evidence for premaxillary facial processes extending lateral or rostral to the canines. There is a V-shaped notch between the canines (Kramarz et al., 2017), but as all relevant edges are damaged it cannot be determined to what degree *Eoastrapostylops* might have resembled *Tetragonostylops* in this regard (see Paula Couto, 1952). The type of *E. riolorense* (PVL 4216) also preserves both canines, but here too there is no positive evidence for premaxillary structure. However, it should be mentioned that the nasals, as preserved on the holotype, are striplike and do not completely cover the dorsum of the rostrum. Although it is conceivable that the true nasals are actually missing and that the striplike elements

are in fact extensions of the facial processes of the premaxillae, no other SANUs exhibit this kind of rostrum configuration.

Extant perissodactylans vary significantly from one another (fig. 23). In *Equus* the two components of each premaxillary element are differentiated, with a laterally prominent, tooth-bearing facial process completing the dental arcade, and a slender palatal process extending across (and thus partially subdividing) the incisive foramen (see Sisson and Grossman, 1953: fig. 43). The palatal processes are rostrally connected to the premaxilla's facial portion by narrow bridges, but their caudal ends are free. They are obviously not involved in buttressing the facial process and serve only to frame the incisive foramen. By contrast, in extant ceratomorphs palatal processes seem to be either completely absent or barely suggested by tiny prongs situated on the rostral margin of the undivided incisive foramen (see fig. 23; cf. Moyano and Giannini, 2017). In tapirs each facial process is robust and bears a full incisor dentition, as in the horse, but in rhinos the process is small, bearing either one incisor or none at all (Nowak, 1999). In ruminant artiodactylans narrow palatal processes are also present, but they terminate rostrally against the flat surfaces of the facial processes supporting the dental pad (e.g., *Saiga*, fig. 23D).

Normal ontogeny of the premaxillae in perissodactylans and artiodactylans has not been investigated in sufficient detail to know precisely how they ossify, although it is claimed that in the horse each premaxilla ossifies from a single center (Sisson and Grossman, 1953: 62). This does not exclude the possibility that, during an early stage of intramembranous ossification, the palatal processes differentiate in mesenchyme separately from the facial portions, but seamlessly fuse thereafter as is known to happen in the development of calvarial bones (Teng et al., 2019). As already mentioned, the existence of multiple centers of ossification in the fetus does not indicate that the bone in question is made up of phylogenetically independent elements that have undergone primordial fusion (cf. multiple

centers in petrosal; De Beer, 1937; Hall, 2015). For example, palatal processes are not likely to represent suppressed septomaxillae, because there are taxa in which septomaxillae and premaxillary palatine processes arguably cooccur (e.g., *Priodontes*, *Euphractus*; Starck, 1967).

Frontals. The partly reconstructed right orbital (or zygomatic) process of the frontal of AMNH VP-28700 may have been somewhat projecting, but there is no reason to believe that it contributed to a once-complete postorbital bar (fig. 25). Complete postorbital bars are also lacking in the best-known astrapotheriids (*Astraponotus*, *Astrapotherium*, and *Parastrapotherium*; Scott, 1928, 1937b; Kramarz et al., 2010), as well as all notoungulates. By contrast, a complete bar occurred in many litopterns (proterotheriids, the macraucheniine *Macrauchenia* and its close relatives). Among extant perissodactylans only *Equus* exhibits a complete bar.

Infraorbital foramina. The outlet for the infraorbital neurovascular bundle is represented by four or five daughter foramina on the preserved right lower face of *Trigonostylops wortmani* AMNH VP-28700 (fig. 24). The equivalent area on MLP 52-X-5-98 exhibits at least three infraorbital foramina (fig. 21D), indicating that AMNH VP-28700 is not unique in this regard. Because of damage it was not practicable to trace all the foramina back to the main infraorbital canal. The ventralmost aperture in this specimen may be an artifact.

Simpson (1933a: 6) regarded multiple infraorbital foramina as "one of the most striking of the many very unusual features" of *Trigonostylops*, but duplication is seen in other placental species, including various SANUs. Although *Astrapotherium magnum* AMNH VP-9278 and YPM PU 15117, 15261, and 15332 exhibit a single foramen, *Astrapotherium* sp. MLP 38-X-30-1 has three (Kramarz et al., 2010). *Astraponotus* sp. MPEF PV 1279 has two foramina, as does *Tetragonostylops apthomasi* DGM 216-M and *Scaglia* cf. *kraglievichorum* MPEF PV 5478, while the juvenile *Astraponotus* sp. MPEF PV 1296 has at least three (Paula Couto, 1952; Kramarz et al., 2010, 2019b). *Scaglia kraglievi-*
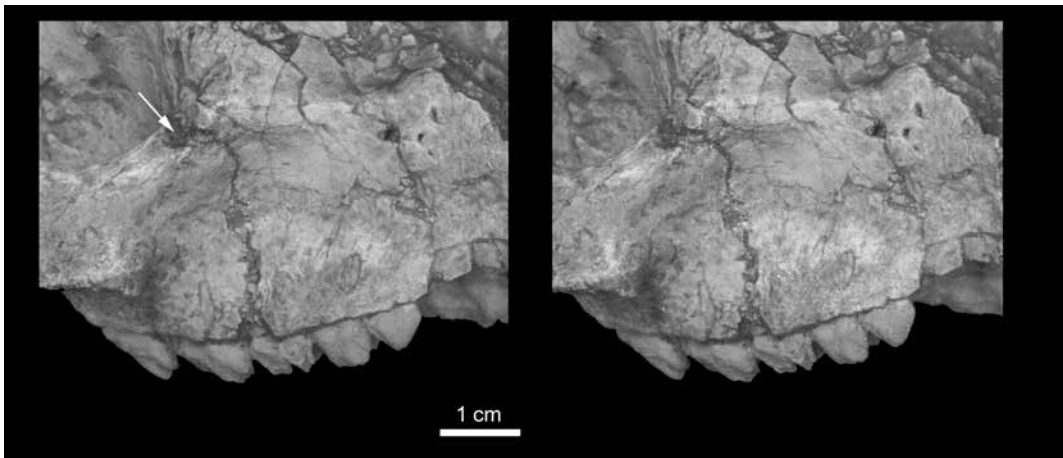
FIG. 24. *Trigonostylops wortmani* AMNH VP-28700, right facial region, showing multiple infraorbital foramina (stereopair). See also figure 25. Lacrimal foramen (**arrow**) and tubercle also visible on orbital rim.

chorum MMP M-207 and *Eoastrapostylops riolorense* PVL 4216 exhibit single foramina (Soria and Powell, 1981; Kramarz et al., 2017), insofar as can be determined. Two foramina are also seen in *Pyrotherium romeroi* FMNH P13515 (Billet, 2010) and the "condylarthran" *Didolodus multicuspis* (Simpson, 1948). Multiple foramina have not been reported for any notoungulates, but a few examples are known in proterotheriid litopterns (Soria, 2001). In extant perissodactylans a single infraorbital foramen is the rule, but there are certainly exceptions (including left-right foraminal asymmetry in *Tapirus indicus* AMNH M-180030; see Witmer et al., 1999). In *Equus* the dorsal labial branch of the maxillary nerve, which supplies the upper lip, may have a separate foramen on the rostrum (Leisering, 1888: plate 38, fig. 2), but it is always comparatively tiny and is not here regarded as an example of an additional infraorbital foramen. In any case, there are no known functional correlates of multiple foramina, and Simpson's enthusiasm for this character seems misplaced.

Nasals (C85, C88, C90). Although the nasal bones are not preserved on AMNH VP-28700, Simpson (1933a: fig. 1) inferred that they were probably short and jutting in *Trigonostylops*, suggesting an arrangement something like that of extant *Tapirus*. This is incorrect: the partially intact nasals found on MACN Pv 47, MACN A

11078, and MLP 52-X-5-98 (fig. 21) establish that these elements extended to the end of the fairly lengthy rostrum (Soria and Bond, 1984). On these specimens the proximal and distal ends of the nasals are slightly flared compared with the middle section, which imparts a waisted appearance to the rostrum as seen from above. Due to damage or incompleteness almost nothing can be ascertained about the internal anatomy of the nasal cavity in *Trigonostylops* (see fig. 12B, C).

Nasals are notably abbreviated in extant tapirs and rhinos, but much less so in horses. As noted, astrapotheriids have highly reduced nasals; conditions in *Eoastrapostylops riolorense* PVL 4216 are uncertain. Nasal reduction is even more extreme in some macraucheniids (Forasiepi et al., 2016), all of which might be correlated with hyperdevelopment of the soft tissues of the lower face in the form of proboscises, hydrostats, or similar structures in these taxa.

Choanae. Simpson (1933a: 7) considered one other feature of the nasal region of *Trigonostylops* as worthy of mention: "Within the choanae the palatines send upward a stout median process, fully united to the presphenoid or vomer, so that the choanae are divided into two wholly separated orifices." Simpson drew attention to this feature not because it was unusual—in adult therians the choanae are normally separated into two orifices by a
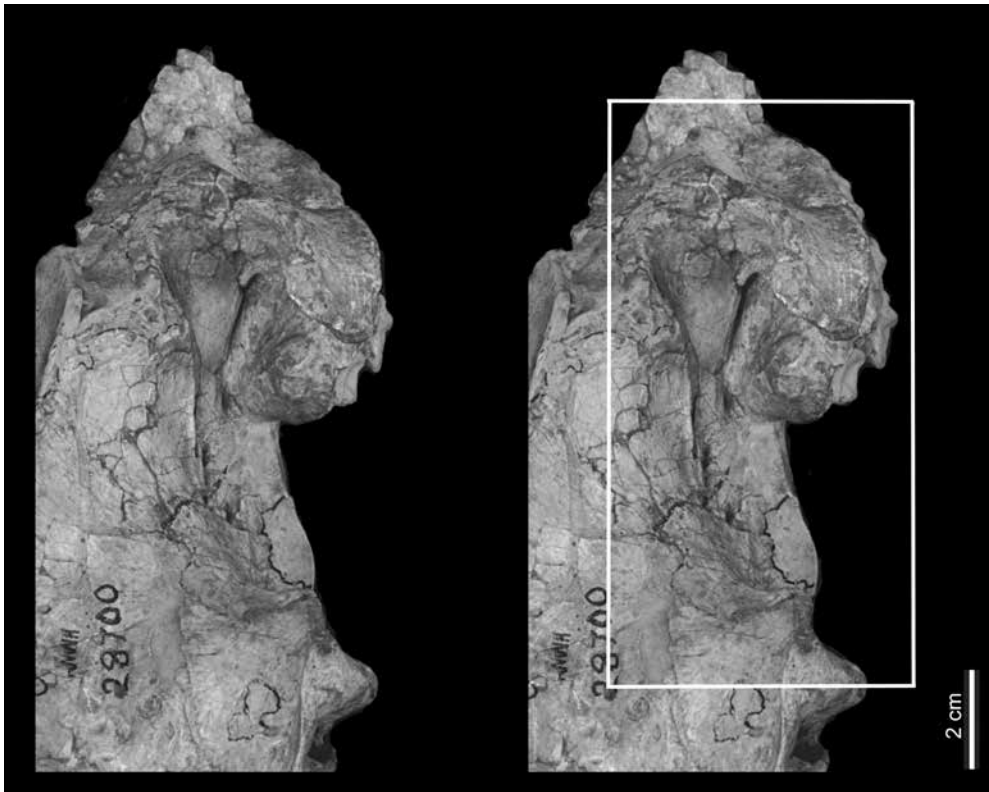
FIG. 25. *Trigonostylops wortmani* AMNH VP-28700, right orbital and infratemporal regions. **A,** oblique right lateral aspect (stereopair), **B,** interpretative diagram (on page opposite), based on Simpson's (1933a) original figure 2 but relabeled to conform with identifications and nomenclature used in this paper. Zygomatic arch shown in section (hachure). Conspicuous groove running dorsorostrally from cranioorbital foramen is probably vascular; in some mammals (e.g., rodents, many eulipotyphlans) a similarly positioned trackway carries retained orbital branch of stapedial ramus superior (Bugge, 1974). Multiple infraorbital foramina are more obvious in figure 24. **Single asterisk**, small aperture, possibly but not certainly a foramen. **Double asterisks**, groove for lesser palatine neurovascular bundle, passing around caudal end of maxillary tuberosity.

bony septum (Moore, 1981)—but because *Astrapotherium* was supposedly different and therefore unlike *Trigonostylops*. In characterizing the choanae of *Astrapotherium* as "tubular, undivided," Simpson (1933a) unfortunately did not specify whether he meant that the choanae were undivided for their whole length, or only at their caudal outlet due to the vomer and perhaps the palatines failing to extend all the way to the far end of the choanal opening. Although the term *choana* means "funnel," not "aperture," recent investigators have chosen to define choanal characters on the basis of the latter reading (e.g., Johnson and Madden, 1997;

Kramarz and Bond, 2009; Vallejo-Pareja et al., 2015). The distinction between *Trigonostylops* and *Astrapotherium*, such as it is, seems trivial, especially in comparison to the remarkable similarity in the diminutive size of their choanal openings in relation to nasal cavity volume (figs. 1A, 4A).

Orbital and Infratemporal Regions

The capacious area of origin for temporalis musculature in *Trigonostylops* is bounded rostrally by the temporal lines and ventrally by a nearly continuous crest running from the mar-

gin of the mandibular fossa to the medial wall of the orbit (fig. 1C, D). Within the orbit the crest presumably supported periorbital dense connective tissue. Below the crest lies the infratemporal surface, which presents the series of foramina noted below. The rostral and ventral orbital walls of AMNH VP-28700 are mostly preserved, but other borders are in poorer condition.
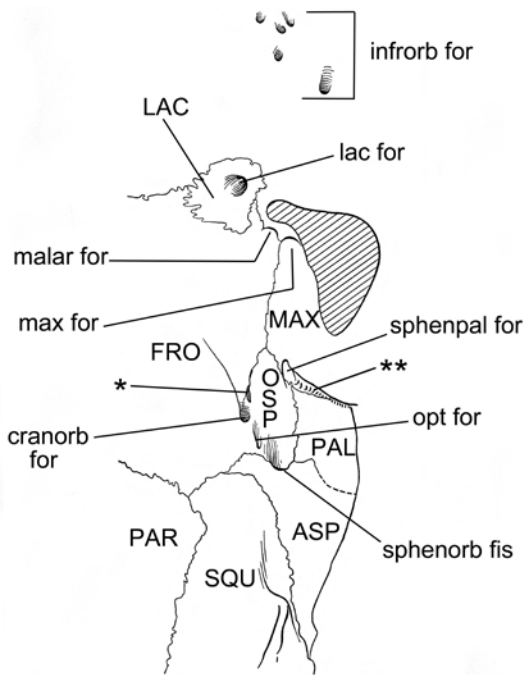
Orbit and orbital mosaic (C92, C94). Simpson attempted to define sutural boundaries in the orbital mosaic of *Trigonostylops* but admitted uncertainty in some areas. According to his reconstruction (Simpson, 1933a: fig. 2; reproduced here in revised form as fig. 25), the palatine and maxilla played only a small role in framing the lower part of the medial wall of the orbit, which was otherwise almost entirely formed by the orbital wing of the frontal. Segmental information agrees with Simpson's depiction. In *Astrapotherium magnum* AMNH V-9278 the maxillary contribution to the orbital mosaic is either absent or very minor. Other astrapotheriid specimens are either damaged or reconstructed in this area.

The frontal is also the largest member of the orbital mosaic in living perissodactylans. In *Tapirus indicus* AMNH M-77875, in which the sutures of the mosaic are well defined, the maxilla does not extend dorsomedial to the sulcus that directs the maxillary nerve toward the maxillary foramen and thus makes no contribution to the orbital wall. The maxilla also lacks an orbital projection in the rhinos *Ceratotherium simum* AMNH M-51882 and *Rhinoceros unicornis* AMNH M-274636, both of which are young specimens with open sutures. The juvenile horse *Equus caballus* AMNH M-204155 is similar to these ceratomorphs.

Simpson did not indicate the caudal part of the frontoorbitosphenoid suture in his illustration of AMNH VP-28700 (fig. 25), and because of breakage it is not evident where the suture would have been situated. The large ascending process of the orbitosphenoid (presphenoid of Hillman, 1975) seen in *Equus caballus* AMNH M-204155 and *Tapirus indicus* AMNH M-77875 is lacking in extant rhinos.

Cranioorbital sulcus and ethmoidal foramen. Simpson's (1933a: fig. 2) candidate for the optic canal of *Trigonostylops* in AMNH VP-28700 is a small opening on the rear wall of the orbit, but segmental data reveal that this aperture leads into the sulcus for the cranioorbital sinus (fig. 8, top). Segments also show that the true opening of the optic canal is situated just below and behind the latter, as depicted in figure 25. On the medial wall of both orbits a deep groove runs out from the cranioorbital foramen. This may have conducted a branch of the supraorbital artery toward the dorsal wall of the orbit (Cartmill and MacPhee, 1980; Diamond, 1992). Billet and Muizon (2013) discussed the likelihood of cranioorbital arterial presence in several notoungulates (*Plesiotypotherium*, *Mesotherium*, *Leontinia*; see also Martínez et al., 2016).

Because the forebrain and interorbital region are extensively damaged in AMNH VP-28700 it is not certain where the bony aperture for the ethmoidal neurovascular bundle would have been located. In endocasts of extant perissodactylans it

consistently appears as an eminence on the side-wall of the olfactory tract, a typical position in mammals (fig. 10: feature d). There are small openings in the vicinity of the cranioorbital foramen in AMNH VP-28700 (e.g., fig. 25: asterisk), but whether they were functional foramina, as opposed to artifacts, cannot be determined from inspection or segmental data given the amount of breakage. None seems large enough to be the ethmoidal foramen, which in the horse transmits a thick bundle (cf. fig. 5D). A remote possibility is that the cranioorbital sinus and the ethmoidal nerve and its associated vasculature shared the same aperture, or—more likely—their outlets were so closely positioned that they cannot be separately distinguished on this damaged specimen. On the endocast of *Tapirus indicus* AMNH M-200300, indicia for these features are situated at almost the same position in lateral view (fig. 10: feature d), although on the skull itself their foramina are not interconnected. In *Equus* the aperture in the equivalent place is always called the ethmoidal foramen (e.g., Hillman, 1975: 339, fig. 15-142), but in this taxon no confusion exists because the cranioorbital vasculature is either absent or reduced to a twig.

Russell and Sigogneau (1965: fig. 3) distinguished separate cranioorbital and ethmoidal foramina in the Paleocene placentals *Pleuraspidotherium* and *Arctocyon*, but that has not been possible to do for the fossils of most interest here. For example, in *Astrapotherium magnum* YPM PU 15332 there is only one major opening in the dorsal part of the orbital area on the skull's better-preserved left side. This opening might be tentatively identified as an ethmoidal foramen on the argument that indicia for the cranioorbital sinus are not visible in the reconstruction of *A. magnum* MACN A 8580 (fig. 8), but this needs confirmation. The orbital areas of *A. magnum* AMNH VP-9278 are relatively intact, but an aperture in the position expected for the sinus could not be identified on this specimen either. *Parastrapotherium* sp. AMNH VP-29575 is again too damaged for interpretation. Nevertheless, ostensible absence of the cranioorbital venous sinus

and artery in fossils or dry skulls should not be inferred automatically merely because "ethmoidal foramen" is the default choice in the literature.

No aperture conforming to the foramen for the frontal diploic vein sensu Wible and Rougier (2017) could be securely identified in *Trigonostylops wortmani*. Whether one is present in *Astrapotherium* is uncertain. The skull of *Astrapotherium magnum* AMNH VP-9278 (fig. 4B, D) bears an exceptionally large foramen (intact on specimen's left side, reconstructed on right) that penetrates the roof of the orbit just medial to the dorsal postorbital process. This area is damaged in the scanned specimen of *Astrapotherium*, MACN A 8580, but segmental data indicate that the foramen joined a short canal suspended within the massive frontal sinus. As in the case of the channel for the temporal sinus in the highly pneumatized retroarticular process of the same specimen (see fig. 14C), the osseous canal in the frontal sinus simply terminates and its contents cannot be traced further. Because of the aperture's proximity to the orbit we tentatively regard it as equivalent to a supraorbital foramen, but the possibility that it is a homolog of the frontal diploic foramen cannot be excluded.

Lacrimal foramen and jugal (C91, C93). The lacrimal foramen of AMNH VP-28700 is relatively large and the bone lacks a tubercle, as Simpson (1933a) noted. The bone itself is preserved on the right side only, and is incomplete. None of the other available specimens of *Trigonostylops* preserve the orbital area, so the accuracy of Simpson's reconstruction of the sutures bounding the lacrimal (figs. 24, 25) cannot be evaluated.

In *Astraponotus* sp. MPEF PV 1279 the lacrimal foramen is small and well exposed, and no sutures are in evidence. However, there is a tubercle, immediately dorsal to the foramen and situated on or near the weakly defined orbital margin. Simpson (1933a) stated that the lacrimal foramen is wholly intraorbital in *Astrapotherium*, although this is not evident on AMNH VP-9278, the orbital rims of which are heavily reconstructed. In his description of *Scaglia kraglievichorum*, Simpson

(1957: 14) noted that the "anterior orbital rim is probably notched, with the lacrimal foramen within the orbit posteromedial to the notch. No facial expansion of the lacrimal is recognized and that bone is probably entirely within the orbit." By contrast, in all extant perissodactylans the lacrimal has a distinct facial component. In tapirs and rhinos, double lacrimal foramina commonly occur on the orbital rim (not within the orbit); *Equus* has a single foramen, also within the orbit (Sisson and Grossman, 1953; O'Leary and Gatesy, 2008; Moyano and Giannini, 2017).

The zygomatic arch is partially present on the right side of *Trigonostylops wortmani* AMNH VP-28700, but Simpson (1933a) gave no description of it. The zygomaticomaxillary suture is not preserved on this specimen. Despite damage to the orbital rim in *Astrapotherium magnum* AMNH VP-9278, it is definite that the jugal exhibits a long rostral extension directed toward the lacrimal. It is not certain, however, whether there was actual lacrimojugal contact. The orbits of *Trigonostylops* are too damaged to permit assessment of this character, and available specimens of *Astraponotus* and *Eoastrapostylops* are similarly problematic. Lacrimojugal contact would not in any case be a distinctive character of this group, as it is also found in notoungulates and *Tetramerorhinus* (and possibly other litopterns) (Muizon et al., 2015).

Sphenoorbital fissure. In *Trigonostylops* this feature is notably elongated, consistent with the length of the mesocranium in this taxon (fig. 25). There is no separate foramen rotundum for CN 5.2, nor recognizably distinct sulci for accompanying blood vessels. Apart from *Granastrapotherium snorki* IGM SCG MGJRG-2018 V4, in which the fissure is undivided (no separate foramen rotundum), available skulls of astrapotheriids are too damaged in this region to evaluate. In the young horse AMNH M-204155 the sphenoorbital fissure is still undivided, but in adult animals there is normally a bony wall defining a separate foramen rotundum (Sisson and Grossman, 1953). In the young *Rhinoceros unicornis* AMNH M-274636 the fissure is also undivided.

In the adult Asian tapir *Tapirus indicus* AMNH M-130108, CN 5.1 and 5.2 share a joint canal, next to which is a separate channel for the maxillary artery. In *Tapirus terrestris* AMNH M-77576 there are separate compartments for CN 5.1 and 5.2 as well as for the maxillary artery, which as in *T. indicus* enters the fissure through the alar canal.

Sulcus and foramen for maxillary nerve and vessels. As is typically the case in mammals, in *Trigonostylops* the channel for CN 5.2 deeply creases the medial margin of the maxillary tuberosity before continuing into the maxillary foramen (fig. 25). This groove, often multipartite in mammals because it also conveys the large maxillary artery and vein, is present in all investigated SANUs as well as extant perissodactylans, although in some it tends to be partly hidden by the large size of the maxillary tuberosity housing the molar roots.

Foramen for malar artery. As already noted (see p. 83, Cranioorbital Sulcus and Ethmoidal Foramen), in AMNH VP-28700 Simpson (1933a: fig. 2) hesitantly identified, as the "ethmoid? foramen," an aperture piercing the frontomaxillary suture immediately dorsal to the maxillary foramen. As he realized, so rostral a position for an aperture normally situated close to the transverse plane of the cribriform plate was improbable.

In a location similar to the one Simpson specified, the horse possesses a foramen (sometimes double) for the malar artery, a small ascending branch of the maxillary/infraorbital artery (Ghosal, 1975: 577, fig. 22-22; Budras et al., 2008: 41). Whether there is also a malar vein has not been reported. Although there are no conclusive indicia for this feature, roughly similar apertures occur in *Rhinoceros unicornis* AMNH M-274636 and *Tapirus indicus* AMNH M-200300. In the former the foramen pierces the lacrimomaxillary suture, while in the latter it is enclosed within the lacrimal. In the case of *Trigonostylops*, it is probably reasonable to conclude that the foramen in question was primarily vascular, conducting vessels irrigating the nasal chamber, but homology with the malar artery of the horse is tentative.

Sphenopalatine foramen (C100, C101). Simpson (1933a) described the sphenopalatine foramen of *Trigonostylops* under the terms "interorbital foramen" and "internal orbital foramen" and noted that it pierced the suture between the maxilla and the orbitosphenoid (fig. 25). Segmental data indicate that the foramen opens medially, directly into the nasal cavity, which is consistent with its having lodged the pterygopalatine ganglion, as in mammals generally. Because of internal damage the distal end of the canal for the nerve of the pterygoid canal could not be identified.

In *Equus*, the sphenopalatine foramen and canal for the greater palatine neurovascular bundle are located immediately next to each other and are housed within a deep joint recess (pterygopalatine fossa), which also includes the entrance to the maxillary foramen further rostrally. By contrast, in *Rhinoceros unicornis* AMNH M-274636 and *Tapirus indicus* AMNH M-200300 these three apertures pierce the medial orbital wall through individual, widely separated ports, and there is no single fossa as such.

In some mammals, including extant perissodactylans, the sphenopalatine foramen may be conspicuously large, seemingly much larger than required for the transmission of the relatively small sphenopalatine vessels and nerves to the nasal cavity. In the white rhinoceros specimen, *Ceratotherium simum* AMNH M-51882, the sphenopalatine foramen is particularly sizeable, although whether it lodged soft-tissue structures other than the ones just mentioned is not known. Sisson and Grossman (1953: 699) note that in *Equus* (the sphenopalatine foramen of which is relatively much smaller) the sphenopalatine vein "forms a rich plexus of valveless vessels on the turbinate bones and the septum nasi… [and the] venous plexuses are remarkably developed in certain parts of the nasal mucosa," yet even in this case the gap seems much larger than required for transmission of vessels. This suggests that the likeliest explanation for the oversized foramen is that it is simply an unossified part of the skull wall, closed by membrane through which vessels

and nerves freely passed. On the right side of *Astrapotherium magnum* AMNH VP-9278, there is a candidate sphenopalatine foramen situated medial to the massive maxillary tuberosity, but it seems to have been artificially enlarged. No similar features have been described in litopterns and notoungulates.

Greater and lesser palatine nerves and vessels. In AMNH VP-28700, the route of the greater palatine nerve and accompanying vasculature could be traced for only a short distance into the damaged palate/rostrum (fig. 12C). Simpson (1933a: 14) stated that a "posterior palatine foramen" (for the greater palatine nerve) could be identified "on the maxillopalatine suture near the antero-external angle of the palatine, with subsidiary foramina in the palatine." The foramina in question are all notably small. Shallow longitudinal grooves, which likely transmitted the palatine neurovascular bundles, run close to the palate's midline in MACN Pv 47 and MACN A 11078 but are not seen in AMNH VP-28700. Greater palatine foramina are also relatively small in *Astrapotherium magnum* AMNH VP-9278 and *Parastrapotherium* sp. AMNH VP-29575, but are always large in extant perissodactylans. Such contrasts in relative foraminal size are surely due to differences in the calibers of related vasculature. In the horse, the greater palatine vein is conspicuously large and terminates in an extensive plexus of valveless veins in the submucosal tissues of the hard palate, through which the greater palatine artery passes to anastomose with its contralateral partner (Leisering, 1888, pl. 4; Sisson and Grossman, 1953: 389). Unfortunately, there are no osteological markers associated with these features, but given foraminal size in the fossil taxa it seems probable that vascularization of palatal soft tissues, at least from this source, was less developed.

In *Equus* the lesser palatine artery is a small vessel that enters the soft palate with its accompanying nerve and vein by passing freely around the maxillary tuberosity (Bradley, 1923: 127; Budras et al., 2008: 40). A groove in the same

position in AMNH VP-28700 suggests the routing of this neurovascular bundle in *Trigonostylops* was similar (i.e., unenclosed by bone; fig. 25D: double asterisk).

CAUDAL CRANIUM

Simpson (1933a: 11) paid special attention to the well-preserved auditory region of AMNH VP-28700 because it was "highly distinctive, fundamentally unlike [that of] any true notoungulate, with some distant and doubtful resemblances to the astrapotheres, and unique in general, although with some minor details suggestive of diverse groups of mammals manifestly quite unrelated to *Trigonostylops*." While it is true that the basicranium of *Trigonostylops* markedly differs from that of known notoungulates, it is not because its "distinctive" features are very much like those of non-SANUs. Indeed, many of the characters to which Simpson drew special attention are better regarded as basal placental apomorphies. Others are specifically much more like those of astrapotheriids than Simpson allowed; a few are closely comparable to equivalents in extant perissodactylans or are sui generis.

Basicranial Foramina and Related Features

Continuous basicapsular fenestra and transiting structures (C110, C114). In *Trigonostylops wortmani* AMNH VP-28700 the petrosal is attached to the rest of the skull only along its lateral and caudolateral surfaces (figs. 12H–K, 26). On its other margins, the petrosal freely projects into the continuous basicapsular fenestra (for definition, see appendix 1). Simpson (1933a: 21) realized that the fenestra, the Γ-shaped gap situated between the petrosal on the one hand and the squamosal, alisphenoid, and central stem elements on the other, was widely open in *Trigonostylops* (see below), especially rostrally, but his figure 5 fails to make this point unambiguously. In his original drawing, reproduced and updated here as figure 26, several features were labeled as separate foramina (e.g., foramen ovale, carotid foramen, "Eustachian" canal) situated at the rostral end of the auditory region. In fact, none of these features appears to have existed as a discrete, bone-bounded aperture, because the vascular, neural, and cartilaginous structures transiting this zone simply passed through (or over) the membranous covering of the continuous basicapsular fenestra. His diagram also suggests that the petrosal closely abuts the elements of the central stem, whereas there is always a narrow gap between them, still filled with matrix in most areas. Simpson (1933a: 23) was more explicit in his text, noting, for example, that the exit point of the CN 5.3 was "not distinctly separated from the [basicapsular fenestra], and the alisphenoid is not pierced anywhere on its exposed surface."

The areas immediately in front of the right and left auditory regions of AMNH VP-28700 were deeply excavated during its original preparation. As may be seen in figure 26A–D, pits are discernible within the excavated areas, bounding the presumed locations of the ports for CN 5.3 and internal carotid artery. Segmental data show that the partitions between the pits, which as prepared appear quite asymmetrical, are largely artifacts, composed of matrix rather than bone. Whether there were notches equivalent to incisurae for the nerve and the artery cannot now be determined. Nor is there a bony canal for the auditory tube; this structure would have simply passed into the tympanic cavity between the rim of the ectotympanic and the rostral pole of the promontorium without being tightly enclosed by either.

The continuous basicapsular fenestra is a normal stage of mammalian basicranial development that allows a variety of neurovascular structures to pass between the ecto- and endocranium (e.g., internal carotid artery and nerve, emissary veins, several cranial nerves). Whether the gap persists as such into adulthood, or resolves into a series of discrete bone-bounded foramina, varies greatly within and among major clades. In the horse the persistent gap is notably wide (fig. 39B), filled with a sandwich of dense connective tissues (Ellenberger and Baum, 1894: 201) resembling those forming sutural boundar-
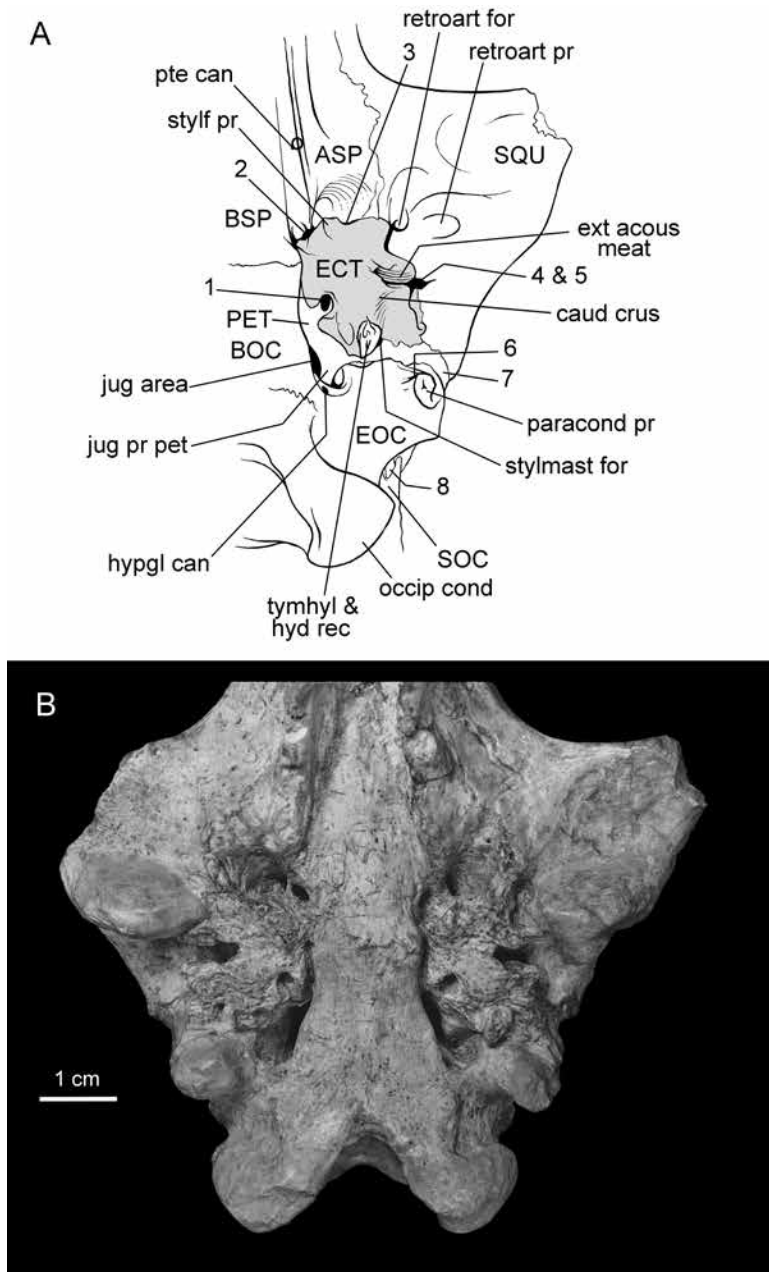
FIG. 26. *Trigonostylops wortmani* AMNH VP-28700. **A, B,** basicranium in rostroventral aspect, with interpretative diagram based on updated version of Simpson's (1933a) figure 5, drawn in similar orientation; **C,** left auditory region (stereopair) in oblique rostroventral aspect, to reveal matrix-filled rostral (piriform) part of basicapsular fenestra; and **D,** left auditory region (stereopair) in oblique caudoventral aspect, to reveal close proximity of tympanic cavity and aditus of extratympanic sinus. In A, contour lines on basicranium rostral to ectotympanic (not in original illustration) approximate extent of matrix-filled basicapsular fenestra (see C). Labeling conforms to identifications and nomenclature used in this paper. **Key: 1,** caudal carotid incisure in ectotympanic; **2,** Simpson's "foramen lacerum medium & Eustachian canal," actually medial limit of matrix-

filled basicapsular fenestra and probably corresponding to internal carotid artery's endocranial entry-point (auditory tube would have lacked canal); **3,** Simpson's "foramen ovale," corresponding to ?incisure in basicapsular fenestra for CN 5.3; **4, 5,** aditus of extratympanic sinus (laterally) and lateral limit of tympanic cavity (medially), better seen in D; **6,** canal X (function uncertain); **7,** petrosal exposure on lateral wall of skull; **8,** caudal end of lambdoidal process of petrosal, projecting through posttemporal foramen.
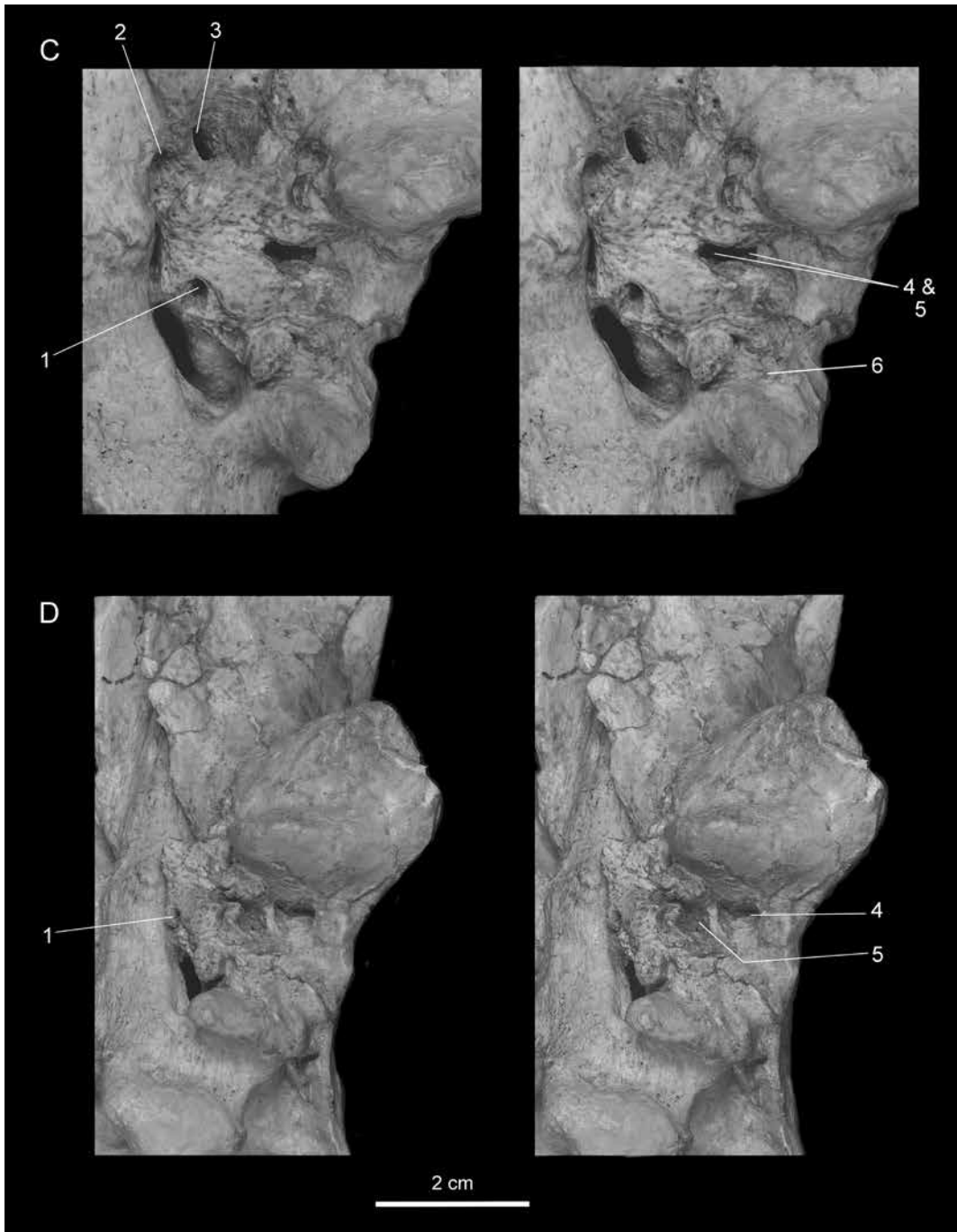
ies between bones but rarely or never ossifying (MacPhee, 1981). A similarly wide gap appears to have been the rule in "condylarthrans" such as *Meniscotherium*, *Hyopsodus*, *Phenacodus*, and *Periptychus* (Gazin, 1965, 1968; Williamson and Lucas, 1992; Shelley et al., 2018).

A wide fenestra may persist into the adult stage as a structural feature without its being externally visible. This happens when other structures, notably the auditory bulla, overlap it. Thus, in many notoungulates exhibiting well-inflated bullae (e.g., *Cochilius*, *Paedotherium*), no continuous basicranial gaps are in evidence because bullar walls impinge on the central stem's lateral margins, hiding most of the still-open fenestra from ventral view (e.g., fig. 18). Proterotheriids exhibit another pattern: the fenestra is wide open caudally and medially, but rostrally it is subdivided by a large alisphenoid wing that is pierced by a complete bony foramen ovale (Scott, 1910). In *Scaglia kraglievichorum* MMP M-207 and *Eoastrapostylops riolorense* PVL 4216 the exit point for CN 5.3 is also a separate, complete foramen, as in *Tetramerorhinus cingulatum* MACN A 5971 and probably most other litopterns (e.g., macraucheniids: Forasiepi et al., 2016). *Astrapotherium*, like *Trigonostylops*, lacks any bony foramina in the trailing edge of the alisphenoid (fig. 27A; contra Simpson, 1933a: 23). In these specimens the rostral portion of the basicapsular fenestra is especially wide, with the caudal portion narrower, as in many notoungulates (e.g., *Homalodotherium*) and all extant perissodactylans.

Retroarticular foramen and glaserian fissure (C108). In AMNH VP-28700 a short sulcus courses along the gap (glaserian fissure) between the squamosal and the rostral crus of the ectotympanic (figs. 11C, 26A). It leads into a foramen, which Simpson correctly recognized as the retroarticular (= postglenoid) foramen. In segmental data the channel can be followed to its union with the sulcus for the temporal sinus (fig. 8). Although the chorda tympani travels out of the tympanic cavity through the glaserian fissure, its extratympanic route to the position of the lingual nerve could not be separately identified on the skull.

A distinct retroarticular foramen is present in many "condylarthrans" (Russell and Sigogneau, 1965; Thewissen, 1990; Williamson and Lucas, 1992), including *Meniscotherium*, and on comparative grounds it is reasonable to assume that it has always had an exclusively venous function in placentals. It is unquestionably present in notoungulates (e.g., *Homalodotherium, Cochilius*) and litopterns (e.g., *Tetramerorhinus*, *Macraucbenia*), but in astrapotheres there is an interesting variation on the usual theme. As noted in *Astrapotherium* (figs. 7, 14C, 15D) the aperture in the retroarticular process seems to have done double duty, acting as a venous foramen as well as a pneumatic aditus (see p. 51, Interpreting Pneumatization). *Granastrapotherium snorki* IGM SCG MGJRG-2018 V4 possesses a large aperture in the same position, but nothing has been reported concerning the extent of retroarticular pneumatization in this taxon. Skulls of *Parastrapotherium* are too poorly preserved for assessment. All known skulls of *Astraponotus* lack a retroarticular foramen (Kramarz et al., 2010), but in this genus there is a large suprameatal foramen that could have acted as an alternative conduit for passing blood to the external jugular. As previously noted, in *Eoastrapostylops riolorense* PVL 4216 there is a remarkably large aperture in the retroarticular process, but its connections have not been investigated (cf. Kramarz et al., 2017). In living perissodactylans the retroarticular vein is large and functional, but it departs the skull through a ragged incisure continuous with the membranous tympanic roof rather than a complete foramen (figs. 35A, 37A, 39A).

For the notoungulate *Gualta cuyana* MCNAM-PV 3951, Martínez et al. (2020: fig. 9) reconstructed a shared trunk for the suprameatal vein and the retromandibular vein (= capsuloparietal emissary vein), but unusually it is shown as arising from the sigmoid sinus as well as the temporal sinus at a markedly caudal location (compare *Cochilius*, fig. 9).

Caudal carotid incisure/foramen (C133). Simpson (1933a: 13) identified the large notch indenting the caudomedial margin of the ecto-

tympanic in *Trigonostylops wortmani* AMNH VP-28700 (fig. 26) as the "posterior carotid foramen." As the aperture is incomplete we will refer to it as the "caudal carotid incisure" to distinguish it from the incisura carotidis associated with the alisphenoid. As an indicium Simpson's identification remains strong because there is no obvious alternative explanation for the notch's presence. Incisures in this position are not known to occur for certain in any other SANUs (see below).

Except for the cartilage of the auditory tube and the internal carotid artery itself (and the proximal stapedial artery in the few mammalian groups in which this vessel departs from the internal carotid outside the middle ear: van der Klaauw, 1931; Wible and Shelley, 2020), the structures that frequently pass through the caudomedial wall of the tympanic cavity tend to be of negligible caliber (e.g., tympanic nerve of CN 9, auricular branch of CN 10). Nor can the caudal carotid incisure in *Trigonostylops* represent an aperture for an emissary of the ventral petrosal sinus because the notch faces into the tympanic cavity, not the endocranium or the basicapsular fenestra (see fig. 12H). At the transverse level of the incisure, the dorsoventral gap between the medial margin of the ectotympanic and the promontorium is notably restricted (fig. 12H), seemingly too narrow to accommodate a vessel of any size. However, this appearance may be a consequence of either postmortem distortion, sediment pressure having pushed the loosely articulated ectotympanic toward the petrosal, or overpreparation making the caudal carotid incisure wider than it was in life.

With regard to other SANUs, Simpson (1936) claimed that the internal carotid artery may have been functionally present and intratympanic in the notoungulate *Oldfieldthomasia debilitata* AMNH VP-28600, but the aperture he identified as the caudal carotid foramen is miniscule and its supposed track (which begins within the jugular foramen) has the wrong relations for this vessel. It is much more likely to be an aperture for the tympanic nerve of CN 9—a

constant feature of the mammalian auditory region (see MacPhee, 1981)—and perhaps the ventral tympanic artery, if one was present (see MacPhee, 2011).

Promontorial vascular features. Virtual reconstruction of the petrosals of AMNH VP-28700 failed to show a distinct transpromontorial sulcus (sensu Wible, 1986) for the internal carotid artery (**C133**). This indicium is therefore not available to additionally corroborate our conclusion that the artery was present. Mineral deposits precluded identification of any features connected with the presence of the proximal stapedial artery or its branches, if present.

Whether a functional internal carotid artery existed in various SANU clades has long been a matter for conjecture (van Kampen, 1905; Simpson, 1936; Patterson, 1936; Gabbert, 2004; Billet et al., 2009; Billet and Muizon, 2013; García-López, 2011; MacPhee, 2014; Martínez et al., 2016, 2020), and evidence for an intratympanic routing of the artery has proven to be especially rare. However, there are some exceptions. A good case for an intratympanic internal carotid artery can be made for *Tetramerorhinus lucarius* AMNH VP-9245, the promontorium of which exhibits a shallow parasagittal groove with a raised medial border (fig. 19). *Thoatherium minusculum* YPM PU 15721 exhibits the same features, which are frequently encountered in mammals with intratympanic carotids (MacPhee, 1981; Wible, 1984), but whether they exist in other protertotheriid litopterns has not been explored.

In specimens of *Astrapotherium* there is also a promontorial sulcus, generally very large but of variable definition, which runs from a position just below the lip of the fenestra vestibuli laterally to the medial or rostromedial margin of the petrosal, i.e., transversely rather than parasagittally (fig. 27H). Given its position on the promontorium, Kramarz et al. (2017) suggested that the groove might represent a trackway for the internal carotid artery. An alternative possibility, that the sulcus represents a passageway for the proximal stapedial artery, is quite unlikely despite its proximity to the fenestra vestibuli. Supporting this conclusion is
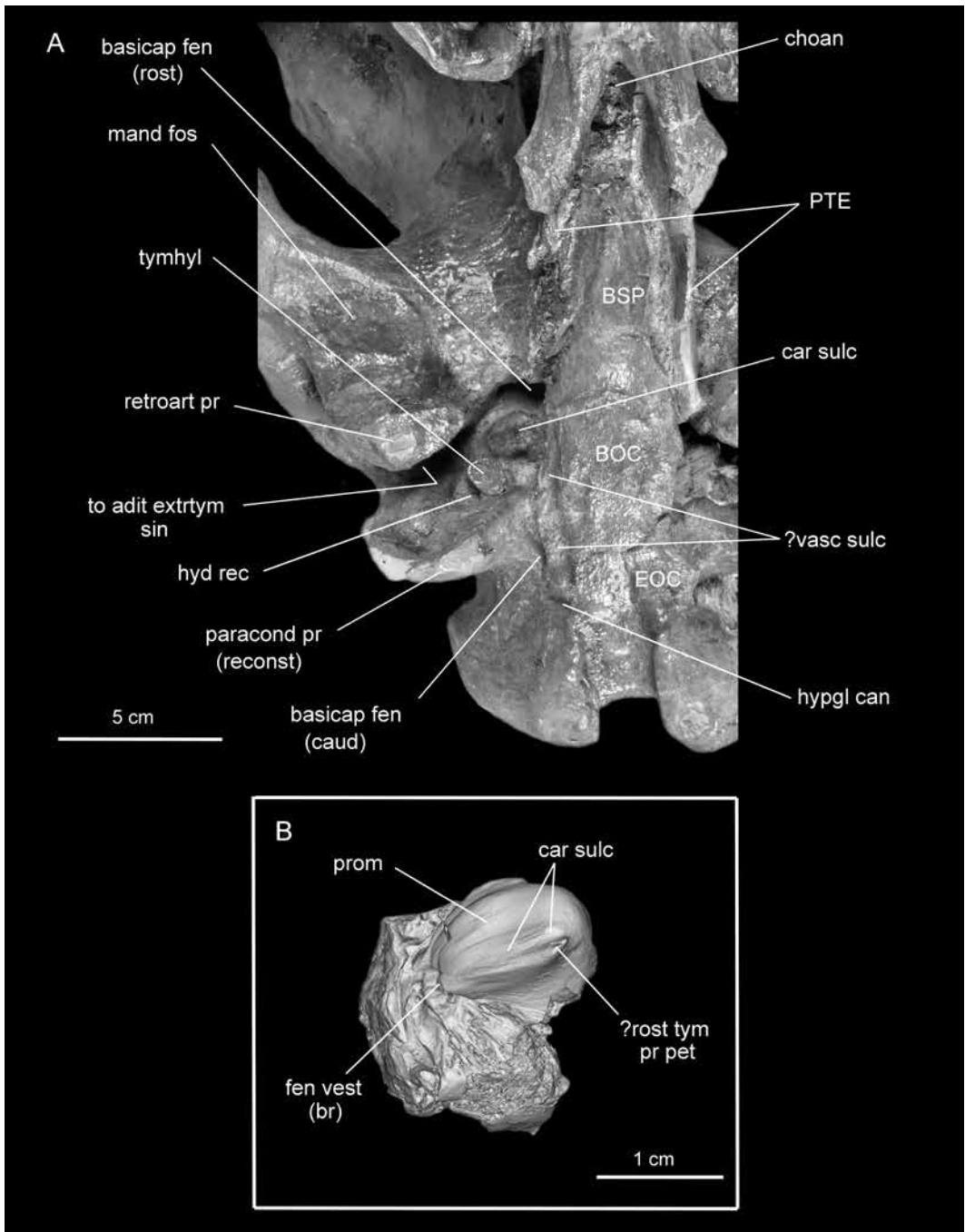
FIG. 27. *Astrapotherium magnum*, selected basicranial features. **A,** AMNH VP-9278, right basicranium in ventral aspect. Prominent impression labelled "?vasc sulc" may have conducted extracranial venous structures similar to basicranial plexuses seen in extant *Equus* (fig. 6; see also similarly positioned sulcus in *Tapirus*, fig. 38: feature 5). Basicapsular fenestra is hidden in this perspective, except for extreme rostral and caudal ends. **B,** Digitally reconstructed left petrosal of *A. magnum* MACN A 3208, reversed and rotated to permit com-

the fact that the stapes of *Astrapotherium magnum* MACN A 3208 is essentially imperforate, save for a small "nutrient" foramen that is out of proportion to the promontorial sulcus (fig. 33) (see p. 103, Neurological and Associated Structures). Furthermore, like other late astrapotheriids *Astrapotherium* was megafaunal (Vallejo-Pareja et al., 2015); extant mammals of very large body size uniformly lack functional proximal stapedial arteries in the adult stage (cf. Conroy, 1982; Wible, 1987; table 6).

In their report on a specimen of the "notohippid" toxodontian *Rhynchippus equinus* (MPEF PV 695), Martínez et al. (2016) noted that the rostral or piriform portion of the basicapsular fenestra "seems to be divided by a delicate strip of bone into an anterior fenestra and a posterodorsal fissure." This configuration appears to be similar to the subdivision of the piriform portion found in some *Toxodon* specimens (fig. 29B, C). If so, this would arguably represent another instance of an extratympanic routing for the internal carotid artery in a SANU, in which the vessel would have passed into the endocranium via the "posterodorsal fissure" (i.e., rostromedial portion of basicapsular fenestra of this paper). However, Martínez et al. (2016) propose a different interpretation of the artery's course: they suggest that a true caudal carotid canal may exist in MPEF PV 695, situated on the bullar wall next to the jugular foramen (cf. Billet and Muizon, 2013), in which case the posterodorsal fissure must have had another function. As in other cases discussed here, the aperture in the bullar wall is much more likely to represent the caniculus of the tympanic nerve (cf. *Homalodotherium*, fig. 28), especially because there do not appear to be any promontorial features supporting intratympanic routing.

Extant perissodactylans vary in regard to the presence and definition of promontorial vascular features. In *Equus* the internal carotid artery unquestionably travels outside the tympanic cavity (Sisson and Grossman, 1953; fig. 5B), but except for the incisura carotidis there are no exclusive indicia related to its preendocranial routing. The reason for this appears to be related to the fact that this artery as well as the pterygoid/pharyngeal plexuses feeding the craniooccipital vein are isolated within a sac of connective tissue as they transit the guttural pouch, and thus make no extracranial contact with basicranial elements (cf. cross sections in Bradley, 1923: fig. 24; Ellenberger and Baum, 1894: fig. 54, features 2, 3; Sisson and Grossman, 1953: fig. 706; Budras et al., 2008: 46). *Rhinoceros unicornis* AMNH M-274636 also lacks a promontorial sulcus, although there is a deep groove for the artery on the entotympanic and (usually) a carotid incisure on the alisphenoid (see van Kampen, 1905; Cave, 1959; see also appendix 2 and figs. 35A, 36A). *Tapirus* specimens sometimes show a short, shallow groove for the internal carotid artery on the rostral pole of the promontorium (appendix 2, fig. 38A). Finally, there is no evidence of the proximal stapedial artery in adult perissodactylans (Tandler, 1899; van der Klaauw, 1931), which is unsurprising in view of their body sizes.

Rostral carotid incisure/foramen. In *Trigonostylops*, the internal carotid artery presumably left the middle ear for the endocranium at the place expected in a typical placental, i.e., rostromedial to the promontorium's rostral pole, via the bony successor to the original chondrocranial foramen (see Forasiepi et al., 2019). Damage, overpreparation, and mineral deposits make it impossible to reconstruct this part of the artery's predicted passage in AMNH VP-28700, although the exit point would have been situated within the large excavation seen in figure 12F (asterisks).

In *Astrapotherium* the rostral portion of the basicapsular fenestra is widely open and there is

parison to petrosal in A. Alignment of inferred internal carotid sulcus varies among *Astrapotherium* specimens, but it is most often positioned as here, i.e., facing more medially than rostrally, although the vessel it conducted (if internal carotid artery) presumably passed into endocranium through rostral part of basicapsular fenestra. Whether raised sidewall of sulcus also functioned as a rostral tympanic process of petrosal is uncertain. On this point see text and Kramarz et al. (2017).
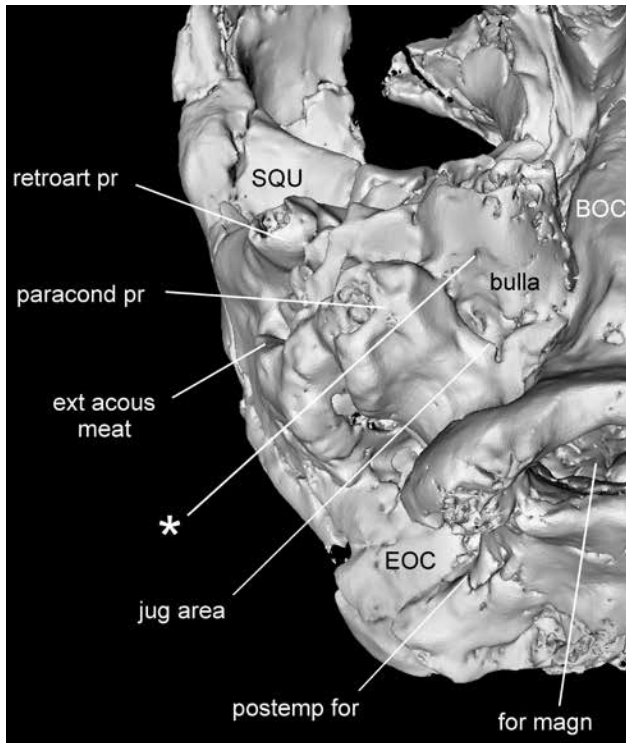
FIG. 28. *Homalodotherium* sp. MPM PV 17490, oblique caudoventral aspect. Patterson (1934a) claimed that in this taxon a carotid foramen existed on bulla's caudal surface, lying close to jugular area of basicapsular fenestra. In this specimen, only transbullar aperture in this location (**asterisk**) is very small and more readily interpreted as a canaliculus for tympanic nerve. If adult *Homalodotherium* possessed an intact internal carotid artery at all (see p. 114), it must have entered endocranium through exposed rostral part of basicapsular fenestra (not visible from this angle), as in *Toxodon* (see fig. 29). Note fully caudal position of posttemporal foramen, as in other notoungulates (cf. fig. 30).

no separately identifiable rostral carotid foramen. Assuming that the internal carotid artery was present and intratympanic in the adult (fig. 27B), the artery must have entered the endocranium through the membranous covering of the fenestra, from a position within the tympanic cavity (fig. 27A). In most *Toxodon* individuals there is usually no separate rostral foramen because the piriform section of the basicapsular fenestra is rarely subdivided (fig. 29A). In examples in which subdivision does occur, as a result of the growth of a distinct **carotid spinous process of the alisphenoid**, an externally situated rostral carotid notch or foramen can be identified (fig. 29B, C). We emphasize that internal

carotid presence/absence in notoungulates is something that needs to be demonstrated on the basis of indicia, not simply assumed (see p. 113, Discussion: Vascular Indicia).

Caudal aperture of pterygoid canal. A small aperture for the pterygoid canal lies in the expected position in AMNH VP-28700 (fig. 12D), and the canal can be traced in segments for a distance into the damaged mesocranium. Although the vidian artery (= embryonic mandibular artery of Padget, 1948: 230), a branch of the preendocranial part of the internal carotid artery, is plesiomorphous at least at the level of Mammalia (Wible, 1984, 1986), evidence for it is rarely encountered even in extant taxa (see MacPhee, 1981, *Erinaceus*; Aplin,

1990, *Tarsipes*). The vidian artery has never been identified in equine anatomies and is not likely to exist in other perissodactylans.

Stylomastoid incisure/foramen. Except in a few highly derived instances (van Kampen, 1905), in mammals the facial nerve follows a stereotypic course by tightly curling around the base of the tympanohyal in order to leave the middle ear (O'Gorman, 2005). In AMNH VP-28700 the facial nerve left the middle ear in the usual manner, passing through the gap between the caudal crus of the ectotympanic and the petrosal, immediately next to the tympanohyal (figs. 12J, 26). Despite its moderately expanded ectotympanic, *Trigonostylops* did not possess a completely ossified tympanic floor and the exit point of the facial nerve is a notch rather than a complete foramen. *Trigonostylops* agrees with "condylarthrans," astrapotheres, and litopterns, as well as numerous unrelated mammals, in lacking an ossified facial canal.

By contrast, in large-bodied notoungulates with well-inflated middle ears there is often a lengthy facial canal, as in *Toxodon* and *Nesodon*. Simpson (1933a: 18) argued that the stylomastoid foramen was positioned differently in notoungulates compared with *Trigonostylops*: in the former it was situated "between porus acusticus and vagina processus hyoidei," whereas in the latter it was located "posterior to porus, between it and paroccipital process." Patterson (1934a, 1977) and Billet et al. (2009) have also noted minor differences in foraminal position in notoungulates, which are presumably related to the extent of ossification around the nerve route and intratympanic pneumatization.

Tympanic aperture of the prootic canal (C141). In mammalian embryos, the lateral head vein becomes for a time the principal conduit for venous drainage of the head (Butler, 1957, 1967), acting as the primary rostral distributary of the developing transverse sinus (Wible and Hopson, 1995). This vein runs lateral to the geniculate ganglion, otic capsule, and glossopharyngeal nerve. Rostrally, it joins the medial head vein behind the trigeminal ganglion, their junction in the prootic

venous sinus marked by the passage of the posttrigeminal vein (Wible and Hopson, 1995; Rougier and Wible, 2006). Among extant mammals the lateral head vein is functionally retained in adult stages of extant monotremes and some marsupials, but is thought to be rare in adult placentals (Wible, 1990, 2003, 2008; Wible and Hopson, 1995; Sánchez-Villagra and Wible 2002; Wible et al. 2001, 2009; Ekdale et al. 2004; Rougier and Wible, 2006; Wible and Rougier, 2017; Muizon et al., 2018).

The prootic canal was first described in the echidna *Tachyglossus aculeatus* as a distinct conduit occupied by the prootic sinus at the endocranial end and by the lateral head vein at the tympanic end (Wible and Hopson, 1995). Among therians, however, the posttrigeminal vein is indistinct or lost, making it difficult to decide whether the prootic canal includes only the prootic sinus or a segment of the lateral head vein as well (Wible and Hopson, 1995; Rougier and Wible, 2006).

In *Cochilius volvens* AMNH VP-29651 a small opening in the tympanic roof of the petrosal, situated in close proximity to the secondary facial foramen, connects the middle ear to the endocranial cavity (figs. 16–18). As the proximal stapedial artery is absent in this taxon, the foramen must be interpreted as the tympanic aperture of the prootic canal. Whether this feature is commonly present in notoungulates is not known, but it is certainly possible.

Unfortunately, due to the combination of mineral deposits, breakage, and low resolution we were not successful in locating the prootic canal in the scanned specimens of *Trigonostylops* and *Astrapotherium* (AMNH VP-28700, MACN A 8580, MACN A 3208). It may, of course, have been absent in the adult stage of these taxa. In perissodactylans the lateral head vein has been identified in late embryonic *Equus* (Vitums, 1979), but at that developmental stage involution is already taking place and there do not appear to be any observations of the vein as an adult anomaly. A tiny aperture can be identified in the expected location in *Tapirus indicus* AMNH M-200300 (present but not visible in fig. 38D), but its identity cannot be verified.
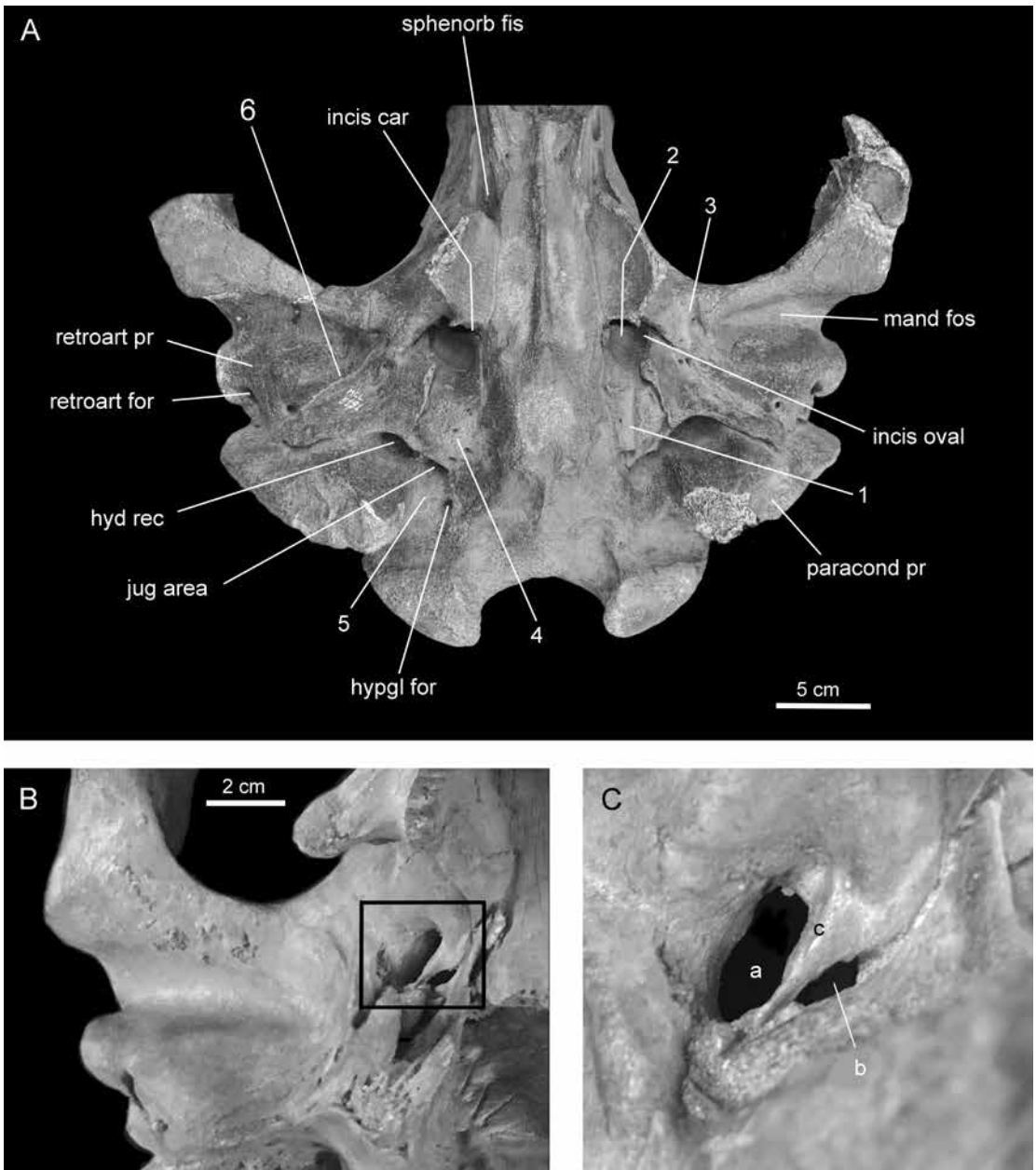
FIG. 29. *Toxodon* sp., selected basicranial features. **A,** MCL 5192 (adult), caudal cranium in ventral aspect, with undivided rostral (piriform) portion of basicapsular fenestra; **B,** MACN Pv 16615 (juvenile), right auditory region in ventral aspect, with divided fenestra (**C,** closeup of area in box in B). **Key: 1,** vascular sulcus crossing tympanic tympanic floor externally; **2,** medial portion of rostral basicapsular fenestra, transmitting internal carotid; **3,** vascular sulcus crossing entoglenoid region, presumably conducting tributaries of basicranial venous plexuses; **4,** auditory bulla; **5,** vascular sulcus between jugular area and hypoglossal canal, ?for anastomosis between ventral petrosal sinus and condylar emissary vein; **6,** squamoectotympanic suture. Van Kampen (1905: 615) reasonably assumed that feature 1, seen crossing external surface of bulla in A, was a

Canal X. A small foramen of unknown function is situated at the base of the paracondylar process in AMNH VP-28700, on the latter's rostral side (fig. 26A: feature 6). It is far enough away from the bounds of the tympanic cavity to make it doubtful that it transmitted the tympanic nerve of CN 9. It is equally unlikely that it gave passage to the auricular branch of CN 10, which would be expected to lie in or near the track of the facial nerve as the latter transited the stylomastoid foramen/incisure. A branch of the caudal auricular artery is possible but unconfirmable. Canal X is better defined on the specimen's right side than the left. It is not known to occur in other relevant taxa.

Trackways for ventral and dorsal petrosal sinuses. Because of mineral deposition the petrosal sinuses could not be adequately reconstructed. In figure 8 the ventral petrosal sinus as shown simply conforms to the margins of the basicapsular fenestra; accurate size and shape details could not be recovered. Patterson (1937) identified an apparent dorsal petrosal sinus in *Rhynchippus* as an "anterior petrosal sinus," but this homology seems improbable because the feature in question was directed toward the foramen ovale. In their treatment of *Rhynchippus*, Martínez et al. (2016: 16) also identified the dorsal petrosal sinus, in this case in relation to the suprameatal vein, but did not discuss Patterson's interpretation. A different possibility is the "rhinencephalic vein" seen in embryos of *Equus* (see Vitums, 1979, fig. 6), but there are no other details on this vessel and it is not known to be present in the adult horse. A similar feature could not be detected in AMNH VP-28700.

Hypoglossal foramen (C113). As Simpson (1933a) originally noted, the placement of the single hypoglossal foramen of *Trigonostylops* is unusual (figs. 11C, 26). Rather than being tucked into a cleft next to the occipital condyle or situated on the exoccipital planum close to the foramen magnum, as in most therians, in AMNH VP-28700 its aperture is located on the internal sidewall of the jugular area in the caudalmost portion of the basicapsular fenestra. In extant monotremes (Zeller, 1989), CN 12 passes through the fissura metotica (= combined jugular + hypoglossal foramina), but in therians there are very few examples of the hypoglossal canal opening into the jugular area (known exceptions include *Megaptera*, *Balaenoptera* [De Beer, 1937] and elephantids [Loomis, 1914]). The hypoglossal foramen is relatively small in *Trigonostylops* compared to its equivalents in *Astraponotus* and *Astrapotherium* (e.g., AMNH VP-9278).

Billet (2010) observed that the hypoglossal foramina of *Astrapotherium* and *Trigonostylops* could be considered to lie in a "common depression" within the jugular area. However, in both *Astrapotherium* and *Astraponotus* the depression is located on the exoccipital planum and does not face into the basicapsular fenestra per se, so their conditions are not strictly comparable to that of *Trigonostylops*. This justifies our reinterpretation of the **C113** character state for *Astrapotherium* as shared not with *Trigonostylops* but instead with *Astraponotus*. In *Astraponotus* the foramen and fenestra are separated by a thin wall; in *Astrapotherium* the separation is somewhat greater. In *Scaglia*, which may have had multiple hypoglossal foramina, the apertures lie close to the jugular area but are not actually situated within it (Kramarz et al., 2019b). Conditions in *Eoastrapostylops*, all relevant specimens of which are damaged, are unknown. Despite the large size of the basicapsular fenestra in extant perissodactylans, the hypoglossal foramen is located in the usual position, well separated from the jugular area.

groove for internal carotid because it terminated in the piriform area; however, function as a venous channel is also a possibility. In B and C, (**a**) incisura ovalis and (**b**) incisura carotidis are essentially complete foramina, separated by spikelike (**c**) carotid spinous process of alisphenoid. Such complete subdivision of rostral part of basicapsular fenestra is rarely seen in toxodontian fossils, either because dividers were negligible (as in A) or broke off post mortem. Note that in B, a juvenile, carotid incisure is only about one-quarter the area of incisura ovalis; in A, artery seems to have been relatively much larger. Difference could be due to age or individual variation, rather than a mark of artery's incipient reduction.
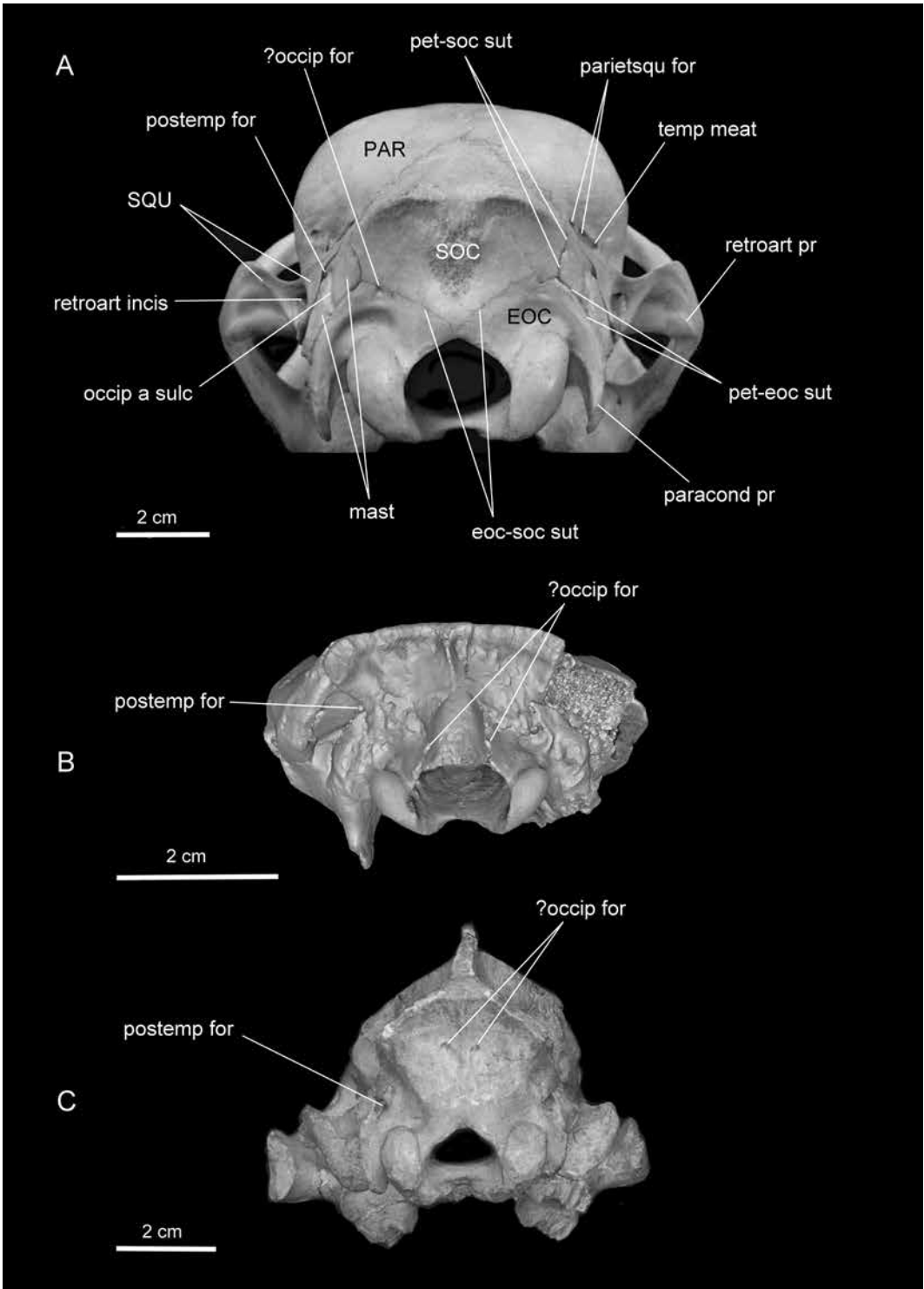
Posttemporal trackway complex (C135). In all known SANUs represented by adequate material, a single large aperture is found on each side of the skull in norma occipitalis. In the recent literature (e.g., Billet and Muizon, 2013; MacPhee, 2014; Martínez et al., 2016, 2020) this feature is almost always denoted as the posttemporal foramen or canal (here denoted together with other markings as the posttemporal trackway complex), in conformity with the naming of similarly positioned apertures in other therians. Simpson (1933a: 15) did not name or attempt to interpret this port in *Trigonostylops*, noting only that it was a "vacuity in the occipital exposure of the exoccipital, through which the mastoid projects."

In toxodontians, and probably notoungulates generally, the external aperture of the posttemporal canal is completely confined to the caudal aspect of the skull (e.g., *Cochilius*, fig. 30B). By contrast, in *Trigonostylops*, *Astrapotherium*, *Tetramerorhinus*, and the majority of other nonnotoungulate SANUs, the posttemporal foramen lies relatively more laterally and rostrally, so that in lateral aspect it appears on the skull's sidewall (see *Trigonostylops*, fig. 30C). Yet the elements involved are seemingly always the same, a point considered in detail later (see p. 119, Discussion: Venous Structures). Such differences in position appear to be related to the degree of expansion of the epitympanic sinus within the squamosal. In taxa with large, cau-dally projecting epitympanic sinuses, such as *Cochilius*, the posttemporal foramen is situated relatively more medially than in taxa in which caudal inflation is absent (e.g., *Trigonostylops*). Extant perissodactylans lack large paratympanic spaces, and, unsurprisingly, their mastoid foramina are positioned relatively laterally (e.g., *Equus*, fig. 39). See Geisler and Luo (1998) for a discussion of variable positioning of the posttemporal foramen/mastoid foramen in euungulates.

Tympanic Floor and Related Features

The auditory region of *Trigonostylops* is framed rostrally by the alisphenoid, laterally by the squamosal, medially by the basisphenoid and basioccipital, and caudally by the exoccipital as indicated by the location of the paracondylar process. Yet none of these bones sends a tympanic process to the floor of the middle ear. As defined by MacPhee (1981), tympanic floor components are projections that arise from their parent elements by growing intramembranously across the surface of the fibrous membrane of the tympanic cavity (or, in the case of most entotympanics, developing in cartilage within that membrane). Obviously, whether or not to call a slight amount of ridging a tympanic process is a matter of judgment, especially in the case of fossils where there are no soft tissues to provide additional indicia.

FIG. 30. Foraminal positions on rear aspect of caudal cranium in **A,** *Equus caballus* AMNH M-204155; **B,** *Cochilius volens* AMNH VP-29651; and **C,** *Trigonostylops wortmani* AMNH VP-28700 (note images not to same scale). In notoungulates generally, external aperture of posttemporal canal faces directly caudad and cannot normally be seen in lateral aspect, as in *Cochilius*. In most other non-notoungulate SANUs for which caudal cranial material is available, posttemporal foramen lies relatively more laterally, on sidewall rather than rear of caudal cranium, as in *Trigonostylops*. Differences may be largely due to degree of expansion of caudally positioned epitympanic sinus in notoungulates, which affects shape of this part of skull. Otherwise, relations are consistent in SANUs: posttemporal foramen is always framed by the squamosal, exoccipital, and petrosal mastoid; posttemporal sulcus/canal always crosses external aspect of lambdoidal process, whether or not process appears externally (e.g., fig. 26A: feature 8). By contrast, exoccipital is not involved in bounding posttemporal foramen ("mastoid foramen") in *Equus* and *Tapirus*; rhinos are different, at least in the juvenile stage when sutures are still open (cf. figs. 36B, 37B). Importantly, separate mastoid emissary foramen in or near petroexoccipital suture could not be distinguished in any of the specimens illustrated. Although there are apertures for ?occipital emissary foramina in supraoccipital bone or supraoccipital-exoccipital suture in specimens illustrated, their homology is questionable and they are often difficult to detect.

Petrosal in tympanic floor. Although the petrosal is a constant member of the auditory region, among mammals generally it rarely produces tympanic processes of large size (van der Klaauw, 1931; MacPhee, 1981; Forasiepi et al., 2016, 2019). In the case of AMNH VP-28700 there is no rostral tympanic process of the petrosal discernible in segmental data. There may be a small caudal tympanic process of the petrosal, but because of the density of mineral deposits in the ear region relevant edges could not be adequately discriminated and it is therefore omitted from consideration here.

Apart from *Astrapotherium* and *Astraponotus*, both of which have promontorial features that could be interpreted as either rostral tympanic processes of the petrosal or internal carotid sulci (see fig. 27B), or conceivably both (Kramarz et al., 2017), the pars cochlearis does not appear to produce significant floor components in any SANU taxa studied to date. Bullae of investigated notoungulates lack this process entirely (cf. *Cochilius*, fig. 18). The caudal tympanic process of the petrosal seems always to be insignificant as well (see Martínez et al., 2016).

Ectotympanic. Simpson (1933a: 11) described the ectotympanic of *Trigonostylops* as "scale-like" with expanded, U-shaped crura (fig. 26). He briefly wondered if it consisted of elements fused together, but he did not point to any supporting evidence and must have concluded that the possibility was doubtful. In AMNH VP-28700 the ectotympanic is preserved bilaterally and has a complicated shape, with a rugose surface (possibly the result of overpreparation) that is deeply incised on its medial, lateral, and caudolateral edges. These notches correspond, in order, to the caudal carotid foramen/incisure, external acoustic meatus, and stylomastoid foramen/incisure.

The rostral crus is in broad contact with the squamosal in the region directly behind the retroarticular process. Simpson discriminated a styliform process on the free rostral margin of the ectotympanic, although the feature he identified is not prominent (fig. 26A) compared with its equivalent in some other panperissodactylans (e.g., *Nesodon*: Patterson, 1932; *Equus*: fig. 41),

and it may be broken. It presumably gave origin to muscle fibers controlling some aspect of pharyngeal or auditory tube function (presumably tensor veli palatini, as in *Equus*: Sisson and Grossman, 1953: 59).

The body of the ectotympanic hides most of the petrosal from ventral view (fig. 26). Its medial margin is closely applied to the petrosal's promontorium, but is not fused to it (fig. 11), nor is there direct contact with the bones of the adjacent central stem. The lateral or meatal border is not smoothly curved but is instead incised by a large notch. Simpson (1933a) interpreted the notch as a "vestige of [the] opening of annulus tympanicus," by which he may have meant the tympanic fenestra (= foramen of Huschke), a naturally occurring developmental defect in the lateral wall of the ectotympanic bulla seen in members of various mammalian clades (MacPhee, 2011). Regarded as an anomaly in human anatomy, it has no known significance in taxa in which it regularly occurs.

The caudal crus tapers upward and backward to meet the tympanohyal, the posttympanic process of the squamosal, and the adjacent portion of the exoccipital. None of these appear to have involved actual articulations, the ectotympanic having been held in place by ligaments in life. The crista tympanica, marking the line of attachment of the tympanic membrane to the internal rim of the ectotympanic, is difficult to detect in transverse segments but is obvious in sagittal slices (fig. 11B). There is nothing corresponding to a crista meatus like that of notoungulates (see Gabbert, 2004).

A relatively unexpanded, U-shaped ectotympanic is usually regarded as representing the element's basal state for therians (MacPhee, 1981; Thewissen, 1990; Muizon et al., 2015). Simpson (1933a) pointed out that the unexpanded ectotympanic of litopterns, then known in only a few instances (e.g., some proterotheriids and macraucheniids: Scott, 1910; Soria, 2001; Forasiepi et al., 2016), was similar to that of *Trigonostylops*, but the resemblance was not very meaningful. Astrapotheriids and xenungulates probably had

unexpanded, loosely attached ectotympanics as well, but despite several new discoveries (e.g., Kramarz et al., 2010, 2019b; Antoine et al., 2015) there is still no direct evidence on this point. Notoungulates and pyrotheres are different in having complete, often well-inflated bullae (Billet, 2010) that are thought to be mainly ectotympanic in composition. Although there are differences in detail, ectotympanics of rhinos and tapirs are moderately expanded and tightly appressed to the tympanohyal, as in many mammals (figs. 35A, 38; appendix 2). Equids by contrast possess a complete ectotympanic-entotympanic bulla (Maier et al., 2013), but it is small and does not completely cover the promontorium medially (fig. 39).

Other features of the tympanic floor. Although the presence of entotympanics and other "adventitious" cranial elements in SANUs has been repeatedly inferred in the past (e.g., Roth, 1903; Patterson, 1934b, 1936; Simpson, 1936, 1948; Chaffee, 1952), only one unambiguous instance of a suture-delimited, compound entotympanic-ectotympanic bulla has been described and illustrated to date (*Cochilius*, fig. 18; see MacPhee, 2014). Patterson (1936) claimed that an entotympanic could be detected in specimens of another typothere, the mesotheriid *Typotheriopsis internum* FMNH P14420 and P14477, but in neither example could we find an unmistakable sign of sutural or other subdivision of the bulla. This is also true of the related taxon *Protypotherium* sp. FMNH P13234, likewise claimed by Patterson (1936) to possess an entotympanic. In this specimen the medial side of the bulla is more rugose than the lateral, but no obvious suture line separates them. Other supposed indicia, like the "septum bullae," have not pointed to any definite cases of entotympanics (see Martínez et al., 2020). However, despite the lack of empirical evidence, entotympanics could have been widespread in SANUs. In extant placentals existence of these elements as separate elements during ontogeny is often brief, because they tend to fuse early in perinatal life with nearby bones like the petrosal or ectotympanic and for that reason are often difficult to demon-strate in adult specimens (see appendix 2). Entotympanics were arguably present in basal placentals, but have been lost, at least as independently developing elements, in many clades (MacPhee and Novacek, 1993).

Tympanic Roof and Related Features

Petrosal in tympanic roof. Apart from the petrosal tegmen tympani and squamosal epitympanic wing, both relatively small, no other structures seem to have participated in the tympanic roof of *Trigonostylops*. A tympanic aperture for the ramus superior of the stapedial artery could not be recognized. Overall, the central part of the tympanic cavity is rather limited in size, with unexpanded walls (fig. 12I). Caudally, the petrosal mastoid is continuous with the squamosal for a short distance due to fusion (fig. 11B: arrows). A discrete fossa for the stapedius muscle could not be identified.

Paracondylar process, hyoid recess, and tympanohyal (C117, C125). *Trigonostylops* differs from *Astrapotherium* and *Astraponotus* in the relative size of the paracondylar process, which is comparatively very short in AMNH VP-28700 (fig. 26). In astrapotheriids the process assumes the form of a massive pyramidal projection that is deeply grooved on its rostral surface by the cranial end of the hyoid apparatus (fig. 27A)—a frequent size-related character of large SANUs (e.g., *Toxodon*, fig. 29A).

Simpson (1933a: 13) identified the "hyoid process" of AMNH VP-28700 as a "roughly hemispherical swelling, which … may be a descending process from the periotic or may be an independent element." The only developmentally independent element expected in this area is the cranialmost portion of Reichert's cartilage, which ossifies as the tympanohyal. In *Trigonostylops*, this feature presents as a thin-walled tube enclosing discontinuous cancellous tissue and matrix (figs. 11A, 12J). We interpret its appearance to mean that, during the perinatal ontogeny of AMNH VP-28700, a low, bony collar developed around the cranialmost part of Reichert's

cartilage, which was undergoing replacement at the same time. The fact that cancellous tissue does not fill the entire volume of the collar may indicate that Reichert's cartilage was incompletely replaced by bone. The result in AMNH VP-28700 is a truncated, honeycombed projection, not a pit, which Simpson (1933a) contrasted with the condition in notoungulate skulls, in which there is a very definite excavation or sheath (vagina processi hyoidei) in the caudal part of the auditory region. A deep or hollow hyoid recess suggests that the tympanohyal may not have been ossified in most notoungulates, with the consequent loss of the entire hyoid apparatus after death.

In extant ceratomorph perissodactylans, the tympanohyal is very robust and only partly encircled by the caudal crus of the ectotympanic; as in *Trigonostylops*, a deep hyoid recess is not present (figs. 38A, 39A). In *Equus* the sheath for the tympanohyal (= tympanostyloid) is formed by the bulla, from the ventrocaudal aspect of which the ossified tympanohyal projects (fig. 39). The tympanohyal is said to remain cartilaginous in the horse (Budras et al., 2008: 34); perhaps it partly ossifies, in the same manner inferred here for *Trigonostylops*.

Lambdoidal process of petrosal. In most SANUs the petrosal mastoid (that is, the caudal end of the pars canalicularis) is short and blunt. In *Trigonostylops* it narrows into a thin spearpoint that projects externally from the posttemporal canal's orifice (figs. 12L, 19), which is likely the reason that Simpson (1933a: 18) drew attention to it even though he did not name it. This feature is here identified as the lambdoidal process (fig. 26A: feature 8). In his illustration of the basicranium of *Trigonostylops*, Simpson (1933a: fig. 5) labelled the jugular exposure of the petrosal as "mastoid," whereas the actual process projecting into the posttemporal foramen is depicted but not identified. Thanks to the lambdoidal part of the mastoid being "clasped between sutures with the exoccipital" (Simpson, 1933a: 10), the petrosal—otherwise only lightly attached to surrounding bones—is firmly locked into the lateral wall of the skull.

In *Astrapotherium* there was also a definite lambdoidal process (figs. 13B: inset; 14F), but as in many other SANUs no part of the mastoid passed through the posttemporal foramen to appear on the caudal aspect of the skull. Gabbert (2004) argued that the "small sliver of bone" visible within the posttemporal canal of certain toxodontians was supraoccipital in origin. In our scans, except for very minor supraoccipital representation in some cases (e.g., *Cochilius*, fig. 17D), the "sliver" is always continuous with the petrosal mastoid. The mastoid produces a lambdoidal projection in some other investigated SANUs (e.g., *Rhynchippus*; Martínez et al., 2016) as well as extant perissodactylans, although it varies in length, robusticity and externalization and is never spearlike (e.g., figs. 35C, 36C).

Sagittal and temporal crests. The sagittal crest of *Trigonostylops* is well developed by comparison to that of most other SANUs in its body size range (figs. 1B, 12E). A crest is also found in adult *Scaglia* cf. *kraglievichorum* MPEF PV-5478 (Kramarz et al., 2019b); the fact that it is absent in the holotype (a juvenile of the same or a closely related species) indicates that it grows significantly in postnatal life, doubtless in concert with development of the temporalis muscle. Moyano and Gianinni (2017) have examined sagittal crest development in selected stages of *Tapirus terrestris*, in which there is also pronounced postnatal growth of this feature.

Simpson's statement that the temporal crests of AMNH VP-28700 are "virtually absent" should be read in conjunction with conditions in adult *Astrapotherium*, to which he compared *Trigonostylops*. In *Astrapotherium* the whole dorsal aspect of the skull is swollen into a prominent dome as a result of massive pneumatization (figs. 4, 14). Temporal crests are present as sharp margins on the dome's sidewalls. In this astrapotheriid the dorsal part of the skull must have grown at an accelerated rate during postnatal ontogeny, because in young animals (e.g., MLP 38-X-30-1) the calvarium is rather flat and inflation is almost negligible. Rapid differential growth in *Astrapotherium* is also reflected in the implied size of the areas of origin of temporalis musculature.

Interparietal. Simpson (1933a) noted that the interparietal bone may be present in *Trigonostylops*, although no external sutures are in evidence on AMNH VP-28700 to confirm this. However, in CT segments containing the relevant region there appear to be vestiges of a suture in the correct location, concealed by later bone deposition. The interparietal bone is widely distributed in extant and fossil mammals (cf. Koyabu et al., 2012); it was probably present in the majority of SANUs.

Neurological and Associated Structures

Brain Endocasts. Therian brains vary widely in morphology and size across and within clades, and there is little agreement at present as to the factors that may have triggered such high levels of disparity (Willemet, 2013). Although endocasts reconstructed from segmental data provide a means for visualizing certain aspects of fossil neuroanatomy, specimens are often more or less severely compromised, which limits interpretation in various ways. In the case of *Trigonostylops wortmani* AMNH VP-28700, for example, crushing and loss of the rostral parts of the cranial cavity obviates description of the lateral olfactory tracts and bulbs. Although the ventral surface of the forebrain region is mostly preserved in this specimen, mineral deposits within the cranial cavity complicated our making a good reconstruction (e.g., evident artifacts on dorsal and lateral faces of endocast in fig. 8).

In the following sections we describe the endocast of AMNH 09

-28700 (fig. 8) in terms of the traditional regions of the brain as seen in the living animal (forebrain, midbrain, and hindbrain). Overall, the endocast exhibits a low angle of basicranial flexure (~15°, calculated according to the method of Macrini et al., 2006). Relative lack of flexure between forebrain and hindbrain occurs in various "condylarthrans," including *Hyopsodus* (Gazin, 1968; Orliac et al., 2012), *Phenacodus* (Edinger, 1929; Simpson, 1933a; Tilney, 1933), and *Meniscotherium* (Gazin, 1965; fig. 9), all of which display flexure values of <25°. Relative lack

of flexure is also found in SANUs of different geological ages, such as Eocene *Notostylops* (Simpson, 1933a), Early-Middle Miocene *Cochilius* (fig. 9), and late Cenozoic notoungulates including mesotheriid typotheres (*Trachytherus spegazzinianus*, Fernández-Monescillo et al., 2019; *Typotheriopsis*, Patterson, 1937) and the toxodontan *Homalodotherium* (Patterson, 1934a). Other Oligocene and Miocene notoungulates, including the leontiniid *Gualta*, the "notohippid" *Rhynchippus*, and the nesodontines *Adinotherium* and *Nesodon*, exhibit a degree of endocast basicranial flexure equal to or above 30° (Martínez et al., 2020; Hernández Del Pino, 2018).

In the Miocene proterotheriid *Tetramerorhinus lucarius* AMNH 9245 (fig. 9; Radinsky, 1981; Forasiepi et al., 2016), recorded values are somewhat higher, ~30°. *Astrapotherium magnum* MACN A 8580 yielded a value of 37° (fig. 8), which correlates well with conditions in some extant perissodactylans, including *Tapirus indicus* AMNH M-200300 (31°) and *Ceratotherium simum* AMNH M-51882 (29°) (fig. 10). In *Equus caballus* AMNH M-204155 (fig. 10), however, the angle is only 23°, which suggests a very low angle of flexure in this specimen. In fact significant flexure between forebrain and hindbrain is present, but the value provided by the method of Macrini et al. (2006) is affected by the relatively low position of the olfactory bulbs relative to the foramen magnum in the horse (see table 4).

The therian forebrain is structurally divided into the telencephalon and diencephalon, but these regions are difficult to separate in endocasts. Although progress is being made in developing proxy boundaries for forebrain components in certain clades (e.g., Walsh and Milner, 2011; Balanoff et al., 2013, Walsh et al., 2013), good samples of extant representatives are required for cross-validation—obviously not possible for SANUs.

The olfactory bulbs of the telencephalon receive signal input from the olfactory epithelium of the dorsal nasal cavity and vomeronasal organ, which is then transmitted via the olfactory tracts to the piriform lobe and associated cortical centers for processing. Although the

bulbs are not preserved in AMNH VP-28700, the portion that normally contains the lateral olfactory tracts and tubercles is still partly represented on the endocast. The tracts were evidently proportionately large, but the endocast surfaces are smooth with no indication that differentiated olfactory tubercles were present. *Astrapotherium magnum* MACN A 8580 exhibits well-developed, relatively rounded olfactory bulbs that are separated from the rest of the forebrain by short, conspicuous peduncles connected to the smooth-walled lateral olfactory tracts. As in *Trigonostylops* olfactory tubercles are not distinctly indicated.

Expansion of the neopallium (= isocortex, neocortex), the portion of the telencephalon that processes so-called higher functions involving integration of perceptual, cognitive, and motor information is a crucial feature of mammalian evolution (e.g., Jerison, 1985; Allman, 1990; Arbib et al., 1998; Aboitiz and Montiel, 2007). As seen indirectly in endocasts, such transformations involved the progression from the narrow, tubular cerebral hemispheres characteristic of early therapsids to the relatively expanded telencephalons seen in crown-group mammals (e.g., Hopson, 1979; Quiroga, 1980; Kielan-Jaworowska et al., 2004). In most mammals, the neopallial cortex occupies most of the superior and temporal surfaces of the telencephalon while leaving exposed the olfactory cortex and associated structures (= paleopallium, paleocortex) (Allman, 1990). Relative size is not the only feature of interest, as cortical folding provides another solution to the problem of amplifying the neural surface area of the neopallium. To the degree that cortical folding can be visualized on endocasts, smooth or lissencephalic cortices can be contrasted with ones that are more convoluted or gyrencephalic. Although the lissencephalic condition appears to be plesiomorphic for mammals, lissencephaly is seen in extant representatives of various major clades of extant mammals (e.g., *Platypus*, didelphids, some small primates and rodents). The degree of gyrencephaly varies widely among mammalian

clades, and is largely correlated with brain and body size rather than phylogenetic affinity (Zilles et al., 2013). In the case of *Trigonostylops,* its long, lissencephalic cerebral hemispheres are less expanded laterally than in some "condylarthrans" (e.g., *Meniscotherium*, *Hyopsodus*; Gazin, 1965, 1968; Orliac et al., 2012). Although descriptively lissencephalic, the endocast of *Astrapotherium* displays relatively shorter and laterally expanded cerebral hemispheres compared to that of *Trigonostylops* (fig. 8).

As we do not possess a complete endocast of *Trigonostylops*, we used the neopallial height ratio (NPH maximum neopallial height/EH maximum endocast height; see table 4) because it has been shown to be a good predictor of total neopallial surface area in some extant taxa (e.g., in rodents; see Bertrand et al., 2018). It has recently been used as a proxy for estimating neopallial surface area in a number of extinct taxa (see Bertrand et al., 2020). For *Trigonostylops* and *Astrapotherium*, neopallial height ratios are 0.42 and 0.36 respectively, suggesting that the former had a relatively more expanded neopallial surface than did the latter. Compared with estimates for other early Cenozoic placentals calculated by Bertrand et al. (2020), *Trigonostylops* possessed a higher neopallial height ratio than did *Chriacus baldwini* (0.25), *Diacodexis ilicis* (0.31), *Hyopsodus lepidus* (0.33), and *Alcidedorbignya inopinata* (0.20). Within our comparative sample, *Meniscotherium* (0.29), *Cochilius* (0.35), and *Tetramerorhinus* (0.38) also present lower values for this ratio, while *Homalodotherium* (0.44) and perissodactylans (ranging from 0.46 to 0.62) are higher. Although *Cochilius* and *Tetramerorhinus* exhibit lower values than *Trigonostylops*, it needs to be recognized that the effect of neocortical folding, although modest in these taxa, is probably not adequately accounted for with this ratio.

The longitudinal fissure separating the hemispheres, which tends to be well marked on "condylarthran" endocasts, was surely present in *Trigonostylops wortmani* AMNH VP-28700 and *Astrapotherium magnum* MACN A 8580 even though barely indicated in the reconstructions

(fig. 8). The shallow rhinal fissure, marking the approximate line of separation between neopallium and paleopallium in extant taxa (Edinger, 1929, 1964), is also poorly visualized, especially on the endocast of AMNH VP-28700. In that specimen the fissure's rostral portion is hidden by artifacts, but its partially preserved caudal portion is situated high on the piriform lobes, similar to conditions in *Meniscotherium* (Orliac et al., 2012). This indicates that the paleopallium must have also been comparatively large in *Trigonostylops*, as in *Phenacodus*, *Meniscotherium*, and *Arctocyon* (Simpson, 1933a; Gazin, 1965; Orliac et al., 2012).

As seen in lateral and ventral view, the piriform lobes of the AMNH VP-28700 endocast appear relatively large and constitute a significant fraction of total endocast surface. On the better-preserved right side, the piriform lobe makes up much of the endocast's vertical height, resulting in a relative height ratio (lobe height/total forebrain height: 10.4 mm/25.0 mm) of approximately 0.41. This correlates with other evidence indicating that the cerebral hemispheres were little expanded ventrally in *Trigonostylops*. The comparable value for *Astrapotherium magnum* MACN A 8580 is 0.50 (38.1/76.8). Interestingly, in *Cochilius volvens* AMNH VP-29651 the ratio is much lower at 0.19 (3.1/15.9). This result is at least partly due to overlap of the piriform lobe by the large temporal lobe, which (together with a certain amount of postmortem dorsoventral compression in the specimen) affects the position of the rhinal fissure. As noted previously, neopallial expansion was independently achieved in numerous clades of mammals and is therefore a trait of limited systematic value at the hierarchical levels of interest here.

Although the mammalian diencephalon is traditionally divided morphologically into several regions, the only ones that can be plausibly identified on endocasts are the hypophyseal fossa and optic chiasm. The hypophyseal fossa houses the ventralmost portion of the hypothalamus, hypophyseal gland, and associated tissues. In *Trigonostylops* AMH VP-28700 it is small and connected to the still-patent cranio-pharyngeal canal, formed during development of the adenohypophysis (De Beer, 1937; Lang, 1983). Situated immediately in advance of the canal is a discrete midsagittal bulge, conceivably representing the tuber cinereum. In *Astrapotherium*, the area corresponding to the hypophyseal fossa is long, smooth, and flat, showing no distinctive features. The optic chiasm is discernible in the casts of both taxa, but it is relatively longer and wider in *Trigonostylops*. In AMNH VP-28700 the optic nerves diverge at an angle of ~42°. Endocasts of other taxa in which divergence could be adequately measured include those of *Astrapotherium magnum* MACN A 8580 (64°), *Homalodotherium* sp. MPM PV 17490 (~35°, slightly damaged), *Cochilius volvens* AMNH VP-29651 (~56°, slightly damaged), *Gualta cuyana* (~54° [Martínez et al., 2020: fig. 2F]), *Tetramerorhinus lucarius* AMNH VP-9245 (~57°, slightly damaged), and *Equus caballus* AMNH M-204155 (86°).

In AMNH VP-28700 the midbrain is exposed to a minor degree in dorsal aspect, a similarity to *Rhyphodon*, *Meniscotherium*, and *Hyopsodus* (Simpson, 1933a, 1933b; Orliac et al., 2012). By contrast, wide midbrain exposure, due to marked separation of the cerebral hemispheres and cerebellum, is seen in many basal placentals and is often correlated with a weak degree of neopallial expansion (Edinger, 1964; Orliac et al., 2012). The surface anatomy of the midbrain tends to be hidden in all groups by vascular sinuses and associated meninges, the caudal expansion of the cerebral hemispheres, and /or the rostral expansion of the cerebellum (Edinger, 1964; Macrini et al., 2007). For example, although the corpora quadrigemina were surely present in *Trigonostylops*, their expected positions are not marked by any special feature on the endocast. This is contrary to what is seen in *Hyopsodus*, in which the position of the corpora quadrigemina are indicated by small bulges on the tectum (see Orliac et al., 2012).

The hindbrain consists of the cerebellum (which plays a key role in coordination and balance) and the medulla oblongata (Butler and Hodos, 2005). Both portions usually exhibit endo-

cast features that permit their discrimination. In *Trigonostylops* the cerebellum occupies approximately one quarter to one fifth the estimated length of the endocranium. Broad, shallow declivities separate the lateral cerebellar hemispheres from the vermis cerebelli, which occupies approximately two thirds of the cerebellar dorsal surface. Unlike the case in many mammals, *Trigonostylops* and *Astrapotherium* show no convolutions on the cerebellar hemispheres, although this is present to some degree in *Tetramerorhinus* and *Equus*. The parafloccular lobes of the cerebellum integrate vestibular and visual stimuli to control eye movements (Zee et al., 1981). On the endocast of *Trigonostylops* the parafloccular impression (hidden by vasculature in fig. 8) presents as a small, undivided eminence. Bertrand et al. (2020) reported a similar appearance of the paraflocculus in "condylarthrans," and this also appears to apply to specimens of *Meniscotherium*, *Astrapotherium*, and *Homalodotherium* in the comparative set (see also Orliac et al., 2012). The same condition (paraflocculus evident but small) has been reported for the Oligocene taxa *Mendozahippus* and *Gualta* (Martínez et al., 2020) as well as the Miocene toxodontids *Adinotherium* and *Nesodon* (Hernández Del Pino, 2018). A relatively large paraflocculus is often considered to be a basal trait of Mammalia (e.g., Kielan-Jaworowska, 1986; Jerison, 1973; Nieuwenhuys et al., 1998; Macrini et al., 2007), and according to some authors there is evidence that parafloccular size in extant species is correlated with locomotor activities demanding high maneuverability and fine coordination (e.g., Jerison, 1973; Zee et al., 1981; Gannon et al., 1988; Macrini et al., 2007). However, Ferreira-Cardoso et al. (2017: 1) found in their sample of extant birds and mammals that parafloccular size was not a good indicator of function, being "better explained by a combination of factors such as anatomical and phylogenetic evolutionary constraints" (Ferreira-Cardoso et al., 2017: 3).

In summary, the brain endocast of *Trigonostylops* displays the following combination of neurological traits thought to be basal in placentals: (1) linear arrangement of the forebrain and hindbrain; (2) lissencephalic neopallium with relatively low ventrolateral expansion, (3) some degree of exposure of the nearly featureless midbrain (possibly in correlation with the previous two features); and (4) large paleopallium exposure (due to feature 2). Aside from outward conservativism, endocast morphology in *Trigonostylops* exhibits values for the neopallial height ratio that are notably higher than those available for basal placentals or other SANUs in the comparative set. Other potentially derived features (e.g., morphology and size of the paraflocculus) need further study in extant and fossil mammals in order to assess their usefulness. It is also important to note that several endocast characters considered to be derived were probably independently acquired by different clades. This points to their being of functional importance, but reflecting the limited capacity of the brain to adapt to evolutionary challenges except along the same heavily constrained pathways.

Cranial Nerves. As in many SANUs, in *Trigonostylops* the mandibular nerve (CN 5.3 in fig. 8) passed through the wide basicapsular fenestra rather than through a separate foramen. The proximal portions of the ophthalmic (CN 5.1) and maxillary (CN 5.2) nerves could be traced up to the severely damaged mesocranium, and again at their bony terminal outlets. As always, there are discrete features representing the facial (CN 7) and vestibulocochlear (CN 8) nerves at the site of the internal acoustic meatus. There are no other aspects of the main cranial nerves that require commentary, other than to repeat that *Trigonostylops* is distinctive in positioning the hypoglossal foramen for CN 12 on the caudal lip of the jugular area rather than well behind it.

Auditory Apparatus

Osseous Labyrinth. In figures 31 and 32, the endocast of the left osseous labyrinth of *Trigonostylops wortmani* AMNH VP-28700 is compared digitally to those of members of the comparative

Trigonostylops
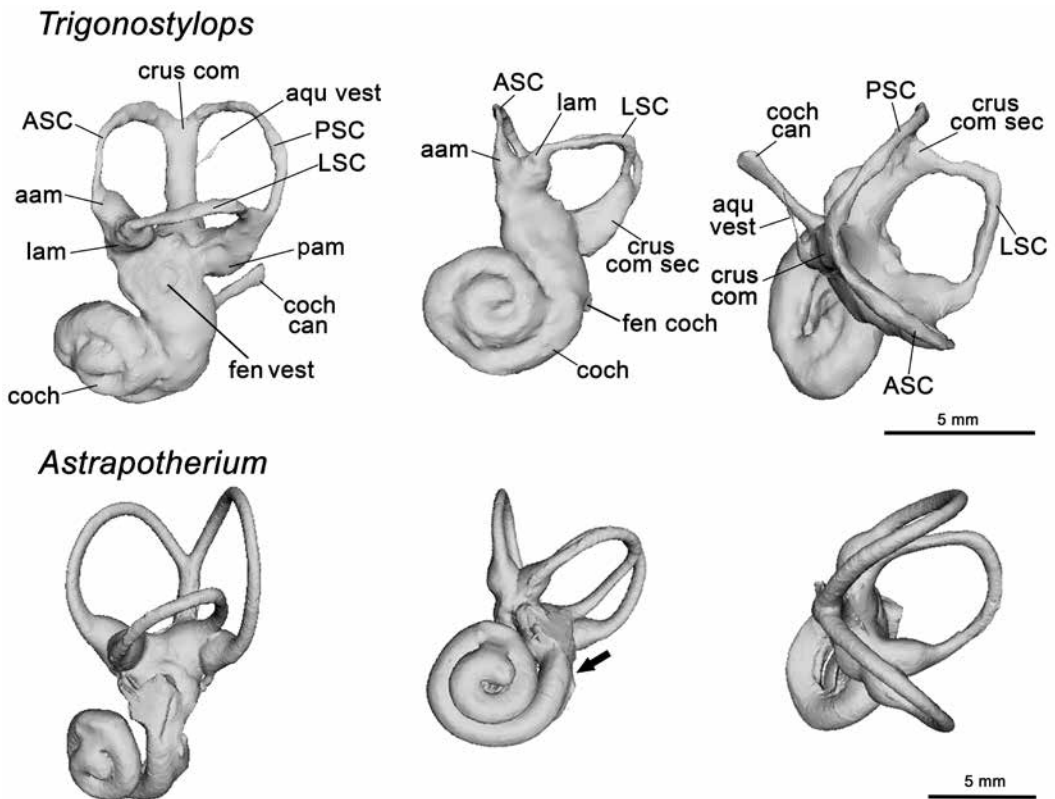
Astrapotherium

FIG. 31. Digital 3D reconstructions of left osseous labyrinths of *Trigonostylops wortmani* AMNH VP-28700 and *Astrapotherium magnum* MACN A 3208 in lateral, ventral, and dorsal views. Both specimens are damaged (area of fenestra vestibuli in AMNH VP-28700; fenestra cochleae in MACN A 3208: arrow).

set in lateral, ventral, and dorsal orientations (**C145, C149**; see also table 5). Although surface detail is poorly recorded in some cases, all expected features are observable in each specimen (see table 2). As noted below, there is reason to believe that considerable individual variation in labyrinth features may exist in some taxa in the comparative set, as has been documented in other instances (e.g., extant sloths; Billet et al., 2015). For most taxa of relevance to this study, our knowledge of labyrinth morphology is based on only one or a few specimens; care therefore needs to be taken in scoring inner ear characters (see appendices 3 and 4).

As in all mammals, the labyrinth of *Trigonostylops* consists of a series of interconnected spaces: the cochlea, which in life housed the sense of hearing, together with the vestibule and the three semicircular canals involved in the sense of balance (e.g., Ekdale, 2013, 2015). The tightly packed cochlear canal of AMNH VP-28700 completes 2 full turns, as does that of *Astrapotherium magnum* MACN A 3208. This agrees with findings for most other panperissodactylans, in which cochlear coiling is usually found to involve 2 or more turns (e.g., Simpson, 1936; Macrini et al., 2010, 2013; Billet et al., 2015; Forasiepi et al., 2016). Known exceptions include *Ceratotherium simum* AMNH M-51882 (<2 turns) and Colhuehuapian *Cochilius volvens* AMNH VP-29651 (>3 turns). This last value stands in sharp contrast to the value (2 turns only) recorded by Macrini et al. (2013) for *Cochilius* sp. SGOPV 3774, a Deseadan specimen of
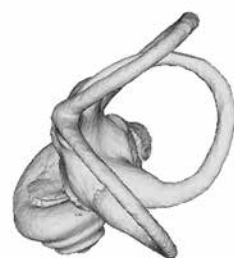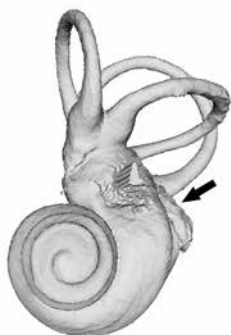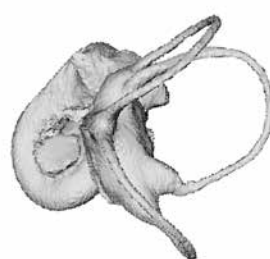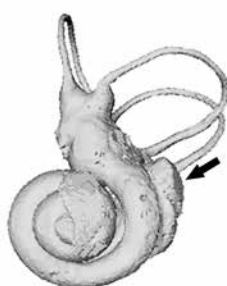
FIG. 32. Digital 3D reconstructions of the osseous labyrinths of *Cochilius volvens* AMNH VP-29651, *Tetramerorhinus lucarius* AMNH VP-9245, *Tapirus indicus* AMNH M-200300, *Ceratotherium simum* AMNH M-51882, and *Equus caballus* AMNH M-204155 (above and on opposite page), in lateral, ventral, and dorsal views. In each ventral view, arrow indicates position of fenestra cochleae.

Cochilius. Whether the difference in this case reflects evolutionary change over an interval of ~1 Ma or merely within-taxon variability is unknown, but characters based on such features (**C145, C148, C149**) should take account of the possibility of polymorphism.

Because of the amount of sinter in AMNH VP-28700 it was not feasible to identify external sulci marking the location of the (internal) primary and secondary osseous spiral laminae, which incompletely separate the scalae tympani and vestibuli within the cochlear canal (Meng and Fox, 1995). In the scan of *Astrapotherium* both sulci can be identified, although the secondary sulcus is feeble and extends along only halfway along the basal turn, as in some other notoungulates (e.g., *Notostylops*, *Altitypotherium*,

and *Pachyrukhos*; Macrini et al., 2013; Billet et al., 2015).

The fenestra vestibuli is positioned slightly ventrocaudal to the lateral ampulla. The cochlear canaliculus (= aqueductus cochleae) for the membranous perilymphatic duct opens at the base of the basal turn of the cochlea, caudomedial to the fenestra cochleae, and its endocast projects beyond the level of the PSC as seen in dorsal view. In life the vestibule contains the membranous utricule and saccule (Meng and Fox, 1995; Macrini et al., 2010; Ekdale, 2015). In AMNH VP-28700 the vestibule is rostrocaudally elongated. The aqueductus vestibuli, for the membranous endolymphatic duct, is very narrow; it projects dorsocaudally from the vestibule, at an oblique angle to the crus commune.
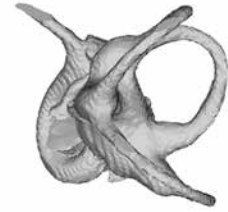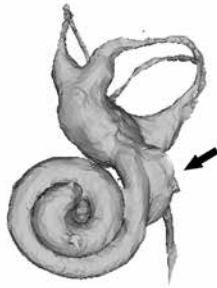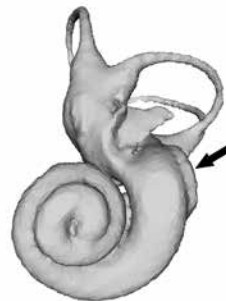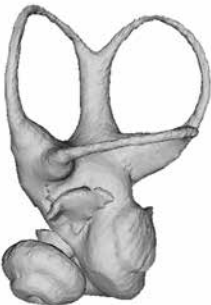
The variable width of the semicircular canals seen in the reconstructed labyrinth of AMNH VP-28700 is artifactual, and results from the sinter obscuring their outlines. The ASC and PSC are subequal in size (PSC slightly longer), with maximum radial height close to 1.0 in each case, much as in *Astrapotherium* (table 5). However, the relative sizes of the semicircular canals may exhibit intraspecific variation, as in some other mammals (Billet et al., 2012). In lateral view, the dorsalmost point on the ASC is coplanar with that of the PSC in *Trigonostylops*. This condition differs from that of *Astrapotherium*, in which the dorsalmost point on the PSC projects above that of the ASC, similar to *Ceratotherium* (table 5). Conversely, there is greater projection of the ASC in extant *Tapirus* (fig. 32), the hegetotheriid *Pachyrukhos* (Macrini et al., 2013), the mac-
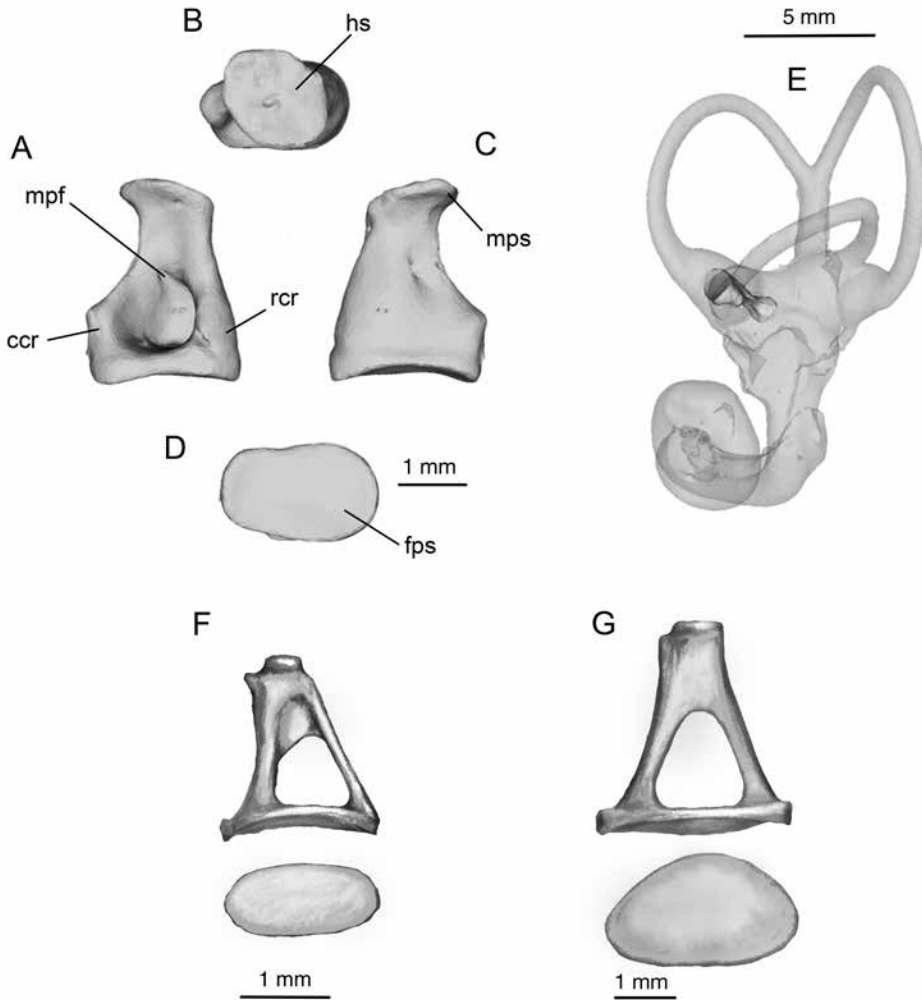
FIG. 33. Stapes in selected members of comparative set. **Top:** Digital 3-D reconstruction of left stapes of *Astrapotherium magnum* MACN A 3208 in **A,** medial; **B,** tympanic; **C,** lateral; **D,** vestibular views. **E,** Dislocated stapes lodged in vestibule of left osseous labyrinth of MACN A 3208 (note scale). **Bottom:** Left stapes of *Tapirus indicus* (**F**) and *Equus caballus* (**G**) in medial and distal views (after Fleischer, 1973: figs. 48, 49). All to same scale as *Astrapotherium*.

raucheniids *Huayqueriana cristata* IANGLIA Pv 29 (Forasiepi et al., 2016) and *Macrauchenia*, and the proterotheriids "*Proterotherium*" MNHN-F-SCZ 205 and *Diadiaphorus* (Billet et al., 2015: fig. 17). However, there is obviously significant variability in this last family, because in *Tetramerorhinus lucarius* AMNH VP-9245 the dorsalmost points on the ASC and PSC are situated at the

same level (table 5). Similarly, while Macrini et al. (2013: fig. 4) found greater ASC projection in the Deseadan specimen of *Cochilius* sp., in the Colhuehuapian species *Cochilius volvens* AMNH VP-29651 (fig. 32) the ASC and PSC display almost no difference in height.

In the panperissodactylans compared here, angular relationships among the three semicircu-

TABLE 5

Inner ear metrics for *Trigonostylops wortmani* AMNH VP-28700 and comparative set[1]

	Trigonostylops	*Astrapotherium*	*Cochilius*	*Tetramerorhinus*	*Equus*	*Tapirus*	*Ceratotherium*
Cochlear turns[2]	2.0	2.0	3.5	2.5	2.2	2.0	1.9
ASC L/W[3]	1.0	1.0	1.3	1.0	1.2	1.3	1.0
LSC L/W[3]	1.0	1.23	1.0	1.15	1.0	1.15	1.16
PSC L/W[3]	1.0	1.25	1.0	1.0	1.0	1.16	1.12
Angle between ASC and PSC[4]	94°	80°	87°	90°	90°	90°	90°
Angle between the PSC and LSC[5]	90°	60°	90°	90°	90°	90°	90°
ASC dorsal projection/PSC height ratio[6]	0	-0.15 (PSC higher)	0	0	0	0.18 (ASC higher)	-0.1 (PSC higher)

[1] Museum numbers for scanned specimens are listed in table 1.

[2] Counted following protocol of West (1985).

[3] Measurements taken from inner side of canal following protocol of Schmelzle et al. (2007).

[4] Measured on a plane parallel to LSC. Angle originates at crus commune (Schmelzle et al., 2007).

[5] Measured on a plane parallel to ASC (Schmelzle et al., 2007).

[6] Distance between dorsalmost point of ASC to dorsalmost point on PSC/ height of PSC measured in straight line from LSC to dorsalmost point on PSC (Schmelzle et al., 2007).

lar canals vary. In *Trigonostylops* the ASC and PSC are set at approximately a right angle to each other in dorsal view, but the angle between the ASC and LSC is slightly acute (~80°). In *Astrapotherium* the departure from orthogonality for the latter angle (~70°), as well as the one between the PSC and LSC (~60°), is much more noticeable (table 5). In dorsal view, the caudalmost projection of the LSC is almost equal to that of the PSC in *Trigonostylops* (fig. 31). We found the same condition in our sample of perissodactylans (fig. 32). A similar relationship holds in the litopterns *Diadiaphorus* and "*Proterotherium*" and the notoungulates *Notostylops*, *Altitypotherium*, and *Pachyrukhos,* but in *Macrauchenia*, *Cochilius*, and *Tetramerorhinus* the PSC is more extended (cf. Macrini et al., 2010, 2013; Billet et al., 2015). The fact that specimens formerly assigned to *Proterotherium* are often found on closer study to be examples of *Tetramerorhinus* (Soria, 2001) raises the question whether this taxon is polymorphic for this and perhaps other labyrinth characters.

The ampullae, situated at the rostral ends of the ASC and LSC and the ventral end of the PSC where it unites with the ventricle, are conspicuously swollen in *Trigonostylops* (fig. 31). Large ampullae are seen in all of the panperissodactylans in the comparative set, including *Cochilius volvens* AMNH VP-29651 (fig. 32). This is of interest because Macrini et al. (2013) found that the ampullae of *Cochilius* sp. SGOPV 3774 differed little in width from their associated semicircular canals.

In all mammals the crus commune is formed by the caudal arm of the ASC and the rostral arm of the PSC (Ekdale, 2013). In *Trigonostylops* the dorsal surface of the crus is almost level with the maximum curve of both semicircular canals in lateral view. Members of the comparative set vary, with the ASC (but not the PSC) projecting above the level of the crus commune (e.g., *Tapirus*, *Ceratotherium*), or with both canals significantly projecting above the crus (e.g., *Astrapotherium*). Macrini et al. (2013) reported significant projection of the ASC compared to the PSC in Deseadan *Cochilius* sp. SGOPV 3774, but in *Cochilius volvens* AMNH VP-29651 the difference between semicircular canals in this

regard is trivial (fig. 32). Variation also occurs in litopterns as well as notoungulates (Macrini et al., 2010, 2013; Billet et al., 2015).

The secondary crus commune is formed where the ventral arm of the PSC and the caudal arm of the LSC join to form a short joint canal (Schmelzle et al., 2007), as seen in *Trigonostylops* but not in *Astrapotherium* (fig. 31). The presence of a secondary crus commune is considered to be plesiomorphic at the level of Mammaliaformes (Ruf et al., 2013; Ekdale, 2015). In our sample of panperissodactylans, it is present in *Trigonostylops*, *Equus*, and *Tapirus*; it is also found in Early Eocene notoungulates (Billet and Muizon, 2013) and litopterns (Billet et al., 2015).

Derived features of the semicircular canals of panperissodactylans may have phylogenetic as well as functional significance. Macrini et al. (2013) found several characters of the inner ear that seem to correlate well with aspects of notoungulate phylogeny. As evident in table 5, the nonorthogonal position of the LSC in *Astrapotherium* and *Trigonostylops* is of particular note; the LSC/PSC ratio of *Astrapotherium* is exceptionally small, both in comparison to other panperissodactylans and to extant mammals in general (see Ekdale, 2013). An inflected lateral canal may have broad ecological implications. Studies focusing on xenarthrans (Coutier et al., 2017) and rhinocerotids (Schellhorn, 2018) suggest that certain values for the LSC/basisphenoid angle may indicate functional differences, affecting head position, diet, and ecomorphotype. More broadly, Berlin et al. (2013) found that non-orthogonal relationships among the semicircular canals may have some relation to fossorial behavior across a broad taxonomic sampling of small mammals. Although drawing analogous ecological conclusions from these studies to panperissodactylans is tenuous without supporting research, these studies just mentioned are representative of a growing body of work illustrating the evolutionary and functional role of semicircular canals, which may eventually help to explain the derived conditions observed in these panperissodactylans.

Stapes. The left stapes of *Astrapotherium magnum* MACN A 3208 is fortuitously preserved inside the osseous labyrinth, having fallen through the fenestra vestibuli postmortem (fig. 33). As usual the element comprises a head, body, and footplate. In tympanic view, the stapedial head is almost circular (length/width ratio of the stapedial head = 1.1), with a faintly convex facet for articulation with the lenticular process of the incus. A blunt process extends from the head's caudal border for attachment of the tendon of the stapedius muscle. In vestibular view, the footplate is slightly compressed with the major axis oriented caudorostrally (footplate length/width = 1.7). The fenestra vestibuli is damaged and therefore could not be separately measured, but its length/width ratio would likely be similar (Segall, 1970). The body of the stapes is essentially imperforate; instead of a large obturator foramen there is only a minute hole situated closer to the stapedial head than to the footplate. However, the bone otherwise has an appearance commonly seen in therians, marked by well-differentiated crura (e.g., Doran, 1878; Novacek and Wyss, 1986; Gaudin et al., 1996; Gaillard et al., in press). The outside border of the rostral crus is almost straight, but that of the caudal crus is deeply concave. The two are separated by a deep pit in medial view. In lateral view, the thin lamina of bone that occupies the space between the crura is weakly convex.

The stapes of *Astrapotherium* differs considerably in appearance from that of *Tapirus indicus, Diceros bicornis,* and *Equus caballus* (fig. 33). A large obturator or intracrural foramen is present in all of these species, although in the tapir and the rhino the size of the foramen is reduced by a small flange of bone draped between the proximal halves of the crura (Doran, 1878; Fleischer, 1973). Functional proximal stapedial arteries are not known to exist in any perissodactylan (Wible, 1987). *Astrapotherium* was evidently similar: the tiny hole mentioned above undoubtedly transmitted a vessel, but it could not have had a wide area of supply even if derived ontogenetically from the stapedial artery. Additionally, there is

no evidence of a promontorial groove (other than the one assumed to be for the internal carotid artery) that might indicate the presence of a true stapedial artery (see p. 91, Promontorial Vascular Features). In the classification scheme adopted by Gaudin et al. (1996), the stapes of *Astrapotherium* resembles the "concave-sided" type as exemplified by the roe deer, *Capreolus capreolus* (in which, however, both crural sidewalls are concave; see Fleischer, 1973; Gaillard et al., in press).

DISCUSSION: INDICIAL AND MORPHOLOGICAL INTERPRETATION

Most of the morphological topics covered in this paper do not require commentaries additional to those already provided in preceding pages. However, some novel insights provided by CT scanning are worth further emphasis, especially ones related to the utilization of indicia to analyze particular morphological problems.

Vascular Indicia

Arterial Structures

In most respects cranial arterial circulation in SANUs seems to have been fundamentally conservative, both within major clades and by comparison to extant perissodactylans and representative archaic "ungulates" such as *Meniscotherium* (figs. 7–10; see also Dechaseaux, 1958a, 1958b; Russell and Sigogneau, 1965; Orliac et al., 2012). For this reason, vessels that are essentially invariant in endocast reconstructions or otherwise of limited interest need only brief review, especially if they leave little or no indication of their passage on dry skulls or fossils. Thus, the vertebral arteries and veins will not be treated in detail, although their significance for interpreting the remarkable conditions encountered in *Homalodotherium* requires emphasis. By contrast, the proximal stapedial artery and (especially) the vasa diploetica magna are reviewed at length precisely because a number of issues connected with their identification and interpretation in SANUs can now be addressed (consult table 6 throughout following sections).

1. Internal carotid artery present and presumably functional in adult: extratympanic routing.

The indicial approach adopted for this paper supports the inference that the internal carotid artery was present and functional in most SANU major taxa (except Xenungulata, for which no applicable data exist at present). Because the route followed by the internal carotid artery to its termination in the circulus arteriosus is of general morphological interest, in this section we outline how different indicia correlate with specific conclusions (extratympanic vs. intratympanic routing, artery absent vs. ambiguous).

It now seems fairly certain that the dominant carotid routing pattern in most SANU clades was extratympanic, not intratympanic (table 6). Presence of IC1 (carotid incisure present) is consistent with an extratympanic route, and this inference is strengthened in certain instances if IC2 (groove on bulla present) can be interpreted as an artery-related feature. The principal caveat is that, in isolation, a bullar groove is ambiguous, signifying presence of internal carotid artery, or a large basicranial vein, or conceivably both. Large emissary veins leave trackways in various places in members of the comparative set (cf. fig. 29A: feature 1; fig. 39B: white asterisks). Their nature can often be settled if the grooves pass into the caudal part of the basicapsular fenestra or the hypoglossal canal (e.g., fig. 38A: feature 5), neither of which are ports for the internal carotid artery. For living species of perissodactylans such features can be unequivocally interpreted as venous channels because internal carotid artery presence is already accounted for, but interpretation may be more difficult where extinct taxa are concerned. Markings associated with the cerebral carotid artery do not verify the presence of a functional internal carotid, because the former vessel always completes the circulus arteriosus, regardless of the fate of the artery's preendocranial section.

Obviously, a lengthy arterial sulcus on the ventral surface of the promontorium (IC3) would be inconsistent with an inference of extratympanic routing, but *Tapirus indicus* AMNH M-200300 presents an intermediate condition (IC5) in which a very short promontorial sulcus is present, limited to the area of the rostral pole (fig. 37B; see appendix 2). In tapirs the internal carotid artery evidently ascends more or less directly into the endocranium from the neck, probably only grazing the petrosal along the way (hence the short sulcus) rather than penetrating the actual membranous envelope of the tympanic cavity (i.e., true cavum tympani, as defined by MacPhee, 1981). For this reason, in tapirs the internal carotid artery should probably be classed as traveling extratympanically, as in other perissodactylans, or its routing defined in terms of an intermediate character state. In other cases it may be more difficult to evaluate IC5, as the fossa for the tensor tympani or even a cochlear turn may leave an impression that could be misinterpreted as a carotid trackway.

2. Internal carotid artery present and presumably functional in adult: intratympanic routing.

The intratympanic course is unambiguously present in *Meniscotherium* and some other "condylarthrans" and may have been the basal condition for euungulates. As discussed earlier (see p. 91, Promontorial Vascular Features), *Tetramerorhinus* (IC3, lengthy promontorial sulcus present) and *Trigonostylops* (IC4, caudal carotid foramen present) were the only SANU taxa investigated in detail for this paper that meet basic indicial requirements for inferring the existence of an intratympanic internal carotid artery. To these *Astrapotherium* could probably be added, although indicia are not entirely conclusive because of the strongly transverse orientation of this sulcus in a large proportion of specimens (IC5, ambiguous). As noted, the *Astrapotherium* condition is unlike the quasisagittal orientation of the sulcus typically seen in placentals exhibiting a transpromontorial internal carotid artery (cf. MacPhee and Cartmill, 1986). It is conceivable that the artery followed a

kind of looping trajectory before entering the endocranium in this astrapotheriid, perhaps in a more drawn-out version of the course seen in modern *Equus* (fig. 5B) and possibly also *Tapirus* (fig. 38A: feature 4). Other plausible, nonarterial explanations for the sulcus (e.g., fossa for tensor tympani muscle, articular facets for ectotympanic or entotympanic) are less likely still. If it were known whether astrapotheriid ectotympanics bore a carotid foramen or notch (IC4) like that of *Trigonostylops*, the matter could be settled.

If in a fossil no reliable indicia can be identified for the presence of an intratympanic carotid, then this particular routing was presumably absent. This does not, however, mean by default that there had to have been a functional but extratympanic carotid, as opposed to no artery at all; choosing between those alternatives must be based on appropriate independent criteria.

As previously remarked, Patterson (1932: 23; 1936: 206, fn.) argued that a "posterior carotid foramen" existed on the caudal aspect of the bulla in several notoungulate specimens, including *Homalodotherium segoviae* FMNH P13092 (fig. 28), *Plagiarthrus* (= *Argyrohyrax*) *proavus* FMNH P13415, *Interatherium robustum* FMNH P13057, and others. Billet and Muizon (2013) made a similar argument for the presence of a caudal carotid foramen in skulls of a number of other notoungulates (*Pleurostylodon*, *Nesodon*, *Posnanskytherium*, *Plesiotypotherium*). However, in all cases that we have personally investigated the only aperture in the stipulated location is relatively tiny, and much more likely to have conducted the tympanic nerve of CN 9 than the internal carotid artery (see also Gabbert, 2004).

Patterson (1936) was unable to bolster his original argument by referencing strong supporting indicia, which in this case might have been either a definite vascular sulcus on the promontorium's ventral surface or a rostral foramen for the alleged artery. The intratympanic "ventral ridge," a partial septum that Patterson (1936: 205, fig. 46) illustrated as extending from his carotid foramen onto the caudal pole of the promontory in *Interatherium robustum* FMNH P13057, can-

TABLE 6

Analysis of Vascular Indicia in Selected Panperissodactyls and Relatives

A. Evaluation of Vascular Indicia[1]

Character States[2,3]	Indicium	Criteria and Notes
IC1 ET presence	Incisura carotidis	Must present definite scalloped edge or sulcus on fenestral lip
IC2 ET presence[4]	Groove on medial bullar wall	Must lead into basicapsular fenestra; must exclude basicranial veins as only occupant
IC3 IT presence	Lengthy ventral promontorial sulcus or canal	Typically caudorostrally oriented, with/without stapedial branch, terminating in intratympanic rostral carotid foramen
IC4 IT presence	Caudal carotid aperture in bulla/ectotympanic	Must exclude tympanic canaliculus
IC5 IT ambiguous	Promontorial sulcus abbreviated, unusual orientation	Must exclude tensor fossa, cochlear turn; absence of definite carotid incisure indicative but not conclusive
IC6 absence	No indicial markings for either course	Absence of promontorial markings may be ambiguous; that, combined with absence of both carotid foramina and tegminal stapedial foramen, would be more indicative
		Evidence of alternative supply to circulus arteriosus may be conclusive
ST1 presence	Sulcus crossing lip of fenestra vestibuli	Must exclude tympanic nerve plexus, especially if no indication of intratympanic internal carotid
ST2 ambiguous	Foramen/sulcus on tympanic roof	If proximate to CN 7 opening, see LHV
ST3 absence	No roof foramen or promontorial markings	Suggests proximal stapedial absent; rami may be present if annexed by other arteries (e.g., ramus inferior in *Equus*)
ST4 absence	Stapes foramen condition	Partly or completely imperforate bicrural stapes indicates stapedial involution during ontogeny
ST5 absence	Body size	Megafaunal body size[e]
ADM1 presence	Squamosopetrosal bounding as in *Dasypus*, canal Y	Bounded posttemporal foramen + canal Y or equivalent trackway; in SANUs bounding includes exoccipital
ADM2 ambiguous	Posttemporal foramen only, no canal Y	Positive for presence of vasa, but not specific as to arteria or vena (or both) if no separate trackways
ADM3 absence	No applicable foramina with artery	Absence of definite posttemporal complex; mastoid emissary foramen venous only
VDM1 presence	Posttemporal complex as in *Dasypus*	Trackways must be evident for vena as well as arteria diploetica magna
VDM2 presence	Posttemporal complex as in *Cochilius*, *Trigonostylops*	Trackway organization suggests venous circulation only; possibly arteria absent, reduced, or functionless
VDM3 absence	Posttemporal complex as in *Equus*	Artery only
AL1 presence	Small channels within calvarial bone	Marrow spaces must link together as a network, join transverse sinuses
AL2 presence	Channels + large extraneural space	As in *Homalodotherium*; must exclude other explanations

TABLE 6 *continued*

Character States[2,3]	Indicium	Criteria and Notes
AL3 absence	Absent or minor	Few or no linked channels (e.g., *Equus*); also interpretable as ambiguous
SS1 presence	Sulcus	Often poorly defined along petrosal-exoccipital suture, better in jugular area
SS2 ambiguous	No evident sulcus	No jugular impression implies involution or diminution to thread
LHV1 presence	Tympanic aperture on or in secondary facial foramen for CN 7	Must be located proximate to CN 7 opening; must exclude cavum suprachochleare & foramen for stapedial ramus superior
LHV2 ambiguous	Sulcus/canal from temporal sinus on tympanic roof	May be hard to distinguish sulcus + trackway for LHV from that for stapedial ramus superior (?may share joint foramen)
LHV3 ambiguous	Sulcus associated with track of CN 7 toward stylomastoid foramen	May be hard to separate from track of CN 7 & ramus posterior; also trackway for auricular ramus of CN 10
LHV4 absence	No trackway uniquely attributable to LHV	No basis for assuming presence

B. Distribution of Indicia in Comparative Set

Taxon	Internal carotid artery	Proximal stapedial artery	Arteria diploetica magna	Vena diploetica magna	Accessory lacunae of transverse sinuses	Sigmoid sinus	Lateral head vein
Trigonostylops AMNH VP-28700	**IC4**	***	ADM2	**VDM2**	**AL1**	**SS1**	***
Astrapotherium MACN A 8580	IC5	*ST3, ST4, ST5*	***	**VDM2**	***	**SS1**	***
Homalodotherium MPM PV 17490	IC6?	*** (ST5)[5]	ADM2	**VDM2**	**AL1, AL2**	**SS1**	***
Toxodon MACN Pv 16615	**IC1, IC2**	*** (ST5)[5]	***	**VDM2**	***	***	***
Cochilius AMNH VP-29651	IC6	ST3[6]	ADM2	**VDM2**	**AL1**	SS2	**LHV1**
Tetramerorhinus AMNH VP-9245	**IC3**	ST2	ADM2	**VDM2**	***	**SS1**	LHV2, LHV3
Equus AMNH M-204155	**IC1, IC2**	*ST3, ST5*	**ADM1**	VDM3	*AL3*	SS2	*LHV4*
Tapirus AMNH M-200300	**IC1**, IC5	ST3, ST5	ADM2	***	*AL3*	**SS1**	***
Ceratotherium	**IC1, IC2**	ST3, ST5[7]	ADM2	***	***	**SS1**	***

TABLE 6 *continued*

Taxon	Internal carotid artery	Proximal stapedial artery	Arteria diploetica magna	Vena diploetica magna	Accessory lacunae of transverse sinuses	Sigmoid sinus	Lateral head vein
AMNH M-51882							
Meniscotherium	**IC3**[8]	**ST1**[8]	ADM2	***	***	**SS1**	LHV2
AMNH VP-4412							

[1] IC, internal carotid artery; ST, proximal stapedial artery; ADM, arteria diploetica magna; VDM, vena diploetica magna; AL, accessory lacunae of transverse sinuses; SS, sigmoid sinus; LHV, lateral head vein.

[2] Font style conventions for character states: **bold** = presence, positive indicial evidence for character state; roman = ambiguous, evidence inconclusive; *italics* = absence, no indicia supporting presence; ***, damaged features(s) or not investgated.

[3] Internal carotid course: ET, extratympanic ; IT, intratympanic.

[4] Intrabullar carotid canals rather than external grooves exist in some placental clades (e.g. extant feliform carnivorans); not known in SANUs

[5] Absence inferred in case of large body size (defined as "aardvark limit," > 50-70 kg; see Wible, 2012; Nowak, 2018)

[6] Tympanic roof foramen present, but interpreted as port for lateral head vein.

[7] Stapes foramen partially obliterated in *Diceros bicornis* (fig. 33).

[8] According to Cifelli (1985), for an unnumbered AMNH specimen (see text).

not be considered an exclusive marker for an intratympanic internal carotid artery. For example, *Cochilius volvens* AMNH VP-29651 and *Oldfieldthomasia debilitata* AMNH VP-28600 exhibit a similar feature, but it almost certainly conducted the tympanic nerve, not the internal carotid artery (contra Simpson, 1936: 17; see MacPhee, 2014: fig. 14C).

Recently, Martínez et al. (2016, 2020) have also argued for an intratympanic routing of the internal carotid in another series of notoungulates (*Rhynchippus equinus, Mendozahippus fierensis*, *Gualta cuyana*), based on the same kinds of evidence as Patterson's. *Mendozahippus fierensis* MCNAM-PV 4004 preserves the auditory bullae, allowing some degree of certainty about foraminal position and relations. Figure 5 of Martínez et al. (2020) depicts, on the virtually reconstructed right petrosal of this specimen, the proximal stapedial artery originating from the internal carotid artery on the caudomedial aspect of the promontorium, just before the latter's main trunk enters the endocranium. No promontorial trackway is identified as belonging to the internal carotid, but "there

is a clearly distinguishable duct that connects the extracranial space (at the level of the jugular foramen) with the tympanic cavity" (Martínez et al., 2020: 17, fig. 6). This duct or foramen was not identified in an earlier description of the skull (Cerdeño and Vera, 2015), suggesting that the aperture is probably quite small. Interestingly, the left bulla exhibits what appears to be a well-developed groove running along its medial aspect toward the piriform fenestra (= medial lacerate foramen), but whether this groove accommodated an artery or a vein is not addressed. In light of these several ambiguities, the best course is to defer reaching a conclusion about the presence of a caudal carotid foramen in this specimen pending an evaluation of the alternative explanation, which is that the "duct" represents the canaliculus for the tympanic nerve.

Note that such tests as there are relate to very specific features, and that single indicia are rarely dispositive. Thus the ?carotid foramen in *Archaeohyrax*, cautiously identified by Billet et al. (2009: fig. 7) halfway down the medial side of the bulla, is much more likely to have been a

port for an emissarial connection between the ventral petrosal sinus and basicranial veins. The so-called intrabullar route, by which the vessel travels within the substance of the auditory bulla (as in a number of carnivorans and other taxa; Wible, 1984, 1986), may seem superficially similar, but in all investigated cases the artery actually enters the circulus arteriosus at the same place, i.e., the position of the ontogenetically primary (rostral) carotid foramen. The same arrangement would also be expected in *Archaeohyrax* if Billet et al. (2009) were correct. Simpson (1948: 187) described a carotid routing in *Notostylops* that cannot be distinguished from one that would be expected for the inferior petrosal sinus.

Finally, it is known that promontorial nerve tracks may mimic the route of the internal carotid artery in certain taxa in which the vessel involutes during fetal life (e.g., some strepsirrhine primates; Conroy and Wible, 1978; MacPhee, 1981). However, any confusion on this score is improbable in the case of SANUs, few of which exhibit transpromontorial sulci of any sort. It should also be kept in mind that such finely branching sulci are unlikely ever to represent carotid pathways in large mammals.

3. Internal carotid artery absent in adult.

Trying to determine whether a soft-tissue structure was completely absent in an extinct taxon is often a frustrating exercise. Indeed, with respect to vasculature, "complete absence" is often not a meaningful category, as parts of vessels present in early stages of ontogeny may be annexed by others and repurposed (Bugge, 1974; Wible, 1987). With respect to whether the internal carotid artery was actually absent in the adult stage of certain SANUs, at present the only potentially useful indicium is IC6, which denotes bullar expansion across most of the basicapsular fenestra, sealing it over nearly completely, and with no contradictory indicia suggesting functional arterial presence. We offer this observation as a correlation; no cause-effect relationship is implied, and as a reliable indicator it needs further testing as noted below.

Possible examples of absence are so far restricted to smaller notoungulates, especially typotheres, in which the enlarged bulla covers all expected local entry points except for the obligatory channel for CN 5.3 (e.g., *Paedotherium, Cochilius, Protypotherium, Oldfieldthomasia, Colbertia, Mesotherium*; see van Kampen, 1905: 610-611; García-López, 2011; MacPhee, 2014).

In principle even a highly reduced basicapsular fenestra, in which the dehiscence is diminished rostrally to the equivalent of the foramen ovale, could have functioned as a joint port for both the internal carotid artery and the mandibular nerve. However, in extant placentals these structures do not usually travel in such close proximity. In SANU specimens with expanded bullae in which the apparent foramen ovale is exceptionally small (e.g., MLP 79-IV-16-1, partial skull of "*Campanorco inauguralis*"), carotid absence might be reasonably suspected, but this point has not been adequately investigated in taxa other than the ones named here. Species of middling body sizes, with very large but unincised piriform openings, are more difficult to assess and should be classed as ambiguous for arterial presence unless positive indicia suggest otherwise (e.g., bony subdivision of rostral section of basicapsular fenestra). In taxa of truly large body size the bulla may be medially expanded, but in taxa such as *Toxodon* other indicia for carotid presence may be found in well preserved material (fig. 29B). Still, it is evident that the carotid recognition problem has not yet been satisfactorily solved for all SANUs.

Equus exhibits yet another character state: it possesses a complete ectotympanic-entotympanic bulla, but it also has a fully functional, extrabullar internal carotid artery (figs. 5, 39). The relevant negative contrast is that the horse's relatively small bulla does not actually cover any part of the basicapsular fenestra, so the piriform portion is widely open, unlike the situation in interatheriids. There is also a positive indicator for arterial presence in the form of the incisura carotidis. (Note that perissodactylans

may be considered to be on a spectrum with regard to the degree of tympanic floor ossification: O'Leary [2010] considered the bulla to be present in tapirs because of wide contacts between the tympanic roof and ectotympanic crura.)

4. Inferring the contribution of noncarotid vasculature to cerebral circulation.

Assuming for the sake of argument that some SANU taxa lacked a functional internal carotid artery in the adult stage, how would they have irrigated their brains? To make progress on this issue it will be important to look for new indicia that could point to the involvement of other vessels in cerebral arterial circulation. For example, in extant artiodactylans, almost all clades of which lack intact internal carotid arteries in the adult stage, major anastomoses between the external and cerebral carotids significantly supplement the relatively small blood supply brought to the circulus arteriosus by the vertebral arteries (Daniel et al., 1953; O'Brien et al., 2016; O'Brien, 2017). Whether a similar solution existed in some SANUs, perhaps via an anastomotic link (arteria anastomotica) passing through the foramen ovale, has not been previously considered but should not be ruled out without a thorough search for potential indicia.

Although there are many examples of strikingly different carotid routings in Mammalia (see van Kampen, 1905; van der Klaauw, 1931; MacPhee, 1981; Wible, 1984, 1986), there also tends to be fairly strong uniformity within individual major clades, which makes any supposed examples of significant within-group variation of great interest. For example, it would be intriguing if Du Boulay et al. (1998) were correct in asserting that the extratympanic vessel universally regarded as the internal carotid in *Equus* is in fact the homolog of the ascending pharyngeal artery, although the only ground offered for their interpretation is that "the cervical course of the ascending pharyngeal is almost exactly the same as that of the internal carotid until it comes close to the skull base."

While position is important, whenever possible it should not be exclusively relied upon for homological determinations, and in this case more evidence is certainly required. (For a good example involving multiple criteria for inferring functional replacement of the internal carotid by the ascending pharyngeal in certain extant primates, see Cartmill, 1975.)

In a different category are the transclival foramina of the basioccipital (fig. 17C), seen in various notoungulates (e.g., *Paedotherium chapadmalense* AMNH VP-45914, *Plagiarthrus proavus* FMNH P13425, *Cochilius volvens* FMNH P13424, *Protypotherium* sp. FMNH P13234) as well as many other taxa, including stem eutherians and marsupials where they often go unremarked or described as "nutrient foramina" (e.g., Kielan-Jaworowska, 1981; Aplin, 1990). In some SANUs they may be relatively large (e.g., *Interatherium*; Sinclair, 1909: pl. 8, fig. 18). Simpson (1933c) even wondered whether the ones exhibited by *Hegetotherium* might be entry points for the internal carotid artery, but this seems very improbable given the ontogenetic development of true carotid foramina in therians (see Forasiepi et al., 2019). Much smaller apertures may occur in similar positions in *Homo*, where they transmit transclival emissary veins that connect the basilar venous plexus with the pharyngeal plexuses (see Altafulla et al., 2019). The SANU versions, assumed here to have been similar in function, might have had some importance for venous circulation on the basis of their size alone, but there is currently no basis for inferring that they were also ports for the internal carotid or any other artery for that matter.

Venous Structures

As in the case of the main cranial arteries, variation in the chief endocranial veins appears to have been rather modest in SANUs, to the degree that this can be assessed with the tools available and in the virtual absence of complementary studies for this group. Smaller branches

are more variable, reflecting their stochastic origin as dominant routes of flow within larger embryonic networks, but few of these were traceable in this study. In table 6 we list indicia for inferring presence/absence of certain venous structures, some of which have never previously been the subject of detailed study in SANUs.

1. Evaluating the comparative dominance of the internal jugular and vertebral venous systems.

The basal mammalian patterns of cerebral drainage investigated by Wible and Hopson (1995) and Wible and Rougier (2000) illustrate the frequent dominance of the vertebral venous system over the internal jugular system, something still seen in many extant mammals (e.g., *Ailuropoda*; see Davis, 1964: fig. 23). In SANUs there is certainly endocast evidence for large anastomoses between the vertebral veins and one or more of the large dural sinuses or their associated outlets in the rear of the cranial cavity (ventral petrosal sinus, condylar vein) (figs. 7–10). Much less can be said about the proportional roles of the sigmoid sinus and internal jugular vein in fossils, largely because endocast impressions for assessing their presence and size are frequently inadequate for the purpose (Kielan-Jaworowska et al., 1986). At present, it is more instructive to note the incidence and limitations of some of the indicia currently available for these features in actual specimens.

To begin with a clearcut example, the endocast of *Tetramerorhinus lucarius* AMNH VP-9245 (figs. 9; 40F, G) exhibits a well-marked sulcus for the sigmoid sinus (SS1, present), consistent with the existence of a large internal jugular vein. The sulcus for the sigmoid sinus also communicates with impressions for the ventral petrosal sinus and the short, wide hypoglossal canal. The latter is in turn continuous with a feature directed toward the foramen magnum, representing the vertebral vein. Here a reasonable case can be made for a continuous chain of endocranial anastomoses that would have caudally united the caudodorsal and rostroventral arrays and permitted cerebral venous return along several pathways, not just the internal jugular route (e.g., retroarticular vein, fig. 40H, I). Whether plexuses on the basicranial exterior were also part of the total venous network is probable but not assured.

By contrast, no definable sulcus for the sigmoid sinus (SS2, ambiguous) is seen in the young specimen of *Equus* illustrated in figure 10, nor is there osteological evidence for a channel running between the hypoglossal canal and sulcus for the ventral petrosal sinus (but see Bradley, 1923: 144). Further, caudodorsal and rostroventral arrays do not appear to directly communicate within the endocranium, a feature noted in staged fetuses by Vitums (1979). However, the temporal meatus and retroarticular incisure are notably large (fig. 41), which would allow for drainage of the transverse/temporal sinuses even if the sigmoid sinus were absent. As shown previously, dissection evidence for *Equus* reveals that the rostroventral array in the horse mostly drains through rostrally positioned emissaries, basicranial plexuses, and the craniooccipital vein discharging into the vertebral venous system (fig. 6A, B; Montané and Bourdelle, 1913). Obviously, in the absence of soft-tissue evidence these routings would be hard or impossible to reconstruct.

The skull of *Ceratotherium simum* AMNH M-51882 (figs. 10; 36B, C) exhibits large sulci and other markings for the sigmoid sinus, ventral petrosal sinus, and hypoglossal canal. This is consistent with the presence of a functional internal jugular in this taxon, but does not obviate the possible importance of an extracranial network integrated with the vertebral venous system. In *Tapirus terrestris* AMNH M-77576 (fig. 38A) there is an evident connection between the ventral petrosal sinus and the hypoglossal canal (feature 6) that may have also involved an inferred ?craniooccipital vein (feature 5). There appears to be no published dissection evidence for ceratomorphs on these points.

In the specimens of *Cochilius* and *Meniscotherium* there are strong impressions for the condylar emissary vein and vertebral vein (fig. 9: features 4, 5; see also Williamson and Lucas, 1992). These indicia are consistent with the importance of

drainage through the foramen magnum in these taxa. In *Cochilius* the impression for the sigmoid sinus is relatively small, but in *Meniscotherium* it is notably larger (fig. 9: feature 7). Descriptions and illustrations published by Martínez et al. (2016) suggest that endocranial drainage in *Rhynchippus equinus* was mostly accomplished via the retroarticular and internal jugular veins, but given the large size of the hypoglossal canal in this species it cannot be discounted that an extracranial pathway to the vertebral venous system was significant as well (compare dural venous reconstructions for the notoungulates *Mendozahippus* and *Gualta* by Martínez et al., 2020). Unnamed sulci seen on the basicranium of large notoungulates in the vicinity of the basicapsular fenestra probably also involved such connections (see *Toxodon*, fig. 29A: feature 5).

2. Homologies and function of the accessory lacunae of the transverse sinuses.

The accessory lacunae of the transverse sinuses have not previously been clearly recognized as a morphological entity, although they are probably common. Because there is no external indication of the size of these large hematopoietic marrow spaces within calvarial diploe, scanning is the only way to model them, which explains why they usually escape notice. Because of limitations of time, we undertook thorough reconstruction of these spaces in only one case (*Homalodotherium*, fig. 7), although if extensive their presence is easily detected in segments (e.g., *Cochilius*, fig. 17C).

Three conditions of the accessory lacunae can be discriminated in our comparative set. The first or typical condition (AL1, present) consists of networks or fields of fine channels concentrated within the diploe in the caudal part of the parietal and supraoccipital; these communicate directly with the transverse sinuses via a few larger canals, as seen in *Cochilius* (figs. 9: feature b; 17C) and *Trigonostylops* (fig. 8) among the taxa reviewed here. These networks are not especially noteworthy by themselves and might be regarded as simply a well-developed system of diploic veins.

Their identity becomes of interest only in light of the second condition, exemplified in the much more elaborate structure capping the dorsal surface of the cerebellum (AL2, present) on the endocast of *Homalodotherium* (fig. 7). The structure's composition during life is of course unknown, but given its highly unusual position and structure it seems improbable that it was composed of neural or ordinary dural tissues. Although situated where the vermis of the cerebellum dorsally arches in many mammals, including SANUs (see MacPhee, 2014: *Paedotherium*, fig. 12B). its highly vermiculated surface and continuity with sulci for dural sinuses bolsters the inference that this feature was vascular. Additionally, segmental data indicate that in *Homalodotherium* large channels extended from the inferred extraneural mass into the local calvarial bone, a resemblance to the typical condition AL1 but in this case much more developed. Although not specifically mentioned by Patterson (1937), the same features can be identified on the latex endocast of *Homalodotherium segoviae* FMNH P13092, showing that conditions in MPM PV 17490 are not anomalous. Also, under magnification the surface of this part of the FMNH P13092 endocast appears riddled with small foramina and canals that were truncated when the latex impression was removed, further supporting the inference that it was composed of or included vascular tissues.

The third condition is apparent absence of accessory lacunae (AL3, absent). In this case parietal diploe presents as cancellous tissue only (e.g., some *Gorilla*; Hershkovitz et al., 1999), with few or no continuous diploic veins detectable radiographically. Clearly, however, there is a continuum in morphology, probably largely driven by species-specific variation in the number of hematopoietic centers maintained during ontogeny. In *Equus*, for example, extensive lacunar fields were not found. However, the sinus communicans, part of the confluence of the sinuses (Sisson and Grossman, 1953), is normally housed within the tentorial process of the supraoccipital where it communicates with both transverse sinuses (fig. 5), and thus presents an intermediate morphology.

It should be easy to resolve whether the sinus communicans is part of an active hematopoietic center throughout life in *Equus*. Martínez et al. (2020) describe similar connections in *Mendozahippus* in regard to what appears to be the equivalent of the sinus communicans ("accessory connection with temporal sinuses").

Much more remarkably, extraneural volumes grossly similar to that of *Homalodotherium* occur in approximately the same place on endocasts of certain fossil cetaceans (e.g., Bajpai et al., 1996; Geisler and Luo, 1998). On endocasts of basilosaurid archaeocetes the inferred extraneural mass is especially large, continuing around the sides and base of the brain all the way to the position of the hypophysis. In extant mysticetes and some odontocetes the same locations are known to be filled with massive intracranial retia mirabilia (e.g., Ommanney, 1932; Walmsley, 1938; Breathnach, 1955; Vogl and Fischer, 1981; Wible, 1984). Geisler and Luo (1998) provide reasons for concluding that the extraneural volumes detected on endocasts of fossil whales were occupied in life by elaborate retial structures, and indeed there seems to be no other plausible explanation for them.

Although cranial retia in extant cetaceans are primarily arterial, Walmsley (1938) noted that components dorsal to the cerebellum in the finwhale *Balaenoptera physalus* may be largely venous. In describing the rostralmost part of the spinal vascular rete in a fetus of this species, Walmsley (1938: 164) also noted that:

> In the anterior part of the vertebral canal the [spinal] rete lies entirely ventral to the spinal cord and as it passes through the foramen magnum it divides into right and left halves. Each passes forwards and laterally on the side wall of the skull as a wide vascular lamina…. Each sweeps medially to the body of the sphenoid on which the two sides join together and form a vascular mass 60 mm. thick in which the hypophysis is embedded.

Judging from Walmsley's (1938) morphological descriptions, he thought that the vascular lamina of the finback whale were highly derived versions of the vertebral arteries seen in mammals generally. On the basis of a study of a fetus of the narwhal *Monodon monoceros*, Wible (1984) regarded the vertebral arteries as absent and the spinal rete mirabile as sui generis. Geisler and Luo (1998) raised the question whether (in addition to rostrally situated epidural retia) small caudal retia might exist in some extant noncetacean artiodactylans, which could imply that retia are an ancient adaptation not specifically linked to aquatic environments. To our knowledge, extraneural spaces of the kind discussed here have never been identified on endocasts of fossil members of noncetacean Artiodactyla, nor have accessory lacunae, but the possibility surely remains.

As discussed in the description of the endocast of *Homalodotherium*, impressions for vascular channels also occur on the floor of the brain case in this taxon (fig. 7). Patterson (1936) interpreted these as vertebral arteries per se, a determination with which we tentatively agree, although the homology of their rostral continuations is uncertain. In any case, there is no evidence at present that might indicate whether the vertebral arteries of *Homalodotherium*, even if correctly identified, were linked to the conjectured vascular mass situated over the cerebellum. If a true intracranial retial system had been present in this SANU, then it would presumably have had a physiological regulatory function of some sort, as in artiodactylans.

Finally, it is relevant to mention that the elaborate cranial retia of whales are associated with the reduction or obliteration of the internal carotid artery (Ommanney, 1932; Walmsley, 1938; Wible, 1984). Whether this correlation would have applied to *Homalodotherium* is undetermined. As noted previously, although the piriform portion of the basicapsular fenestra is large in this taxon, indicia for the internal carotid artery are inconclusive.

3. Identification of the true ventral petrosal dural sinus.

It is often assumed that the ventral petrosal sinus may be either intra- or extracranial,

because in different species grooves attributed to this vessel may be found on either surface of the central stem. This assumption overlooks deep organizational features of the cranial venous system that need to be considered when making homological decisions. A fundamental distinction is ordinarily made between venous channels that develop within dural tissues, and are thus intracranial by definition, versus those that do not, which are classed as extracranial if they lie outside the skull (Butler, 1957, 1967). Topologically, these two categories of cranial veins can be readily separated because the skeletogenic anlagen that form the bones of the skull differentiate in dense connective tissues situated between the dural sinuses and external systemic veins (Butler, 1967; Padget, 1956; Warwick and Williams, 1973: 144). From this it follows that the ventral petrosal sinus, as a vein differentiating on the endocranial side of the bones of the central stem, should be classed as intracranial. A vessel differentiating on the basicranial exterior, even if its course parallels that of the ventral petrosal sinus, must therefore be something else—and, as a nonhomolog, should be given a different name.

Equus displays just such a dual condition: the ventral petrosal sinus from the cavernous sinus and the craniooccipital vein from the basicranial plexuses travel on opposite sides of the central stem, but communicate via emissaria passing between them through the basicapsular fenestra (fig. 6). Vitums (1979: 135) grouped the emissaria of the basicranial plexuses as the "extracranial portion of the equine ventral petrosal sinus," but this obscures the fact that they are not the same thing from a developmental or, probably, a phylogenetic perspective. *Canis* and *Homo* appear to be fundamentally similar to the horse in these regards, although the anatomical nomenclature is different (see p. 33, Interpreting Vasculature: Veins). From the standpoint of homology, identification of the true ventral petrosal sinus should be restricted to vessels (or trackways in dry skulls and fossils) lying on the floor of the cranial cavity in close relation to the internal aspect of the

basicapsular fenestra or petrobasioccipital suture. Vessels or trackways that are situated on the extracranial side of the same features should be recognized by a different term or terms, as we have done here in connection with the craniooccipital vein and the basicranial venous plexuses with which it communicates (e.g., fig. 6). However, it is acknowledged that this series of inferences cannot account for all conditions that have been described for eutherian fossils, especially stem taxa (e.g., Wible et al., 2001).

4. Potential roles of parietosquamosal vasculature.

Parietosquamosal apertures are ubiquitous in many mammalian clades, not just panperissodactylans (see Wible, 1987). Their number is notably variable within and between phylogenetic groupings, and lack any evident correlation with body size, locomotor behavior, or ecological preference. The prevailing view (e.g., MacPhee and Cartmill, 1986; Wible, 1987), that their occupants—terminal branches of meningeal vessels—act only to irrigate the temporalis muscles and perhaps local scalp tissues or head ornamentation, is possibly too narrow in cases where the number of parietosquamosal foramina/canals is large. Modeling the roles of similar features in extant mammals, including their conceivable involvement in selective brain cooling, would be an interesting project in comparative physiology. The notable dilatation in the caudodorsal dural array on the dorsal side of the petrosal apex, seen in different SANU taxa (see p. 33, Interpreting Vasculature: Veins), may or may not be a related phenomenon.

5. Identifying the tympanic aperture of the prootic canal for the lateral head vein/prootic sinus.

Although the lateral head vein regularly forms in early mammalian vascular ontogeny (Butler, 1967), its apparent functional retention, as indicated by a patent tympanic aperture of the prootic canal in the adult osteocranium, has been established in only a handful of fossil taxa (see p. 95, Tympanic Aperture of Prootic Canal). The aperture is probably present in skulls of extinct

and extant members of many mammalian clades—including SANUs—but it is easily confused with the exit foramen of the stapedial ramus superior (see suggested indicia in table 6).

Generalizing from observations reported by Wible (2008) concerning *Solenodon*, in a mammal the intratympanic entry point for the prootic canal should lie within the petrosal's contribution to the tympanic roof, in close proximity to the secondary facial foramen (LHV1 presence). This is the case in *Cochilius volvens* AMNH VP-29651 (figs. 16A, 17B, 18A), which is thus the first SANU to yield evidence for the presence of the lateral head vein within the tympanic cavity. Although in taxa that possess the ramus superior of the stapedial artery the vessel's exit point also penetrates the tympanic roof, its foramen is usually situated more laterally, near or within the suture between the epitympanic wing of the squamosal and tegmen tympani (see MacPhee, 1981; exceptions noted below)

On the endocranial surface, trackways issuing from the sulcus for the temporal sinus may be indeterminate (LHV2, ambiguous) because the paths for both the lateral head vein/prootic sinus and ramus superior may overlap or intersect. However, this ambiguity can be indirectly resolved in favor of the vein if there are no indicia for any intratympanic components of the internal carotid, including the proximal stapedial artery (ST3, absent). This is the case in *Cochilius* and probably most SANUs (but see Billet and Muizon, 2013).

Another indicator of the vein's presence would be presence of a distinct channel passing to the rear of the tympanic cavity in close association with, but separate from, the groove for the facial nerve. This is not a typical routing for the superior and inferior rami of the stapedial artery or related anastomoses (cf. Wible and Hopson, 1995; Wible, 2008). However, the ramus posterior's trackway follows the same course (Wible, 1984; MacPhee, 2011) and thus may be hard to distinguish from that of the vein, in which case conclusive identification would not be possible (LHV3, ambiguous). In *Cochilius volvens* AMNH VP-29651, a shallow

sulcus on the rostral wall of pars canalicularis, attributed to the vein, is separate from the groove for CN 7 that crosses the lip of the adital opening (fig. 17B). These sulci eventually coalesce in the rear of the tympanic cavity and the distinction between them is no longer evident. In *Cochilius* the lateral head vein would have left the facial sulcus at some point in order to travel medially to the jugular area, where it would have terminated in the internal jugular vein or perhaps the ventral petrosal sinus. Wible (2008) noticed in *Solenodon* that the lateral head vein departs the tympanic cavity through the foramen for the auricular branch of the vagus (mastoid canaliculus). This part of its route would ordinarily be ambiguous (LHV3); fortunately, the vein was fully traceable on a sectioned specimen. Ekdale et al. (2004: fig. 4) illustrated a similar relationship in Zhelestidae. In *Oldfieldthomasia* AMNH VP-28600 there is a candidate aperture for the auricular branch of the vagus nerve that passes between the caudal wall of the bulla and the caudal crus of the ectotympanic, but there is no clear indication that two structures were contained within it. At present, it seems that LHV1 is the only decisive indicium for asserting presence of the lateral head vein in a fossil or dry skull.

Martínez et al. (2016, 2020) concluded that a sulcus for the proximal stapedial artery and the intratympanic part of its ramus superior exists in several notoungulates (*Rhynchippus*, *Mendozahippus*, and *Gualta*), but it is more likely to have accommodated the lateral head vein. At least as illustrated (Martínez et al., 2020: 17, fig. 5A), the trackway that they identified does not cross the fenestra vestibuli, but travels instead through the postpromontorial fossa to the groove for the facial nerve, which it follows. The alleged ramus superior is shown leaving the middle ear through a "conduit that pierces the tegmen tympani at about the anterior extent of the facial canal. It opens dorsally into the sulcus that probably housed the temporal sinus and the arteria diploetica magna." These observations are arguably more consistent with a retained lateral head vein than a stapedial ramus superior.

There are exceptions. In *Ornithorhynchus*, as well as certain fossil nontherians including some multituberculates and the dryolestoid *Necrolestes* (Wible and Hopson, 1995; Wible and Rougier, 2017), both the stapedial ramus superior and lateral head vein seem to be present, sharing a common aperture in the tympanic roof. Although as an indicium the foramen alone would be ambiguous (LHV2), this arrangement of the artery and vein is of great interest morphologically and needs further study.

6. Homological problems concerning posttemporal vasculature and its identification in panperissodactylans.

This study has shown that resolving the identities and connections of the large vessels that pierce the caudal or caudolateral aspect of panperissodactylan skulls, grouped here as the vasa diploetica magna, is more complicated than previously appreciated. For instance, relative to conditions reported or inferred for many other placentals, SANUs may be significantly different in exhibiting a relatively large vena diploetica magna, an absent or highly reduced arteria diploetica magna, and a distinctive bony mosaic enclosing the posttemporal foramen/canal that may signal the coalescence of originally separate vascular ports. Because the posttemporal vasculature of therians is of general interest, in this section we approach the evaluation of individual indicia using as many sources of evidence as are available—vascular, osteological, and developmental (table 6; also see figs. 40, 41). Because the routings of the arteria and vena diploetica magna are closely linked, it is simplest to consider these vessels together. And, as will be clear from this examination, although the identity of the arteria diploetica magna in numerous therian clades has been satisfactorily resolved, the homology of vena diploetica magna in SANUs remains uncertain.

Posttemporal vasculature of *Dasypus* and *Equus*. The fact that the arteria and vena diploetica magna are co-labeled may be thought to imply that the vena is responsible for draining the same tissues that the arteria supplies. The

evidence suggests that this is correct only in a general sense, for the two vasa tend to be in rather brief association in the few mammals in which their relations have been closely studied.

Wible (1984, 2010, 2012) and Wible and Rougier (2017) have provided a number of important observations regarding the basic anatomical relations of the vasa diploetica magna in therians. In his detailed investigations of conditions in the nine-banded armadillo, *Dasypus novemcinctus*, Wible (1984, 2010) correlated information reported by Hyrtl (1854) and others with his own observations on two prenatal specimens. Because of its completeness we utilize Wible's *Dasypus* study as the standard against which conditions in SANUs can be compared.

After passing through the posttemporal foramen, in *Dasypus* the arteria diploetica magna enters the short, medially directed posttemporal canal formed between the dorsal surface of the petrosal and overlying squamosal. The vessel then passes rostrally across the petrosal to anastomose with (or become) the cranioorbital artery (= orbitotemporal artery) (VDM1). Hyrtl's (1854) dissection notes suggest that in *Dasypus* the arteria diploetica magna retains much of the original area of supply of the stapedial ramus superior (cf. Tandler, 1899; Wible, 2010].

In *Dasypus* the posttemporal canal also transmits the vena diploetica magna, which runs from the point of furcation of the transverse and sigmoid sinuses to the occipital vein "on the occiput and [later] joins the internal jugular vein" (Wible, 2010: 18, fig. 10) (VDM1). Whether distinct trackways for the artery and vein can be detected within the posttemporal canal of *Dasypus* is not stated, but Wible (2010: fig. 10) depicts them as traveling in close association along the entire posttemporal complex of sulci.

How frequently such a close spatial relationship between the vena and arteria diploetica magna occurs within placentals is not known, but it is not invariant because there is at least one relevant case (*Equus*) in which the presumed homolog of the artery travels unaccompanied by any vein. A number of other relevant details important for this dis-

cussion, not reported in equine anatomies but inferable from isolated petrosals, are provided in appendix 2 (see also figs. 39A, 40, 41).

Inferred posttemporal vasculature of SANUs. Determining the occupancy of the posttemporal sulcus/canal is important because in adult SANUs the posttemporal complex may have primarily, and perhaps exclusively, conducted veins. Two observations support this. First, in our scanned SANU material an identifiable groove for an independent arteria diploetica magna, comparable to that of *Dasypus* (Wible, 2010) or its caudal meningeal equivalent in *Equus* (figs. 40, 41), was not detectable anywhere along the path of the posttemporal sulcus. Secondly, and by contrast, the routes emanating from the sulcus that we were able to reconstruct in different taxa terminated in relatively large and sometimes enormous dural sinuses, principally the transverse and temporal sinuses (figs. 7–9; see also Martínez et al., 2020: fig. 9B). These points do not necessarily mean that the arteria diploetica magna was completely absent (VDM2, ambiguous); indeed, given how widely distributed the vessel is assumed to be among mammalian clades (Wible, 1987, 2010), it would be more surprising if an anlage for it never developed during SANU ontogeny. Involutions, reductions, annexations, and reorganizations are common occurrences in normal mammalian vascular ontogeny, affecting even major vessels like the internal carotid artery and internal jugular vein (Tandler 1899; Bugge, 1974; Wible, 1987; Tubbs et al., 2020). Thus, Wible (2008: 365) found that in a sectioned juvenile of the eulipotyphlan *Solenodon* that the primary occupant of the posttemporal sulcus was venous; instead of being a primary arterial channel as in *Dasypus* the sulcus contained only "a tiny arteria diploëtica magna arising from the ramus superior dorsal to the piriform fenestra and well-developed accompanying veins." The small size of what appears to be the distal part of the arteria diploetica magna could be related to the fact that the almiquí possesses an unreduced stapedial system (MacPhee, 1981), making supplementation by the occipital artery or its branches unnecessary. The *Solenodon* pattern

may be more common than currently appreciated, although for taxa of very large body size other causes would have to be invoked for the reduction of the arteria diploetica magna. The point, however, is that if this vessel was actually present and functionally significant in adult stages of SANUs, this needs to be inferred on grounds other than the mere presence of the posttemporal sulcus.

Mastoid emissary vein as the vena diploetica magna. The argument that will be developed in this section is that, in SANUs at least, the vein inferred to have been the chief occupant of the posttemporal complex was not the occipital vein per se, as construed for *Dasypus* by Wible (2010), but instead an independent emissarium related to the occipital vein that underwent massive enlargement. The likeliest candidate for this role is the **v. emissaria mastoidea**, which relays blood between the occipital vein and the caudodorsal array and seems to be universally represented in early mammalian development (see Butler, 1957, 1967; Lang, 1983; Tubbs et al., 2020; see also Geisler and Luo, 1998). Much the same homology was inferred for the multituberculate posttemporal vein by Kielan-Jawowska et al. (1986: 588), which suggests that the emissarial connection between the transverse sinus (or prootic sinus, depending on nomenclature) and the occipital vein connection is basal for Theriiformes.

First, however, it is necessary to address an anomaly in emissary nomenclature. In the literature the vein of the mastoid foramen is sometimes named the **v. emissaria occipitalis** rather than v. mastoidea. This is confusing; the occipitalis and mastoidea veins are developmentally distinct, even if for other reasons they are difficult to discriminate. Both appear during early ontogeny (Butler, 1957, 1967), both normally penetrate the caudal aspect of the skull (through separate and often variably placed foramina; see fig. 30), and both run between the caudodorsal array and the true occipital vein or nearby vessels. In *Homo*, the two emissaria arise very close together, on or near the angle formed by the confluence of the transverse and sigmoid sinuses—the occipitalis usually emerging from the former and the mastoidea from the latter,

but with much individual variation (Okudera et al., 1994; Lang, 1983; Mortazavi et al., 2011). The source of nomenclatural confusion, at least in comparative anatomy, may be the influential canine anatomy published by Evans and Christensen (1979 and other editions). These authors depicted the emissary vein of the mastoid foramen in *Canis* as originating from branches from both the transverse sinus and the sigmoid sinus, forming a common trunk that anastomoses with the occipital vein (Evans and Christensen, 1979: 793, fig. 12-23). For unstated reasons the authors chose to describe the common trunk as the "occipitalis [emissary] vein" despite the fact it was transmitted through an aperture routinely called the mastoid foramen. The v. emissaria mastoidea is not mentioned as such in their text. This usage is inconsistent with best practice in comparative anatomy. Here we refer to any vein transmitted by the mastoid foramen as the mastoid emissary vein or, more simply, the mastoidea vein (including occipitalis-mastoidea anastomoses).

Although generally small in caliber, some emissaria (e.g., internal jugular vein, retroarticular vein) regularly enlarge significantly during ontogeny. Others may also, contingent on the physiological demands placed upon them. Thus in *Homo*, if cerebral drainage through the sigmoid sinus/internal jugular vein develops in an abnormal manner, the body may compensate by shunting almost all the blood transmitted by the transverse sinus into the mastoid emissary vein, thereby causing its caliber to drastically increase (from ~1 mm up to ~7.0 mm in diameter in *Homo*; Butler, 1967: 50; Tubbs et al., 2020). This response is facilitated by the fact that the sigmoid sinus lumen is small relative to that of the mastoid emissary vein until after birth (Okudera et al., 1994). The existence of fluctuating dominance along potentially alternative developmental pathways suggests how evolutionary variability might arise in mammalian vascular systems (Padget, 1957; Butler, 1957, 1967; Bugge, 1974). Thus, in the case of some panperissodactylans (figs. 7–9), it is possible to imagine how the dominant method for returning cerebral

blood to the heart from the caudodorsal array could have easily transitioned from the sigmoid sinus/internal jugular vein/vena cava to one comprising the sigmoid sinus/mastoidea emissarium/occipital vein/vertebral plexuses/vena cava, or conversely. In the first case it is the basicapsular fenestra that functions as the main portal for linking the extra- and intracranial circulations, while in the second it is the posttemporal foramen. Such transitions might induce a cascade of other effects, such as the relative location and dimensions of foramina, canals, and trackways.

Bounding the posttemporal trackway complex in SANUs. According to Wible (1987, 2008, 2010, 2012), the basal condition of the therian posttemporal foramen includes its framing by only two bone territories: the caudal border of the squamosal and the lateral face of the petrosal mastoid (= "mastoid extension"). By contrast, the independent foramen for the mastoid emissary vein, when properly identified, is generally situated more medially, in or near the petrooccipital suture on the caudal aspect of the skull. This roughly corresponds to the position of the capsulooccipital fissure of the chondrocranium (De Beer, 1937), which is closed by the expansion of the exoccipital and petrosal ossification centers. Therefore, at least as traditionally understood, the recognition criteria for these two apertures seem to be fundamentally distinct.

SANUs are different: no such distinction between apertures can readily be made, for in all examined cases in which bony fusions do not mask composition, the apparent posttemporal complex is always framed by at least three elements, not two. In addition to the squamosal and the petrosal mastoid, the exoccipital bone (sometimes assisted by the supraoccipital bone) always forms the foramen's ventral or ventromedial rim (e.g., *Trigonostylops,* fig. 11C; *Cochilius,* fig. 17D; *Tetramerorhinus,* fig. 40F–I; see also MacPhee, 2014: fig. 12A). This fact has long been recognized as characteristic of SANUs, if rarely considered important morphologically. Thus, despite

his errors in other regards (Simpson, 1933a; MacPhee, 2014), Roth (1899, pl. 1, fig. 2) correctly showed that the "foramen temporale" (= posttemporal foramen) was ventrally bounded in *Toxodon* by the petro(ex)occipital suture. Scott (1912: pl. 18, fig. 1) as well as other authorities occasionally mentioned or illustrated the posttemporal foramen and its bounding sutures, including the petro(ex)occipital suture, but usually without any interpretative comments (but see Billet and Muizon, 2013: 466).

In ceratomorphs the framing of the posttemporal foramen is variable, and its composition can be accurately determined only in young animals. As we had limited young material to examine, this accounting should not be considered exhaustive. In *Rhinoceros unicornis* AMNH M-274636 and *Ceratotherium simum* AMNH M-51882 the foramen is bordered as in SANUs, with the squamosal and exoccipital hiding the petrosal mastoid, which participates in the floor of the posttemporal sulcus but does not appear externally (figs. 35C, 36B). By contrast, in *Tapirus indicus* AMNH M-77576 a thin strip of petrosal intervenes externally between the exoccipital and squamosal, so the foramen is bordered as in *Equus* (fig. 39B). An independent mastoid emissary foramen could not be securely identified in the available material of tapirs and rhinos, although several small apertures could usually be found perforating the caudally exposed petrooccipital suture. This incomplete survey suggests that exclusive squamosal/petrosal bounding of the posttemporal foramen is not the prevalent character state in most examined panperissodactylan taxa. Other mammalian taxa also differ from the *Dasypus* pattern: for example, O'Leary et al. (2013) identified supraoccipital involvement in the framing of the posttemporal foramen as a candidate afrothere synapomorphy.

Conclusions. According to the available evidence, the arteria diploetica magna is present in *Equus* (as the caudal meningeal artery of equine anatomy). Its occurrence as a functional entity in other extant perissodactylans is likely although

not yet properly documented. By contrast, it is beyond reasonable doubt that a vein—but perhaps only a vein—was transmitted by the posttemporal complex in SANUs. The possible homologs of this vein in other placentals remain unresolved. Wible (2010) considers the vena diploetica magna in all cases to be a branch of the true occipital vein, but as discussed here it might be better thought of as an enlarged emissarium. Indeed, the vena diploetica magna of *Dasypus* is essentially a very short pipeline between extra- and intracranial venous networks, which is essentially the definition of an emissary vein.

But this nomenclatural swap merely exchanges one problem in homological interpretation for another. To settle the matter a test is needed, which would involve establishing whether an identifiable mastoid emissary vein and vena diploetica magna ever coexist simultaneously in any extant species. Wible (2012) thought this might be the case in *Orycteropus*, but as he noted his evaluation was based on dry skulls, not on dissection of vascular networks. In the case of *Solenodon*, Wible (2008) was careful to note variability in the position of ostensible mastoid foramina in different dry skulls of this genus, even noting that in some specimens there were openings that "bear a resemblance in position to posterior openings into the posttemporal canal. However, they do not lead into a canal between the pars canalicularis and squamosal and, therefore, are not posttemporal foramina." As regards extinct species, Martínez et al. (2016) stated that a separate mastoid foramen might exist in their scanned specimen of *Rhynchippus equinus*, lying just within the lip of the larger posttemporal foramen but evidently separate from it. In a reconstruction of vascular relations in *Gualta cuyana* they show the "occipitalis" emissary vein as traveling in apparently close association with the inferred arteria diploetica magna, although whether an independent vena diploetica magna might have also existed in this taxon is not indicated (Martínez et al., 2020: fig. 6D).

Finally, given that the vasa diploetica magna are well distributed in all major clades of Theria

(e.g., Rougier et al., 1992), and therefore likely to be basal features of the subclass, what has happened to these vessels in extant mammals that lack an obvious posttemporal foramen (ADM3)? Are these vessels still present in some form but go unrecognized as such? In humans, the mastoidea emissarium is often not alone within the mastoid foramen, because "the meningeal branch of the occipital artery usually passes through it [i.e., the mastoid foramen] into the skull" (Lang, 1983: 336). This vessel is described as "small in size and sometimes absent…[but] it gives branches to the mastoid air cells and ramifies in the dura mater, anastomosing with the middle meningeal artery" (Warwick and Williams, 1973: 628). Similarly, Davis (1964: 54, fig. 23) described the contents of the "mastoid foramen" (= posttemporal foramen) of *Ailuropoda* as including a meningeal branch of the posterior auricular artery (presumably the arteria diploetica magna) as well as a "vein from the transverse sinus," elsewhere identified as "v. mastoidea" (= v. mastoidea or occipitalis?).

The examples could be multiplied, but such isolated datapoints have little probative value. For the problem at hand a much broader sample of mammalian taxa would be needed to determine whether the stipulated mastoid emissary foramen frequently houses a meningeal branch of the occipital artery or one of its branches. Further insights would then depend on the location of the foramen relative to the petro(ex)occipital suture, a key issue. Parsimony and the indicial method might be on the side of the assumption that, in SANUs, the vein of the posttemporal foramen is a retooled emissarium rather than a novel entity, but correspondence is not identity, and parsimony is not always the best way to reach a conclusion. Apart from inevitable homological questions concerning the veins under consideration here, we recommend continued use of "arteria diploetica magna" and "vena diploetica magna," both well-established terms in comparative anatomy, but encourage care in assuming that both are present when separate trackways cannot be detected.

Pneumatization Indicia

The various bone-remodeling processes grouped under the term "pneumatization" profoundly affect cranial features and proportions during ontogeny, and thus have implications for character description and analysis. This section summarizes what evidence there is for epitympanic and extratympanic sinus formation in *Trigonostylops* and *Astrapotherium*, and how this may bear on larger questions of homology.

1. Major indicia for the identification of the epitympanic sinus include position of its aditus (1) directly adjacent to the fenestra vestibuli (i.e., within or adjacent to the expected locations of the epitympanic recess and incudomalleolar joint), and (2) entirely within the confines of the tympanic cavity (i.e., epitympanic sinus is a derivative of the middle ear and thus paratympanic in origin).

2. Major indicia for identification of the extratympanic sinus include position of its aditus (1) well rostral to the position of the fenestra vestibuli/auditory ossicles and epitympanic recess/sinus and (2) on or slightly beyond the conventional osteological boundary between the tympanic cavity and the external acoustic meatus/retroarticular process.

As discussed earlier under Interpreting Pneumatization: Ontogeny of Cranial Pneumatization (p. 51), a true epitympanic sinus, defined as an ontogenetic expansion of the epitympanic recess, can be demonstrated in members of each SANU ordinal clade for which adequate cranial material exists. This includes *Astrapotherium*, in which the paratympanic epitympanic sinus is arguably present but small (figs. 13A, 14D). The skull of *Trigonostylops* AMNH 28700 is damaged in the relevant area, but if there was a sinus extension of the epitympanic recess it must have been inconsiderable. This is more or less typical for the vast majority of investigated mammalian taxa (van der Klaauw, 1931; MacPhee, 1981; Wible et al., 2009; Wible, 2012) and therefore of minor interest from a character analytic standpoint.

The situation with extratympanic sinuses, which both taxa express in similar but not identical ways, is more complicated. Large, continuous air spaces occur within the retroarticular process and related parts of the squamosal in many therians, but they are almost always paranasal in origin (van der Klaauw, 1931; Forasiepi et al., 2019). *Trigonostylops* and *Astrapotherium* significantly differ in this regard. CT results for *Trigonostylops* AMNH VP-28700 indicate that the air space in the base of the articular process cannot be paranasal in origin because it lacks any connection with the nasal cavity. The only logical source for the inducting epithelium is therefore the tympanic cavity (see p. 65, Interpreting Pneumatization). By contrast, in *Astrapotherium* the retroarticular air space is indisputably continuous with the nasal cavity, as is ordinarily the case in other mammals in which this region is highly pneumatized (see van der Klaauw, 1931).

What is not ordinarily seen in other cases, however, is the presence of a very large aperture on the caudal surface of the retroarticular process that connects this air space with the external acoustic meatus (fig. 15C). The aperture, which opens onto a series of chambers and incomplete septa within the retroarticular process (fig. 14B), is seemingly far too large to have functioned solely as a retroarticular foramen. If as we argue in life this aperture was subdivided into an aditus for the extratympanic sinus as well as an outlet for the retroarticular vein, the two would still have been separated by their respective epithelial coverings, their volumes touching but not merging. This is indicated because it makes no functional sense for there to have been a continuous hollow space running through the skull from the nasal cavity to the external acoustic meatus.

This is as far as morphological speculation can usefully be driven. However, assuming there is a phylogenetic relationship between astrapotheriids and trigonostylopids (see p. 131, Phylogenetic Analyses), it is worth trying to harmonize the differences in the organization of their pneumatic spaces to the degree possible. The massive scale of paranasal inflation charac-

teristic of Neogene astrapotheriids is unquestionably derived, whereas in *Trigonostylops* paranasal pneumatization was just as clearly limited to the rostrum and related areas, as would have presumably also been the case in basal astrapotheres. However, lateral outpocketing of the tympanic cavity may have occurred in early (and currently unknown) members of both groups, affecting the walls of the bony external acoustic meatus and retroarticular process to at least a minor extent. Hypothetically, as body size dramatically increased in Oligo-Miocene astrapotheriids, novel paranasal expansion would have eventually come to involve much of the cranium. For unknown reasons in this group the epitympanic sinus did not scale up at the same time, persisting only as a small excavation in the tympanic roof. However, paratympanic outpocketing into the area of the external acoustic meatus evidently did occur, producing a well-marked aditus in the retroarticular process in some lineages but not others (i.e., in *Astrapotherium* but not *Astraponotus*). By contrast in trigonostylopids massive paranasal pneumatization did not take place, perhaps because gigantism failed to occur in this group and there was thus no need to reduce skull mass. In the immediate ancestry of *Trigonostylops* paratympanic expansion may have developed further, perhaps for functional reasons related to audition and resulting in the relatively large extratympanic sinus and aditus characteristic of the adult. In any case aperture sharing with the retroarticular vein did not occur.

Although this scenario is hypothetical, it permits recognition of possible operational homology between the extratympanic sinuses of *Trigonostylops* and *Astrapotherium*, providing an ontogeny-based explanation for apparently shared features in these two very different taxa. Whether lateral outpocketings also occurred in non-SANU panperissodactylans (as may have been the case in palaeotheres, for example) is an interesting question to consider but beyond the scope of this paper. In future it needs to be seen whether it is possible to differentiate the true ret-

roarticular venous foramen from the aditus of the extratympanic sinus in astrapotheres. *Eoastrapostylops riolorense* PVL 4216 might be helpful here: although lying outside Astrapotheria (fig. 34), it exhibits relatively large, apparently natural apertures on its low and crestlike retroarticular processes (Kramarz et al., 2017). Whether these holes were related to veins or air spaces—or both—cannot be determined by external inspection (hence a score of "?" in **C108** for this taxon), but this ambiguity might be resolved with scanning.

PHYLOGENETIC ANALYSES

Simpson (1933a) presented three lists of characters in which he summarized the features that he considered to be the most important for resolving the affinities of *Trigonostylops*. These were reprinted in his 1967 paper, with nearly identical content. His first list (Simpson, 1933a: 14) consisted of 19 cranial foramina that he was able to identify and interpret satisfactorily, plus three additional "miscellaneous" openings whose identity and function were uncertain. Most of these were reviewed in the second (p. 18) and third (p. 21) lists, in which he contrasted conditions in *Trigonostylops* with those found in nonspecific "Notoungulata" and *Astrapotherium*. Only one solid resemblance to Notoungulata emerged from these comparisons, the absence of foramina in the alisphenoid between the sphenoorbital fissure and the basicapsular fenestra, a reference to the absence of the alar canal. In the case of Astrapotheria Simpson—never a cladist—mentioned at least six "special resemblances" to *Trigonostylops*, but noted that litopterns were also similar "to some degree" for these characters as well as others. In the end, his suspicion was that Trigonostylopoidea, Litopterna, and Astrapotheria "may have been derived from the same, but perhaps rather remote, [i.e., probably 'condylarthran'] ancestral group," with trigonostylopids being "possibly nearer to or even in the most ancient astrapothere line, but diverging strongly in a third direction" (Simpson, 1933a: 27).

In light of the vast increase in our knowledge of mammalian skull morphology and development during the past nine decades, Simpson's character evidence for the relationships of *Trigonostylops* needs both expansion and reevaluation. In line with modern methods, this evidence needs to be scrutinized using an approach that bases conclusions about relationships on resolved character distributions, focusing on shared derived states. The next section is designed to do this and to place *Trigonostylops* in its proper phylogenetic position.

Placing *Trigonostylops*

A parsimony analysis (fig. 34) was conducted to examine the phylogenetic relationships of *Trigonostylops* to other panperissodactylans and potentially related archaic ungulates, denoted in this paper as "condylarths." We used the dataset developed by Billet et al. (2015), which provides an exhaustive covering of South American native ungulates with an emphasis on notoungulates and dental and otic characters. We have modified this matrix by redefining some characters and adding three others of potential phylogenetic interest. After conducting our own specimen examinations we changed some of the scorings made by Billet et al. (2015), mostly for *Trigonostylops*, but also for *Astrapotherium* and certain litopterns and notoungulates. Additionally, 13 characters used by Billet et al. (2015) were not included in the present analysis, either because they were invariant in the taxa scored for our version of the matrix or because differences among defined character states were too vague to permit consistent evaluations. Omitted characters have nevertheless been kept in the matrix, with their original enumeration, as inactive characters. This allowed us to preserve the original numbering while adding the three new characters to the end of the character list. All revisions and additions are documented in appendix 3.

In regard to taxon representation, a number of terminal taxa (mostly xenarthrans and late diverging notoungulates) in the original matrix

were removed because they were not relevant to the objectives of this study. By contrast, to increase resolution for targeted taxa we added the early astrapotheriid *Astraponotus*, the supposed basal astrapothere *Eoastrapostylops,* and several extant and extinct representatives of Perissodactyla (*Palaeotherium*, *Equus*, *Tapirus*), none of which were sampled in the original matrix. The monophyly of Perissodactyla is unquestioned, with robust support from both molecular and morphological evidence (e.g., Rose et al., 2014, 2020; Westbury et al., 2017). However, because the unity of this order is largely founded on postcranial synapomorphies (Rose, 2006; Rose et al., 2014)—none of which were included in the data matrix—we introduced a topological constraint to ensure that Perissodactyla was recovered as a monophyletic unit in our analyses.

Our reworked data matrix encompassing 146 active characters and 41 terminal taxa was analyzed with the program TNT 1.1 (Goloboff et al., 2008) using maximum parsimony with equally weighted characters. Analysis involved a heuristic search of Wagner trees with 1000 random addition sequences, followed by TBR (tree bisection reconnection), saving 10 trees per round. This produced 138 most parsimonious trees (MTPs) of 467 steps each (fig. 34), with a moderately high level of homoplasy (HI = 0.63). In all MTPs, *Trigonostylops* clustered with the clade *Astrapotherium* + *Astraponotus* (i.e., Astrapotheriidae) on the basis of 4 unambiguous synapomorphies: C114.1, complete basicapsular fenestra; C157.1, facial process of premaxilla absent; C158.1, diverging canines; and C159.1, cheekteeth enamel displaying vertical HSB. The presence of the extratympanic sinus aditus (C108.1), shared by *Trigonostylops* and *Astrapotherium* but not by *Astraponotus*, is an ambiguous synapomorphy of Astrapotheria. *Trigonostylops* is excluded from Astrapotheriidae in lacking 6 synapomorphies shared by *Astrapotherium* and *Astraponotus*: C20.0, P1 absent; C21.1, hypsodont cheekteeth; C55.1, shallow lingual sulcus on i1-i2; C61.1, mesial lophid

(paralophid?) on lower cheekteeth; C90.1, length of nasals reduced; and C97.0, anterior zygomatic root posterior to M1. The hypoglossal foramen opening into the jugular area (C113.2) and the ASC and PSC not extending well dorsal to crus commune (C149.2) are here interpreted as autapomorphies of *Trigonostylops*.

Bootstrap and Bremer supports are relatively low across the taxon sample and in some cases the metrics appear contradictory. With regard to our focal taxa, we found that the clade *Trigonostylops* + (*Astrapotherium* + *Astraponotus*) is only indifferently supported with this data set, exhibiting less than 50% bootstrap support. While these results suggest that the ultimate placement of *Trigonostylops* is still not well constrained, it is worth noting that in suboptimal trees (+1 step) *Trigonostylops* groups closer to notoungulates, astrapotheres, and *Pyrotherium* than to basal placentals or "condylarthrans." Firmer support for an affiliation with astrapotheres may come through discovery of earlier (and cranially less-derived) astrapotheriids, but it will be equally important to discover new characters like the ones proposed here.

With regard to higher-level SANU interrelationships, on the whole our results agree with previous analyses (Muizon et al., 2015; Kramarz et al., 2017) in recovering the conventional content of Astrapotheria (i.e., *Trigonostylops* + Astrapotheriidae) as the sister group of the clade encompassing *Pyrotherium* + Notoungulata. They also agree with the analysis of Kramarz et al. (2017) concerning the position of *Eoastrapostylops* as the earliest diverging taxon within the clade encompassing astrapotheres, notoungulates, and *Pyrotherium*. However, note that placement of several taxa (including *Eoastrapostylops*) is associated with comparatively high Bremer support but low bootstrap scores; these nodes should therefore be interpreted with caution. (Incidentally, the base of Notoungulata exhibits only marginal support, in contrast to that for Litopterna, which is quite solid.) Such inconsistencies are most likely a result of missing data and homoplasy in the underlying
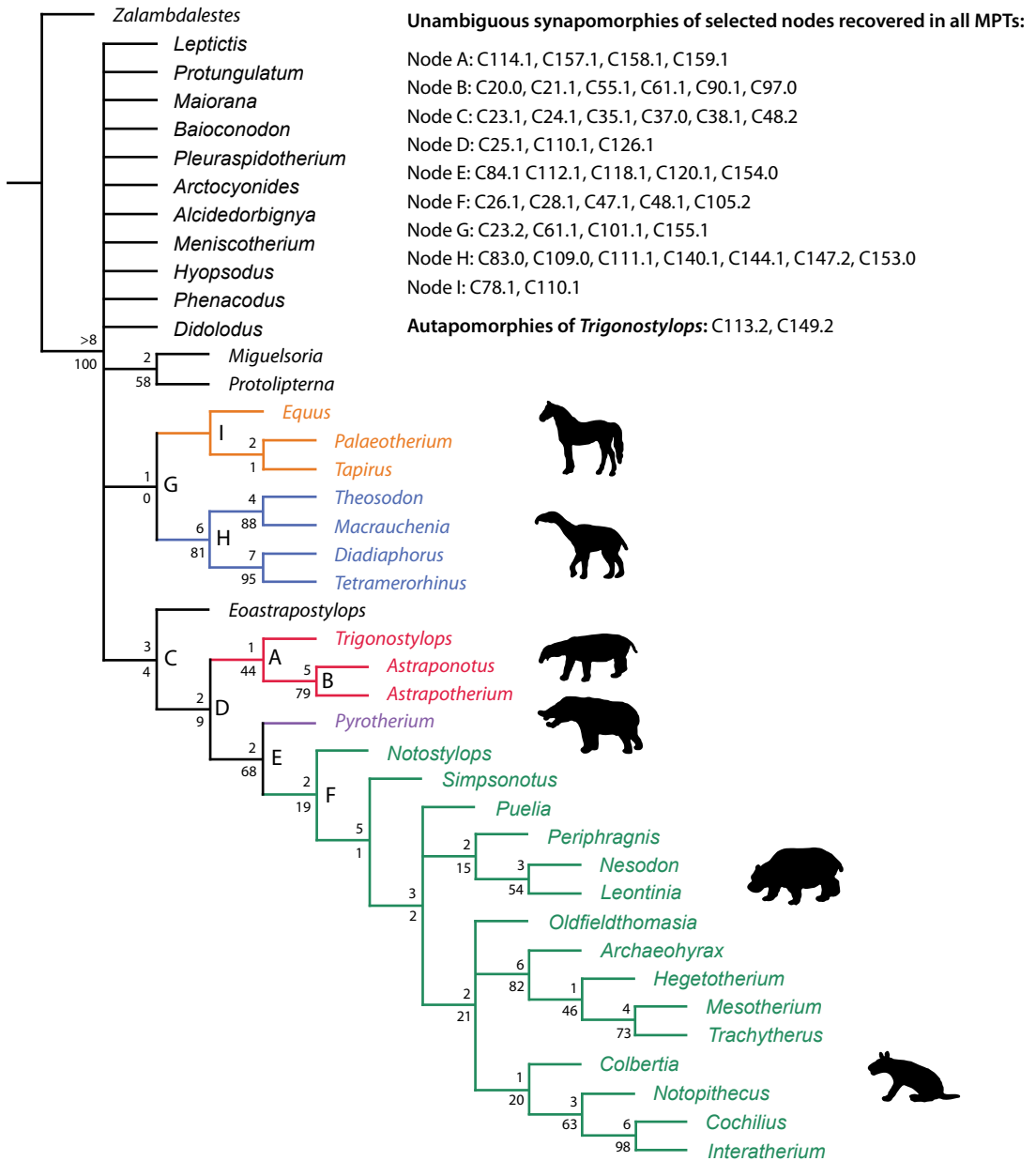
FIG. 34. Strict consensus of 138 most parsimonious trees (MTPs) of 467 steps each, obtained from parsimony analysis of modified version of data matrix developed by Billet et al. (2015) (see appendix 3, 4). Monophyly of Perissodactyla (*Tapirus* + *Equus* + *Palaeotherium*) was imposed using "force" command in TNT 1.1 (Goloboff et al., 2008). Numbers above and below nodes are Bremer and bootstrap values, respectively. Bremer support values were calculated by searching for suboptimal trees (up to 8 extra steps). Bootstrap values were assessed from 10,000 iterations of bootstrap resampling on consensus tree, with standard resampling, absolute frequencies, and perissodactylan monophyly enforced.

matrix, which contributes uncertainty to the resulting consensus tree.

One other result is worth brief comment. Few previous studies have explored the relationships of SANUs and perissodactylans on the basis of a simultaneous analysis of morphological characters (but see Horovitz, 2004; O'Leary et al., 2013; Beck and Lee, 2014). Ours is the first to include both a large sample of SANUs as well as representative living and extinct perissodactylans. One result of our study, perhaps predictable because it is exclusively based on morphology, is an indication that litopterns may be more closely related to perissodactylans than to other SANUs, in contrast to recent proteomic analyses that have come to the opposite conclusion (Welker et al., 2015; Buckley, 2015). In the present investigation, the Litopterna + Perissodactyla affiliation is supported by the occurrence of the following characters: C23, paracingulum high but not connecting to parastyle-paracone; C61, paralophid? on lower cheekteeth; C101, sphenopalatine foramen at level of middle of orbit floor (anteroposterior length); and C155, astragalar neck and head expanded and axis subparallel to tibial trochlea. Note also that the position of the South American "condylarthran" *Didolodus*, as well as that of the putative basal litopterns *Protolipterna* and *Miguelsoria*, could not be established unambiguously. Nevertheless, in all MTPs these taxa are positioned closer to the Litopterna + Perissodactyla clade than they are to other SANU groupings, although our results do not specifically support the brigading of didolodontids and litopterns (e.g., Cifelli, 1993).

In regard to this topic, Chimento and Agnolín (2020) recently argued for a quite different thesis, that "Perissodactyla" should include not only the traditional crown group, but also stem taxa from India and Pakistan, now grouped as Anthracobunia by Rose et al. (2019), and austral "condylarthrans" (e.g., *Escribania* spp.) from South America. Litopterna is excluded from this arrangement but positioned as its sister group. Their matrix is difficult to directly compare to ours because cranial features comprise only 18% of their total character list. Furthermore, because

their taxon set inexplicably omitted notoungulates and other SANU clades, their results cannot be regarded as a meaningful test of panperissodactylan systematic relationships. It need hardly be said that the book is not yet closed on SANU inter- and intraordinal relationships (see Croft et al., 2020).

Trigonostylops in the Context of SANU Evolution

The earliest unquestionable records of *Trigonostylops* are Vacan (early Casamayoran) in age (43 Ma, Lutetian, Middle Eocene; Dunn et al., 2015) or more doubtfully Riochican (49 Ma, late Ypresian; Woodburne et al., 2014, but see Krause et al., 2017). Nevertheless, the occurrence of *Tetragonostylops* in the Itaboraí fauna (?early Ypresian) implies that the divergence of *Trigonostylops* from a basal astrapotheriid lineage predates the Itaboraian SALMA, and likely took place in earliest Eocene. The sediments at the South Barranca near Lago Colhué Huapí, which yielded AMNH VP-28700, are dated as younger than 41.7 Ma (Dunn et al., 2012). Consequently, this fossil documents the results of more than 11 Ma of morphological evolution separate from that of the astrapotheriids.

Trigonostylops is represented in later Casamayoran (Barrancan) contexts (43 to 39 Ma, Dunn et al., 2015) by dozens of specimens, all of which have been assigned to *T. wortmani* (Simpson, 1967). A second, probably valid species, *T. gegenbauri* (Roth, 1899), occurs in somewhat younger levels (Mustersan SALMA, ~38 Ma, Dunn et al., 2015), although it is differentiated from the former only by the absence of p1 (Simpson, 1967). However, a small assortment of undescribed, isolated *Trigonostylops*-like molars, unequivocally coming from Mustersan rocks (Cladera et al., 2004), exhibit some subtle but clearly distinctive traits. These fossils might belong to yet another taxon, suggesting that trigonostylopids experienced a moderate but otherwise undocumented diversi-

fication during the clade's tenure of ca. 15 Ma in South American ecosystems.

In his treatment of *Tetragonostylops apthomasi*, Paula Couto (1952: 391) drew attention to the fact that "the facial part of the maxilla has a very prominent…swelling lateral to the large roots of the canine, and resulting from the enormous development of this root." By contrast, although MACN Pv 47 is highly incomplete it is obvious that the canine alveolus in this taxon cannot be described as greatly enlarged (see also MLP 52-X-5-98, fig. 21). This is of interest because canine enlargement and associated facial reorganization are hallmark traits of derived astrapotheriids not found in *Tetragonostylops* or *Trigonostylops*.

Simpson´s view that *Trigonostylops* shared a remote "condylarthran"—but probably no later—ancestry with other SANUs is not supported by our investigation. On the contrary, our results are consistent with the interpretation that *Trigonostylops* and its close allies shared a unique common ancestry with astrapotheres and notoungulates, to the exclusion of litopterns. The common ancestor would have had relatively enlarged canines (C18), molars with a high protoloph (C23) and ectoloph (C24), indistinct paraconule (C35), parastyle lacking labial projection (C37) and separated from paracone by subvertical sulcus (C38), M1 much smaller than M3 (C48), double crescent pattern on lower cheekteeth (C62), and foramen ovale merged with rostral (piriform) portion of basicapsular fenestra (C110).

In our parsimony analysis, *Trigonostylops* does not occupy a basal position within Astrapotheria + Notoungulata, but instead consistently groups within a clade that also includes *Astrapotherium* and *Astraponotus*. Despite low analytical metrics and the small number of synapomorphies underlying this result, *Trigonostylops* still stands as the earliest-diverging definite astrapothere represented by good fossil material. The morphological gap between the skulls of *Trigonostylops* and *Astrapotherium* is indeed wide (figs. 1, 4)—hardly surprising in view of the 30 Ma gap

separating them, which is only partially filled by *Tetragonostylops*, *Scaglia*, and *Astraponotus*. At the same time, almost all of the dental and cranial features of *Trigonostylops* interpreted by Simpson as distinctive of that genus are better interpreted as either autapomorphies or plesiomorphies shared with basal astrapotheriids (but not with *Astrapotherium*).

The skull of *Astraponotus*, despite being highly autapomorphic, displays several features that could be regarded as morphologically transitional between *Trigonostylops* and *Astrapotherium*. For example, in *Astraponotus* the orbital rim is low and rounded, the sagittal crest is longer and more marked than the temporal crests, the occiput is not emarginated and situated low on the cranium, and the lacrimal foramen is located on the orbital rim. All of these features are similarities to *Trigonostylops* but not to *Astrapotherium*. In addition, *Astraponotus* exhibits multiple (double) infraorbital foramina, and the hypoglossal foramen opens nearer the jugular area than in *Astrapotherium*. Simpson (1933a: 21) also pointed out that *Trigonostylops* has a very long basisphenoid-presphenoid exposure compared with *Astrapotherium*. In *Astraponotus*, the exposure is short only because the pterygoids are expanded medially and in contact at the midline, hiding the bones of the central stem. In *Astrapotherium*, the exposure is short for another reason, which is that the palate is expanded caudally in correlation with the greatly enlarged molars. If Simpson conceived this character as capturing the relative length of the basicranium, then *Astraponotus* is closer to *Trigonostylops* in having a short palate and long basicranium. Certainly, *Astraponotus* exhibits several highly derived cranial characters also seen in *Astrapotherium*, such as the extreme reduction of the length of the nasals, interpreted as synapomorphies here and in previous analyses (e.g., Kramarz et al., 2019a). Similarities to *Trigonostylops* are therefore largely due to retention of plesiomorphic states.

As Simpson (1933a: 19) noted, "the dentition gives the best evidence for astrapothere affinities

of *Trigonostylops.*" In addition to the shared presence of vertical HSB in *Trigonostylops* and all astrapotheriids, the dentitions of *Trigonostylops*, *Albertogaudrya*, and *Astraponotus* represent successive structural variations on the same basic morphological theme (Carbajal et al., 1977: 160). This succession, characteristic of dental evolution in Paleogene astrapotheriids, primarily involved gradually increasing hypsodonty, lophodonty, occlusal complexity, and premolar reduction. Simpson's "patristic" approach for evaluating the phylogenetic content of dentitions involved tracing combinations of perceived evolutionary trends backward in time in order to infer the most likely ancestral pattern. For Astrapotheria, the pattern culminates in *Trigonostylops.* Our unweighted parsimony approach affirms this basic calculus.

ACKNOWLEDGMENTS

REFERENCES

Aboitiz, F., and J. Montiel. 2007. Origin and evolution of the vertebrate telencephalon, with special reference to the mammalian neocortex. Berlin: Springer.

Allman, J. 1990. Evolution of neocortex. *In* E.G. Jones and A. Peters (editors), Cerebral cortex: comparative structure and evolution of cerebral cortex, vol. 8a: 269–283. New York: Plenum Press.

Altafulla, J.J., et al. 2019. Transclival venous circulation: anatomic study. World Neurosurgery 121: e136–e139.

Ameghino, F. 1901. Notices préliminaires sur des ongulés des terrains crétacés de Patagonie. Boletín de la Academia de Ciencias en Córdoba 16: 349–426.

Anthwal, N., and H. Thompson. 2016. The development of the mammalian outer and middle ear. Journal of Anatomy 228: 217—232.

Anthony, R. 1920. La poche gutturale du tapir. Bulletin de la Société des Sciences Vétérinaires de Lyon (December 1920), p. 1-15.

Antoine, P.-O., et al. 2015. A new *Carodnia* Simpson, 1935 (Mammalia, Xenungulata) from the Early Eocene of northwestern Peru and a phylogeny of xenungulates at species level. Journal of Mammalian Evolution 22: 129–140.

Aplin, K.P. 1990. Basicranial regions of diprotodontian marsupials: anatomy, ontogeny, and phylogeny. Ph.D. dissertation, School of Biological Sciences, University of New South Wales, Sydney, 389 pp.

Arbib M.A., P. Erdi, and J. Szantagothai. 1998. Neural organization: structure, function and dynamics. Cambridge, MA: MIT Press.

Archer, M. 1976.The basicranial region of marsupicarnivores (Marsupialia): interrelationships of carnivorous marsupials and affinities of the insectivorous marsupial peramelids. Zoological Journal of the Linnaean Society of London 59: 217–322.

Arnautovic, K.I., O. Al-Mefty, T.G. Pait, A.F. Krisht, and M.M. Husain. 1997. The suboccipital cavernous sinus. Journal of Neurosurgery 86: 252–262.

Bajpai, S., J.G.M. Thewissen, and A. Sahni. 1996. *Indocetus* (Cetacea, Mammalia) endocasts from Kachchh (India). Journal of Vertebrate Paleontology 16: 582–584.

Balanoff, A.M., G.S. Bever, T.B. Rowe, and M.A. Norell. 2013. Evolutionary origins of the avian brain. Nature 501: 93–96.

Batson, O.V. 1957. The vertebral vein system. American Journal of Roentgenology, Radium Therapy, and Nuclear Medicine 78: 195–212.

Beck, R.M., and M.S. Lee. 2014. Ancient dates or accelerated rates? Morphological clocks and the antiquity

of placental mammals. Proceedings of the Royal Society B281: 20141278.

Berlin, J.C., E.C. Kirk, and T.B. Rowe. 2013. Functional implications of ubiquitous semicircular canal nonorthogonality in mammals. PLoS One 8:e79585.

Bertrand, O.C., F. Amador-Mughal, M.M. Lang, and M.T. Silcox. 2018. Virtual endocasts of fossil Sciuroidea: brain size reduction in the evolution of fossoriality. Palaeontology 61: 919–948.

Bertrand, O.C., et al. 2020. Virtual endocranial and inner ear endocasts of the Paleocene 'condylarth' *Chriacus*: new insight into the neurosensory system and evolution of early placental mammals. Journal of Anatomy 236 (1): 21–49.

Billet, G. 2010. New observations on the skull of *Pyrotherium* (Pyrotheria, Mammalia) and new phylogenetic hypotheses on South American ungulates. Journal of Mammalian Evolution 17: 21–59.

Billet, G. 2011. Phylogeny of the Notoungulata (Mammalia) based on cranial and dental characters. Journal of Systematic Palaeontology 9 (4): 481–497.

Billet, G., and C. de Muizon. 2013. External and internal anatomy of a petrosal from the Late Paleocene of Itaboraí, Brazil, referred to Notoungulata (Placentalia). Journal of Vertebrate Paleontology 33: 455–469.

Billet, G., C. de Muizon, and B. Patterson. 2009. Craniodental anatomy of late Oligocene archaeohyracids (Notoungulata, Mammalia) from Bolivia and Argentina and new phylogenetic hypotheses. Zoological Journal of the Linnean Society 155: 458–509.

Billet, G., et al. 2012. High morphological variation of vestibular system accompanies slow and infrequent locomotion in three-toed sloths. Proceedings of the Royal Society B279: 3932–3939.

Billet, G., et al. 2015. Petrosal and inner ear anatomy and allometry amongst specimens referred to Litopterna (Placentalia). Zoological Journal of the Linnean Society 173: 956–987.

Blanke, A., A. Aupperle, J. Seeger, C. Kubrick, and G.F. Schusser. 2014. Histological study of the external, middle and inner ear of horses. Anatomia, Histologia Embryologia: Journal of Veterinary Medicine. [doi: 10.1111/ahe.12151]

Boscaini, A., et al. 2020. Digital cranial endocasts of the extinct sloth *Glossotherium robustum* (Xenarthra, Mylodontidae) from the Late Pleistocene of Argentina: description and comparison with the extant sloths. Journal of Mammalian Evolution 27: 55–71.

Boyer, D.C., et al. 2016. Internal carotid arterial canal size and scaling in Euarchonta: re-assessing implications for arterial patency and phylogenetic relationships in early fossil primates. Journal of Human Evolution 97: 123–144.

Bradley, O.C. 1923. The topographical anatomy of the head and neck of the horse. Edinburgh: Green.

Breathnach, A.S. 1955. Observations on endocranial casts of recent and fossil cetaceans. Journal of Anatomy 89: 532–546.

Buckley, M. 2015. Ancient collagen reveals evolutionary history of the endemic South American "ungulates." Proceedings of the Royal Society B282: 20142671.

Budras, K.-D., W.O. Sack, and S. Röck. 2008. Anatomy of the horse, 5th ed. Hannover: Schültersche.

Bugge, J. 1974. The cephalic arterial system in insectivores, primates, rodents and lagomorphs, with special reference to the systematic classification. Acta Anatomica 87, supplement 62: 1–160.

Butler, A.B., and W. Hodos. 2005. Comparative vertebrate neuroanatomy: evolution and adaptation. John Wiley & Sons.

Butler, H. 1957. The development of certain human dural venous sinuses. Journal of Anatomy 91: 510–526.

Butler, H. 1967. The development of mammalian dural venous sinuses with especial reference to the postglenoid vein. Journal of Anatomy 102: 33–56.

Cabanac, M. 1996. Human selective brain cooling. New York: Springer Verlag.

Caputa, M. 2004. Selective brain cooling: a multiple regulatory mechanism. Journal of Thermal Biology 29: 691–702.

Carbajal, E., R. Pascual, R. Pinedo, J. Salfity, and M.G. Vucetich. 1977. Un nuevo mamífero de la Formación Lumbrera (Grupo Salta) de la comarca de Carahuasi (Salta, Argentina). Edad y correlaciones. Publicaciones del Museo Municipal de Ciencias Naturales de Mar del Plata 'Galileo Scaglia' 2: 148–163.

Cartmill, M. 1975. Strepsirhine basicranial structures and the affinities of the Cheirogaleidae. *In* W.P. Luckett and F.S. Szalay (editors), Phylogeny of the primates, a multidisciplinary approach: 313–354. New York: Plenum.

Cartmill, M., and R.D.E. MacPhee. 1980. Tupaiid affinities: the evidence of the carotid arteries and cranial skeleton. *In* W.P. Luckett (editor), Comparative biology and evolutionary relationships of tree shrews: 95–132. New York: Plenum.

Cave, A.J.E. 1959. The foramen ovale in the Rhinocerotidae. Proceedings of the XVth International Congress of Zoology, London: 419–421.

Cerdeño, E., and B. Vera. 2015. A new Leontiniidae (Notoungulata) from the late Oligocene beds of

Mendoza Province, Argentina. Journal of Systematic Palaeontology 13: 943–962.

Chaffee, R.G. 1952. The Deseadan vertebrate fauna of the Scarritt Pocket, Patagonia. Bulletin of the American Museum of Natural History 98 (6): 509–562.

Chimento, N., and F.L. Agnolín. 2020. Phylogenetic tree of Litopterna and Perissodactyla indicates a complex early history of hoofed mammals. Scientific Reports 10:13280. [doi.org/10.1038/s41598-020-70287-5]

Cifelli, R.L. 1982. The petrosal structure of *Hyopsodus* with respect to that of some other ungulates, and its phylogenetic implications. Journal of Paleontology 56: 795–805.

Cifelli, R.L. 1983. The origin and affinities of the South American Condylarthra and early Tertiary Litopterna (Mammalia). American Museum Novitates 2772: 1–49.

Cifelli, R.L. 1985. Biostratigraphy of the Casamayoran, early Eocene of Patagonia. American Museum Novitates 2820: 1–26.

Cifelli, R.L. 1993. The phylogeny of the native South American ungulates. *In* F.S. Szalay, M.J. Novacek, and M.C. McKenna (editors), Mammal phylogeny, vol. 2, Placentals: 195–216. New York: Springer.

Cladera, G., E. Ruigómez, E. Ortiz Jaureguizar, M. Bond, and G. López. 2004. Tafonomía de la Gran Hondonada (Formación Sarmiento, Edad—Mamífero Mustersense, Eoceno Medio) Chubut, Argentina. Ameghiniana 41: 315–330.

Conroy, G. 1982. A study of the cerebral vascular evolution in primates. *In* E. Armstrong and D. Falk (editors), Primate brain evolution, methods and concepts: 247–261. New York: Plenum.

Conroy, G., and J.R. Wible. 1978. Middle ear morphology of *Lemur variegatus*: some implications for primate paleontology. Folia Primatologica 29: 81–85.

Cooper, L.N., et al. 2014. Anthracobunids from the Middle Eocene of India and Pakistan are stem perissodactyls. PLoS One 9: e109232.

Cope, E.D. 1880. On foramina perforating the posterior part of the squamosal bone of the Mammalia. Proceedings of the American Philosophical Society 18: 452–461.

Coutier, F., L. Hautier, R. Cornette, E. Amson, and G. Billet. 2017. Orientation of the lateral semicircular canal in Xenarthra and its links with head posture and phylogeny. Journal of Morphology 278: 704–717.

Croft, D.A., J.N. Gelfo, and G.M. López. 2020. Splendid innovation: the extinct South American native ungulates. Annual Review of Earth and Planetary Sciences, 48: 259–290.

Curé, J.K., P. Van Tassel, and M.T. Smith. 1994. Normal and variant anatomy of the dural venous sinuses. Seminars in Ultrasound, CT and MRI 15: 499–519.

Daniel, P.M., J. D.K. Dawes, and M.M.L. Prichard. 1953. Studies of the carotid rete and its associated arteries. Philosophical Transactions of the Royal Society, London B237: 173–204.

Davis, D.D. 1964. The giant panda: a morphological study of evolutionary mechanisms. Fieldiana: Zoology Memoirs 3: 5–339.

De Beer, G.R. 1929. The development of the skull of the shrew. Philosophical Transactions of the Royal Society of London B217: 411–480.

De Beer, G.R. 1937. The development of the vertebrate skull. Oxford: Clarendon Press.

Dechaseaux, C. 1958a. Encéphales de condylarthres. *In* J. Piveteau (editor), Traité de paléontologie, vol. 6 (2), Mammifères: 28–30. Paris: Masson.

Dechaseaux, C. 1958b. Encéphales de proboscidiens fosiles. *In* J. Piveteau (editor), Traité de paléontologie, vol. 6 (2), Mammifères: 296–298. Paris: Masson.

Diamond, M.K. 1991. Homologies of the stapedial artery in humans, with a reconstruction of the primitive stapedial artery configuration of Euprimates. American Journal of Physical Anthropology 84: 433–462.

Diamond, M.K. 1992. Homology and evolution of the orbitotemporal venous sinuses of humans. American Journal of Physical Anthropology 88: 211–244.

Doran, A.H.G. 1878. Morphology of the mammalian ossicula auditûs. Transactions of the Linnean Society of London, Zoology 1: 371–497.

Du Boulay, G.H. 1991. A note on the cerebral arteries of Perissodactyla: the rete caroticum of *Diceros bicornis*. Dubious nomenclature of the internal carotid artery of horses. Neuroradiology 33, supplement: 462–463.

Du Boulay, G.H., and P.M. Verity. 1973. The cranial arteries of mammals. London: Heinemann.

Du Boulay, G.H., M. Lawton, and A. Wallis. 1998. The story of the internal carotid artery of mammals: from Galen to sudden infant death syndrome. Neuroradiology 40: 697–703.

Dunn R.E., et al. 2012. A new chronology for middle Eocene–Early Miocene South American Land Mammal Ages. Bulletin of the Geological Society of America 125: 539–555.

Dunn, R.E., C.A.E. Strömberg, R.H. Madden, M.J. Kohn, and A.A. Carlini. 2015. Linked canopy, climate, and faunal change in the Cenozoic of Patagonia. Science 347: 258–261.

Edinger, T. 1929. Die fossilen Gehirne. Zeitschrift für gesamte Anatomie, Abteilung III 28: 1–249.

Edinger, T. 1964. Midbrain exposure and overlap in mammals. American Zoologist 4: 5–19.

Ekdale, E.G. 2013. Comparative anatomy of the bony labyrinth (inner ear) of placental mammals. PLoS One 8: e66624.

Ekdale, E.G. 2015. Form and function of the mammalian inner ear. Journal of Anatomy. [doi: 10.1111/joa.12308]

Ekdale, E.G., J.D. Archibald, and A.O. Averianov. 2004. Petrosal bones of placental mammals from the Late Cretaceous of Uzbekistan. Acta Palaeontologica Polonica 49: 161–176.

Ellenberger, W., and H. Baum. 1894. Topographische Anatomie des Pferdes, mit besonderer Berücksichtigung der tierärztlichen Praxis, vol. 2, Kopf und Hals. Berlin: Paul Parey.

Ellenberger, W., and H. Baum. 1908. Handbuch der vergleichenden Anatomie der Haustiere, 12th ed. Berlin: Hirschwald.

Epstein, H.M., H.W. Linde, A.R. Crampton, I.S. Ciric, and J.E. Eckenhoff. 1970. The vertebral venous plexus as a major cerebral venous outflow tract. Anesthesiology 32: 332–337.

Evans, H.E., and G.C. Christensen. 1979. Anatomy of the dog, 2nd ed. Philadelphia: Saunders.

Evans, H.E., and A. de Lahunta. 2013. Anatomy of the dog, 4th ed. St. Louis: Elsevier Saunders.

Evans, H.M. 1912. III. The development of the vascular system. *In* F. Keibel and F.P. Mall (editors), Manual of human embryology, vol. 2: 570–709. Philadelphia: Lippincott.

Fawcett, E. 1921. The primordial cranium of *Tatusia novemcinctus* as determined by sections and models of the embryos of 12 millimetre and 17 millimetre C.R. length. Journal of Anatomy 55: 187–218.

Fernández-Monescillo, M., et al. 2019. Virtual endocast morphology of Mesotheriidae (Mammalia, Notoungulata, Typotheria): New insights and implications on notoungulate encephalization and brain evolution. Journal of Mammalian Evolution 26: 85–100.

Ferreira-Cardoso, S., et al. 2017. Floccular fossa size is not a reliable proxy of ecology and behaviour in vertebrates. Scientific Reports 7: 1–11.

Filippo A., D. Kalthoff, G. Billet, H. Gomes Rodrigues. 2020. Evolutionary and functional implications of incisor enamel microstructure diversity in Notoungulata (Euungulata, Mammalia). Journal of Mammalian Evolution 27: 211–236.

Fischer, M.S., and P. Tassy. 1993. The interrelation between Proboscidea, Sirenia, Hyracoidea, and Mesaxonia: The morphological evidence. *In* F.S. Szalay, M.J. Novacek, and M.C. McKenna (editors), Mammal phylogeny, vol. 2, Placentals: 217–234. New York: Springer.

Fleischer, G. 1973. Studien am Skelett des Gehörorgans der Säugetiere, einschliesslich des Menschen. Säugetierkundliche Mitteilungen 21: 131–239.

Forasiepi, A.M., et al. 2015. New toxodontid (Notoungulata) from the Early Miocene of Mendoza, Argentina. Paläontologische Zeitschrift 89: 611–634.

Forasiepi, A.M., et al. 2016. Exceptional skull of *Huayqueriana* (Mammalia, Litopterna, Macraucheniidae) from the Late Miocene of Argentina: anatomy, systematics, and paleobiological implications. Bulletin of the American Museum of Natural History 404: 1–76.

Forasiepi, A.M., R.D.E. MacPhee, and S. Hernández Del Pino. 2019. Caudal cranium of *Thylacosmilus atrox* (Mammalia, Metatheria, Sparassodonta), a South American predaceous sabertooth. Bulletin of the American Museum of Natural History 433: 1–64.

Frappier, B.L. 2006. Digestive system. *In* J.A. Eurell and B.L. Frappier (editors), Dellmann's textbook of veterinary histology, 6th ed.: 170–211. Ames, IA: Blackwell.

Fukuta, K., et al. 2007. Absence of carotid rete mirabile in small tropical ruminants: implications for the evolution of the arterial system in artiodactyls. Journal of Anatomy 210: 112–116.

Gabbert, S.L. 2004. The basicranial and posterior cranial anatomy of the families of Toxodontia. *In* G.C. Gould and S.K. Bell (editors), Tributes to Malcolm C. McKenna: his students, his legacy (ch. 14). Bulletin of the American Museum of Natural History 285: 177–190.

Gaillard, C, R.D.E. MacPhee, and A.M. Forasiepi. In press. The stapes of stem and extinct Marsupialia: implications for the ancestral condition. Journal of Vertebrate Paleontology.

Gannon, P.J., A.R. Eden, and J.T. Laitman. 1988. The subarcuate fossa and cerebellum of extant primates: comparative study of a skull-brain interface. American Journal of Physical Anthropology 77: 143–164.

García-López, D.A. 2011. Basicranial osteology of *Colbertia lumbrerense* Bond, 1981 (Mammalia, Notoungulata). Ameghiniana 48: 3–12.

García-López, D.A., J. Babot, R. González, and A. Scanferla. 2017. Cranial anatomy of an Eocene notoungulate mammal from northwestern Argentina with special reference on the ear region. Historical Biology. [doi.org/10.1080/08912963.2017.1326112]

Gardner, E., D., J. Gray, and R. O'Rahilly. 1969. Anatomy: a regional study of human structure, 3rd ed. Philadelphia: Saunders.

Gaudin, T.J., J.R. Wible, J.A. Hopson, and W.D. Turnbull. 1996. Reexamination of the morphological evidence for the Cohort Epitheria (Mammalia, Eutheria). Journal of Mammalian Evolution 3: 31–79.

Gaudry, A. 1904. Fossiles de Patagonie: dentition de quelques mammifères. Mémoires de la Société Géologique de France, Paléontologie 12, Mémoire 31: 1–27.

Gaupp E. 1908. Zur Entwickelungsgeschichte und vergleichenden Morphologie des Schädels von Echidna aculeata var. typica. Denkschriften der Medicinisch-Naturwissenschaftlichen Gesellschaft zu Jena 6: 539–788.

Gazin, L.C. 1965. A study of the Early Tertiary condylarthran mammal *Meniscotherium*. Smithsonian Miscellaneous Collections 149 (2): 1–98.

Gazin, L.C. 1968. A study of the Eocene condylarthran mammal *Hyopsodus*. Smithsonian Miscellaneous Collections 153 (4): 1–90.

Geisler, J.H., and Z. Luo. 1998. Relationships of Cetacea to terrestrial ungulates and the evolution of cranial vasculature in Cete. *In* J.G.M. Thewissen (editor), The emergence of whales: evolutionary patterns in the origin of Cetacea: 163–212. New York: Springer.

Getty, R. (editor). 1975. The anatomy of the domestic animals, 5th ed. Philadelphia: Saunders.

Ghosal, N.G. 1975. Equine heart and arteries. *In* R. Getty (editor), The anatomy of the domestic animals, 5th ed., vol. 1: 554–618. Philadelphia: Saunders.

Goloboff, P., J. Farris, and K. Nixon. 2008. TNT, a free program for phylogenetic analysis. Cladistics 24: 774–786.

Gregory, W.K. 1910. The orders of mammals. Bulletin of the American Museum of Natural History 27: 3–524.

Grubb, P. 2005. Order Perissodactyla. *In* D.E. Wilson and D.M. Reeder (editors), Mammal species of the World, a taxonomic and geographic reference: 629–636. Baltimore: Johns Hopkins University.

Habel, S. 1975. Ruminant digestive system. *In* R. Getty (editor), The anatomy of the domestic animals, 5th ed., vol. 1: 861–915. Philadelphia: Saunders.

Hall, B.K. 2015. Bones and cartilage. New York: Academic.

Hare, W.C.D. 1975. General respiratory system. *In* R. Getty (editor), The anatomy of the domestic animals, 5th ed., vol. 1: 113–144. Philadelphia: Saunders.

Harper, T, and G.W. Rougier. 2019. Petrosal morphology and cochlear function in Mesozoic stem therians. PLoS One 14 (8): e0209457.

Hernández Del Pino, S. 2018. Anatomía y sistemática de los Toxodontidae (Notoungulata) de la Formación Santa Cruz, Mioceno temprano, Argentina. Ph.D. dissertation, Facultad de Ciencias Naturales y Museo, Universidad Nacional de La Plata, La Plata, Argentina. 415 pp.

Hershkovitz, I., et al. 1999. The elusive diploic veins: anthropological and anatomical perspective. American Journal of Physical Anthropology 108: 345–358.

Hillman, D.J. 1975. Skull. *In* R. Getty (editor), The anatomy of the domestic animals, 5th ed., vol. 1: 318–348. Philadelphia: Saunders.

Hopson J.A. 1979. Paleoneurology. *In* C. Gans, R.G. Northcutt, and P. Ulinski (editors), Biology of the Reptilia: 39–146. New York: Academic Press.

Horovitz, I. 2004. Eutherian mammal systematics and the origins of South American ungulates as based on postcranial osteology. Bulletin of Carnegie Museum of Natural History 36: 63–79.

Hyrtl, J. 1854. Beiträge zur vergleichenden Angiologie. V. Das arterielle Gefäss-system der Edentata. Denkschriften der Akademie der Wissenschaften, Wien, Mathematisch-Naturwissenschaftliche Klasse, 6: 21–65.

International Committee on Veterinary Gross Anatomical Nomenclature. 2017. Nomina anatomica veterinaria, 6th ed. Online resource (http://www.wava-amav.org/wava-documents.html).

Janis, C.M., and J.M. Theodor. 2014. Cranial and postcranial morphological data in ruminant phylogenetics. Zitteliana B32: 15–31.

Jerison, H.J. 1973. Evolution of the brain and intelligence. New York: Academic Press.

Jerison H.J. 1985. Animal intelligence as encephalization. Philosophical Transactions of the Royal Society of London B308: 21–35.

Jessen, C., et al. 1994. Blood and brain temperatures in free-ranging black wildebeest in their natural environment. American Journal of Physiology 267: R1528–R1536.

Johnson, S.C., and R.H. Madden. 1997. Uruguaytheriine astrapotheres of tropical South America. *In* R.F. Kay, R.H. Madden, R.L. Cifelli, and J.J. Flynn (editors), Vertebrate paleontology in the Neotropics: the Miocene fauna of La Venta, Columbia: 355–381. Washington, D.C.: Smithsonian Institution.

Kampen, P.N. van. 1905. Die Tympanalgegend des Säugetierschädels. Morphologisches Jahrbuch 34: 321–722.

Kielan-Jaworowska, Z. 1981. Evolution of the therian mammals in the latest Cretaceous of Asia. Part IV. Skull structures in *Kennalestes* and *Asioryctes*. Palaeontologia Polonica 42: 25—78.

Kielan-Jaworowska, Z. 1986. Brain evolution in Mesozoic mammals. Rocky Mountain Geology 24, special paper 3: 21–34.

Kielan-Jaworowska, Z., R. Presley, and C. Poplin. 1986. The cranial vascular system in taeniolabidoid multituberculate mammals. Philosophical Transactions of the the Royal Society of London 1164: 525–602.

Kielan-Jaworowska, Z., R.L. Cifelli, and Z. Luo. 2004. Mammals from the age of dinosaurs. New York: Columbia University.

Klaauw, C.J. van der. 1922. Über die Entwickelung des Entotympanicums. Tijdschrift der Nederlandsche Dierkundige Vereeniging 18: 135–174.

Klaauw, C.J. van der. 1931. The auditory bulla in some fossil mammals, with a general introduction to this region of the skull. Bulletin of the American Museum of Natural History 62 (1): 1–352.

Koenigswald, W. von. 2011. Diversity of hypsodont teeth in mammalian dentitions—construction and classification. Palaeontographica, Abteilung A 294: 63–94.

Koenigswald, W. von, T. Martin, and G. Billet. 2014. Enamel microstructure and mastication in *Pyrotherium romeroi* (Pyrotheria, Mammalia). Paläontologische Zeitschrift. [doi: 10.1007/s12542-014-0241-5]

Koyabu, D., W. Maier, and M. Sánchez-Villagra. 2012. Paleontological and developmental evidence resolve the homology and dual embryonic origin of a mammalian skull bone, the interparietal. Proceedings of the National Academy of Sciences of the United States of America 109: 14075–14080.

Kramarz, A.G., and M. Bond. 2009. A new Oligocene astrapothere (Mammalia, Meridiungulata) from Patagonia and a new appraisal of astrapothere phylogeny. Journal of Systematic Palaeontology 7: 117–128.

Kramarz, A.G., M. Bond, and A. Forasiepi. 2010. New remains of *Astraponotus* (Mammalia, Astrapotheria) and considerations on the astrapothere cranial evolution. Paläontologische Zeitschrift 85: 85–200.

Kramarz, A., M. Bond, and G.W. Rougier. 2017. Redescription of the auditory region of the putative basal astrapothere *Eoastrapostylops riolorense* Soria and Powell, 1981, systematic and phylogenetic considerations. Annals of Carnegie Museum 84: 95–164.

Kramarz, A., A. Garrido, and M. Bond. 2019a. *Astrapotherium* from the Middle Miocene Collón Cura Formation and the decline of astrapotheres in Southern South America. Ameghiniana 56: 290–306.

Kramarz, A., M. Bond, and A. Carlini. 2019b. Astrapotheres from Cañadón Vaca, Middle Eocene of central Patagonia: new insights on diversity, anatomy, and early evolution of Astrapotheria. Palaeontologia Electronica 22.2.52A: 1–22.

Krause, J.M., et al. 2017. New age constraints for early Paleogene strata of central Patagonia, Argentina: implications for the timing of South American Land Mammal Ages. Bulletin of the Geological Society of America. [doi: 10.1130/B31561.1]

Lang, J. 1983. Clinical anatomy of the head: Neurocranium, orbit, craniocervical regions. Berlin: Springer. [translated by R.R. Wilson and D.P. Winstanley]

Leisering, A.G.T. 1888. Atlas der Anatomie des Pferdes und der übrigen Hausthiere. Für Thierärzte und Studierende der Veterinärkunde, landwirthschaftliche Lehranstalten und Pferdeliebhaber überhaupt, 2nd rev. ed. Leipzig: Teubner.

Lindenau, C. 2005. Zahnschmelzmikrostrukturen südamerikanischer Huftiere, Ph.D. dissertation, Mathematisch-Naturwissenschaftlichen Fakultät, Rheinischen Friedrich-Wilhelms-Universität, Bonn.

Loomis, F.B. 1914. The Deseado Formation of Patagonia. New Haven: Amherst College.

Louis, R.G., et al. 2008. Clinical anatomy of the mastoid and occipital emissary veins in a large series. Surgical and Radiologic Anatomy 31. [doi:10.1007/s00276-008-0423-5]

Lydekker, R. 1893. Contributions to a knowledge of the fossil vertebrates of Argentina. III. A study of extinct Argentine ungulates. Anales de Museo de La Plata, Paleontología Argentina 2: 2–83.

MacPhee, R.D.E. 1979. Entotympanics, ontogeny and primates. Folia Primatologia 31: 23–47.

MacPhee, R.D.E. 1981. Auditory regions of primates and eutherian insectivores: morphology, ontogeny, and character analysis. Contributions to Primatology 18: 1–282.

MacPhee, R.D.E. 1994. Morphology, adaptations, and relationships of *Plesiorycteropus*, and a diagnosis of a new order of eutherian mammals. Bulletin of the American Museum of Natural History 220: 1–213.

MacPhee, R.D.E. 2011. Basicranial morphology and relationships of Antillean Heptaxodontidae (Rodentia, Ctenohystrica, Caviomorpha). Bulletin of the American Museum of Natural History 363: 1–70.

MacPhee, R.D.E. 2014. The serrialis bone, interparietals, "x" elements, entotympanics, and the composition of the notoungulate caudal cranium. Bulletin of the American Museum of Natural History 384: 1–69.

MacPhee, R.D.E., and M. Cartmill. 1986. Basicranial structures and primate systematics. In D.R. Swindler (editor), Comparative primate biology, vol. 1, Systematics, evolution, and anatomy: 219–275. New York: Liss.

MacPhee, R.D.E., and M.J. Novacek. 1993. Definition and relationships of Lipotyphla. In F.S. Szalay, M.J. Novacek, and M.C. McKenna (editors), Mammal phylogeny, vol 2: 13–31. New York: Springer.

Macrini, T.E., T. Rowe, and M. Archer. 2006. Description of a cranial endocast from a fossil platypus, Obdurodon dicksoni (Monotremata, Ornithorhynchidae), and the relevance of endocranial characters to monotreme monophyly. Journal of Morphology 267: 1000–1015.

Macrini, T.E., T. Rowe, and J.L. Vandeberg. 2007. Cranial endocasts from growth series of Monodelphis domestica (Didelphidae, Marsupialia): a study of individual and ontogenetic variation. Journal of Morphology 268: 844–865.

Macrini, T.E., J.J. Flynn, D.A. Croft, and A.R. Wyss. 2010. Inner ear of a notoungulate placental mammal: anatomical description and examination of potentially phylogenetically informative characters. Journal of Anatomy 216: 600–610.

Macrini, T.E., J.J. Flynn, X. Ni, D.A. Croft, and A.R. Wyss. 2013. Comparative study of notoungulate (Placentalia, Mammalia) bony labyrinths and new phylogenetically informative inner ear characters. Journal of Anatomy 223: 442–461.

Maier, W. 2020. A neglected part of the mammalian skull: the outer nasal cartilages as progressive remnants of the chondrocranium. Vertebrate Zoology 70 (3): 367–382.

Maier, W., A. Tröscher, and I. Ruf. 2013. The entotympanic of Equus caballus (Perissodactyla, Mammalia). Mammalian Biology 78: 231–234.

Marsot-Dupuch, K., M. Gayet-Delacroix, M. Elmaleh-Berges, F. Bonneville, and P. Lasjaunias. 2001. The petrosquamosal sinus: CT and MR findings of a rare emissary vein. American Journal of Neuroradiology 22: 1186–1193.

Martínez, G., M.T. Dozo, J.N. Gelfo, and H. Marani. 2016. Cranial morphology of the Late Oligocene Patagonian notohippid Rhynchippus equinus Ameghino, 1897 (Mammalia, Notoungulata) with emphases in basicranial and auditory region. PLoS One 11: e0156558.

Martínez, G., M.T. Dozo, B. Vera, and E. Cerdeño. 2020. Paleoneurology, auditory region, and associated soft tissue inference in the late Oligocene notoungulates Mendozahippus fierensis and Gualta cuyana (Toxodontia) from central-western Argentina. Journal of Vertebrate Paleontology [doi:10.1080/02724634.2019.1725531]

Mead, J.G., and R.E. Fordyce. 2009. The therian skull: a lexicon with emphasis on the odontocetes. Smithsonian Contributions to Zoology 627: 1–248.

Meng J., and R.C. Fox. 1995. Osseous inner ear structures and hearing in early marsupials and placentals. Zoological Journal of the Linnean Society 115: 47–71.

Minett, F.C. 1925. The organ of Jacobson in the horse, ox, camel and pig. Journal of Anatomy 60: 110–118.

Montané, L., and E. Bourdelle. 1913. Anatomie régionale des animaux domestiques, vol. 1, Cheval. Paris: Baillière.

Moore, K.L. 1985. Clinically oriented anatomy, 2nd ed. Baltimore: Williams & Wilkins.

Moore, W.J. 1981. The mammalian skull. Cambridge: Cambridge University Press.

Mortazavi, M.M., et al. 2011. Anatomy and pathology of cranial emissary veins: a review with surgical implications. Neurosurgery 70: 1313–1318.

Moyano, S.R., and N.P. Giannini. 2017. Comparative cranial ontogeny of Tapirus (Mammalia: Perissodactyla: Tapiridae). Journal of Anatomy 231: 665–682.

Muizon, C. de, G. Billet, C. Argot, S. Ladevèze, and F. Goussard. 2015. Alcidedorbignya inopinata, a basal pantodont (Placentalia, Mammalia) from the Early Palaeocene of Bolivia: anatomy, phylogeny and palaeobiology. Geodiversitas 37: 397–634.

Muizon, C. de, S. Ladevèze, C. Selva, R. Vignaud, and F. Goussard. 2018. Allqokirus australis (Sparassodonta, Metatheria) from the Early Paleocene of Tiupampa (Bolivia) and the rise of the metatherian carnivorous radiation in South America. Geodiversitas 40: 363–459.

Muizon C. de, G. Billet, and S. Ladevèze. 2019. New remains of kollpaniine "condylarths" (Panameriungulata) from the Early Palaeocene of Bolivia shed light on hypocone origins and molar proportions among ungulate-like placentals. Geodiversitas 41: 841–874.

Nathoo, N., E.C. Caris, J.A. Wiener, and E. Mendel. 2011. History of the vertebral venous plexus and the significant contributions of Breschet and Batson. Neurosurgery 69: 1007–1014.

Nickel, R, A. Schummer, E. Seiferle, J. Frewein, and K.-H. Wille. 1977. Lehrbuch der Anatomie der Haustiere, vol. 1, Bewegungsapparat. Berlin: Paul Parey.

Nieuwenhuys, R., H.J. Ten Donkelaar, and C. Nicholson. 1998. The central nervous system of vertebrates. Berlin: Springer.

Novacek, M.J., and Wyss, A.R. 1986. Origin and transformation of the mammalian stapes. *In* K.M. Flanagan and J.A. Lillegraven (editors), Vertebrates, phylogeny, and philosophy. Contributions to Geology, University of Wyoming Special Paper 3: 35–53.

Nowak, R. 1999. Walker's mammals of the world. Baltimore: Johns Hopkins University Press.

Nowak, R.M. 2018. Walker's mammals of the world: monotremes, marsupials, afrotherians, xenarthrans, and sundatherians. Baltimore: Johns Hopkins Press.

O'Brien, H.D. 2017. Cranial arterial patterns of the alpaca (Camelidae: *Vicugna pacos*). Royal Society Open Science 4: 160967.

O'Brien, H.D., and J. Bourke. 2015. Physical and computational fluid dynamics models for the hemodynamics of the artiodactyl carotid rete. Journal of Theoretical Biology 386: 122–131.

O'Brien, H.D., P.M. Gignac, T.L. Hieronymus, and L.M. Witmer. 2016. A comparison of postnatal arterial patterns in a growth series of giraffe (Artiodactyla: *Giraffa camelopardis*). PeerJ 4: e1696.

O'Gorman, S. 2005. Second branchial arch lineages of the middle ear of wild-type and *Hoxa2* mutant mice. Developmental Dynamics 234: 124–131.

Okudera, T. et al. 1994. Development of the posterior fossa dural sinuses, emissary veins, and jugular bulb: morphological and radiological study. American Journal of Neuroradiology 15: 1871-1883.

O'Leary, M.A. 2010. An anatomical and phylogenetic study of the osteology of the petrosal of extant and extinct artiodactylans (Mammalia) and relatives. Bulletin of the American Museum of Natural History 335: 1–206.

O'Leary, M.A., and J. Gatesy. 2008. Impact of increased character sampling on the phylogeny of Cetartiodactyla (Mammalia): combined analysis including fossils. Cladistics 24: 397–442.

O'Leary, M.A., et al. 2013. The placental mammal ancestor and the post-KPg radiation of placentals. Science 339: 662–667.

Ommanney, F.D. 1932. The vascular networks (retia mirabilia) of the fin whale (*Balaenoptrna physalus*). Discovery Reports 5: 327–362.

Orliac, M. J., C. Argot, and E. Gilissen. 2012. Digital cranial endocast of *Hyopsodus* (Mammalia, "Condylarthra"): a case of Paleogene terrestrial echolocation? PLoS One 7: 1–10.

Owen, R. 1854. Description of some species of the extinct genus *Nesodon*. Proceedings of the Royal Society of London 6: 272–273.

Oyanagi, T., J. Hyun-Kim, M. Yamamoto, M. Ishii, G. Murakami, F. F. Rodríguez-Vásquez, and S. Abe (2020). Topographical anatomy of the tentorium cerebelli and venous confluences in human midterm fetuses. Annals of Anatomy/Anatomischer Anzeiger 233: 151596.

Padget, D.H. 1948. The development of the cranial arteries in the human embryo. Contributions to Embryology of the Carnegie Institute of Washington 32: 207–261.

Padget, D.H. 1956. The cranial venous system in man in reference to development, adult configuration, and relation to the arteries. American Journal of Anatomy 98: 307–355.

Padget, D.H. 1957. The development of the cranial venous system in man, from the standpoint of comparative anatomy. Contributions to Embryology of the Carnegie Institute of Washington 36: 81–139.

Parker, W.N. 1882. On some points in the anatomy of the Indian tapir (*Tapirus indicus*). Proceedings of the Zoological Society of London 1882: 768–777.

Parrington, F.R., and T.S. Westoll. 1940. On the evolution of the mammalian palate. Philosophical Transactions of the Royal Society of London B230: 305–355.

Patterson, B. 1932. The auditory region of the Toxodontia. Field Museum of Natural History, Geological Series 6: 1–27.

Patterson, B. 1934a. Cranial characters of *Homalodotherium*. Field Museum of Natural History, Geological Series 6: 113–117.

Patterson, B. 1934b. The auditory region of an upper Pliocene typotherid [sic]. Field Museum of Natural History, Geological Series 6: 83–89.

Patterson, B. 1934c. Upper premolar-molar structure in the Notoungulata with notes on taxonomy. Field Museum of Natural History, Geology Series 6: 91–111.

Patterson, B. 1936. The internal structure of the ear in some notoungulates. Field Museum of Natural History, Geological Series 7: 199–227.

Patterson, B. 1937. Some notoungulate braincasts. Field Museum of Natural History, Geological Series 6: 273–301.

Patterson, B. 1977. A primitive pyrothere (Mammalia, Notoungulata) from the early Tertiary of northwestern Venezuela. Fieldiana: Geology 33: 397–422.

Paula Couto, C. de. 1952. Fossil mammals from the beginning of the Cenozoic in Brazil. Condylarthra, Litopterna, Xenungulata, and Astrapotheria. Bulletin of the American Museum of Natural History 99 (6): 359–394.

Presley, R. 1979. The primitive course of the internal carotid artery in mammals. Acta Anatomica 103: 238–244.

Presley, R. 1993. Development and the phylogenetic features of the middle ear region. *In* F.S. Szalay, M.J. Novacek, and M.C. McKenna (editors), Mammal Phylogeny, vol. 2, Placentals: 21–29. New York: Springer.

Quiroga, J. 1980. The brain of the mammal-like reptile *Probainognathus jenseni* (Therapsida, Cynodontia). A correlative paleo-neurological approach to the neocortex at the reptile mammal transition. Journal für Hirnforschung 21: 299–336.

Radinsky, L. 1981. Brain evolution in extinct South American ungulates. Brain, Behavior and Evolution 18: 169–187.

Remy, J.-A., 1992. Observations sur l'anatomie crânienne du genre *Palaeotherium* (Perissodactyla, Mammalia): mise en évidence d'un nouveau sous-genre, *Franzenitherium*. Palaeovertebrata 21: 203–224.

Rensberger, J.M., and H.U. Pfretzschner. 1992. Enamel structure in astrapotheres and its functional implications. Scanning Microscopy 6: 495–510.

Rose, K.D. 2006. The beginning of the age of mammals. Baltimore: Johns Hopkins University.

Rose, K., et al. 2014. Early Eocene fossils suggest that the mammalian order Perissodactyla originated in India. Nature Communications 5: 5570.

Rose, K.D., et al. 2019. Anatomy, relationships, and paleobiology of *Cambaytherium* (Mammalia, Perissodactylamorpha, Anthracobunia) from the Lower Eocene of western India. Journal of Vertebrate Paleontology 39 (suppl. 1): 1–147.

Rossie, J.B. 2006. Ontogeny and phylogeny of the paranasal sinuses in Platyrrhini (Mammalia: Primates). Journal of Morphology 267: 1–40.

Roth, S. 1899. Aviso preliminar sobre mamíferos mesozoicos encontrados en Patagonia. Revista del Museo de La Plata 9: 381–388.

Roth, S. 1903. Los ungulados sudamericanos. Anales de Museo de La Plata, Sección Paleontología 5: 1–36.

Rougier, G.W., and J.R. Wible. 2006. Major changes in the ear region and basicranium of early mammals. *In* M. Carrano, T.J. Gaudin, R. Blob, and J.R. Wible (editors), Amniote paleobiology: phylogenetic and functional perspectives on the evolution of mammals, birds, and reptiles: 269–311. Chicago: University of Chicago Press.

Rougier, G.W., J.R. Wible, and J.A. Hopson. 1992. Reconstruction of the cranial vessels in the Early Cretaceous mammal *Vincelestes neuquenianus*: implications for the evolution of the mammalian cranial vascular system. Journal of Vertebrate Paleontology 12: 188–216.

Ruf, I., Z. Luo, and T. Martin. 2013. Re-investigation of the basicranium of *Haldanodon exspectatus* (Mammaliaformes, Docodonta). Journal of Vertebrate Paleontology 33: 382–400.

Rusconi, C. 1932. Nuevos restos de *Scalabrinitherium* del Terciario de Paraná y apuntes relativos a su anatomía craneana. Revista de Medicina y Veterinaria 15–19: 3–18.

Russell, A.P., and J. Thomason. 1993. Mechanical analysis of the mammalian head skeleton. *In* J. Hanken and B.K. Hall (editors), The skull, vol. 3, Functional and evolutionary mechanisms: 345–383. Chicago: University of Chicago Press.

Russell, D.E., and D. Sigogneau. 1965. Etude de moulages endocraniens de mammifères paleocènes. Mémoires de Museum National d'Histoire Naturelle, sér. C16: 1–34.

Saban, R. 1963. Contribution à l'étude de l'os temporal des primates. Description chez l'homme et les prosimiens. Anatomie comparée et phylogénie. Mémoires du Museum National d'Histoire Naturelle, sér. A, Zoologie 29: 1–377.

Sánchez-Villagra, M.R., and J.R. Wible. 2002. Patterns of evolutionary transformation in the petrosal bone and some basicranial features in marsupial mammals, with special reference to didelphids. Journal of Zoological Systematics and Evolutionary Research 40: 26–45.

Schellhorn, R. 2018. A potential link between lateral semicircular canal orientation, head posture, and dietary habits in extant rhinos (Perissodactyla, Rhinocerotidae). Journal of Morphology 279: 50–61.

Schliemann, H. 1987. The solum nasi of the mammalian chondrocranium with special reference to the Carnivora. *In* H.-J. Kuhn and U. Zeller (editors), Morphogenesis of the mammalian skull: 91–103. Hamburg: Paul Parey.

Schmelzle, T., M.R. Sánchez-Villagra, and W. Maier. 2007. Vestibular labyrinth evolution in diprotodontian marsupial mammals. Mammal Study 32: 83–97.

Schummer, A., H. Wilkens, B. Vollmerhaus, and K.-H. Habermehl. 1981. The circulatory system, the skin, and the cutaneous organs of the domestic mammals. Heidelberg: Springer.

Scott, W.B. 1909. Typotheria of the Santa Cruz Beds. *In* W.B. Scott (editor), Reports of the Princeton University Expeditions to Patagonia, 1896–1899, vol. 6, Paleontology. Mammalia of the Santa Cruz Beds, part 1: 1–110. Stuttgart: Schweizerbart'sche Verlagshandlung.

Scott, W.B. 1912. Toxodonta and Entelonychia of the Santa Cruz Beds. *In* W.B. Scott (editor), Reports of the Princeton University Expeditions to Patagonia, 1896–1899, vol. 6, Paleontology. Mammalia of the Santa Cruz Beds, part 2–3: 111–300. Stuttgart: Schweizerbart'sche Verlagshandlung.

Scott, W.B. 1928. Astrapotheria of the Santa Cruz Beds. *In* W.B. Scott (editor), Reports of the Princeton University Expeditions to Patagonia, 1896–1899, vol. 6, Paleontology. Mammalia of the Santa Cruz beds, part 4: 301–351. Stuttgart: Schweizerbart'sche Verlagshandlung.

Scott, W.B. 1937a. A history of land mammals in the Western Hemisphere. New York: MacMillan.

Scott, W.B. 1937b. The Astrapotheria. Proceedings of the American Philosophical Society 77: 309–393.

Segall, W. 1970. Morphological parallelism of the bulla and auditory ossicles in some insectivores and marsupials. Fieldiana Zoology 51: 169–205.

Shelley, S.L., T.E. Williamson, and S.L. Brusatte. 2018. The osteology of *Periptychus carinidens*: a robust, ungulate-like placental mammal (Mammalia: Periptychidae) from the Paleocene of North America. PLoS One 13 (7): e0200132.

Simpson, G.G. ᴍꜱ. [Scarritt—Patagonian Exped. Field Notes.] Online resource (http://research.amnh.org/paleontology/notebooks/simpson-1930a/index.html).

Simpson, G.G. 1932. *Cochilius volvens* from the Colpodon Beds of Patagonia. American Museum Novitates 577: 1–13.

Simpson, G.G. 1933a. Structure and affinities of *Trigonostylops*. American Museum Novitates 608: 1–28.

Simpson, G.G. 1933b. Braincasts of *Phenacodus, Notostylops,* and *Rhyphodon*. American Museum Novitates 622: 1–19.

Simpson, G.G. 1933c. Braincasts of two typotheres and a litoptern. American Museum Novitates 629: 1–18.

Simpson, G.G. 1934. Provisional classification of extinct South American hoofed mammals. American Museum Novitates 750: 1–21.

Simpson, G.G. 1936. Structure of a primitive notoungulate cranium. American Museum Novitates 824: 1–31.

Simpson, G.G. 1948. The beginning of the age of mammals in South America. Part 1. Introduction. Systematics: Marsupialia, Edentata, Condylarthra, Litopterna, Notioprogonia. Bulletin of the American Museum of Natural History 91: 1–232.

Simpson, G.G. 1957. A new Casamayoran astrapothere. Revista del Museo Municipal de Ciencias Naturales y Tradicional de Mar del Plata 1 (3): 11–18.

Simpson, G.G. 1967. The beginning of the age of mammals in South America, Part 2, Systematics: Notoungulata, concluded (Typotheria, Hegetotheria, Toxodonta, Notoungulata incertae sedis), Astrapotheria, Trigonostylopoidea, Pyrotheria, Xenungulata, Mammalia incertae sedis. Bulletin of the American Museum of Natural History 137: 1–259.

Simpson, G.G. 1975. Recent advances in methods of phylogenetic inference. *In* W.P. Luckett and F.S. Szalay (editors), Phylogeny of primates, a multidisciplinary approach: 3–19. New York: Plenum.

Sinclair, W.J. 1910. Litopterna of the Santa Cruz Beds. *In* W.B. Scott (editor), Reports of the Princeton University Expeditions to Patagonia, 1896–1899, vol. 7, Paleontology. Mammalia of the Santa Cruz Beds, part 1: 1–156. Stuttgart: Schweizerbart'sche Verlagshandlung.

Sisson, S., and J.D. Grossman. 1953. The anatomy of the domestic animals, rev. 4th ed. Philadelphia: Saunders.

Soria, M.F. 1982. *Tetragonostylops apthomasi* (Price y Paula-Couto, 1950): su asignación a Astrapotheriidae (Mammalia; Astrapotheria). Ameghiniana 19: 234–238.

Soria, M.F. 1988. Estudios sobre los Astrapotheria (Mammalia) del Paleoceno y Eoceno. Parte II: Filogenia, origen y relaciones. Ameghiniana 25: 47–59.

Soria, M.F. 2001. Los Proterotheriidae (Mammalia, Litopterna): sistemática, origen y filogenia. Monografías del Museo Argentino de Ciencias Naturales "Bernardino Rivadavia" 1: 1–167.

Soria, M.F., and M. Bond. 1984. Adiciones al conocimiento de *Trigonostylops* Ameghino 1897 (Mammalia, Astrapotheria, Trigonostylopidae). Ameghiniana 21: 43–51.

Soria, M.F., and J.E. Powell. 1981. Un primitivo Astrapotheria (Mammalia) y la edad de la Formación Río Loro, provincia de Tucumán, República Argentina. Ameghiniana 18: 155–168.

Sprinz, R. 1952. The innervation of the trunk of the Indian elephant. Proceedings of the Zoological Society of London 122: 621–624.

Starck, D. 1967. La crâne des mammifères. *In* P.-P. Grassé (editor), Traité de zoologie, Mammifères: téguments et squelette, 16/1: 405–549, 1095–1102. Paris: Masson.

Tandler, J. 1899. Zur vergleichenden Anatomie der Kopfarterien bei den Mammalia. Denkschriften der Kaiserlichen Akademie der Wissenschaften, Mathematisch-Naturwissenschaftliche Classe, Wien 67: 677–784.

Teng, C.S., L. Cavin, R.E. Maxson, M.R. Sánchez-Villagra, and J.G. Crump. 2019. Resolving homology in the face of shifting germ layer origins: Lessons from a major skull vault boundary. eLife 8: e52814.

Thewissen, J.G.M. 1990. Evolution of Paleocene and Eocene Phenacodontidae. University of Michigan Papers on Paleontology 29: 1–107.

Tilney, F. 1933. Fossil brains of some early Tertiary mammals of North America. Bulletin of the Neurological Institute of New York 1: 430–505.

Tsutsumi, S., et al. 2015. Cerebrospinal fluid drainage through the diploic and spinal epidural veins. Journal of Anatomy 227: 297–301.

Tubbs, R.S., K. Watanabe, M. Loukas, and A.A. Cohen-Gadol. 2014. Anatomy of the inferior petro-occipital vein and its relation to the base of the skull: application to surgical and endovascular procedures of the skull base. Clinical Anatomy 27: 698–701.

Tubbs, R.S., et al. (editors). 2020. Anatomy, imaging and surgery of the intracranial dural venous sinuses. New York: Elsevier.

Vallejo-Pareja, M.C., et al. 2015. *Hilarcotherium castanedaii*, gen. et sp. nov., a new Miocene astrapothere (Mammalia, Astrapotheriidae) from the Upper Magdalena Valley, Colombia. Journal of Vertebrate Paleontology: e903960.

Vitums, A. 1979. Development of the equine venous sinuses of the dura mater. Zentralblatt für Veterinärmedizin, Reihe C: Anatomie, Histologie, Embryologie 8: 124–137.

Vogl, A.W., and H.D. Fisher. 1981. Arterial circulation of the spinal cord and brain in the Monodontidae (Order Cetacea). Journal of Morphology 170: 171–180.

Walmsley, R. 1938. Some observations on the vascular system of a female fin back. Contributions to Embryology of the Carnegie Institute of Washington 27: 107–178.

Walsh, S., and A. Milner. 2011. *Halcyornis toliapicus* (Aves: Lower Eocene, England) indicates advanced neuromorphology in Mesozoic Neornithes. Journal of Systematic Palaeontology 9: 173–181.

Walsh, S.A., et al. 2013. Avian cerebellar floccular fossa size is not a proxy for flying ability in birds. PLoS One 8(6): e67176.

Warwick, R., and P.L. Williams. 1973. Gray's anatomy, 35th British ed. Philadelphia: Saunders.

Webster D.B. (1975) Auditory systems of Heteromyidae: postnatal development of the ear in *Dipodomys merriami*. Journal of Morphology 146: 377–394.

Welker, F., et al. 2015. Ancient proteins resolve the evolutionary history of Darwin's South American ungulates. Nature 522: 81–84.

West, C.D. 1985. The relationship of the spiral turns of the cochlea and the length of the basilar membrane to the range of audible frequencies in ground dwelling mammals. Journal of the Acoustical Society of America 77: 1091–101.

Westbury, M., et al. 2017. A mitogenomic timetree for Darwin's enigmatic South American mammal *Macrauchenia patachonica*. Nature Communications 8: 15951.

Wible, J.R. 1984. The ontogeny and phylogeny of the mammalian cranial arterial pattern. Ph.D. dissertation, Department of Anatomy, Duke University, Durham, NC, 705 pp.

Wible, J.R. 1986. Transformations in the extracranial course of the internal carotid artery in mammalian phylogeny. Journal of Vertebrate Paleontology 6: 313–325.

Wible, J.R. 1987. The eutherian stapedial artery: character analysis and implications for superordinal relationships. Zoological Journal of the Linnaean Society 91: 107–135.

Wible, J.R. 1990. Petrosals of Late Cretaceous marsupials from North America and a cladistic analysis of the petrosal in therian mammals. Journal of Vertebrate Paleontology 10:183–205.

Wible, J.R. 2003. On the cranial osteology of the short-tailed opossum *Monodelphis brevicaudata* (Didelphidae, Marsupialia). Annals of Carnegie Museum 72: 137–202.

Wible, J.R. 2008. On the cranial osteology of the Hispaniolan solenodon, *Solenodon paradoxus* Brandt, 1833 (Mammalia, Lipotyphla, Solenodontidae). Annals of Carnegie Museum 77: 321–402.

Wible, J.R. 2010. Petrosal anatomy of the nine-banded armadillo, *Dasypus novemcinctus* Linnaeus, 1758 (Mammalia , Xenarthra, Dasypodidae). Annals of Carnegie Museum 79: 1–28.

Wible, J. R., 2012. The ear region of the aardvark, *Orycteropus afer* (Pallas, 1766) (Mammalia, Placentalia, Tubulidentata). Annals of Carnegie Museum 80: 115–146.

Wible, J.R., and T.J. Gaudin. 2004. On the cranial osteology of the yellow armadillo *Euphractus sexcinctus* (Dasypodidae, Xenarthra, Placentalia). Annals of Carnegie Museum 73: 117–196.

Wible, J.R., and J.A. Hopson. 1995. Homologies of the prootic canal in mammals and non-mammalian cynodonts. Journal of Vertebrate Paleontology 15: 331–356.

Wible, J.R., and G.W. Rougier. 2000. Cranial anatomy of *Kryptobaatar dashzevegi* (Mammalia, Multituberculata), and its bearing on the evolution of mammalian characters. Bulletin of the American Museum of Natural History 247: 1–124.

Wible, J.R., and G.W. Rougier. 2017. Craniomandibular anatomy of the subterranean meridiolestidan *Necrolestes patagonensis* Ameghino, 1891 (Mammalia, Cladotheria) from the Early Miocene of Patagonia. Annals of Carnegie Museum 84: 183–252.

Wible, J.R. and S.L. Shelley. 2020. Anatomy of the petrosal and middle ear of the brown rat, *Rattus norvegicus* (Berkenhout, 1769) (Rodentia, Muridae). Annals of Carnegie Museum 86: 1–35.

Wible, J.R., G.W. Rougier, M.J. Novacek, and M.C. McKenna. 2001. Earliest eutherian ear region: a petrosal referred to *Prokennalestes* from the Early Cretaceous of Mongolia. American Museum Novitates 3322: 1–44.

Wible, J.R., G.W. Rougier, M.J. Novacek, and R.J. Asher. 2009. The eutherian mammal *Maelestes gobiensis* from the Late Cretaceous of Mongolia and the phylogeny of Cretaceous Eutheria. Bulletin of the American Museum of Natural History 327: 1–123.

Willemet, R. 2013. Reconsidering the evolution of brain, cognition, and behavior in birds and mammals. Frontiers in Psychology 4: 396.

Williamson, T. E., and S.G. Lucas. 1992. *Meniscotherium* (Mammalia, "Condylarthra") from the Paleocene-Eocene of western North America. Bulletin of the New Mexico Museum of Natural History and Science 1: 1–75.

Witmer, L.M., S.D. Sampson, and N. Solounias. 1999. The proboscis of tapirs (Mammalia: Perissodactyla): a case study in novel narial anatomy. Journal of Zoology 249: 249–267.

Woodburne, M.O., et al. 2014. Revised timing of the South American early Paleogene land mammal ages. Journal of South American Earth Sciences 54: 109–119.

Zancanaro, C. 2014. Vomeronasal organ: a short history of discovery and an account of development and morphology in the mouse. *In* C. Mucignat-Caretta (editor), Neurobiology of chemical communication. Boca Raton, FL: CRC/Taylor & Francis.

Zee, D.S., A. Yamazaki, P.H. Butler, and G. Gucer. 1981. Effects of ablation of flocculus and paraflocculus of eye movements in primate. Journal of Neurophysiology 46: 878–899.

Zeller, U. 1989. Die Entwicklung und Morphologie des Schädels von *Ornithorhynchus anatinus* (Mammalia: Prototheria: Monotremata). Abhandlungen der Senckenbergischen Naturforschenden Gesellschaft 545: 1–140.

Zenker, W., and S. Kubik. 1996. Brain cooling in humans—anatomical considerations. Anatomy and Embryology 193: 1–13.

Zilles, K., N. Palomero-Gallagher, and K. Amunts. 2013. Development of cortical folding during evolution and ontogeny. Trends in Neurosciences 36: 275–284.

Zollikofer, C.P.E., and J.D. Weissmann, 2008. A morphogenetic model of cranial pneumatization based on the invasive tissue hypothesis. Anatomical Record 291: 1446–1454.

APPENDIX 1

Glossary and Notes

This appendix provides brief definitions or additional characterizations of some of the principal features named in the main text, particularly those that have not been widely utilized in similar investigations in the past. It is not intended to be definitive. For additional definitions and information, see relevant papers cited in References (e.g., MacPhee, 1981; Mead and Fordyce, 2009; O'Leary, 2010; Wible and Gaudin, 2004; Wible, 2008; Muizon et al., 2015; Forasiepi et al., 2019). New names are noted where necessary, as are synonyms frequently encountered in the paleontological and comparative morphological literature. Names often come with or are embedded in associated hypotheses concerning structural change. In this paper we emphasize hypotheses developed from the known ontogeny of extant taxa and, where useful, we have made these explicit in the definitions listed below. More information on chondrocranial and osteocranial elements not separately defined can easily be found in classic compendia (e.g., De Beer, 1937). Where possible *NAV* names have been used except where indicated (e.g., non-*NAV* jugal bone rather than zygomatic bone).

Accessory lacunae of the transverse sinuses. As described in this paper, recognizably large network of venous channels associated with diploic marrow spaces of calvarium and draining to transverse sinuses and confluence of sinuses. Organization takes form of interlacing small channels draining to larger ones, but size and complexity in some taxa suggest functions beyond drainage of occipital diploe. Frequency not investigated here, but accessory lacunae surely have a wider representation among mammals than currently known (e.g., in *Homo*; Warwick and Williams, 1973: 693). Non-*NAV* term.

Aditus (foramen pneumaticum). Any narrow connector between continuous major pneumatic spaces, marking original sites of intense bone remodeling during ontogeny (e.g., in *Homo*, aditus of mastoid antrum, aditus of maxillary sinus;

see MacPhee, 1981). See also p. 65, Interpreting Pneumatization: Epitympanic Sinus, Extratympanic Sinus, and Other Pneumatic Spaces.

Alar canal (alisphenoid canal). In some mammals (e.g., extant perissodactylans), bony conduit for maxillary artery, perforating basicranial surface of alisphenoid. Typically, canal opens into sphenoorbital fissure, from which artery emerges on rear wall of orbit (Nickel et al., 1977: figs. 256, 282).

Auditory tube foramen/canal/incisure (canalis musculotubarius). When present as a distinct aperture, conducts auditory tube into tympanic cavity. Normally associated in placentals with cartilage of auditory tube, an independent cranial element mostly derived from mesoderm with a lesser component originating from neural crest (Anthwal and Thompson, 2016). If a foramen or other osseous feature is lacking, as is normally the case in abullate taxa, passageway for auditory tube may be marked by a groove in rostromedial angle of tympanic cavity (MacPhee, 1981: 48).

Auricular branch of vagus nerve. Somatic afferent nerve providing sensation to part of ear and related area of scalp. In *Homo*, "the vagus nerve emits its auricular branch… [which] runs laterally to reach the lateral wall of the jugular fossa and the entrance to the mastoid canaliculus, which transmits it. It crosses the facial nerve, running more or less laterally, then leaves the temporal bone…in company with the facial nerve" (Lang, 1983: 444). In many mammals, especially smaller taxa, auricular branch may travel superficially to stylomastoid foramen to meet CN 7, in which case a bony mastoid canaliculus will be lacking.

Basicapsular fenestra (fissura petrooccipitalis, basiotic fissure). Anatomy of this feature and its various named subdivisions can be best understood from an ontogenetic viewpoint. In fetal placentals, it is the initially continuous gap (ignoring transitory cartilaginous commissures) between ossifying auditory capsule, central stem components (basioccipital, basisphenoid, ala temporalis), and rostrolateral bones developing in

membrane (pterygoid, alisphenoid, squamosal). Caudal part of gap may remain as large dehiscence in osteocranium (e.g., in *Equus*, *NAV* "foramen lacerum posterius"), or it may narrow in relative width once ossification centers differentiate and expand, leaving only jugular area/jugular foramen. Similarly, rostral part of gap may be reduced or largely obliterated due to growth of petrosal and facing membrane bones. There are as a result many styles or degrees of closure seen in adults of different taxa. Distinguishing feature of *continuous* basicapsular fenestra is that it is *widely* open in adult stage, as opposed to cases in which only small gaps or sutures separate petrosal from circumjacent elements. Persistent rostral part of basicapsular fenestra between alisphenoid and petrosal is often designated by other terms, e.g., "piriform fenestra" (MacPhee, 1981; Wible and Shelley, 2020), "sphenotympanic fissure" (Gabbert, 2004), "foramen lacerum anterius" (in *Equus*, *NAV*), "lateral carotid fenestra" (Aplin, 1990). Non-*NAV* term.

Basilar artery. Formed ontogenetically by fusion of bilateral vertebral arteries beneath hindbrain; forms caudal section of circulus arteriosus (Warwick and Williams, 1973: 158).

Basilar plexus/sinus. From cavernous sinus, "connects [endocranially] the two inferior petrosal sinuses and communicates inferiorly with the internal vertebral venous plexus" (Moore, 1985: 867).

Canal X. In *Trigonostylops*, small aperture at base of paracondylar process. Function uncertain (fig. 26A).

Canal Y. In *Equus*, dorsally positioned conduit that transmits distal part of caudal meningeal artery (= arteria diploetica magna) or its anastomosis with cranioorbital branch of stapedial artery to rostral end of petrosal (figs. 40, 41).

Carotid spinous process of alisphenoid. In *Toxodon* and perhaps other notoungulates, prominence on trailing edge of alisphenoid that helps to sharply define incisura carotidis (fig. 29).

Carotid foramen/incisure (foramen caroticum, incisura carotidis). Aperture or notch transmitting internal carotid toward endocranium, where vessel (now as cerebral carotid)

joins circulus arteriosus. If internal carotid travels through two separate foramina on basicranium, as in extant primates, many carnivorans, and some other placentals (van der Klaauw, 1931), the one providing access to endocranium is rostral (or anterior) carotid foramen. The other—often, but not exclusively, found in taxa with completely ossified tympanic floors—is distinguished as caudal (or posterior) carotid foramen or incisure. Also, artery may travel rostrally within bullar wall, or pass through it into middle ear (MacPhee, 1981).

Cavernous sinus. "Occupies the intracranial surface of the basisphenoid bone, lying beneath and around the hypophysis, and medial to the trigeminal ganglion. It is derived from the medial segment of primary head vein and receives blood from ophthalmic veins and various duro-cerebral sinuses" (Aplin 1990: 95).

Cerebrospinal venous system. Consists of two interconnected venous networks draining brain (cerebral venous system, mainly dural sinuses) and spine (vertebral venous system, mainly plexuses associated with vertebral canal) (Batson, 1957; Nathoo et al., 2011). Continuity between networks achieved by means of emissary veins, linkages between temporal sinus and occipital vein. See Dural sinuses, Vertebral venous system.

Condylar emissary vein (condyloid sinus). "A vertebral vein (sinus condyloideus), connecting the sigmoid sinus to the vertebral venous plexus, is also a constant feature [of mammalian development] and frequently forms the main termination of the sigmoid sinus" (Butler, 1957: 53). Preferred to *NAV* term, v. emissaria canalis n. hypoglossi.

Condylar foramen. See Hypoglossal foramen.

Craniooccipital vein (rostral root of occipital vein). In *Equus*, formed by pterygoid/pharyngeal plexuses in combination with emissaries that anastomose beneath central stem, together joining or becoming rostral component of occipital vein (see Sisson and Grossman, 1953: 698, fn.). Possible homologs include (inferior) petrooccipi-

tal vein in *Homo* and other primates (Cartmill, 1975; MacPhee, 1981). See also Ventral petrosal sinus. Non-*NAV* term.

Cranioorbital sulcus/foramen (orbitotemporal sulcus; lateral cerebral sulcus). Channel for vein that "accompanies the anterior division of the ramus superior of the stapedial artery. It runs across the inner face of the squamosal and alisphenoid bones, and extends from the postglenoid foramen, posteriorly, to the cranio-orbital foramen, anteriorly…. [T]he cranio-orbital sinus communicates with the superior ophthalmic vein in the orbit in certain primates" (Diamond, 1992: 225). Rostral branch of stapedial ramus superior also supplies, or continues into orbit as, supraorbital artery (Cartmill and MacPhee, 1980; Diamond, 1992). Non-*NAV* term.

Craniopharyngeal canal. Midline aperture or blind pit in ventral surface of presphenoid in dry skull, not always present in adult. Developmentally, a remnant of "pathway traversed by Rathke's pouch as it grew upwards from the stomodeum to form the adenohypophysis" (Lang, 1983: 136). Non-*NAV* term.

Dorsal petrosal sinus (superior petrosal sinus). From transverse sinus, "runs forward in the tentorial fold and crosses [trigeminal] ganglion to join the cavernous sinus" (Butler, 1967: 50), thus linking caudodorsal and rostroventral arrays. May leave no clear impression on dry skull.

Dorsal sagittal sinus (superior sagittal sinus). Lies in convex dorsal border of falx cerebri; transmits venous cerebral blood to transverse sinuses and communicates with diploic and meningeal veins (Gardner et al., 1969: 625). In *Equus*, this sinus joins transverse sinus by passing through a foramen piercing ossified tentorium (see Sisson and Grossman, 1953; *NAV* Osteologia, fn. 16).

Dural sinuses. Venous channels formed between inner and outer layers of dura mater, roughly triangular in section and sheathed solely by endothelium. In addition to being valveless, dural sinuses lack capacity for physiological compliance because dural tissues are nondistensible (Warwick and Williams, 1973). Their extensive drainage fields include not only brain and diploe but also various soft tissues related to orbital adnexa, face, and deep portions of certain cranial muscles.

Emissary and diploic veins. See p. 33, Interpreting Vasculature: Veins, for definitions and descriptions. *NAV* lists 11 emissary veins, not all of which are significantly functional in different species. In rough order from caudal to rostral these are: Vv. emissaria mastoidea, occipitalis, canalis n. hypoglossi, foraminis jugularis, foraminis retroarticularis, canalis carotici, foraminis ovalis, foraminis laceri, foraminis rotundi, fissurae orbitalis, and foraminis orbitorotundi. There are others (e.g., transclival emissary veins) not included in this list, which is focused on conditions in domesticants. V. emissaria canalis n. hypoglossi is referred to here as V. emissaria condylaris (condylar emissary vein).

Entotympanics. Independent elements of tympanic floor, traditionally regarded as of two kinds (rostral and caudal) that usually arise in cartilage (see MacPhee, 1979, 1981; MacPhee and Novacek, 1993; Maier et al., 2013). Variably present as distinct bones in most major clades of placentals, but unknown in other therians. Among perissodactylans, entotympanics as independently developing entities have been securely identified in developmental stages of extant horses and rhinos but not tapirs (van Kampen, 1905; van der Klaauw 1931; MacPhee and Novacek, 1993; Maier et al., 2013; see also appendix 3). Entotympanics probably present in many SANU taxa but rarely recognized as such (e.g., *Cochilius*; see MacPhee, 2014). *Pars endotympanica* (*NAV* Osteologia, fn. 22) should not be regarded as an acceptable synonym for ontogenetically independent element.

Epitympanic and extratympanic sinuses. These air spaces pneumatize different parts of squamosal from different initiation areas (epitympanic recess vs. lateral border of tympanic cavity/external acoustic meatus) and for this reason are considered nonhomologous. In notoungulates, proterotheriid litopterns, and *Pyrotherium*, aditus of epitympanic sinus situated well within tympanic cavity, inflating caudal

portion of squamosal as in many other mammals. By contrast, in *Trigonostylops* and *Astrapotherium*, aditus of extratympanic sinus positioned within external acoustic meatus on caudal surface of retroarticular process (fig. 19). Size of extratympanic sinus can be accurately estimated for *Trigonostylops* because it was pneumatized from only one source are (tympanic cavity). Size in *Astrapotherium* is more difficult to assess because, as interpreted here, only part of retroarticular process was pneumatized from tympanic cavity; remainder pneumatized from nasal cavity via frontal sinus, with no bony indicia to mark limits of each source's activity. Note that term "epitympanic recess" has been applied historically to a variety of spaces with quite different topological positions. As employed in this paper, term refers strictly to "dorsal extension of tympanic cavity that lies above upper level of tympanic membrane; contains incudomalleolar articulation," in close proximity to vestibular fenestra (MacPhee, 1981: 53).

Ethmoidal foramen (ethmoid foramen). Foramen in dorsal part of medial orbital wall, for ethmoidal division of nasociliary nerve and associated vasculature. Apertures for persistent cranioorbital sinus and artery and frontal diploic vein occur in same region, complicating discrimination in dry skulls and fossils (e.g., Russell and Sigogneau, 1965; Wible and Rougier, 2017).

Foramen ovale/incisura ovalis. Transmits CN 5.3, emissary venous plexus of foramen ovale, and occasionally middle meningeal artery (or other vessels, e.g., arteria anastomotica in ruminants). See also Basicapsular fenestra.

Greater petrosal nerve. Communicating branch of CN 7 consisting chiefly of taste fibers distributed to mucous membrane of palate. Also contains preganglionic parasympathetic fibers destined for pterygopalatine ganglion. From its morphological origin at geniculate ganglion in cavum supracochleare, greater petrosal nerve passes through hiatus of facial canal runs beneath trigeminal ganglion, then meets and travels coaxially with sympathetic deep petrosal nerve (MacPhee, 1981: 55–56; Lang, 1983: 293).

Hyoid recess (vagina processi hyoidei). Walled depression immediately adjacent to stylomastoid foramen marking position of tympanohyal. Recess forms during ontogeny when petrosal alone, or in combination with ectotympanic and sometimes exoccipital, grows around tympanohyal to form a short tube or partial socket. In many SANUs recess is notably deep, suggesting that tympanohyal was large but remained persistently cartilaginous (and therefore fell away after death, leaving empty recess).

Hypoglossal foramen/canal. For CN 12 and associated vasculature (condylar emissary vein, condylar artery). Mammals may have one or several foramina for these structures (Forasiepi et al., 2019). Developmentally they are in evidence as soon as occipital arches chondrify early in cranial ontogeny (De Beer, 1937). When two such foramina are present, it is a common if arbitrary practice to describe one as the hypoglossal foramen (for CN 12) and the other as the condylar or condyloid foramen (for vasculature), but in many cases such a distinction cannot realistically be made (Lang, 1983). Medullary rootlets of CN 12 characteristically segregate into bundles, which in some taxa may leave developing skull through separate foramina in occipital arches, with or without accompanying vasculature. This organizational pattern reflects nerve's phylogenetic history: CN 12 is thought to be a composite of several primitive ventral root (somatic motor) nerves that for morphological purposes are considered to comprise a single entity, serially homologous with ventral (motor) roots of mixed spinal nerves. At least in the case of fossils, because of persistent confusion regarding whether a particular aperture is "condylar" (and thus considered mainly vascular) or "hypoglossal" (mainly neural), it is recommended that all such foramina be identified as "hypoglossal" unless there are firm grounds for inferring otherwise. However, condylar emissary vein should continue to be identified as such, to conform to general usage in comparative morphology. In fossils trackways for artery and vein cannot be distinguished.

Incisurae on rostral margin of basicapsular fenestra. In taxa of interest here, caudal edge of alisphenoid may be notched (not always distinctly) by incisures corresponding to routes of transiting vessels and nerves. (These components are not usually separately identifiable in fossils, but are mentioned here for completeness.) *NAV* terms for these features in extant euungulates, adopted here for SANUs, are: *incisura carotidis*, for internal carotid artery plus associated sympathetic nerve and venous plexuses; *incisura ovalis*, for mandibular nerve plus associated venous plexuses; and *incisura spinosa*, for middle meningeal artery (of maxillary artery) and vein, and recurrent meningeal branch of CN 5.3 (see Ellenberger and Baum, 1894: 98–99; Sisson and Grossman, 1953: 660). Positions of transiting structures may vary somewhat. In *Equus*, middle meningeal vein may pass more caudally, close to squamosal incisure for retroarticular vein (Ellenberger and Baum, 1908: 96, fig. 89; Nickel et al., 1977: fig. 241).

Infraorbital foramen. Typically but not always single in placentals; transmits CN 5.2 and associated vasculature (Sisson and Grossman, 1953; Evans and Christensen, 1979; Moore, 1981). Sensory and vascular targets include teeth, gums, upper lip, cheeks, and rostral part of snout.

Internal carotid artery. See p. 26, Interpreting Vasculature: Arteries.

Internal carotid nerve. Nerve, morphologically originating from cranial (or dorsal) cervical ganglion of sympathetic system and carrying postganglionic fibers to targets in head (e.g., lacrimal gland, nasal mucosa). Normally closely associated with preendocranial portion of internal carotid artery (MacPhee, 1981: 56). See also Pterygoid canal.

Internal jugular vein. In *Homo* largest vein of head, extending from sigmoid sinus to subclavian/brachiocephalic vein, and draining brain, superficial parts of face, and upper neck. Direct intracranial tributaries include ventral petrosal sinus and sigmoid sinus (Tubbs et al., 2020). However, its size and detailed relations vary in mammals; in horse, internal jugular may be absent or insignificant.

Jugular area/foramen/incisure of basicapsular fenestra. For CN 9, 10, 11, rostral end of sympathetic trunk, and internal jugular vein (last if functionally present in adult). Term "jugular area" is specifically intended for "featureless" cases, i.e., no discrete foramen or incisure for jugular vein and nerves separable from continuous basicapsular fenestra.

Lambdoidal process of petrosal. Caudal extension of petrosal mastoid, especially in SANUs, often forming part of floor of posttemporal foramen/canal, but rarely extending onto exterior of skull. See also character "wedge-shaped mastoid" defined by O'Leary (2010). Non-*NAV*.

Lateral head vein (vena capita lateralis). In mammalian embryos, lateral head vein becomes, for a time, principal means of draining head end (Butler, 1957, 1967), where it acts as primary rostral distributary of developing transverse sinus (Wible and Hopson, 1995). Known functional retention in adult stages of extant monotremes, some marsupials, and eulipotyphlan *Solenodon* (Wible, 2003, 2008; Wible and Hopson, 1995; Wible and Rougier, 2000; Sánchez-Villagra and Wible 2002; Rougier and Wible, 2006). Indicia for its existence in zhelestids (Ekdale et al., 2004) and *Prokennalestes* and *Maelestes* (Wible et al., 2001, 2009) have also been reported. For SANU example see figure 17B. Non-*NAV* term.

Lesser petrosal nerve. Nerve formed mainly by preganglionic parasympathetic fibers of tympanic nerve (relayed via tympanic plexus). Travels across tympanic roof, leaves through glaserian fissure or own foramen, lateral to position of auditory tube, and terminates in otic ganglion (MacPhee, 1981: 57; Warwick and Williams, 1973: 1018).

Mastoid emissary vein/foramen (v. emissaria mastoidea). "The emissary vein of the superior part of the occipito-capsular fissure is, in fact, a mastoid emissary vein and, in the adult skull, leaves via an irregular fissure bounded by the occipital and petrous temporal bones" (Butler,

1967: 48, referencing condition in lagomorphs). Present in prenatal stages of many investigated mammals, and retained in many species into adult stage as a link between caudal dural sinuses and occipital vein. Its origin normally lies close to transverse sinus/sigmoid sinus junction and it may drain either channel. Individual variation data exist only for *Homo* (see Lang, 1983; Louis et al., 2008; Tubbs et al., 2020) but other mammals probably similar. Not to be confused with mastoid canaliculus, for auricular branch of CN 10.

"Mastoid foramen" (of *Equus*). In equine anatomies, defined as aperture conducting caudal meningeal artery into endocranium. If as accepted here this artery is homolog of arteria diploetica magna, then foramen in horse should be called posttemporal foramen (q.v.) in conformity with usage in modern comparative anatomy, as well as to prevent confusion with mastoid emissary foramen (q.v.).

Middle meningeal artery. Blood supply to meninges may come from a variety of potential arterial sources not covered here (see Bugge, 1974; Wible, 1987). Ontogenetically, middle meningeal artery is a derivative of stapedial ramus superior (Tandler, 1899; but see Wible, 1987) and usually feeds meninges and related periosteal tissues. Rostral (= anterior) branch travels to orbit as cranioorbital artery; caudal (= posterior) branch becomes or anastomizes with arteria diploetica magna. Middle meningeal is frequently annexed by maxillary artery (e.g., in *Homo*), its original ontogenetic connection to proximal stapedial artery having been lost with latter's involution (Bugge, 1974; MacPhee and Cartmill, 1986; Wible and Shelley, 2020).

Parietosquamosal foramina/canals (foramina for rami temporales, squamoparietal foramina). Foramina of varying sizes piercing caudal sections of parietal and squamosal (and sometimes elsewhere) are found in many mammals (Cope, 1880). Limited dissection evidence indicates that parietosquamosal foramina transmit both veins (to transverse and temporal sinuses) and arteries (from meningeal branches) (Cart-mill and MacPhee, 1980; Wible, 2008). Physiological function of parietosquamosal veins uncertain, although given range of taxa possessing them there may be more than one such function. Non-*NAV* term.

Petromastoid canaliculus. In *Homo*, conducts parafloccular (= subarcuate) artery and vein to periantral mastoid cells. Simpson (1936: 22) saw a petromastoid canaliculus in *Old-fieldthomasia* AMNH VP-28600 but did not name it. Billet and Muizon (2013) identified this channel in a presumed notoungulate petrosal from Itaboraí. Present and very large in *Cochilius* (fig. 9: feature f). Non-*NAV* term.

Posttemporal canal/foramen (posttemporal trackway complex). For vasa diploetica magna (q.v.). In panperissodactylans, canal is situated where combinations of squamosal, petrosal mastoid, and exoccipital (rarely supraoccipital) form complex interdigitating sutures (see p. 119, Vascular Indicia: Venous Structures; see also Geisler and Luo, 1998; Wible and Gaudin, 2004). "Mastoid foramen" of *Equus* is synonymous but potentially misleading and should not be used (cf. Wible, 1987). Non-*NAV* term.

Prootic canal, tympanic aperture of (apertura tympanica canalis prootici). Prootic canal first described under that name by Gaupp (1908) in echidna *Tachyglossus aculeatus*, as tube running within petrosal from endocranial cavity to facial sulcus (more precisely, from prootic venous sinus within endocranium to aperture in roof of tympanic cavity where sinus joins lateral head vein). For conditions in *Cochilius*, in which this aperture has been detected, see p. 119, Discussion: Venous Structures.

Pterygoid canal, sulcus for nerve of. Nerve of pterygoid canal carries both sympathetic and parasympathetic fibers to a variety of targets in head (e.g., structures in orbit, glands) (MacPhee, 1981). Nerves that comprise it morphologically (deep petrosal and greater petrosal nerves) typically leave confines of tympanic cavity together, to enter sutural gap (pterygoid canal) between pterygoid and basisphenoid/presphenoid; sulci marking their course often present (see fig. 18).

Pterygoid plexuses (pterygoid/pharyngeal plexuses). As seen in *Equus*, large venous arrays situated alongside pharynx and paralleling basicapsular fenestra (see fig. 6). In horse, this complex morphologically terminates in cranio-occipital vein (see fig. 6).

Rete mirabile epidurale, arteria anastomotica, and ramus anastomoticus. Epidural retia and their components comprise a system of extracarotid arterial structures supplying brain in various mammalian groups. Among extant terrestrial and semiaquatic euungulates, presence apparently universal in nontragulid artiodactylans (Fukuta et al., 2007). Not found in any perissodactylans (but see Du Boulay, 1991, regarding apparent rete in *Diceros bicornis*). Artiodactylan version consists of complex networks of small, intertwined, thin-walled arteries situated in cavernous sinus on either side of hypophysis, where they join cerebral carotid. Cerebral carotid and epidural retia are fed by anastomotic branches, often multiple, from maxillary artery; these vessels travel through sphenoorbital fissure (arteriae anastomoticae) or foramen ovale (rami anastomotici) or both (Daniel et al., 1953). In taxa possessing these structures, preendocranial portion of internal carotid often undergoes complete involution, having been functionally supplanted during development by external carotid and related retial anastomoses (O'Brien, 2017; for possible physiological functions of various retial arrangements, see Jessen et al., 1994; Caputa, 2004; O'Brien, 2017). Cetaceans may also possess a caudal arterial rete located either rostral to foramen magnum on cranial floor or in vertebral canal at level of atlas. Arterial feed in this case is from vertebral and occipital arteries (Geisler and Luo, 1998).

Retroarticular emissary vein (postglenoid vein; capsuloparietal emissary vein). Vein connecting temporal sinus to external jugular vein (or its tributaries). See Wible and Hopson (1995) and Wible and Gaudin (2004) for discussions of homology in different eutherians.

Retroarticular foramen/canal/incisure (postglenoid foramen). Outlet for retroarticular emissary vein, normally situated within squamosal, or in suture between latter and petrosal or ectotympanic.

Retroarticular process (postglenoid process; retromandibular process). Eminence on squamosal that clasps head of mandible.

Secondary facial foramen, facial sulcus, and stylomastoid foramen. An aperture-groove-aperture complex by means of which CN 7 morphologically enters, crosses, and finally exits tympanic cavity to enter neck. If exit-point is an incisure or gap between tympanohyal and ectotympanic/petrosal, a foramen stylomastoideum primitivum is distinguished. If bone territories form a complete orifice, a foramen stylomastoideum (definitivum) is identified (MacPhee, 1981: 63).

Sigmoid sinus. "The sigmoid sinus … runs behind the petrous temporal bone and receives the occipital sinus. It then divides into a vein [joining the vertebral vein] and a terminal sigmoid sinus which joins the inferior petrosal sinus" (Butler, 1967: 50, referencing *Erinaceus*). In older equine anatomies, sigmoid sinus is often identified as "occipital sinus" (e.g., Bradley, 1923: 144), but these sinuses are morphologically distinct and this usage is therefore confusing.

Sinus communicans. In *Equus*, the "two [transverse] sinuses are connected by the sinus communicans, which extends across the cranial vault in a channel at or in the base of the internal occipital protuberance" (Sisson and Grossman, 1953: 701; see also Nickel et al., 1977: fig. 284). Functionally same as confluence of sinuses in *Homo*, but presence of a bony channel (rarely or never seen in humans) should be regarded as a separate indicium because of its relationship with accessory lacunae of the transverse sinus (q.v.). Similar feature described for *Mendozahippus* by Martínez et al. (2020).

Sphenoorbital fissure (foramen orbitale). Transmits trunks or divisions of CN 3–6 (excepting CN 5.3) plus infraorbital artery, ophthalmic vein, and other structures. Separate foramen rotundum, for CN 5.2, often appears during development within ala temporalis of chondrocranium (De Beer, 1937), but foramen may be

present in osteocranium whether or not there is a chondrocranial precursor (Moore, 1981).

Stapedial ramus superior, foramen for. Aperture on tympanic roof to permit exit of stapedial ramus superior into endocranium. Not to be confused, especially in fossils, with epitympanic recess or tympanic aperture of prootic canal (q.v.).

Tegmen tympani. In placentals, process of petrosal, sometimes large, that springs from rostrolateral section of pars canalicularis of auditory capsule to form part of tympanic roof. Root of tegmen is characteristically crossed by facial sulcus (De Beer, 1929: 418).

Temporal canal/sinus (petrosquamous sinus, posterolateral venous sinus, prootic canal in part). When present, extends rostrally from transverse sinus as a canal or prominent sulcus in squamosal, to terminate in retroarticular foramen (*Equus*; see Ellenberger and Baum, 1894: 183; Nickel at al., 1977: fig. 284). Also communicates with parietosquamosal, cranioorbital, and retroarticular canals when present. Homologies of temporal sinus are complicated by fact that veins that depart retroarticular foramen of marsupials and placentals appear to have different origins (Wible et al., 2001: 19; see also Ekdale et al., 2004; Rougier and Wible, 2006). Other synonyms of temporal sinus, in whole or in part, include "dorsal cerebral vein" (Sisson and Grossman, 1953: 698), "*confluent pariéto-temporal*" (Montané and Bourdelle, 1913), and Simpson's (1936: 27) term "quadrate sinus."

Tensor tympani fossa. For tensor tympani muscle, which originates in *Homo* from dorsal wall of tympanic cavity (tensor tympani canal) and cartilage of auditory tube, and inserts onto muscular process of malleus. A fossa for this muscle is frequently identified in dry skulls where tegmen tympani meets promontorium (see van der Klaauw, 1931; MacPhee, 1981). According to some veterinary anatomies, muscle is often very small and without a petrosal origin in domestic ungulates (Sisson and Grossman, 1953), although for horse this observation is not correct (see Blanke et al., 2014).

Transverse sinus(es) (posterolateral venous sinuses). Right and left transverse sinuses, draining cerebral hemispheres, exist in all mammals (Edinger, 1929). In *Canis*, each transverse sinus "begins mid-dorsally by receiving the sagittal and occasionally the straight sinus, and merges with its fellow to form the confluence of the sinuses…located within the dorsal part of the occipital bone [and] terminates at the distal end…by dividing into the temporal and sigmoid sinuses" (Evans and Christensen, 1979: 791–793). In panperissodactylans and perhaps other mammals, transverse sinus may be connected to a network of ancillary spaces within diploe (see Accessory lacunae of the transverse sinuses). Other frequently seen direct connections of transverse sinuses include parietosquamosal veins and vena diploetica magna.

Tympanic nerve. Branch of CN 9 containing preganglionic parasympathetic fibers, entering middle ear through tympanic canaliculus in rear of tympanic cavity. Morphologically terminates in tympanic plexus (sometimes detectable as a series of fine radiating grooves on promontorium). Its fibers are then relayed by lesser petrosal nerve, synapsing in otic ganglion (MacPhee, 1981: 65).

Tympanohyal (tympanohyoideum). In fetus, cranialmost element forming in Reichert's cartilage in continuity with crista parotica of cartilaginous auditory capsule. Usually by late fetal life indistinguishably fused with, or ossifying from, petrosal [see De Beer, 1937: 372], but may also remain partly or wholly cartilaginous. With stylohyal (independent element immediately distal to it) forms hyoid process of adult anatomy.

Vasa diploetica magna. Here used to refer to both arteria and vena diploetica magna (vasa, L. "vessels"). As defined by Tandler (1899), arteria diploetica magna is an anastomotic link between occipital artery and caudal branch of stapedial ramus superior, supplying (depending on taxon) cranioorbital artery, parietosquamosal arteries, branches to dura mater, and others (see Hyrtl, 1854; Wible, 1984, 1987; Harper and Rougier, 2019). Wible (1987) defines arteria diploetica magna as an inherent part of stapedial system,

but morphologically it is better understood as a link with the latter and the occipital artery (or posterior auricular artery in some cases). When present, vena diploetica magna likewise serves as a link from transverse sinus/sigmoid sinus to occipital vein, posterior auricular vein, or vertebral plexuses (which are themselves often linked by additional anastomoses). See also Mastoid emissary vein. Non-*NAV* terms.

Vein of temporal meatus. Proposed name for venous channel between temporal sinus and superficial temporal vein in *Equus* exiting skull through temporal meatus. This vessel is sometimes called "dorsal cerebral vein" in older equine anatomies (e.g., Ellenberger and Baum, 1908: 746, fig. 693), but a replacement is needed as this is a now defunct synonym for a branch of the temporal sinus per se (which in any case does not leave skull at this point, but continues rostrally to release or become retroarticular emissary vein). In *Homo* it is described as "temporal emissary vein," a ?rare connection between remnant of cranioorbital sinus and deep temporal vein (Tubbs et al., 2020: 180). Non-*NAV* term.

Ventral petrosal sinus (inferior petrosal sinus, inferior cerebral vein, internal cerebral vein). As defined here, an explicitly endocranial dural sinus running from cavernous sinus to jugular area on either side of central stem. Terminates by discharging into one or more of sigmoid sinus, internal jugular vein, condylar vein, and/or suboccipital plexuses. In some mammals, sinus is enclosed within a bony gutter between petrosal and basisphenoid/basioccipital (e.g., *Homo*, other anthropoid primates; Saban, 1963). In horse, which exhibits a continuous basicapsular fenestra, there is no gutter. Instead, ventral petrosal sinus is simply "enclosed in the thick dura which closes the foramen lacerum" (Sisson and Grossman (1953: 701) and drains via emissaries to large pterygoid/pharyngeal plexus and craniooccipital vein situated beneath basicranium. Ventral petrosal sinus and its distributaries are obviously more extensive in some taxa than others (Wible and Rougier, 2000).

Vertebral artery. "A. vertebralis in the horse is considered to continue through the Fossa atlantis, anastomosing with the A. occipitalis. It then turns dorsally through the For. alare and enters the vertebral canal. Right and left vertebral arteries join to form A. basilaris" (*NAV* Angiologia, fn. 24). This arrangement is probably typical for therians; anastomosis with occipital artery does not normally leave an osteological marking.

Vertebral vein. In *Homo*, usually a "plexus of veins which accompanies the vertebral artery through the vertebral foramina. [It] communicates above [i.e., endocranially] with the suboccipital venous plexus, the inferior petrosal sinus, the jugular vein and numerous other venous channels [including the] cavernous sinus and … the inferior condylar vein" (Lang, 1983: 328). Osteological indicia often weak or absent, but a reliable indicium caudal to "confluence of the inferior petrosal and [sigmoid] sinuses is a groove, which houses the vertebral vein, and continues caudad through the lateral corner of the foramen magnum" where it joins endocranial aperture of hypoglossal canal (e.g., in *Ailuropoda*; Davis, 1964: 59).

Vertebral venous system. Part of larger cerebrospinal venous system (q.v.), consisting of "plexuses of thin-walled veins that…communicate above with the intracranial veins and below with the portal system" (Gardner et al., 1969: 346). In *Homo*, "the vertebral venous plexus is involved in regulating intracranial pressure, transmitting the influence of the respiratory and cardiac pressures to the intracranial compartment and equalizing the pressures within the venous system" (Arnautovic et al., 1997). Like dural sinuses, components of this system uniformly lack valves. Hemodynamically, valvelessness potentially permits bidirectional flow of venous blood, which in turn provides an essential basis for homeostatic regulation of cerebral circulation (Epstein et al., 1970). However, among mammals generally, physiological significance of valveless flow is likely to include other functions beyond regulation of intracranial blood volume during postural movements, such as control of brain temperature (Zenker and Kubik, 1996).

APPENDIX 2

Entotympanics, Vasculature, and Other
Features of the Caudal Cranium
of Extant Perissodactylans

These notes amplify some of the descriptions of the caudal crania of extant perissodactyls provided elsewhere in this paper, but are not meant to be comprehensive treatments. For additional details on basicranial anatomy in a variety of extant and extinct euungulates, see O'Leary (2010).

Indian rhinoceros,
Rhinoceros unicornis AMNH M-274636

Apart from incidental observations by van Kampen (1905) and van der Klaauw (1931), there appear to be no investigations of the development of the auditory region in perinatal stages of extant rhinos. The notes in this section are mostly based on conditions in AMNH M-274636, a very young animal with open sutures (figs. 23, 35). Although its age at death is not recorded in museum records, none of its teeth are fully erupted and the ones that are partially emergent are completely unworn, suggesting the animal was either in the womb or subsisting on mother's milk at the time of death. At some point the skull cap of the specimen was removed in order to expose the endocranium and the caudal part of the nasal cavity and ethmoidal air cells. Fortunately, the basicranium was not dissected, with the result that not only are the ectotympanic and auditory ossicles intact and in life position, so is the rostral entotympanic (identified as such by virtue of its position).

Rostral entotympanic. This element, composed of a shell of thin, compact bone housing a cancellous core, is texturally quite different from the adjacent ectotympanic and petrosal. Complex in form, it may be described as consisting of two processes, one ventral and the other dorsal, joined by a narrow neck (fig. 35A, B). The ventral process lies against the rostral part of the promontorium but is not fused to it. It is deeply scalloped on its medial and lateral sides by sulci for the internal carotid artery and mandibular nerve, the partition between the two pointing rostrally and slightly ventrally. The arterial sulcus is ventrally visible, but the sulcus for the mandibular nerve is better seen from above. The entotympanic's dorsal process is obscured by other structures in ventral view, but in segments it can be seen that the process passes through the rostral or piriform part of the basicapsular fenestra, thus participating in the composition of the endocranium where it forms sutures with both the petrosal and squamosal (fig. 35C). In this way the entotympanic contributes to the tympanic roof, an uncommon but not unique feature (MacPhee, 1981). According to van Kampen (1905), in rhinos the entotympanic may fuse with both the promontorium and tegmen tympani.

The entotympanic has a very irregular surface, perforated by tiny foramina on its tympanic side with a small contact area for the rostral crus of the ectotympanic. Together with the adjacent part of the promontorium, the entotympanic forms a short semicanal that probably acted as a channel for the auditory tube (not visible in the figure) and perhaps the tensor veli palatini muscle. In taxa possessing the rostral entotympanic, a close ontogenetic relationship with the tubal cartilage—often including primordial continuity—is almost always present (see van der Klaauw, 1922, 1931; MacPhee, 1979; Maier et al., 2013). Modification of gene expression in mice strains has now established that the tubal cartilage has a dual origin (mesoderm and neural crest; see references cited by Anthwal and Thompson, 2016). It would be of interest to know whether the neural crest is associated with entotympanic development, as it is in the case of the auditory ossicles.

In this specimen carotid incisurae are not evident, but in some rhino species or individuals such notches may be fairly prominent on the trailing edge of the alisphenoid (Cave, 1959). By virtue of its position, the relatively large entotympanic would have kept the internal carotid artery well away from the promontorium, explaining why a carotid sulcus is lacking on the latter.

In *Ceratotherium simum* AMNH M-51882, a juvenile (most sutures open, third molar not erupted, second molar partially erupted), the (rostral) entotympanic has a similar, rather amorphous form, with a shallow sulcus for the internal carotid artery. It appears to be already fused to the promontorium at this stage of development. The ectotympanic (fig. 36A) is preserved on the right side; it has a complicated shape, with excavations on its medial and lateral surfaces that may have conducted the auditory tube and the tendon of the tensor tympani, although this is not certain These elements seem to be at least partly fused to the petrosal in this specimen.

?CAUDAL ENTOTYMPANIC. Tiny tablike ossifications, facing on the basicapsular fenestra, occur at various positions along the medial aspect of both petrosals in the *Rhinoceros* specimen (fig. 36C: white asterisks). They are obviously not derived from the ossification of the petrosal because they are not continuous with it. Most are flat rather than nodular, perhaps indicating an origin within membrane continuous with the fibrous membrane of the tympanic cavity (see MacPhee, 1981). Because there is already a notably large, rostrally positioned rostral entotympanic in *Rhinoceros*, the homological value of these exostoses is uncertain. They could signal the presence of another developing entotympanic, but a more diffuse process seems likely, in which bone spicules differentiate ectopically within dense connective tissue. Similar exostoses occur in the same areas in the donkey *Equus asinus* AMNH M-204141 and the Sumatran rhinoceros *Dicerorhinus sumatrensis* AMNH M-81892, both adult, and they may therefore be a general feature of auditory region development in certain perissodactylans (see also similar structures in the armadillo *Dasypus* [Wible, 2010]).

Asian tapir, *Tapirus indicus* AMNH M-77875

?ROSTRAL ENTOTYMPANIC. A prominent bony nodule, here identified as the articular process of the tegmen tympani, occurs in this juvenile specimen (erupted cheekteeth are deciduous) in much the same place as the dorsal process of the entotympanic found in young *Rhinoceros unicornis* (fig. 38A). In an adult specimen of *Tapirus indicus*, AMNH M-130108, the nodule is unquestionably continuous with the petrosal, with no suggestion of a separate origin (fig. 38B). An adult of the species *T. terrestris*, AMNH M-77576 (fig. 38A), exhibits the same feature. In *T. indicus* AMNH M-200300 the process' ventral surface exhibits a flat, downward-facing surface with an articular facet for the ectotympanic (fig. 38D, E). The astrapothere *Scaglia kraglievichorum* MMP M 207 has an eminence on the rostrolateral end of the tegmen that is also pillarlike. O'Leary (2010) identified a somewhat similar outgrowth in artiodactylans as the anterior process of the tegmen.

While there is certainly positional and shape similarity between the developmentally ambiguous articular process of *Tapirus* and the definite entotympanic of *Rhinoceros*, a proper ontogenetic investigation will be required to settle the process's origin. Van Kampen (1905) did not find an entotympanic in the material of *Tapirus* available to him, but wondered whether one was regularly present but so loosely attached that it always fell away during preparation. Van der Klaauw (1931) interpreted comments by Parker (1882) as indicating the existence of an entotympanic cartilage in a fetus of *T. indicus*, although given that the cartilage of the auditory tube would have differentiated in the same area this cannot be regarded as conclusive. Moyano and Giannini (2017) did not specifically discuss the entotympanic, but as their study is based on numerous specimens it is likely that a separate element was never encountered in the tympanic region. For the present entotympanic presence in tapirs must remain undetermined.

OTHER FEATURES. Unlike young *Rhinoceros*, there are no lamellar spicules bridging the basicapsular fenestra on this specimen (fig. 38A, B). However, this might simply be due to more vigorous cleaning during osteological preparation, because such spicules are present in *Tapirus indicus* AMNH

M-130108 (although not seen in the segment illustrated in fig. 38A). Once again these minor outgrowths do not give the impression of an organized ossification comparable to an entotympanic. There is a fossa in the place usually identified as the origin of the tensor tympani muscle (**C130, 132**).

Most tapir specimens investigated for this study display a short and very weak longitudinal depression, set at various angles, on the ventral surface of the promontorium (fig. 37A). In most circumstances this would be counted as an inadequate basis for identifying a sulcus for the internal carotid artery (see Boyer et al., 2016). However, in *T. terrestris* AMNH M-77576 there is an incomplete ring-shaped process—essentially a very abbreviated tube—that is positioned in the same place on the promontorium as the depression just noted and which surely marks the artery's passage (fig. 38A; see also p. 114). The process was present only on the right side of AMNH M-77576, and no similar feature was encountered on other tapir specimens. This is a good example of a situation in which internal carotid presence might be doubted or overlooked because most specimens lack strong promontorial indicia (see table 6, IC6).

Domestic horse,
Equus caballus AMNH M-204155

Most of the cranial features of adult *Equus caballus* relevant to this study have been adequately covered in the main text, but a few additional points are worth making here. With respect to the auditory region, Maier et al. (2013) have definitively established that the (rostral) entotympanic participates in the composition of the bony tympanic floor of the horse, developing endochondrally and forming much of the medial part of the bulla. This was not previously known for certain, and adds another item to the moderate amount of morphological variety seen in perissodactylan auditory regions (see below). Ectotympanic-entotympanic fusion normally happens early in perinatal life in *Equus*; in the juvenile AMNH M-204155 illustrated in figure 39B, the ectotympanic/entotympanic suture is already obliterated.

With regard to cranial vasculature, Tandler (1899: 697) observed that, in a fresh horse cadaver, the internal carotid artery reached (*angelangt*) the rostral pole of the promontorium, then crossed the dorsal surface of an independent piece of "fibrocartilage" in the basicapsular fenestra before entering the endocranium. Tandler's (1899) fibrocartilage is not otherwise identified. It may have been the developing entotympanic rather than the cartilage of the auditory tube, but in the adult there is no distinct impression for the artery on the entotympanic or the adjacent ventromedial exposure of the petrosal. Nevertheless, a pattern of slight carotid/promontorial contact may be general for perinatal perissodactylans, with differences in adult morphology being due to basicranial growth trajectories or the interposition of the entotympanic if formed.

Morphological notes provided by equine anatomies on the caudal meningeal artery/arteria diploetica magna are insufficiently detailed to permit tracing the course and relations of this vessel on dry skulls. Using indicia, we traced the inferred routes of the artery and related veins in a series of closely spaced transverse segments through the caudal cranium of *E. caballus* AMNH M-204155 (fig. 40 A–E; for approximate locations of slices, see fig. 39A). As an aid to visualization we superimposed reconstructed pathways on a detached petrosal of *E. asinus* in near-dorsal view (fig. 41). Although corroboration by dissection is still needed, essential vascular relations may summarized as follows:

On the lateral aspect of the exposed petrosal mastoid, the occipital artery would have traveled rostrally in a deep sulcus (fig. 40A, B) toward the foramen that conducts its main branch, the arteria diploetica magna (= caudal meningeal artery) into the skull (Tandler, 1899; Sisson and Grossman, 1953). The sulcus on the petrosal is roofed by the squamosal, which creates a canal not only for the artery but also for the more dorsally positioned temporal sinus (fig. 40C, 41). It can be seen that, although physically close together, the trackways of these two vessels remain separate and distinct. The first part of the track for the artery is by definition the posttemporal sulcus/canal. However, about
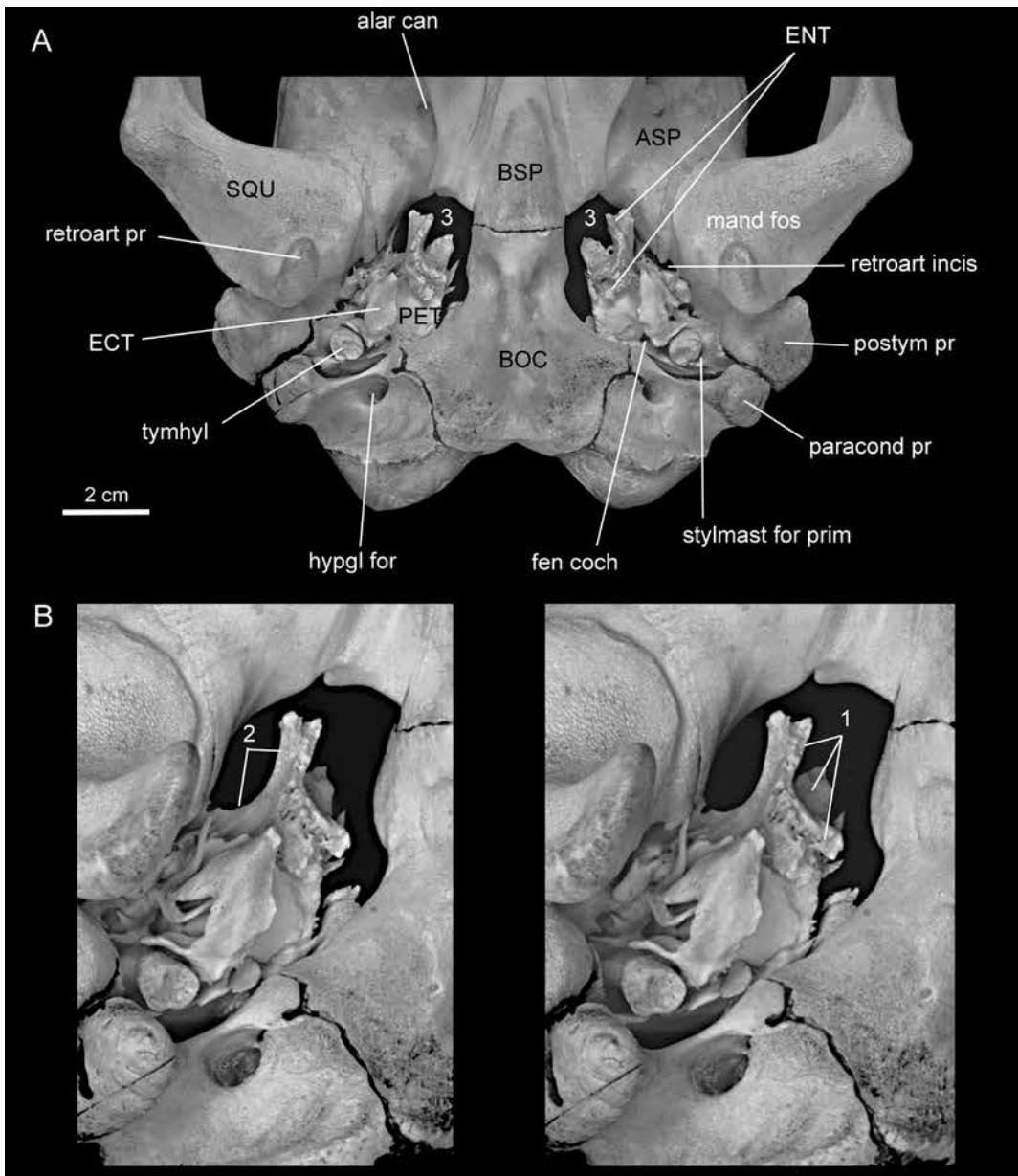
FIG. 35. *Rhinoceros unicornis* AMNH M-274636, perinatal specimen. **A,** general view of caudal cranium, ventral aspect; **B,** right auditory region, oblique ventrolateral view (stereopair); **C,** right auditory region, oblique dorsolateral view (skull cap removed, cut edge indicated by hachure); **D,** aspect as in C, but viewed from slightly different vantage point in order to view entotympanic sulci (stereopair). In ventral views (A, B), note deep grooves on medial and lateral sides of ventral process of entotympanic for accommodation of internal carotid artery (**1**) and mandibular nerve (**2**), as well as incisures (**3**) on alisphenoid's ventral margin (facing basicapsular fenestra). Route of internal carotid is best described as extratympanic, because it grooves rather than tunnels through entotympanic and does not actually touch promontorium. In dorsal views C and D, plane of slice passes through sulci for posttemporal and temporal vasculature, obscuring their relationship. Note entotympanic's dorsal process (**4**) projecting between squamosal and petrosal, to form a small part of endocranial floor. Rostromedially there is a weak depression, probably for cerebral carotid artery (**5**), adjacent
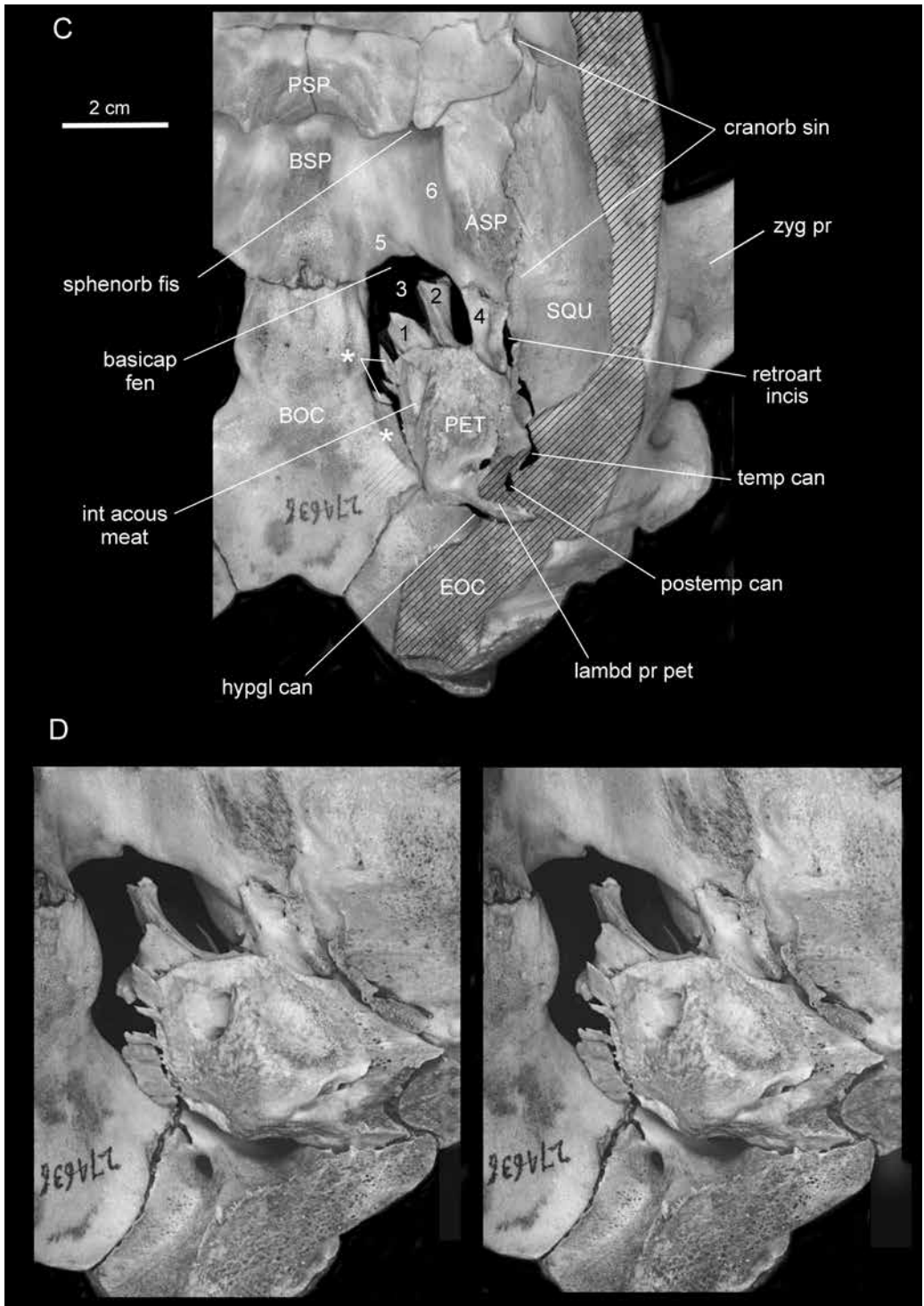
to much wider and deeper trough for trunks of CN 5.1 and 5.2 (**6**). Small lamellae (**asterisks**) attached to but not continuous with petrosal project over basicapsular fenestra. These bony growths are best viewed as adventitious ossifications within dural tissues, but are unexpected in a perinatal specimen.
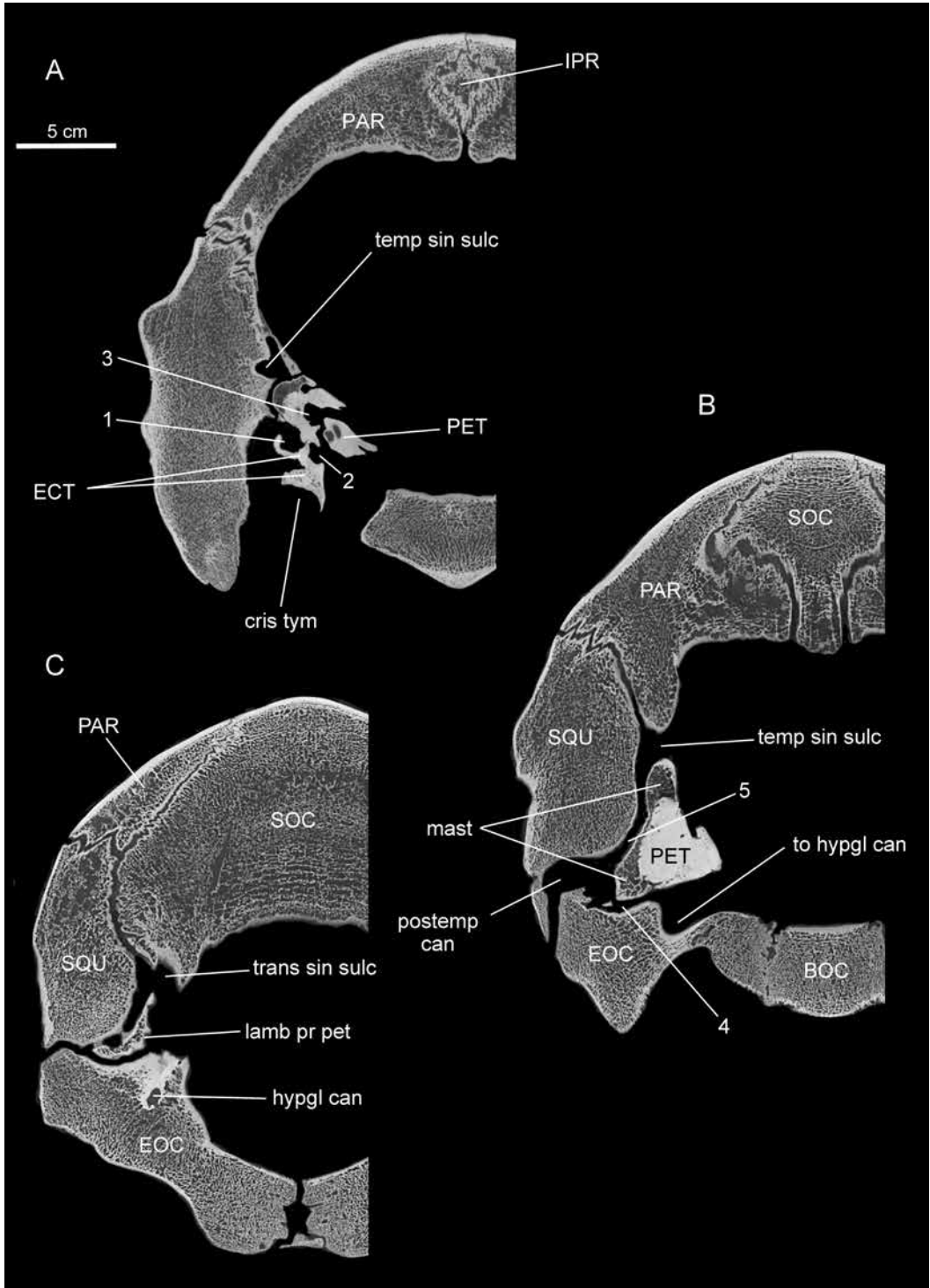
halfway across the dorsal surface of the petrosal the trackway for the arterial sulcus turns abruptly medially and enters a separate canal (canal Y) within the substance of the petrosal. Although canal Y and the trackway crossing the dorsal aspect of the petrosal are not specifically mentioned or illustrated in equine anatomies (e.g., Sisson and Grossman, 1953), these osteological features are consistent with conditions in other taxa (see Wible, 1984, 2010). In the illustrated specimens canal Y is formed exclusively by the petrosal (figs. 40D, E; 41), but petrosquamosal fusion occurs in equines in this area and in some individuals squamosal material probably participates in bounding the canal (as in *Dasypus*; Wible, 2010). After a brief transit canal Y opens into a large cleft in the rostromedial corner of the petrosal, where it terminates.

We distinguish canal Y morphologically from the trackway for the arteria diploetica magna because the former's lumen is somewhat smaller than that of the arterial trunk (as judged by the width of the its sulcus on the petrosal). Apparent reduction is surprising given that there is no published evidence that the artery releases distributaries along the way (but see p. 35, Arteria Diploetica Magna). Whether the inferred artery transmitted by canal Y in *E. caballus* AMNH M-204155 would have been derived (in an ontogenetic sense) primarily from the original arteria diploetica magna or from the caudal branch of the ramus superior of the stapedial artery cannot be decided by inspection. Although conditions in *Dasypus* suggest the former possibility according to Wible (2010), the latter should not be excluded given the sharp angle at which canal Y leaves its parent sulcus and its placement directly over the tympanic cavity (fig. 40D). There is no exit foramen in the tegmen tympani for the trunk of the (intratympanic) ramus superior, indicating, as expected, that this part of the stapedial system was aborted during ontogeny. However, the tegmen's position should roughly mark where the caudal branch of the ramus superior would have departed from the latter's trunk to join the arteria diploetica magna. The vessel transiting canal Y joins (or becomes) the cranioorbital artery no later than the point of its departure into the middle cranial fossa.

As noted previously the equivalent of a vena diploetica magna is absent in the horse. It is not impossible that a vein might pass through canal Y in company with the artery, as speculatively suggested in fig. 41 (dashed line). In this scenario there is no role for a branch of the occipital vein. Nor can the vein of the temporal meatus be regarded as a massively displaced equivalent of the vena diploetica magna of *Dasypus*, as its aperture penetrates the parietal or parietosquamosal suture within the confines of the temporal fossa.

The sequence of segments illustrated for *Equus caballus* AMNH M-204155 in figure 40A–E should be compared to the roughly similar series for *Tetramerorhinus lucarius* AMNH VP-9245 (fig. 40F–I). There are important differences in detail: in the litoptern no deep groove suggestive of a separate arterial trackway exists on the lateral face of the petrosal mastoid, nor is there any evidence of an equivalent to canal Y. This is of course merely negative evidence for the absence of a robust arteria diploetica magna, but it is consistent with similarly negative conditions in other examined SANUs.

FIG. 36. *Ceratotherium simum* AMNH M-51882, juvenile specimen, coronal segments. **A,** rostral portion of tympanic cavity (caudal to position of entotympanic, which is not visible here), showing ectotympanic and promontorium; **B,** caudal portion of petrosal, with posttemporal foramen and entrance to posttemporal canal; **C,** caudal end of petrosal, with lambdoidal process of petrosal. Observations on vascular morphology lacking for this species, so all identifications are inferential. **Key: 1,** ectotympanic sulcus for tensor tympani muscle; **2,** ectotympanic sulcus for auditory tube and its cartilage; **3,** cavum supracochleare for geniculate ganglion of CN 7; **4,** descending sulcus from posttemporal canal passing between petrosal and exoccipital, presumably connected to hypoglossal foramen or sigmoid sinus; **5,** ascending sulcus from posttemporal canal passing between squamosal and petrosal toward sulcus for transverse sinus. In A, B, sulcus for temporal sinus is assumed to have been venous, but could have also transmitted arteria diploetica magna (= caudal meningeal artery of *Equus*). In C, note lambdoidal process of petrosal.
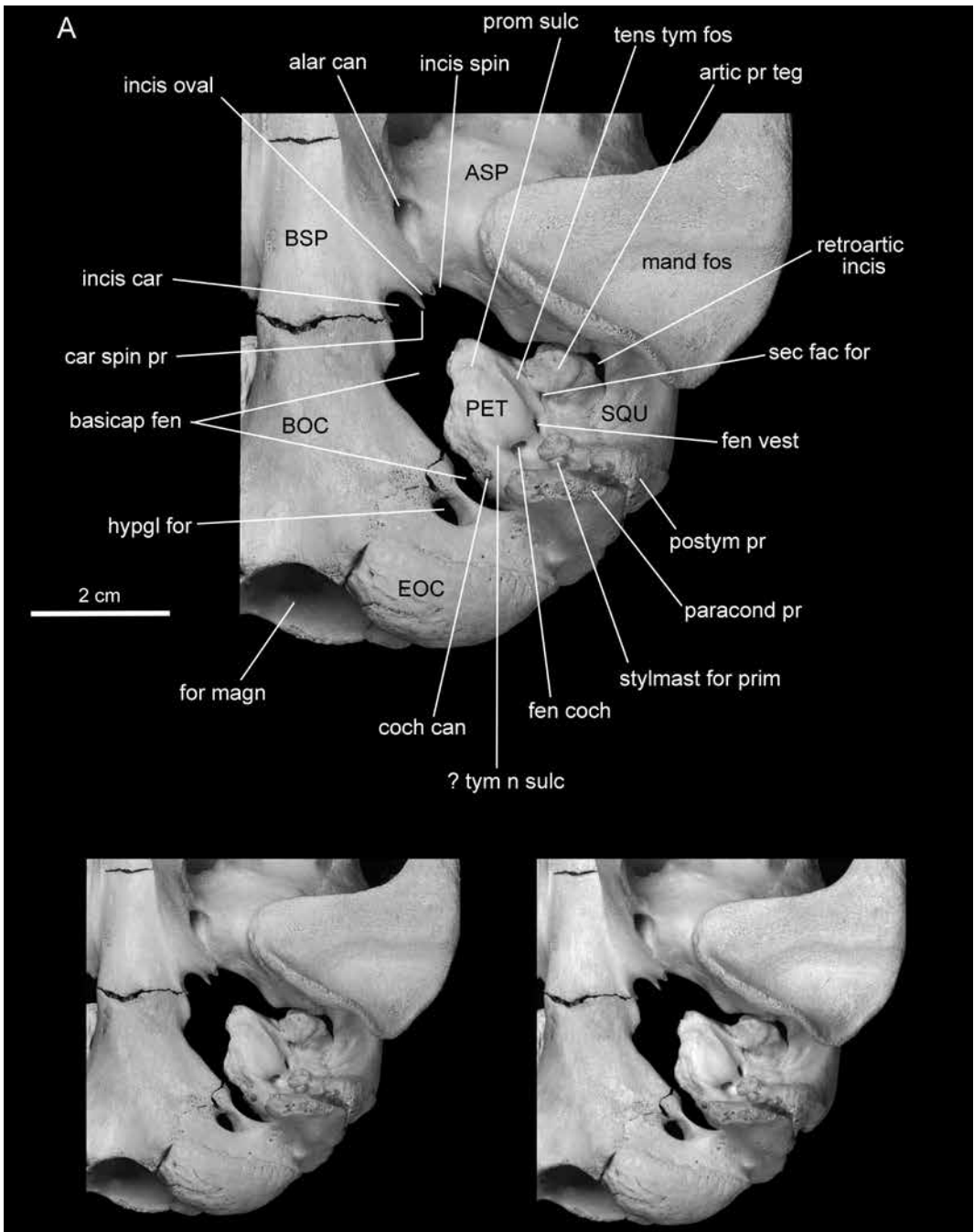
FIG. 37. *Tapirus indicus* AMNH M-77875, juvenile specimen. Left caudal cranium in oblique **A,** ventral and **B**, dorsal views, on facing pages with accompanying stereopairs. In B, endocranial sulcus (**1**) rostral to carotid incisure resembles that of *Equus*, which houses cavernous sinus and S-shaped loop of cerebral carotid before latter pierces dura mater (Bradley, 1923, p. 145; see also fig. 5); a second vascular sulcus (**2**) is situated where
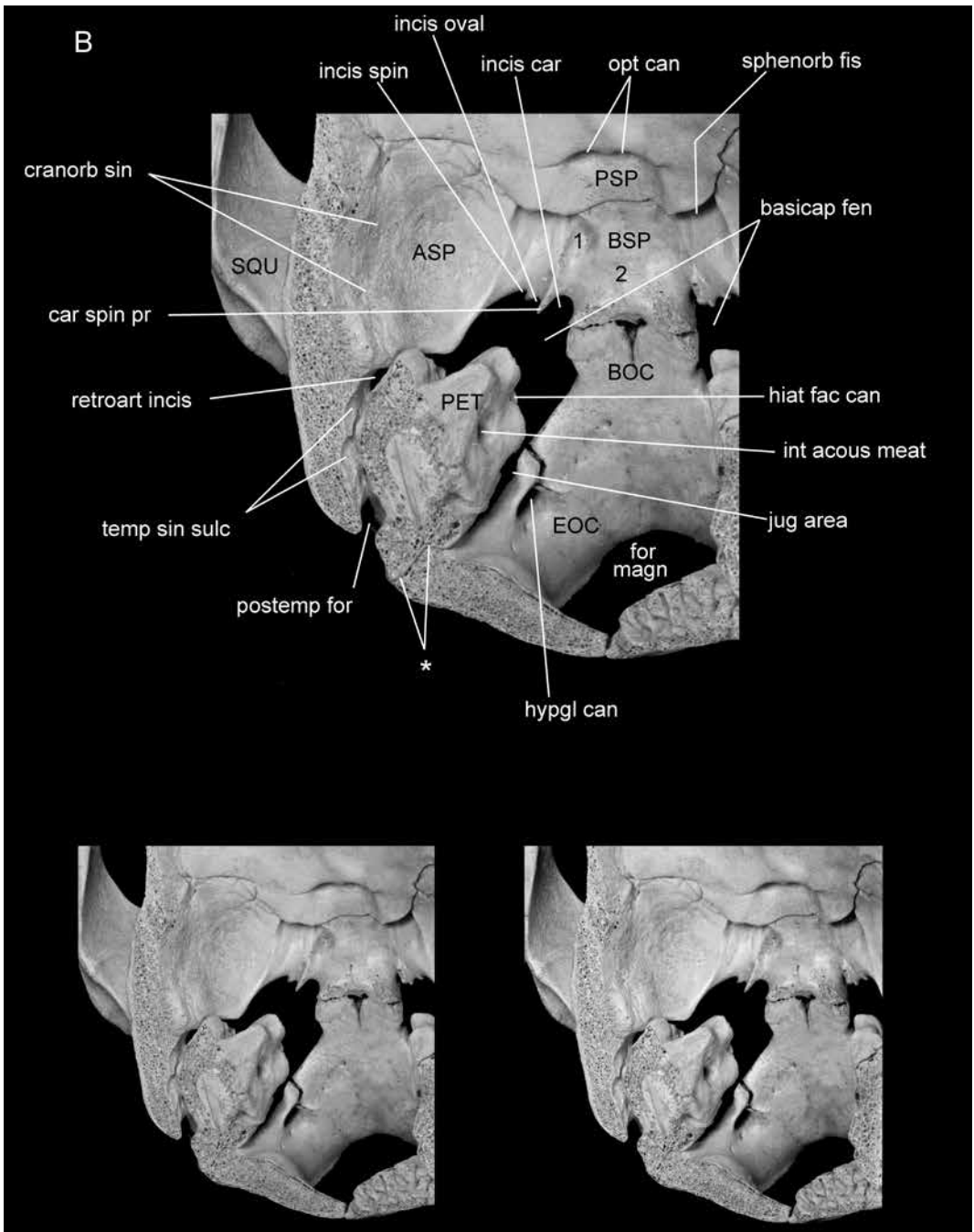
intercarotid artery would be expected to lie in life. **Asterisk** indicates petroexoccipital suture and small strip of exposed petrosal mastoid that isolates exoccipital from posttemporal foramen (as in *Equus*). Incisurae are more prominent here than in specimen of *Rhinoceros unicornis* AMNH M-274636 (fig. 35) at roughly similar stage of development.
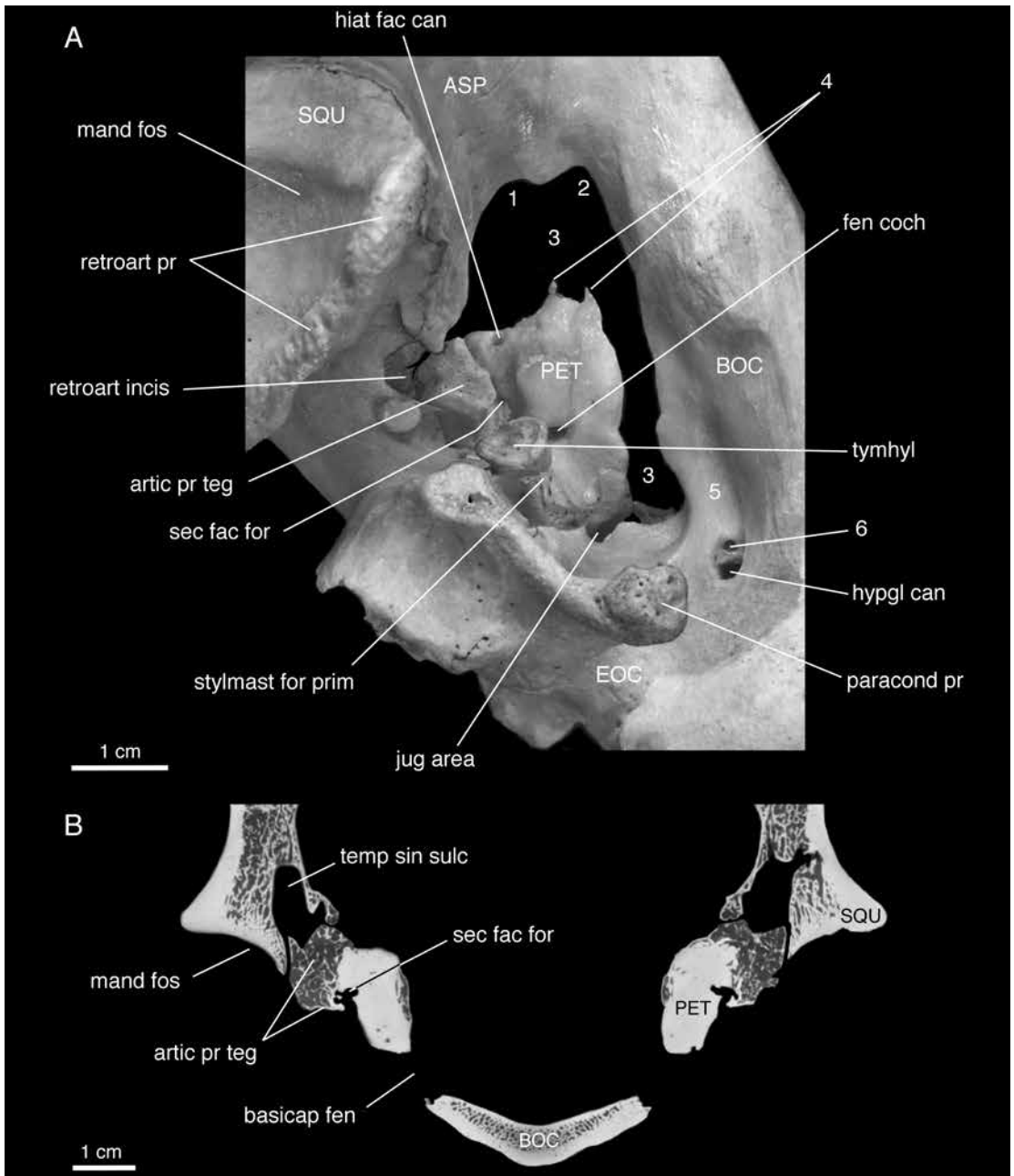
FIG. 38. *Tapirus*, selected basicranial features in subadult and adult specimens on this and facing page. **A,** *T. terrestris* AMNH M-77576 (adult), caudal cranium in ventral aspect; **B,** *T. indicus* AMNH M-130108 (adult), segment through articular process of tegmen tympani; **C, D,** *T. indicus* AMNH M-200300 (subadult), isolated right petrosal in lateral (**top**) and ventral (**bottom**) aspects; **E, F,** *T. indicus* AMNH M-200300, isolated left ectotympanic (stereopair) in oblique medial (**top**) and oblique lateral (**bottom**) aspects. **Key: 1,** incisura ovalis; **2,** incisura carotidis; **3,** rostral (piriform) and caudal (jugular) portions of continuous basicapsular fenestra; **4,** incomplete "canal" for internal carotid artery; **5,** prominent groove for
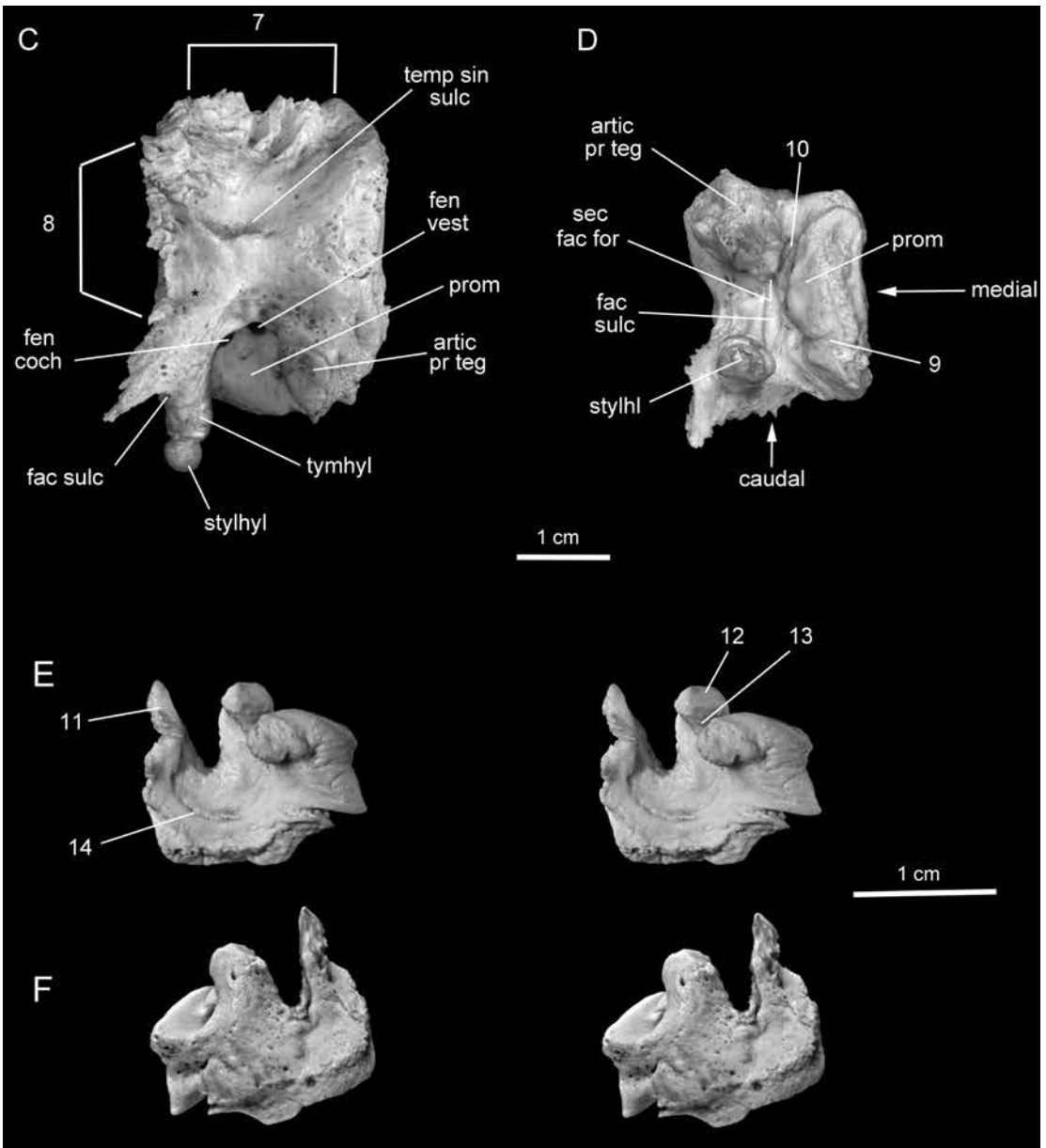
?craniooccipital vein and associated plexuses; **6,** canal linking ventral petrosal sinus and hypoglossal/condylar canal; **7,** petrosal surface of squamopetrosal suture; **8,** petrosal surface of petroexoccipital suture; **9,** sulcus for ?tympanic n.; **10,** ?tensor tympani fossa; **11,** caudal crus of ectotympanic; **12,** rostral crus of ectotympanic; **13,** groove for gonial; **14,** crista tympanica (for tympanic membrane). In A, tympanic aperture of prootic canal for lateral head vein/prootic sinus lies immediately lateral to secondary facial foramen (not visible from this angle). In B, frothy internal texture of articular process of tegmen tympani matches appearance of dorsal process of entotympanic as seen in *Rhinoceros unicornis* AMNH 274636 (fig. 35); if process is actually entotympanic in origin, which cannot be confirmed on this specimen, by this stage it is already continuous with petrosal.
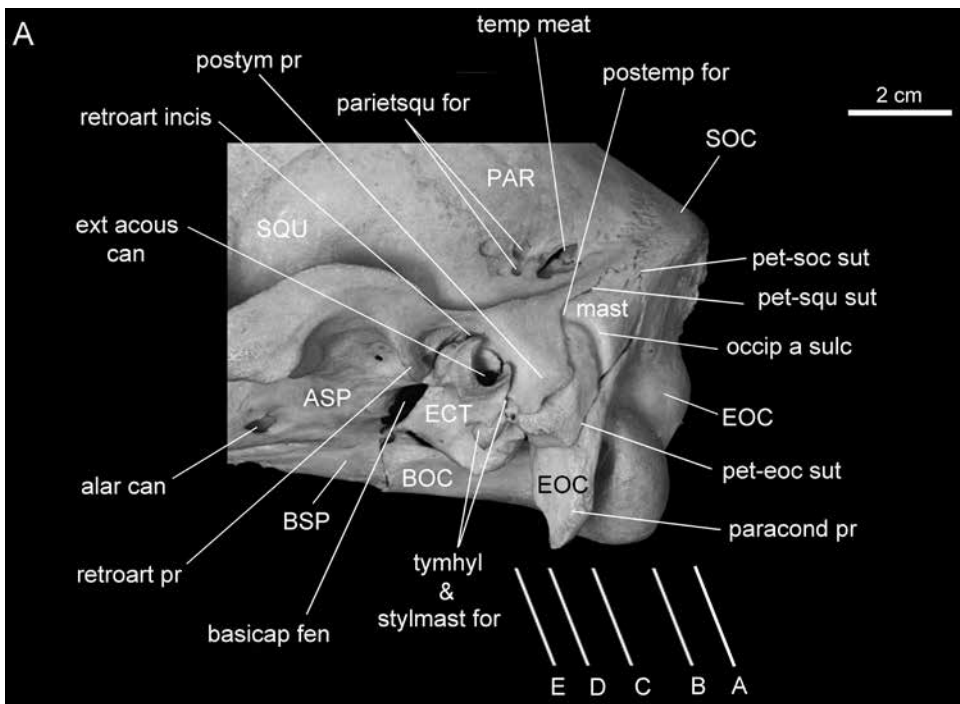
FIG. 39. *Equus caballus* AMNH M-204155, left caudal cranium in **A,** lateral and **B,** ventral aspects, with **C,** ventral stereopair of auditory region. **Key: 1,** incisura carotidis; **2,** incisura ovalis; **3,** incisura spinosa. In A, planes corresponding to approximate location of segments illustrated in figure 40A–E are indicated on lower right. In B, **white asterisks,** impressions for ?tributaries of basicranial plexuses and retroarticular emissary vein; **black asterisk,** impression for ?craniooccipital vein or emissarium from ventral petrosal sinus (see fig. 6). Even though this a young animal, suture line between ectotympanic and entotympanic is already obliterated (see Maier et al., 2013).
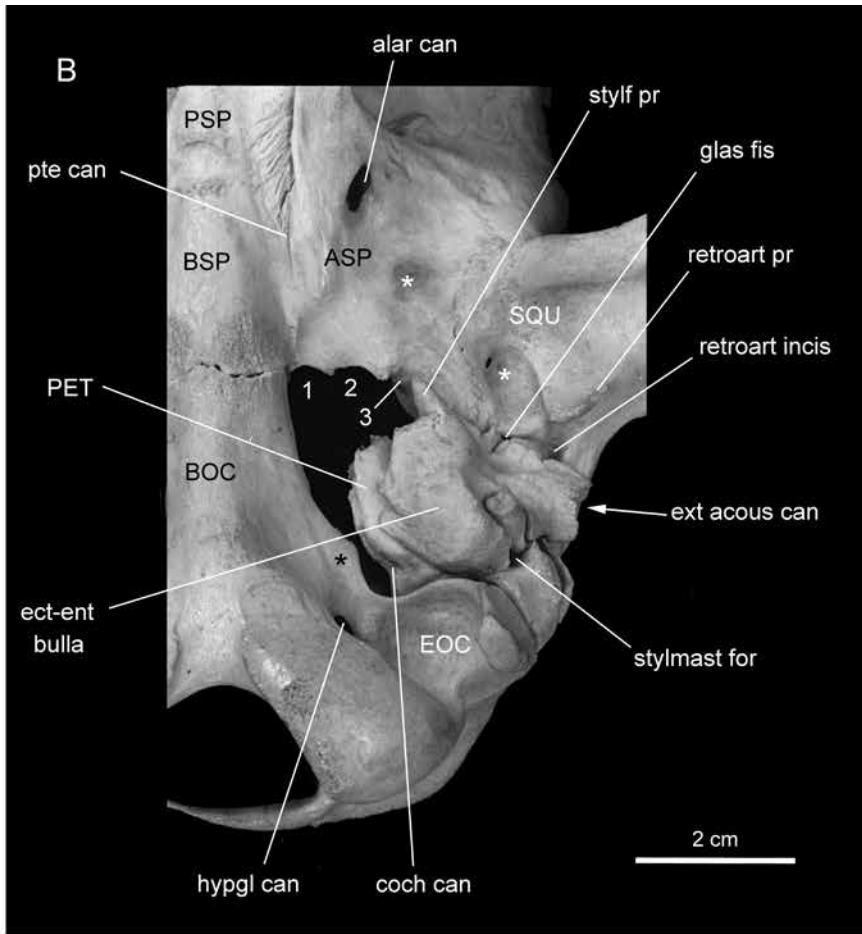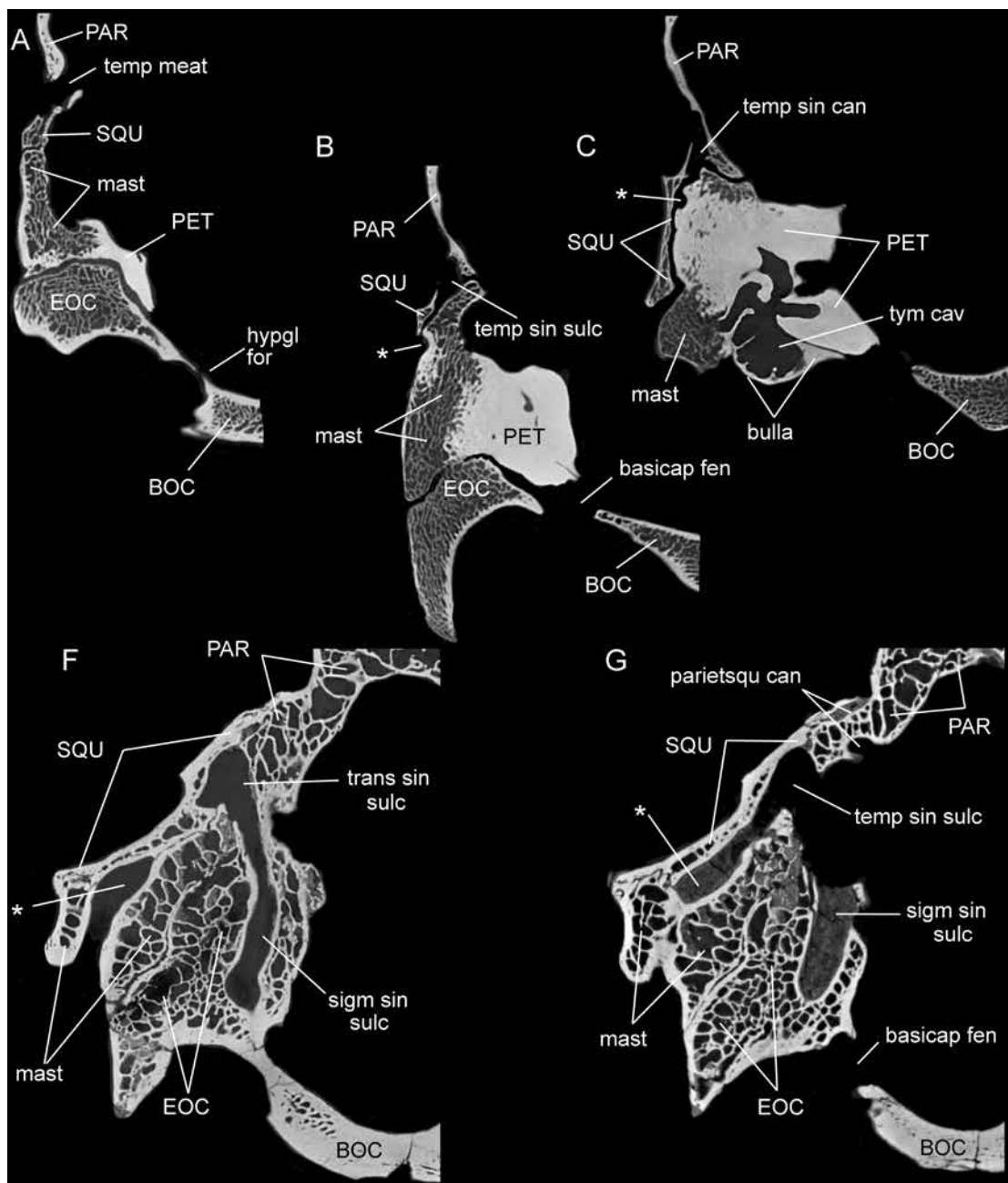
FIG. 40. Transverse segments comparing vascular routes in mastoid region in *Equus caballus* AMNH M-204155 (**A–E**) and *Tetramerorhinus lucarius* AMNH VP-9245 (**F–I**) on this and facing page, each series in caudorostral order. ***Equus* series:** In A–C, sulcus for arteria diploetica magna/caudal meningeal artery (**single asterisk**) crosses lateral face of petrosal mastoid in a deep sulcus covered by overlying squamosal (thus forming posttemporal foramen, so-called mastoid foramen of equine anatomies). Artery's trackway is located below, but converges with, sulcus for temporal sinus in separate compartment. In D, at transverse level of external acoustic meatus, sulcus for artery enters short canal (canal Y) that penetrates dorsal surface of petro-

sal. Trackway reemerges, continues into endocranium where it joins or becomes cranioorbital artery. In E, sulcus for temporal sinus continues rostrally, terminates at retroarticular incisure (for departing retroarticular vein). **Tetramerorhinus series**: In F, G, posttemporal foramen/canal, framed at different levels by combinations of petrosal mastoid, squamosal, and exoccipital, terminates in sulcus for transverse/temporal sinus near origin of sigmoid sinus. In H, I, sulcus for temporal sinus continues rostrally on lateral face of petrosal mastoid, passes around large epitympanic sinus (absent in *Equus*), to terminate in retroarticular foramen. Segments C (*Equus*) and H (*Tetramerorhinus*) are at roughly comparable transverse levels, but a groove incising mastoid for caudal meningeal artery/arteria diploetica magna is evident only in C. In *Tetramerorhinus* there is no conduit equivalent to canal Y, suggesting functional absence of this artery. **Double asterisk** in H marks vascular sulcus, presumably for vertebral vein or its anastomotic link with ventral petrosal sinus.
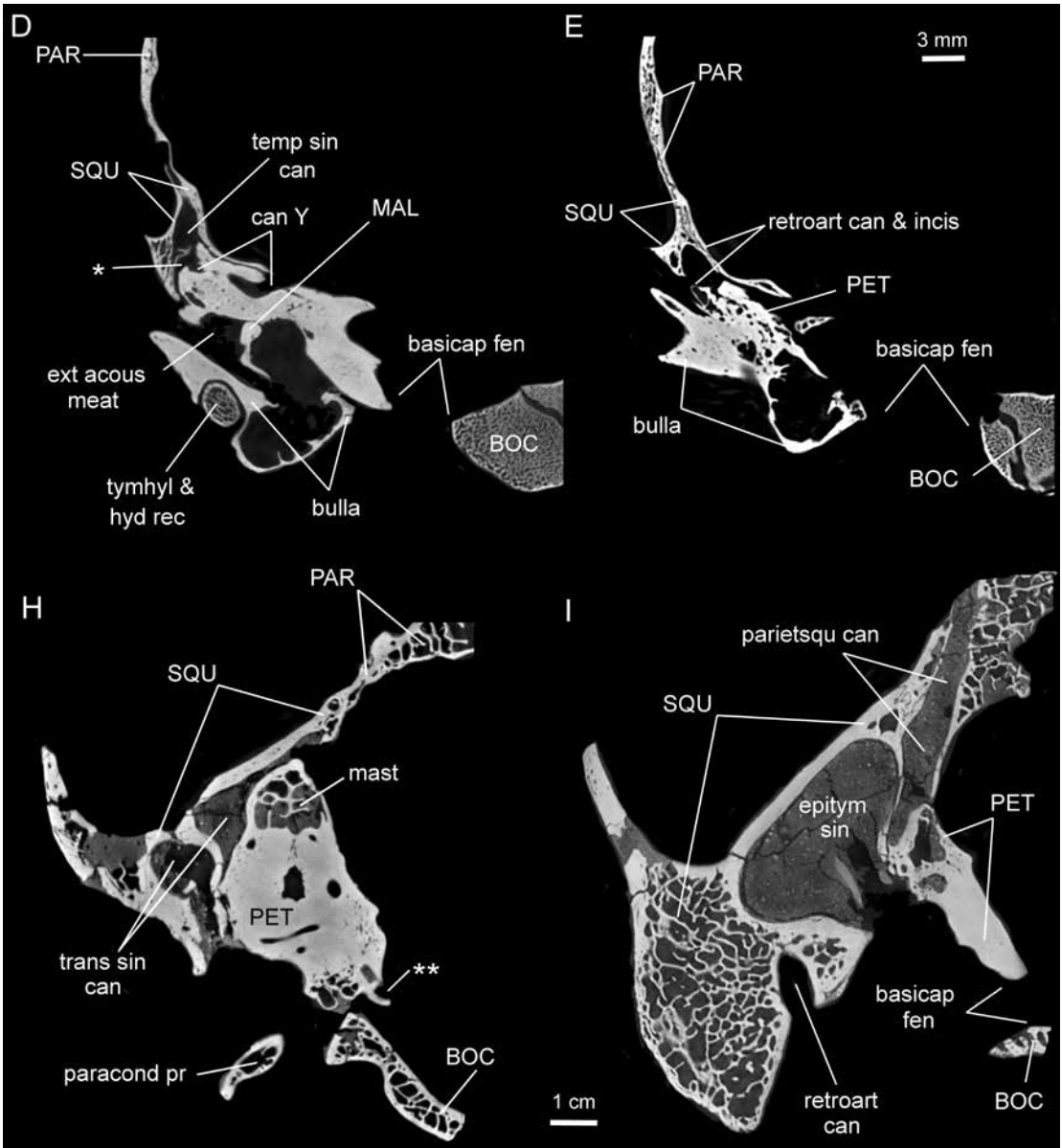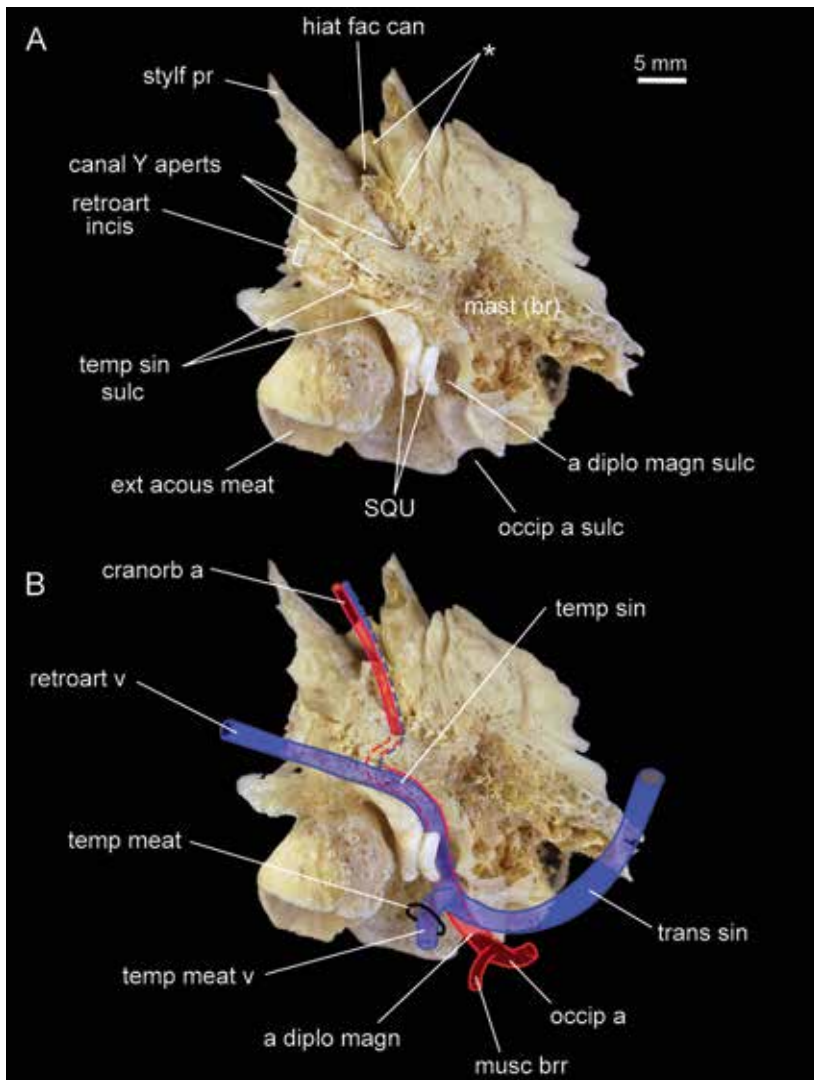
FIG. 41. *Equus asinus* AMNH M-204141, isolated left petrosal in oblique caudodorsal aspect, showing osteological (**top**) and inferred vascular (**bottom**) features based on known anatomy of domestic horse. **Arteries (red):** Sulci for occipital artery and arteria diploetica magna (= caudal meningeal artery of equine anatomies) are continuous; small vessel leaving occipital trunk is meant to suggest muscular branches to m. obliquus capitis cranialis (Ellenberger and Baum, 1908: 672), which leave no trace osteologically. As in figure 40, sulcus for arteria diploetica magna passes dorsally over tympanic roof, then diverges medially along a somewhat narrower trackway that runs through a short tube, canal Y. Trackway reemerges, crosses (**asterisk**) petrosal's mediodorsal face, then continues into middle cranial fossa to join or become cranioorbital artery. **Veins (blue):** In equines there is no equivalent of vena diploetica magna closely accompanying arteria diploetica magna. Small vein (dashed blue line) within canal Y is included for purposes of illustration only; no such vein is found in the horse, but its presence (as vena diploetica magna) would be generally expected in other taxa possessing arteria diploetica magna. Although hard to appreciate from this aspect, transverse sinus, temporal sinus, and vein of temporal meatus are individually situated at higher horizontal positions than trackway for arteria diploetica magna (cf. figs. 39A, 40). Temporal sinus enters canal that partly parallels sulcus for arteria diploetica magna, but continues rostrally to leave skull as retroarticular vein via retroarticular incisure (fig. 40).

APPENDIX 3

CHARACTER LIST

Our taxon/character matrix (see appendix 4) is a modification of the one published by Billet et al. (2015). The modified matrix is also available from MorphoBank (morphobank.org).

All of the characters in the original set were implemented as is, with the following exceptions: 13 were omitted (C52, 74, 77, 82, 92, 102, 104, 115, 124, 128, 131, 134, and 141), and another 22 characters/character states were modified or redefined to comply with our nomenclature or descriptions (C73, 79, 83, 97, 105–110, 112–114, 121, 122, 126, 130, 132, 137, 138, 150, 151). Characters originally classed as additive were treated as in the Billet et al.(2015) analysis and are indicated by asterisks (*). Reasons for omission or modification of the original characters are provided in accompanying notes (texts in *italics*). Three new characters were also added to the matrix (C157, 158, and 159). The character list in its original form was developed from various sources, as documented by Billet et al. (2015, appendix S2), and is here edited where necessary for clarity and terminological usage. Figure 42 provides a guide for scoring states of certain characters.

The main aim of this part of our study was to explore the phylogenetic position of *Trigonostylops,* with special regard to its placement in relation to astrapotheriids. In line with this objective we added to the taxon list, as terminal taxa, the putative astrapothere *Eoastrapostylops* (but see Kramarz et al., 2017), the indisputable astrapotheriid *Astraponotus,* and the perissodactylans *Tapirus, Equus,* and *Palaeotherium.* We also deleted taxa from the original list of Billet et al. (2015) if they were not relevant to the present paper's specific inquiries. Removals included the xenarthrans *Bradypus, Kuntinaru,* and *Dasypus*; the isolated petrosal UFRJ-DG, identified as litoptern (scoreable for only a few characters); and the notoungulates *Pleurostylodon, Scarritia, Rhynchippus, Adinotherium, Protypotherium, Federicoanaya, Plesiotypotherium, Paedotherium,* and MNHN-F-BRD23 (testing internal relationships within Notoungulata was not

a goal of our project). In the matrix the taxon name *Proterotherium* is replaced by *Tetramerorhinus,* in accordance with Soria's (2001) taxonomic allocation of listed specimens (see table 1: fn. 9).

TEETH

1. Presence of variable upper and lower precanine diastemata (= elongation of the premaxillary relative to toothrow size): 0, absent; 1, present.

2. Presence of variable upper postcanine diastemata (= elongation of the anterior part of maxillary relative to toothrow size): 0, absent; 1, present. *Rescoring:* changed *Trigonostylops* and *Astrapotherium,* "-" →1.

3. I1: 0, absent; 1, present.

4. I2: 0, absent; 1, present.

5. I2-C labio-lingually compressed: 0, absent; 1, present.

6. I1 relative size vs. other incisors: 0, smaller or subequal to other incisors; 1, enlarged relative to other incisors.

7. I1 crown highly curved: 0, absent; 1, present.

8. I1 comma shaped in section: 0, absent; 1, present.

9. I1 obliquely implanted, tips meet obliquely: 0, absent; 1, present.

10. Procumbent I1-2, occluding at an angle of 90° (or less) with procumbent i1-2? (wear creates a bevel on upper incisors): 0, absent; 1, present.

*11. I1 crown height and robustness: 0, brachydont or slightly hypsodont, not tusklike; 1, hypsodont and/or tusk-like; 2, hypselodont and tusklike. *Hypsodonty corresponds here to enamel-band or dentine hypsodonty sensu Koenigswald (2011).*

12. (I1-) I2 caniniform, circular in cross section: 0, absent; 1, present.

13. I2 tusk trihedral and divergent: 0, absent; 1, present.

*14. I2 position relative to I1: 0, I2 lateral to I1; 1, posterolateral to I1; 2, I2 immediately posterior to I1 (I1 and I2 in anteroposterior alignment).

15. I3 (+-i3): 0, present; 1, absent. *Rescoring:* changed *Trigonostylops,* 1→?

16. Lingual cingulum on upper incisors creates a fossette: 0, absent; 1, present.

*17. Canine (upper and +- lower): 0, present; 1, vestigial, often absent; 2, always absent.

18. Tusklike upper and lower canines: 0, absent; 1, present.

19. Canine (upper and lower): 0, massive and caniniform; 1, incisiform and subequal to other incisors.

20. P1: 0, absent; 1, present. *Rescoring:* changed *Trigonostylops*, 0 →1.

*21. Cheekteeth: 0, brachyodont; 1, hypsodont (sidewall hypsodonty sensu Koenigswald, 2011); 2, hypselodont.

22. Distal cingulum isolating a deep fossette (postcingulum fossette) on upper cheekteeth: 0, absent; 1, present.

23. Protoloph (high crest or loph joining paracone-parastyle and protocone, in paracingulum position) on upper molars (and premolars): 0, absent; 1, present; 2, paracingulum high but not connected to parastyle-paracone.

24. Ectoloph (high crest joining paracone and metacone) on upper molars (and premolars): 0, absent; 1, present.

25. Metaloph (high crest joining metacone and hypocone) on M1–2 (and premolars): 0, absent; 1, present.

26. Long crochet on upper cheekteeth connected to the ectoloph, thus isolating a posterolabial fossette: 0, absent; 1, present.

27. Anterolabial fossette on upper cheekteeth: 0, absent; 1, present.

28. Central fossette on upper cheekteeth: 0, absent; 1, present.

29. Deep labial extension of central fossette between the protoloph (-crista 1) and the crochet (-crista 2) on upper molars: 0, absent; 1, present.

30. Multiple cristae demarcated mesial to the crochet on upper cheekteeth: 0, absent; 1, present.

31. Crista intermedia running lingually from the ectoloph between the protoloph and the crochet on upper cheekteeth: 0, absent; 1, present.

32. Crista intermedia: 0, not well demarcated but suggested by a bulge; 1, completely demarcated.

33. Posterolabial fossette on upper molars: 0, cooccurs with the central fossette; 1, disappears before the closure of the central fossette.

34. Crochet originating lingually on mesial edge of hypocone: 0, absent; 1, present.

35. Para- and metaconule: 0, absent or indistinct; 1, present.

36. Upper cheekteeth parastyle: 0, absent or indistinct; 1, present.

37. Upper cheekteeth parastyle (at least on molars): 0, not labially projecting (not more labial than paracone); 1, labially projecting relative to metacone.

38. Subvertical parastyle-paracone sulcus on upper cheekteeth (at least premolars): 0, absent; 1, present.

39. Subvertical parastyle-paracone sulcus on upper premolars: 0, shallow; 1, deep.

40. Prominent mesostyle (stylar cusp C) (at least on all upper molars): 0, absent; 1, present.

41. Metacone (fold or cusp) on (P3-)P4: 0, absent, fused with paracone or not visible; 1, present, distinctly individualized from paracone.

42. Deep mesial valley on P2–3 (-4) due to incomplete development of protoloph: 0, absent; 1, present.

43. Persistent lingual sulcus after the isolation of the central fossette on upper molars: 0, absent; 1, present.

44. Persistent lingual sulcus (enamel infolding; tooth not trilobate) between protoloph and metaloph on upper molars: 0, absent; 1, present.

*45. Upper molars trilobate when little worn, with large and rounded median lobe: 0, absent; 1, present but disappears with wear; 2, trilobation persists through all wear stages.

46. Prominent hypocone on upper molars (M1–2 +-M3): 0, absent; 1, formed by bulge of posterocingulum; 2, formed by displaced and expanded metaconule; 3, formed by an additional cusp, possibly due to subdivision of protocone.

47. Size (area) of M1 vs. M2: 0, M1 much larger (>120%) than M2; 1, subequal (80% to 120%); 2, M1 much smaller than M2 (<80%).

48. Size (area) of M1 vs. M3: 0, M1 much larger than M3 (>120%); 1, subequal (80% to 120%); 2, M1 much smaller than M3 (<80%).

49. Size (area) of m1 vs. m2: 0, m1 much larger (>120%) than m2; 1, subequal (80% to 120%); 2, m1 much smaller than m2 (<80%).

50. Size (area) of m1 vs. m3: 0, m1 much larger than m3 (>120%); 1, subequal (80% to120%); 2, m1 much smaller (<80%) than m3.

51. Cusp on precingulum anterolingual to paraconule: 0, absent; 1, present.

52. OMITTED. Separation between paracone and metacone on upper molars (at tip and base): 0, small to moderate, 1, large. *This character was not used because the differences in character states are vaguely stated and it proved difficult to consistently score in most taxa with lophoid cusps.*

53. First lower incisor: 0, well developed; 1, reduced relative to other incisors.

54. Lingual ridge vertical on lower incisors and canine: 0, absent; 1, present.

*55. Lingual face of i1–2 (only i2 when i1 is absent, and conversely): 0, without vertical sulcus; 1, with a shallow vertical sulcus; 2, with a deep vertical sulcus (bifid incisors).

56. Lower incisors: 0, implanted subvertically; 1, highly procumbent.

57. Third lower incisor large (larger than canine) and caninelike (i.e., pointed): 0, absent; 1, present.

58. Tusklike third lower incisor: 0, absent; 1, present.

59. Leaf-shaped lower incisors: 0, absent; 1, present.

60. Metaconid of p4 (or ultimate premolar): 0, small to medium sized and appressed against protoconid; 1, enlarged and distinctly separated from the protoconid.

61. Mesial lophid (paralophid?) in a paraconid position on lower cheekteeth: 0, absent (or just a faint cristid); 1, present.

62. Lower cheekteeth with short mesiodistal protolophid, transverse metalophid, and mesiodistal hypolophid slightly convex labially (double crescent): 0, absent; 1, present.

63. Lower cheekteeth with entoconid transversely expanded into entolophid: 0, absent; 1, transversely expanded; 2, less transverse and attached to the trigonid.

64. Isolated cuspid in front of the metalophid-metaconid on lower cheekteeth: 0, absent; 1, small mesiodistal crest running mesially from the distolingual extremity of the metalophid-metaconid; 2, completely isolated cusp.

65. Lingual connection of lophids of the trigonid and talonid (entolophid connects to metalophid with wear) on lower cheekteeth: 0, absent; 1, isolates a trigonid-talonid fossettid in conjunction with the preceding more labial connection of hypolophid with trigonid; 2, lingual connection trigonid-talonid precedes the labial connection and isolation of fossettid; 3, single lingual connection, producing a deep labial sulcus between trigonid and talonid.

66. Hypoconid: 0, forms labial half or less of talonid, does not invade talonid basin anterior to the hypoconulid; 1, large, conical, extends onto lingual half of talonid and invades talonid basin anterior to hypoconulid.

67. Fossettid of entolophid: 0, absent; 1, present.

68. Trigonid of lower molars with a tiny trigonid fossettid partially or entirely isolated lingually by a crest (premetacristid) running mesially from metalophid: 0, absent; 1, present.

69. Transversely elongated fossettid isolated between entolophid (mesially) and hypolophid (labially and distally) with advanced wear: 0, absent; 1, present.

70. Distolabial crest on trigonid of lower premolars created by a distolabial extension of protolophid: 0, absent; 1, present.

71. Talonid extending well distal to entolophid on lower molars: 0, absent; 1, present.

72. Deep labial and lingual sulci dividing trigonids and talonids on lower cheekteeth crowns at all wear stages: 0, absent; 1, present.

73. Flat, vertical lingual face on all lower molars at all wear stages, for full height of crown: 0, absent; 1, present. *The wording of this character has been modified for clarity.*
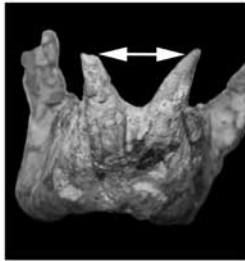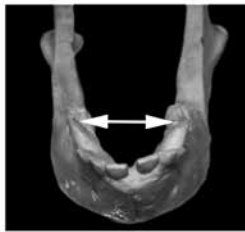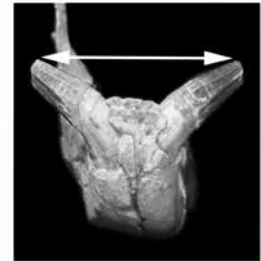
FIG. 42. Visual guide for scoring certain matrix characters. "Slashed zero" symbol indicates "absent" character state. **C113,** Hypoglossal foramen (-ina): **0,** located nearer to occipital condyle than to jugular area (e.g., *Scalabrinitherium bravardi* MACN Pv 13082); **1,** hypoglossal foramen closer to jugular area than to condyle (e.g., *Astraponotus* sp. MPEF PV 1084); **2,** hypoglossal foramen opens directly into jugular area (*Trigonostylops wortmani* AMNH VP-28700). **C157** (new), Facial process of premaxilla: **0,** present (e.g., *Mesotherium angustirostrum* MACN Pv 6040); **1,** absent (e.g., *Astrapotherium magnum* AMNH VP-9278; *Trigonostylops wortmani* MLP 52-X-5-98). **C158** (new), Diverging canines (upper and lowers): **0,** canines diverging at an angle less than 70° in front view (e.g., *Eoastrapostylops riolorense* PVL 4216; *Phenacodus primaevus* MACN Pv 18808, cast of YPM PU 14864); **1,** divergence equal to or larger than 70° (e.g., *Astrapotherium* FMNH 13172; *Trigonostylops* MPEF PV 5483 [right canine reconstructed]). In the case of **C159** (new), consult micrographs in original publication (Lindenau, 2005) for proper scoring.

74. OMITTED. Teeth: 0, differentiated into morphological categories (incisors, canines, premolars, and molars) with enamel or, 1, simple peglike teeth without enamel (or very thin layer in unworn teeth). *This character was not used because, as framed, it is invariant in taxa scored for this matrix (character state 1 applies only to xenarthrans).*

Skull

75. Rostrum length/braincase length <0.5 (braincase more than twice as large as rostrum): 0, absent; 1, present.

76. Premaxillaries defining a long ridge connecting the narial processes to the anterior alveolar border (the nares open much higher than the alveolar border): 0, absent; 1, present. *Rescoring:* changed *Trigonostylops*, 0 →?

77. OMITTED. Development of incisive foramina: 0, small; 1, large (i.e., anteroposteriorly elongated). *This character was omitted because of uncertainty concerning how size is to be evaluated.*

78. Triangular incisive foramina (distal extremities converging): 0, absent; 1, present. *Rescoring:* changed *Astrapotherium*, 0 →?

79. Medial platform of palatines extending palate posterior to M3 and fully continuous with it: 0, absent; 1, present. *The wording of this character has been modified for clarity.*

80. Orientation of the blades of the ectopterygoid crests: 0, sub-parallel and facing ventromedially; 1, diverging and facing mostly posteriorly. *Rescoring:* changed *Eoastrapostylops*, ? →0 (revised from Kramarz et al., 2017).

*81. Position of choanae: 0, mostly anterior to last molar; 1, even with last molar; 2, mostly posterior to last molar.

82. OMITTED. Choanae divided by a vomerian/palatine process: 0, absent; 1, present. *This character was not used because, as framed, it is invariant in taxa scored for this matrix (none lack the vomer/palatine process).*

*83. Premaxillary-maxillary suture disposition on palate: 0, medial portion of suture directed anteriorly; 1, medial portion of suture runs mainly transversely; 2, medial portion of suture is directed posteriorly (but not lateral portion); 3, entire suture directed posteriorly. *The wording of this character has been modified for clarity.*

84. Narial processes of the premaxillaries: 0, absent; 1, present.

*85. Posterodorsal extremity of maxillary contacting nasal: 0, does not reach posterior extremity of nasals; 1, approximately reaches posterior extremity of nasals; 2, reaches much further than posterior extremity of nasals. *Rescoring:* changed *Astrapotherium*, ? → 0.

86. Infraorbital foramen in adult: 0, above premolars; 1, above molars.

87. Strong vertical descending process (masseteric spine) of maxillary: 0, absent; 1, present.

88. Anterior tip of nasals: 0, extends anterior to ascending process of premaxillary; 1, does not extend anterior to ascending process of premaxillary. *Rescorings:* changed *Trigonostylops*, ? → "-"; *Astrapotherium*, 0 → "-."

89. Anterior edge of ascending process of premaxillary shifted posteriorly: 0, absent; 1, present. *Rescorings:* changed *Trigonostylops*, ? → "-"; *Astrapotherium*, 0 → "-"; *Macrauchenia,* "-" →?

90. Length of nasals reduced relative to width: 0, absent; 1, present. *Rescoring:* changed *Trigonostylops*, ? → 0.

91. Large facial extent of lacrimal in direction of nasal bone: 0, absent; 1, present.

92. OMITTED. Postorbital constriction: 0, strong; 1, weak. *This character was not used because of uncertainty about how constriction is to be evaluated.*

93. Jugal excluded from anterior orbital border: 0, absent; 1, present. *Rescoring:* changed *Eoastrapostylops*, ? →0 (revised from Kramarz et al., 2017).

94. Squamosal contacts with frontal at level of postorbital apophysis: 0, absent; 1, present. *Rescorings:* changed *Trigonostylops*, 1 →0; *Eoastrapostylops*, ? →1 (revised from Kramarz et al., 2017).

95. Zygomatic arches in dorsal view: 0, parallel to anteroposterior axis; 1, semicircular and

well expanded laterally. *Rescoring:* changed *Eoastrapostylops*, 1 →0 (revised from Kramarz et al., 2017).

96. Zygomatic plate below and in front of orbit: 0, absent; 1, present.

97. Anterior root of zygomatic arch situated anterior to transverse level of M3: 0, absent; 1, present. *Rescoring:* changed *Trigonostylops*, 0 →1. *The wording of this character has been modified for clarity.*

98. Orbit shape: 0, round; 1, oval (higher than long, dorsal edge of zygomatic arch excavated below orbit).

99. Jugal-squamosal suture strongly curved anteriorly (largely directed dorsally): 0, absent; 1, present.

100. Sphenopalatine foramen: 0, well delimited, between medial orbital wall and orbital floor; 1, poorly delimited, within a groove between medial orbital wall and orbital floor. *Rescoring:* changed *Trigonostylops*, 0 →1.

101. Position of sphenopalatine foramen: 0, in posterior part of orbital floor; 1, at level of middle of orbital floor (in terms of its anteroposterior length). *Rescoring:* changed *Astrapotherium*, ? →0.

102. OMITTED. Very large orbit (the orbit occupies almost all the orbitotemporal fossa): 0, absent; 1, present. *This character was not used because of uncertainty about how orbit size is to be evaluated in some cases.*

*103. Temporal lines (forming sagittal crest): 0, fused temporal lines, sagittal crest well developed; 1, fusion of temporal lines only in most posterior part; 2, no fusion between temporal lines. *Re-scoring:* changed *Macrauchenia*, 0→2.

104. OMITTED. Auditory region (basicranium) large and short (i.e., auditory region much wider than longer, from level of anterior edge of squamosal root of zygomatic process to posterior border of paroccipital processes): 0, absent; 1, present. *This character was not used because the character was invariant in the taxa selected for inclusion in the matrix (in all cases the auditory region was much wider than longer).*

105. Mandibular fossa shape: 0, concave (or concave posteriorly and flat anteriorly), opens

anteriorly; 1, mostly flat anteroposteriorly; 2, concavo-convex (deep and narrow fossa posteriorly). *Rescoring:* changed *Eoastrapostylops*, 1 →? (revised from Kramarz et al., 2017). *The wording of this character has been modified to reflect anatomical nomenclature used in this paper.*

*106. Extent of mandibular fossa surface: 0, transversely elongated; 1, transversely reduced, almost as large anteroposteriorly; 2, anteroposteriorly elongated. *Rescoring:* changed *Eoastrapostylops*, 0 →? (revised from Kramarz et al., 2017). *The wording of this character has been modified to reflect anatomical nomenclature used in this paper.*

107. Retroarticular foramen: 0, posterior or posteromedial to the retroarticular process; 1, anterior to the retroarticular process. *The wording of this character has been modified to reflect anatomical nomenclature used in this paper. Rescorings:* changed *Trigonostylops*, 0 →1; *Astrapotherium*, 0 → "-"; *Cochilius*, ? →0.

108. Extratympanic aditus deeply piercing retroarticular process caudodorsally and defining a large sinus within its base: 0, absent; 1, present. *The wording of this character has been modified to reflect anatomical nomenclature used in this paper. Rescoring:* changed *Cochilius*, ? →0.

109. Alar canal: 0, absent; 1, present. *Rescoring:* changed *Cochilius*, ? →0. *The wording of this character has been modified to reflect anatomical nomenclature used in this paper.*

110. Foramen ovale: 0, within alisphenoid and separated from rostral portion of basicapsular fenestra (i.e., piriform fenestra); 1, mandibular branch of CN5.3 passes through rostral portion of basicapsular fenestra (i.e., piriform fenestra). *The wording of this character has been modified to reflect anatomical nomenclature used in this paper.*

111. Long, large groove on the lateral face of ecto(-ento)pterygoid process immediately in front of the foramen ovale/sphenotympanic fissure: 0, absent; 1, present. *Rescoring:* changed *Cochilius*, ? →0.

112. Well-inflated ossified auditory bulla (tightly) attached to basicranium: 0, absent; 1, present. *The wording of this character has been*

modified to reflect anatomical nomenclature used in this paper. *Rescoring:* changed *Astrapotherium*, ? →0.

*113. Hypoglossal foramen (-ina): 0, located nearer to occipital condyle than to jugular area; 1, hypoglossal foramen closer to jugular area than to condyle; 2, hypoglossal foramen opens directly into jugular area. *This character has been redefined. Original definition: Position of hypoglossal foramen relative to posterior lacerate (jugular) foramen: 0, well separated from it; 1, in a common depression.*

114. Medial part of continuous basicapsular fenestra: 0, incomplete/closed; 1, complete. *This character has been redefined. Original definition: Basicochlear fissure: 0, closed; 1, patent). Incomplete means that there is at least one point of contact between pars cochlearis (i.e., promontorium) and the elements of the central stem. Complete means that there is no contact (i.e., a wide gap) between the pars cochlearis and the elements of the central stem.* Rescorings: changed *Trigonostylops*, ? → 1; *Cochilius*, ? → 0.

115. OMITTED. Large foramen medial to promontorium midlength and/or auditory bulla and lateral to basioccipital: 0, absent; 1, present. *This character was not used because of uncertainty about the target to evaluate: if it is the passageway used by the ventral petrosal sinus to leave the endocranium, this may refer either to its own foramen, or to the jugular foramen (or caudal part of basicapsular fenestra), which is also used by caudal cranial nerves. Either way, a "large foramen" is always present.*

116. Large quadrangular auditory bulla with an anterior border grossly transverse and a medial border defining a long straight line: 0, absent; 1, present. *Rescorings:* changed *Trigonostylops*, "-"→0; *Astrapotherium*, "-"→?

117. Posterior bulla laps up onto paraoccipital process: 0, absent; 1, present. *Rescorings:* changed *Trigonostylops*, "-"→0; *Astrapotherium*, "-"→?

118. Crista meatus: 0, absent; 1, present. *Rescoring:* changed *Cochilius*, ?→ 0.

119. Crista meatus: 0, small; 1, well developed. *Rescoring:* changed *Cochilius*, ? →"-."

120. Ossified tubular external auditory meatus strongly attached to the basicranium: 0, absent; 1, present. *Rescoring:* changed *Eoastrapostylops*, ? →0 (revised from Kramarz et al., 2017).

121. Ossified tubular external auditory meatus: 0, short, does not reach lateral edge of skull (especially lateral edge of retroarticular process); 1, long, reaches lateral edge of skull. *The wording of this character has been modified to reflect nomenclature used in this paper. Rescorings:* changed *Astrapotherium*, "-" →?; *Cochilius*, ? →1; *Eoastrapostylops*, ? → "-" (revised from Kramarz et al., 2017).

122. Retroarticular process appressed or almost fused for its entire length to crista meatus and/or to external auditory meatus, thus defining a channel for retroarticular foramen: 0, absent; 1, present. *The wording of this character has been modified to reflect nomenclature used in this paper. Rescoring:* changed *Eoastrapostylops*, ? → "-" (revised from Kramarz et al., 2017).

123. Crista meatus and post-tympanic process of squamosal: 0, widely separated; 1, very close to or appressed against each other. *Rescorings:* changed *Cochilius*, ? → "-"; *Eoastrapostylops*, ? → "-" (revised from Kramarz et al., 2017).

124. OMITTED. Posterior border of tympanohyal recess: 0, formed by paroccipital process; 1, formed by a tympanic extension and/or post-tympanic process. *This character was not used because tympanohyal may lack a posterior border formed by another element; it is also difficult to score consistently in small taxa.*

125. Very small tympanohyal recess located on posterolateral slope of bulla: 0, absent; 1, present. *Rescorings:* changed *Cochilius*, ?→ 1; *Eoastrapostylops*, ? → "-" (revised from Kramarz et al., 2017).

126. Epitympanic sinus and aditus: 0, absent; 1, present. *This character has been redefined. Original definition: Epitympanic sinus in posterodorsal part of squamosal: 0, absent; 1, present. This character and its states as redefined are meant to refer to the epitympanic sinus arising from the epitympanic recess in the roof of the tympanic cavity, as expressed in notoungulates as well as litopterns and* Pyrotherium. *"Aditus" refers to*

the aperture in the tympanic roof that leads into the epitympanic sinus; it marks the position at which pneumatization begins during ontogeny and is thus an integral part of the feature to be analyzed. Muizon et al. (2015) scored the epitympanic sinus as absent in Trigonostylops, Astrapotherium, and "Proterotherium." Because of the amount of damage to AMNH VP-28700, at present Trigonostylops should be scored with a question mark. The other two should be scored as sinus present, assuming "Proterotherium" specimens represent Tetramerorhinus (see table 1: fn. 9). Rescorings: changed Tetramerorhinus, 0 → [01]; Trigonostylops, 0 →?; Astrapotherium, 0 → 1; Simpsonotus, ? → 1; Macrauchenia, 0 →?

127. Epitympanic sinus in a large swollen triangular area delimited by a medial crest continuous with posterior root of zygomatic arch anteriorly and by lambdoid crest posteriorly: 0, absent; 1, present. Rescoring: changed Eoastrapostylops, "-" →? (revised from Kramarz et al., 2017).

128. OMITTED. Promontorium shape: 0, flat; 1, globose. This character was not used because the differences in character states are too vague to permit consistent scoring.

129. Expanded and fanlike medial flange of tympanic face of petrosal, well demarcated from the bean-shaped promontorium: 0, absent; 1, present. Rescoring: changed Trigonostylops, ?→0; Cochilius, ?→1.

130. Location of apparent tensor tympani fossa: 0, largely (ventro-)medial to the cavum supracochleare; 1, strictly ventral or lateral to it, not medial. The wording of this character has been modified to reflect nomenclature used in this paper. Rescorings: changed Astrapotherium, ? →0; Cochilius, ? →0; Eoastrapostylops, 0 →? (revised from Kramarz et al., 2017).

*131. OMITTED. Facial sulcus (here the distance from fenestra vestibuli to crista parotica): 0, wide; 1, moderate; 2, narrow. This character was not used because the differences in character states are too vague to permit consistent scoring.

132. Subquadrangular feature (presumably tensor tympani fossa) on the promontorium, elongated anteroposteriorly: 0, absent; 1, present. The wording of this character has been modified to reflect nomenclature used in this paper. Rescorings: changed Astrapotherium, 0 →1; Eoastrapostylops, 0→? (revised from Kramarz et al. 2017).

133. Vascular (internal carotid and stapedial) sulci on promontorium: 0, absent; 1, present. Rescorings: changed Astrapotherium, 0 →1; Cochilius, ? →0.

134. OMITTED. Epitympanic recess vs. fossa incudis: 0, subequal; 1, epitympanic recess larger; 2, reduced or no visible depression for epitympanic recess. This character was not used because boundaries of both fossa incudis and epitympanic recess can be difficult to discern in many taxa.

135. Posttemporal canal (or groove) and foramen: 0, absent; 1, present. Rescorings: changed Trigonostylops, ? →1; Cochilius, ? →1.

136. Stapedial ratio: 0, less than 1.8; 1, more than 1.8. Rescoring: changed Cochilius, ? →1.

137. Stapedial fossa and postpromontorial tympanic sinus: 0, distinct features, separated by a crest or sharp break in slope; 1, features merged, almost indistinct. Rescoring: changed Cochilius, ? →0. The wording of this character has been modified for clarity.

138. Hiatus of the facial canal (for the greater petrosal nerve; hiatus fallopii), location: 0, opening on anterior edge of petrosal; 1, opening on the tympanic surface of petrosal. The wording of this character has been modified to reflect nomenclature used in this paper. Rescorings: changed Cochilius, ?→ 0; Eoastrapostylops, 0 →1 (revised from Kramarz et al., 2017).

139. Strongly curved promontorium of petrosal (excavated by a deep notch just anterior to the fenestra vestibuli): 0, absent; 1, present. Rescoring: changed Trigonostylops, ?→0.

140. Tegmen tympani: 0, inflated ventrolaterally; 1, thin, not inflated ventrolaterally. Rescoring: changed Trigonostylops, ?→1.

141. OMITTED. Pierced tegmen tympani: 0, absent; 1, present. This character was not used because of homological ambiguity: without indicia, one cannot tell whether feature is related to stapedial ramus superior or to lateral head vein/prootic sinus (or perhaps both in some cases).

142. Location of crest separating foramen acusticus superius and foramen acusticus inferius in internal auditory meatus (IAM): 0, shallow in IAM; 1, deep in IAM. *Rescorings:* changed *Trigonostylops*, ?→1; *Cochilius*, ?→1.

*143. Parafloccular (= subarcuate) fossa morphology: 0, deep, diameter of aperture is smaller than maximum diameter of the fossa; 1, deep, cylindrical or slightly conical, with diameter more or less constant; 2, conical or shallow depression: aperture is the widest diameter. *Rescoring:* changed *Trigonostylops*, ?→2.

144. Cochlear canaliculus within a large notch at posteromedial edge of promontorium (i.e., lateral wall of cochlear canaliculus notched in a [large] right angle): 0, absent; 1, present. *Rescorings:* changed *Trigonostylops*, ?→0; *Astrapotherium*, ?→1; *Cochilius*, ?→0.

145. Number of cochlear turns: 0, less than 2 (or 2); 1, more than 2. *Rescorings:* changed *Trigonostylops*, ? →0; *Cochilius*, 0 → [0,1].

146. Relative sizes of semicircular canals (from inner perimeter and/or R): 0, ASC clearly the largest (>1.10 from the others); 1, subequal (at least ASC and PSC); 2, PSC the largest (>1.10 from the others). *Rescoring:* changed *Trigonostylops*, ? →1.

147. Secondary common crus: 0, present; 1, just a contact; 2, absent. *Rescoring:* changed *Trigonostylops*, ? →0.

148. Anterior (and posterior) ampullae, dorsoventral girth relative to semicircular canal cross-sectional diameter: 0, ampullar girth in the dorsoventral direction extends well beyond the SSC boundaries; 1, ampullae are not noticeably expanded anterodorsally beyond the plane of the SSC. *Rescorings:* changed *Trigonostylops*, ? →0; *Cochilius*, 1 → [0,1].

149. Dorsal extent of ASC and PSC above the crus commune: 0, only the ASC extends well dorsal to the crus; 1, ASC and PSC both extend well dorsal to the crus commune; 2, neither canal extends well dorsal to the crus. *Rescorings:* changed *Trigonostylops*, ?→2; *Cochilius*, 0 → [0,1].

150. Pars mastoidea of petrosal: 0, well exposed; 1, absent or reduced to a thin strip of bone appearing between squamosal and exoccipital. *The wording of this character has been modified to reflect nomenclature used in this paper. Rescoring:* changed *Astrapotherium*, ? →1.

151. Very high sagittal and lambdoid crests, latter crest being inclined backward: 0, both absent; 1, both present. *Rescorings:* changed *Trigonostylops*, 3 →1; *Astrapotherium*, 3 →1. *The wording of this character has been modified for clarity.*

152. Coronoid process of dentary: 0, rectilinear; 1, bent medially.

153. Mandibular foramen: 0, below alveolar border; 1, at level of alveolar border.

154. Shape of mandibular body: 1, deep, robust; 1, slender.

155. Neck and head of astragalus: 0, not expanded and axis oblique relative to tibial trochlea; 1, expanded and axis subparallel to tibial trochlea.

156. Cotylar fossa of the astragalus: 0, absent; 1, present.

157. NEW. Facial process of premaxilla: 0, present; 1, absent. *As seen in lateral view in most mammals, the facial process of the premaxilla is that part of that bone that contributes to the end of the rostrum and articulates with the maxilla externally along the lateral maxillopremaxillary suture. Astrapotheriids* and Trigonostylops *lack the facial process.*

158. NEW. Diverging canines (upper and lowers): 0, canines diverging at an angle less than 70° when viewed in frontal aspect; 1, divergence angle equal to or larger than 70°.

159. NEW. Cheekteeth enamel with vertical Hunter-Schreger bands (HSB): 0, absent; 1 present. *This character captures the presence of vertical prism decussation in the inner portion of cheektooth enamel, as seen in section and described by Rensberger and Pfretzschner (1992) and Koenigswald et al. (2014). Evaluation is carried out independent of the width of the portion with vertical HSB, or the cooccurrence of HSB with other configurations (see also Lindenau, 2005). Taxa without vertical HSB or with nonvertical HSB (i.e., transverse or curved) are scored as absent. Pyrotherium is scored as absent following Koenigswald et al. (2014).*

APPENDIX 4

CHARACTER/TAXON MATRIX[1]

```
                    0         0         0         0         0         0         0         0         0
                    1         2         3         4         5         6         7         8         9
                    0         0         0         0         0         0         0         0         0

Zalambdalestes    1111?10?0010020?0001000000--------1110-01----0000000000100000000-0-----0000-00002000000000000010100
Leptictis         00010-???0?002000001000000--------1110-01----0102100000000010000-0-----0000-00000010010000010000000
Phenacodus        1111000000001000001000000--------1110-11----11011010000000?10000-0-----0000-00001020100010000000000
Hyopsodus         0011010000001000011000000--------1100-00----121BBA100?0001A000-0-----0000-00001?00?00000010-?0000
Meniscotherium    1111000000001000011000000--------1110-11----1B11111000000010100-0-0---0000-00000020000000000000000
Protolipterna     ?0??????????????010?000000--------1100-00----121B211??????10000-0-----000?????????????00????0?0?00??
Tetramerorhinus   --01-----0-01-1-2--1002010--------1110-11----11A1B01-0010101110000-0-0-0000-00001000000000000000000
Trigonostylops    -1?????????--?-01010011A000--0---01010010--0B2220000000001010000-0-0-000???0011???00--000?000010?
Astrapotherium    -100----------1-010011111100-00----1010000-00-------00110001110000-0-0-00-0??001-20010--10-0?00000
Astraponotus      -100----------1-010010111000-0??-001010010-00122B20-00110001110000-0-0-00-0??000-??000--1?-??10000
Eoastrapostylops  ?0??????????????010100110000--0---0101001----022220-?0?00?71000000-0-0-00-1???000-??000??0?-010010?
Pyrotherium       --11--00012002102--000101000--0----0---0-0-00?222200?001??0?-0----------0010000120?1?00??????0010?
Notostylops       1111-1000110020010-A00111101000-0001010000100D11120?100100010111000000000010000101100000000000100
Simpsonotus       0011000000001000001001110100000-A001010000100DB1B200-000000011200000000001000000010000000000?0000?
Periphragnis      0011000?0000010?000100111101010-00-1010000100D11201110000010110000010000A-0001202000000000?10000
Puelia            0011000000001010011010?1111010?????-????0???00D????0?0?????????????????????010000120210001100000000?
Leontinia         0011000000101000011011111101010-10-1010001-00D22220?0100100111100?100110001000120310010011000?10010
Nesodon           11110-000000100-10-111111101001101-1010000000-------0001010111101?1011100000001203101000000?10011
Colbertia         0011010000001000011001111111010-A001010000100DB1220000000010112000000001000112011220??00000?00?00100
Oldfieldthomasia  0011010000001000011001111111110-00-1010110100D11B201000000010110000000000001120?1100?00000000000
Notopithecus      0011110000001000011001111111100-00-1010000100D11120000100001011000000000100011201120000001000100
Interatherium     11111000010010010-12?111??0????-?-10110?0-10------001100010????0?0??0100100011201120100001?00100
Cochilius         0011110000100100001112?111??0????-?-10110?0-10------001100010????0?0??0?010000011201120100001000100
Trachytherus      1-11011010200100101111111111110-10-1010000001-------0011000111122?2?010000000-0111200011000010100?00000
Mesotherium       --10--10102---1-2--02?111??0????-?-????00?-02-------0001--01????3?0??0000000111201111000010000100
Archaeohyrax      1011010010100100001121111111100-10-1010000000-------00?1000111211?010000000000112001110000100000000
Hegetotherium     1111010110200100001112?????????????-101000??00-------0001000?1????3?0???00100-00112010110000110101000
Macrauchenia      0011000000001000011112010--------1110-11-----------010000111100-?-0-0-0000-100011?00101?1?00?0000?
Alcidedorbignya   1011000000001000101000000--------1110-00----0212200100000010000-0-----0000-0?001000000000110010100
Arctocyonides     111100?????010?0??1000000--------1100-00----1212100??????00000-0-----0000-00000000000001110?10000
Pleuraspidotherium 1111010??70?10100001A000000--------1110-11----2111101??????010100-0-0-0000-000010?0000?00000000000
Baioconodon       ?0??????????????01?1000000--------1110-00----02022?0??????00000-0-----000???002????00????00?0000?
Mairoana          ?0??????????????0??1000000--------1110-00----021??00?????????????????????0????002???000??0?10000000
Diadiaphorus      --01-----0-01-1-2--1002000--------1110-11----1A11101-0010101100-0-0-0-0000-000000?0000001000000000
Miguelsoria       ?????????????????????000000--------1100-00----121B211??????10000-0-----000??????????????????????
Protungulatum     ?????????????????????000000--------1110-00----0212200??????00000-0-----000??????????????????????
Theosodon         0011000000101000011002000--------?110-11----11111?1110001111000000000000-100001000101-1?00?00000
Didolodus         ?0??????????????0??1000000--------1100-10----11A1111??????10000-1-----000??????????00???0?0??00??
Tapirus           0111000000001000000000101000-00----1010010-0-112220-0010000100?00--0-0-0-0--10-0-E00001-10-0000110
Equus             1111000000100001C00A11??0000-0-----110-110---?------000000011?0000-0-0-00-00-10-0-200000101-0000000
Palaeotherium     AA11000000001000001012017?0--00--?1110-110---111120-00000011110000-0-0-00-00-100A-000A00-AA-00A0000
```

APPENDIX 4 *continued*

	1 0 0	1 1 0	1 2 0	1 3 0	1 4 0	1 5 0	1 6 0
Zalambdalestes	100000010000010---0-0-----0-100001011000?00??00000010?1?0000
Leptictis	010200001000100---0-0-----0-100101?01000010000010010?10000?
Phenacodus	00000000010?011---0-0-----0-00?001?11000001?0?????01011?0000
Hyopsodus	??0000100010?001---0-0-----0-00001121A000000B0?????00??10000?
Meniscotherium	000000100100001---0-0-----0-0000111110000020?????0101000000
Protolipterna	??110?1?
Tetramerorhinus	??00021000010A1---0-0-----1-0000112100001102112010100110000
Trigonostylops	100000011010021-000-0-----?-00????1???01?1200100201011??111
Astrapotherium	10-1-00-1010?11-????0-----1--00-11-100001-120012011101101111
Astraponotus	10-0-00-0010?11-????0-----??-00-??-1???0?-????????110?1??111
Eoastrapostylops	??-0-?0??000??-????0-----0?-0?-??-110101-????????0?011???00
Pyrotherium	??0?000?0?101??00111?????1??????????????????????010000-0
Notostylops	0000020000101000011100100101011?00?10?20?02?111111111010??000
Simpsonotus	??000??00?101??0001010000001?????????????????????1001??00?
Periphragnis	000012000010101-0011111100101111?0?????00??????????11001??000
Puelia	00000200001010?000111100010?????????????????????11?????000
Leontinia	??0012000010101-0011110100110?????????????12??????1?20?200?
Nesodon	0?0012000010100?0001111110010?????????????????????110A001000
Colbertia	??000??00?1?100010??10????101?????????????????????100001100?
Oldfieldthomasia	??0002000?1?10?000111?00??10?????????????????????11?00??000
Notopithecus	0100020000101010?0100-10--1111?????????????????????11010??000
Interatherium	??0002000010100?0110-11--1111?????????????????????1000??000
Cochilius	??00020000101000110-111-0111?10??0?1100110120A22AA10000??000
Trachytherus	100002000?1010?00111111111010?????????????2??????11??0000-0
Mesotherium	10000201001010000111111110101?0???????1??????12??????11100000-0
Archaeohyrax	100002000?1?11?1001111101010?????????????????????11000??000
Hegetotherium	1011020000101010?10010111-101011?0???1??1??0?20?????1100000000
Macrauchenia	??0200100001001---0-0-----?-0000101100001?1211B2010100110000
Alcidedorbignya	010000000100001---0-0-----0-0000111110101102000000A000A00000?
Arctocyonides	000000000000000?01--0-0-----0-000011101000???A10000000??1??00?
Pleuraspidotherium	00000000000?0?00--0-0-----0-10000110A010010B0000010000000000?
Baioconodon	00000000010000?1---0-0-----0-00??1????0?001010000000?????00?
Mairoana	00000000010000?1---0-0-----0-00?0??1??0?0??????????????????00?
Diadiaphorus	01000210000100001---0-0-----?-0000112100001102112010000110000
Miguelsoria	??1110???
Protungulatum	?????????????????????????00000120100010000????????100?00
Theosodon	??0000100001001---0-0-----0-00?0??????01???1?????000110000
Didolodus	??100???
Tapirus	00-0-00001100A1-000-0-----0--0A-11-101100-120000001101110000
Equus	11-1-0000110001-000-110--10--01-00-011000-120110010101110000
Palaeotherium	01-0-0000110001---0-0-----??-00-1?-100101-120?????1101110000

[1] Key to symbols and letters: question mark = missing data; dash = inapplicable; recorded polymorphisms, A = [0, 1]; B = [1, 2]; C = [0, 2]; D = [2, 3]; E = [1, 2, 3].

On the cover: Reconstruction of skull and body of *Trigonostylops wortmani*, an Eocene South American native ungulate (Jorge Blanco, 2021).